MULTIFUNCTIONAL CHROMATOGRAPHY SUPPORTS

By

Alison Mary Liddy

A thesis submitted to
The University of Birmingham
for the degree of
DOCTOR OF PHILOSOPHY

School of Chemical Engineering
The University of Birmingham
March 2009

Thesis abstract

Packed bed chromatography is recognised as one of the key techniques for the successful purification of gene therapy vectors such as plasmid DNA. However, as target products have evolved over the years, packed bed chromatography supports have not been re-designed to purify larger nano-sized biomolecules. For example, the purification plasmid DNA via chromatography suffers from significant problems, such as low binding capacities and co elution of contaminants with the target product.

The aim of this study was to create a bi-layered packed bed chromatography support for the purification of nano-sized bioproducts in an attempt to solve the problems discussed above. This bi-layered bead would possess two distinct functional layers, a size exclusion outer layer and a charged anion exchange inner core. The size exclusion layer would address the problem of co elution by preventing the binding of the target product to the support whilst allowing smaller contaminating entities to diffuse into the core of the bead. The charged inner core would still maintain a high binding capacity for contaminants therefore allowing for the collection of the product in a more purified form.

Previous work published to create a bi-layered bead showed that the chemistry approaches applied were not that successful in producing two chromatography functions present in distinct layers. It was apparent from the results that in some cases a size exclusion layer had been fabricated on the surface of the support but that this layer still maintained point charges which allowed for outer surface binding therefore reducing the beneficial effects of the layer. The focus of this study was to develop chemistry methods that construct a bi-layered support that possesses two chromatographic functions present

in distinct layers. This achieved by investigating three different of synthetic chemistry routes and a variety of reaction conditions. Sepharose CL-6B was the base matrix employed in all three synthetic chemistry routes explored. In synthetic routes 1 & 2 the base matrix was firstly activated with allyl glycidyl ether. This resulted in allyl groups been distributed throughout the support. The next step of the synthesis involved the fabrication of the inert outer layer. This step in synthetic route 1 involved the reaction of bromine with the allyl groups present on the surface of the bead, followed by the addition of sodium hydroxide. The creation of the size exclusion outer layer in synthetic route 2 was achieved by an oxidation reaction of the allyl groups present on the surface with potassium permanganate, and again this oxidation step. The final steps of both synthesises (1 & 2) was the same, with the remaining allyl groups present reacted with bromine and then coupled with the charged amine ligand to produce an anion exchange inner core. Synthetic route 3 involved the activation of the base matrix with epichlorohydrin, this introduced three membered epoxide groups throughout the bead. The next step of the synthesis generated the size exclusion outer layer, the epoxide groups present on the surface of the bead were reacted either with sodium hydroxide or hydrochloric acid. In the final step of synthesis, the epoxide groups remaining were reacted with trimethylamine hydrochloride to create an anion exchange inner core. In all three synthesises the chemistry step to fabricate the outer layer was examined with microwave heating and with different solvent conditions in an attempt to improve the inertness of the layer. The chemistry introduced onto the supports was tested using different chemical assays, and the modified supports were tested for ionic capacity, plasmid DNA binding and the protein binding capacity.

One of the bi-layered supports created in synthetic route 1 eliminated 91% of plasmid DNA binding while maintaining a high protein binding capacity. This was achieved by using DMSO as the solvent in the bromination step and employing microwave heating. Synthetic route 2 proved to be the least successful approach in creating a bi-layered support with the best results eliminating only 59% of plasmid DNA binding, however microwave heating did appear to further enhance the reaction occurring at the surface of the bead. Synthetic route 3 again produced some positive results, with the support created under hydrochloric acid-methanol reaction conditions reducing 91% of the plasmid DNA binding whilst maintaining a high protein binding capacity.

The work completed during this study revealed that microwave heating was an extremely useful tool in the chemical synthesis of chromatography supports. Subsequently, a comprehensive study was untaken investigating the effects of microwaves on numerous chromatography matrices. The results from this work showed that only certain types of chromatography support can undergo microwave heating, as some chromatographic materials are damaged by microwave radiation. Furthermore, the results also revealed that certain charged ligands affected the durability of the matrix by microwave heating. This evaluation of the response of chromatographic supports to microwave heating was viewed as crucial to future development in this area.

Dedication

To my family and Matthew; for their constant love and support

Acknowledgements

I am deeply grateful to Professor Owen Thomas and Dr. Eirini Theodossiou for supervising this project and for all their time and effort during my Ph.D.

A very big thanks to John Stenson, Robert Palin, and Professor Colin Thomas for their assistance with the micromanipulation work.

I would also like to thank Nitin Jain, whom it was a delight to supervise during his M.Sc. project, and whose work has contributed to chapter 3.

Thank you to Hazel Jennings and Elaine Mitchell, who were always available to help and advise.

To all my research group colleagues at the Biochemical Engineering Department, University of Birmingham, it was pleasure to work with you all during to my Ph.D.

Table of contents

List of Illustrations

List of tables

Abbreviations

AC: Affinity Chromatography

Ad: Adenovirus

AEC: Anion exchange chromatography

AGE: Allyl Glycidyl Ether

ATPS: Aqueous Two phase systems

BSA: Bovine serum albumin

CHO: Chinese Hamster ovary

CL: Cross-linked

CM: Carboxymethyl

DNA: Deoxyribonucleic acid

DEAE: Diethylaminoethyl

DLRLP: Double layered Rotavirus-like Particles

DSP: Downstream processing

EBA: Expanded bed adsorption

EPC: Epichlorohydrin

FDA: Food and Drug administration

FF: Fast Flow

gDNA: genomic DNA

GF: Gel filtration

GMP: Good manufacturing practice

HEA: Hexylamine

HIC: Hydrophobic interaction chromatography

HPLC: High performance liquid chromatography

HPTFF: High performance tangential flow filtration

HR: High resolution

IEC: Ion exchange Chromatography

IMAC: Immobilized metal affinity chromatography

MAbs: monoclonal antibodies

MPa: Megapascals

OC: open circular

pDNA: plasmid DNA

PEI: Polyethyleneimine

PEG: Polyethylene glycol

PPA: Phenylpropylamine

Q: Quaternary amine

RNA: Ribonucleic acid

RPC: Reversed-Phase Chromatography

RPLC: Reversed phase liquid chromatography

SEC: Size exclusion Chromatography

SEM: Scanning electron microscopy

S: Sulphate

SC : Super-coiled

SP : Sulphopropyl

SC : Super-coiled

TAC: Thiophilic adsorption chromatography

THAC: Triple helix affinity chromatography

TPP: Three-phase partitioning

Symbols

A_0 : cross sectional area of the particle (μm^{2})

E: Young's modulus (MPa)

ε: Strain

ε'': dielectric loss factor

ε': dielectric constant

F: Force (mN)

J: Joules

h: displacement (μm)

h: hours

σ: Pressure Stress (MPa)

K: Kelvin

l_0 : length before deformation (μm)

l : length after deformation (μm)

R_p: Radius of the particle (μm)

s: seconds

μ: Poisson's ratio (0.5)

1. INTRODUCTION

1.1 History of Chromatography

The development of chromatography as a separation technique began with research published by Twett in 1903 (Ettre, 2000). During the next few decades that followed, few scientists employed the chromatography method invented by Twett (Ettre, 2000). It took until the 1930's for researchers to fully appreciate Twett's efforts, and employ chromatography as a laboratory technique for investigating different natural substances (Lederer, 1972). The advancement of chromatography from this point onwards was rapid, with the introduction of synthetic ion-exchange resins by Taylor in 1938 (Lederer, 1972).

By the 1950s researchers were investigating protein purifications on new chromatography matrices (Curling, 2007). However these new supports were comprised of hydrophobic styrene-divinyl benzene which was highly unsuitable for protein separations. The hydrophobic nature of proteins resulted in non specific protein interactions with the supports. Secondly these beads produced low protein binding capacities, when what was required for successful separations were porous hydrophilic supports. During this decade the development of cellulose ion exchangers by Peterson and Sobers (1954) and Sephadex (Porath & Flodin, 1959) significantly improved protein separations with chromatography. The creation of these hydrophilic chromatography supports in 1956 (Peterson & Sobers, 1956), allowed for the first effective protein separations via chromatography. From this point onwards the production of new chromatography supports was swift, with cellulose based ion exchange resin, cross linked dextran beads (1959), polyacrylamide (1961) and agarose beads (1964) (Porath & Flodin, 1964) all becoming commercially available over a four year period. The focus of research was now

on ligand design with the aim of improving purifications by Chromatography. The generation of new chemical synthesises allowed for the activation of supports with a selection of ligands. Axen and co workers (1967) produced the cyanogen bromide chemistry which later contributed to the invention of affinity chromatography by Cuatrecasas *et al.* (1968). These new commercially available supports had a huge impact on protein purifications via chromatography, unfortunately most of these new beads were not applicable for process chromatography as one gram of dry support adsorbed 100 mL of water (Curling, 2007).

The development of chromatography in the early 1970s was lead by a breed of new supports and the introduction of a new chromatographic principle. This new principle was named Hydrophobic Interaction Chromatography (HIC) due to the hydrophobic nature of the ligands attached to the matrix, which allowed for the separation of biomolecules by exploiting their hydrophobic properties. Kopaciewiez *et al*. (1986) synthesised anion exchange stationary phases, which varied in ligand density and hydrophobity, and demonstrated from this work that protein retention and resolution increased when more hydrophobic moieties were incorporated in the resin. These new neutral Hydrophobic Interaction Chromatography beads were a result of research completed by Porath (Porath *et al*., 1973) and Hjertén (Hjertén, 1973) and became commercially available in 1977. Hydrocarbon-coated Sepharose derivatives were also released onto the market in 1972 (Zaidenzaig *et al*., 1972). These Sepharose supports allowed for reverse phase separations leading to the invention of the High Performance Liquid Chromatography (HPLC) in the mid 1970s. Also throughout this decade Pharmacia Fine Chemicals introduced many new chromatography products onto the market, Protein A Sepharose in 1975, HIC products in 1977, and Immobilised metal affinity chromatography 1975 (Porath, 1975).

An abundance of different chromatography beads were developed in the 1980's, mostly based on dextran and agarose, but also using cellulose, polyacrylamide, and methacrylate (Janson & Hedman, 1982). By this stage it was apparent there were many advancements made in the design of chromatography supports since their early primitive beginnings, however chromatography supports still suffered from many inadequacies by the end of the 1980s. Chromatography materials were: polydisperse; had insufficiently wide pores; large particle size, and suffered from low mechanical strength. These problems remained unresolved throughout the 1990s with few new developments made in further enhancing the design of chromatography supports. Ligand chemistry did progress somewhat with the creation of bimodal ligands (Frechet *et al.*, 1994). However, the biology of target molecules had changed from small biomolecules in the 1980's to larger recombinant products and monoclonal antibodies (MAbs).

Since the new millennium, the purification of monoclonal antibodies (MAbs) has dictated the design of chromatography beads. Protein A adsorbents now boast: binding capacities in the 20–30 g/L range; short residence times, and flow rates between 100 and 500 cm/h (Curling, 2007). However, the progression of chromatography material has been slow in comparison to the advancements made upstream and it is still unable to deal with increasing product titres (Afeyan *et al.*, 1990). Subsequently, the chromatography stage is now referred to as the 'bottleneck' of biopharmaceutical processes (Wurm, 2004). Despite the advancements discussed above, in many ways, chromatographic material development has remained stationary with the basic design of chromatography supports not having changed significantly over the past 50 years.

1.2. Types of Chromatography

1.2.1 Ion exchange Chromatography (IEC)

Ion exchange chromatography is an adsorption technique that separates biomolecules on the basis of charge. Separation through ion exchange relies completely on electrostatic interactions between the charged molecules present in the mobile phase (buffer and sample) and oppositely charged ligands attached to the beads.

Ion exchange chromatography is performed in four main steps (Figure 1.1). The first step is the equilibration stage in which the matrix is at a starting point, in terms of pH and ionic strength, and will permit the binding of the desired target molecules. The next step is the sample application and adsorption, in which charged solute biomolecules displace the charged counter ions of the support and bind reversibly to the bead. The third step is the desorption of the target molecules from the bead. This is achieved by introducing a buffer, possessing counter ions that have a greater affinity for the charged ions present on the support, so that the target bimolecules are dissociated from the bead back into the mobile phase. The final step is the regeneration of the beads in which any unbound residual material is removed from the beads by washing typically with sodium hydroxide. The beads are then re-equilibrated with the original counter ions and are ready for another cycle.

The different types of amino acids present in proteins enable them to bind effectively to both an anion exchange and cation exchange adsorbents. Lysine, arginine, and histidine, are positively charged at a physiological pH, in contrast to aspartic acid and glutamic acid which are negatively charge at a physiological pH (Culter, 2004). Typically the retention of proteins on an ion exchange adsorbent can be explained by two possible types of

models, stoichimetric and non stoichiometric. Although stoichiometric models are capable of accurately describing the behaviour of ion exchange chromatography systems, they assume that the individual charges on the protein molecules interact with discrete charges on the ion exchange surface (Bruch *et al*., 2009). In reality the mechanism for retention of proteins on ion exchange support is more complex. It is primarily due to the interaction of the: electrical fields; protein molecules, and bead surface (Bruch *et al*., 2009). In recent years, the theories applied in colloid and surface chemistry have been used to describe the electrostatic and other interactions, behind the retention of proteins in IEC (Jonsson *et al*., 1999)

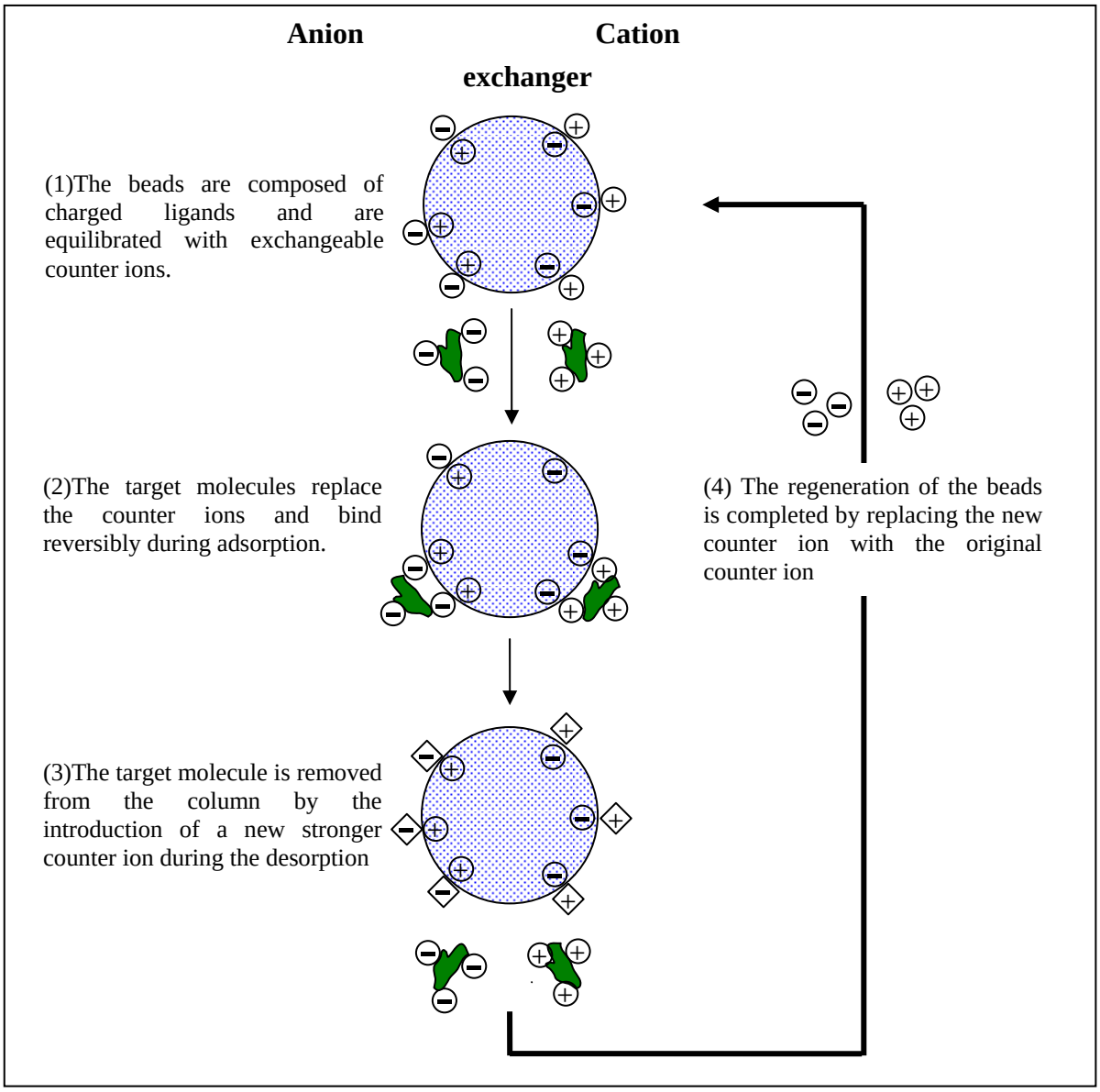

Figure 1.1: The principles of ion exchange chromatography. (Adapted from Theodossiou, 2004)

An ion exchange support is comprised of an insoluble hydrophilic matrix to which charged ligands are covalently attached. The beads may be composed of inorganic compounds, synthetic resins, or polysaccharides.

There are a variety of ligands which maybe attached to matrix, these fall under two general categories of either strong or weak (Table 1.0). Strong ion exchange ligands maintain their charge characteristics, and therefore their ion exchange capacity over a wide pH range, whereas an ion exchanger possessing weak ligands can only be charged over a narrow pH range (Culter, 2004).

Table 1.0: Ligands used as Ion exchangers (data taken from Culter, 2004)

Ion Exchangers	**ligand**	**Type**	**Ionic capacity pH range**	**Functional groups**
DEAE Sepharose FF (AEC)	Diethylaminoethyl (DEAE)	Weak	2.0-9.0	$-O-CH_2-CH_2-N^+H(CH_2CH_3)_2$
Q Sepharose FF (AEC)	Quaternary ammonium (Q)	Strong	2.0-12.0	$-CH_2-N^+(CH_3)_3$
SP Sepharose FF (CEC)	Sulfonpropyl (SP)	Strong	4-13	$-CH_2-SO_3^-$
CM Sepharose FF (CEC)	Carboxymethyl	Weak	6-10	$-CH_2COO^-$

IEC is one of the most of utilized chromatography methods for the purification of biomolecules (Ferreira *et al*., 2000). It produces: fast separations; has no solvent requirements, and there is a wide variety of process-grade adsorbents available (Eon-Duval & Burke, 2004). IEC as a purification technique can be incorporated in the capture stage, intermediate stage, and the polishing stage of a purification process, achieving high binding capacities and high resolution (Figure 1.2).

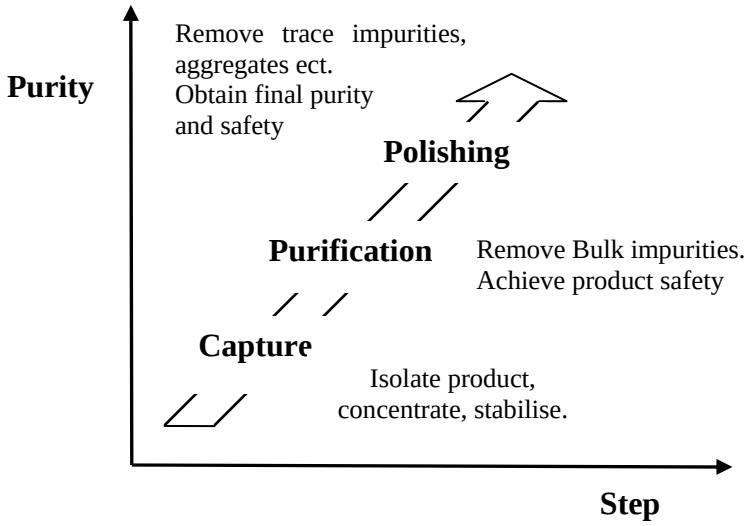

Figure 1.2: The different stages an ion exchanger can by employed in a downstream process (adapted from GE Healthcare handbook, 2008).

Important separation factors, such as efficiency, capacity, and recovery, are controlled by both the physical and chemical properties of the ion exchange bead, as well as the characteristics of the target biomolecule. Although it is reported that high binding capacities are observed for proteins purified with ion exchange chromatography this technique is not as effective in the purification of larger biomolecules such as plasmid DNA. Ferreria *et al.* (2000) showed that when comparing protein and plasmid DNA binding capacities on Q Sepharose FF, the protein binding capacity obtained was 120mg/mL, where as the plasmid DNA binding capacity was only 1.3mg/mL.

1.2.2 Size Exclusion Chromatography (SEC)

Size exclusion Chromatography is a technique which separates biomolecules according to their molecular size. This separation method is extensively used in both laboratory scale and production scale bioprocesses for sample conditioning and final product polishing (Hood *et al.,* 1996). It offers numerous purification advantages such as: high

sample loading capacities and sample buffer exchange in a single step. However there are also disadvantages to this technique such as: cost; co elution of target product with contaminants; limited separation between molecules of similar size, and the product is obtained in a diluted solution (Diogo, 2005; Firestone, 1994).

Several SEC supports have proved effective in the conditioning and polishing stages of biomolecules for example: Superose 6B; Sephacryl S-1000; Sepharose 6 FF, and Sephacryl S-500 HR (Stadler *et al.*, 2004; Transfiguracion *et al.*, 2007; Varley *et al.*, 1999).

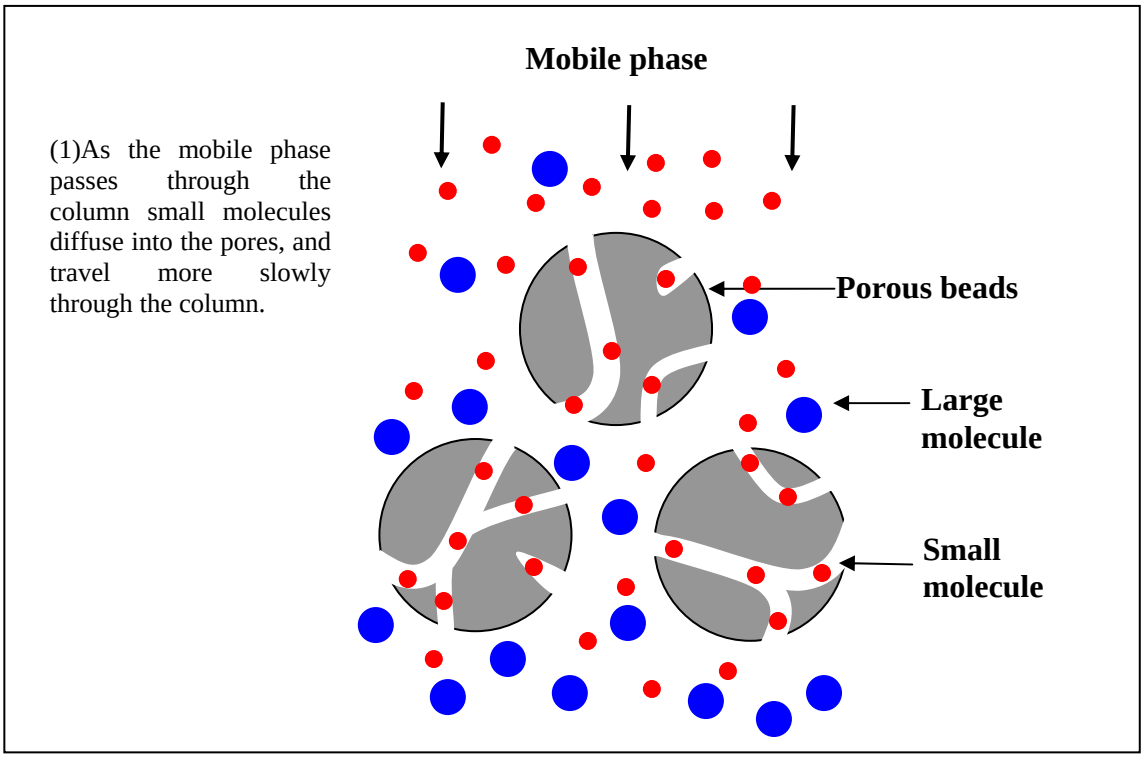

Figure 1.3: Size exclusion chromatography principles

SEC operates (Figure 1.3) by passing a mobile phase (target product and buffer) through the column containing the SEC beads. The smaller molecules diffuse into the beads and are slowed in their passage down the column. Larger molecules have limited or no diffusion into the pores and move more rapidly down the column. The order of elution is

inversely related to the molecular weight of the molecules. Typical separation range of SEC is approximately 10^2 to 10^6 g/mol (Barth & Mori, 1999). The fractionation range of some common commercially available SEC matrices is shown in Table 1.1. The choice of a certain SEC support depends on the fractionation range of the bead, with regard to the size of a specific biomolecule, for example the SEC bead employed is usually dependent on the size and properties of the target product. Correct working conditions are also paramount for effective separations with SEC, for example: high flow rates can give low resolution, which is also dependent upon bead size (GE Healthcare handbook, 2008)

Table 1.1 Size exclusion ranges of some commercially available supports (data taken from GE Healthcare handbook 2008)

Gel type	**Bead size (μm)**	**Fractionation range Globular proteins**
Sephacryl S-400 HR	25-75	20 0000 – 8 000 000
Superdex 200	11-15	10 000-600 000
Superose 6	11-15	5 000- 5 000 000
Sepharose 6B	45-65	70 000- 40 000 000

There are many published models that describe how molecules behave during size exclusion chromatography (McGreavy *et al*., 1990; Porath, 1963). Most of the earlier models were based on a theoretical approach which described the mechanism of SEC with sterric effects and prohibited diffusion from a porous bead (Kubin, 1975). Recently more advanced models have investigated the influence of pore morphology on SEC mechanisms focusing more on retention and band broadening (McGreavy *et al*., 1990). This study revealed that pore volume morphology can play an important part in band broadening behaviour in SEC columns.

SEC matrices typically have a porous structure, are hydrophilic, and comprised of cross-linked agarose, dextran or synthetic polymers. Recently, there have been some interesting new developments in the design of SEC beads. For example, Adrados and co workers (2001) recently created a thermo-responsive cellulose based support which boasts of possessing temperature dependent porosity, and this can produce very high resolution. In more recent developments Malik *et al*., (2009) created nano-porous polymeric SEC adsorbents for blood purification.

1.2.3 Affinity chromatography (AC)

Affinity Chromatography separates biomolecules on the basis of a reversible interaction between the target molecule, and a specific ligand coupled to a chromatography matrix (Table 1.2). Affinity Chromatography is extensively used for the purification of proteins (Mallik *et al*., 2008). It is also an attractive unit operation for the isolation of larger biomolecules such as viruses, as it offers high selectivity and capacity (Lute *et al*., 2008). As of yet this technique has not been used extensively for larger biomolecules such as plasmid DNA purifications, nevertheless there are some interesting reports which claim to have effectively separated nucleic acids with a specific ligand immobilized on an AC stationary phase (Woodgate *et al*., 2001).

The main advantage to AC is its ability to obtain high binding capacities for a specific biomolecule. The disadvantages to this technique: are possible loss of ligand from the matrix; distortion of the beads morphology, and strong protein interactions with the supports which causes problems at the elution stage (Lute *et al*., 2008).

Table 1.2: Example of Ligand-target molecule interactions on Affinity matrices (GE Healthcare, 2008)

Ligand	Target Product
Antibody	Antigens Virus cells
Lectin	Polysaccharides Glycoprotein Cell surface-receptors
Nucleic acid	Complementary base sequences Histones Nucleic acid polymerase
Glutathione	Gluthathione-S-transferase GST fusion proteins
Metal affinity	Poly (his) fusion proteins Native proteins with histidine cysteine troptophan on their surface.

The separation of process of AC occurs through the target biomolecule interacting with the ligand attached to the matrix through: electrostatic; or hydrophobic interactions; van der Waals' forces, or hydrogen bonding (Mohr, 1985). The target molecule can be eluted from the support by introducing a competitive ligand, or by changing the pH, ionic strength, or polarity of the solvent.

1.2.4 Hydrophobic Interaction Chromatography

Hydrophobic Interaction Chromatography is a widely used chromatographic technique for the purification of proteins, it's popularity for protein purifications is due to it's capability to remove aggregated forms of antibody from a process stream (Valliere-Douglas *et al.*, 2008). It has also proved effective in purifying a variety of larger

biomolecules including plasmid DNA (Diogo *et al*., 2003) and viruses (Chahel *et al*., 2007).

HIC is a separation technique, which purifies biomolecules by exploiting their hydrophobic properties, these interactions are possible due to the fact that hydrophobic molecules in an aqueous solvent will self associate (Jansson & Ryden, 1998). HIC interactions occur through the hydrophobic region present on the biomolecule and hydrophobic ligands (alkyl or aryl groups) covalently attached to the beads. The retention of biomolecules is achieved using high salt concentrations while the elution is performed by decreasing the salt concentration of the mobile phase (Xiao *et al*., 2007).

The level of binding on HIC beads increases with the chain length of the ligand. It is reported that with proteins more than one ligand is involved in adsorption process, and so multi-point attachment of the protein to the matrix is possible (Jansson & Ryden, 1998). Other factors that significantly influence target product retention are temperature, pH, and chaotropic salts (Gagnon & Grund, 1996).

The base of HIC matrices is typically composed of carbohydrates, for example cross-linked agarose or synthetic copolymer materials with covalently attached ligands.

1.2.5 Reversed-Phase Chromatography (RPC)

Reversed Phase Chromatography is a technique that separates biomolecules through a hydrophobic interaction between biomolecules present in the mobile phase and immobilised hydrophobic ligands on the stationary phase. The basis of separation is similar to HIC where biomolecules with the highest degree of hydrophobity are bound

more tightly to the column and are eluted last (McNeilly, 2001). It is assumed that the binding interactions in RPC are entropy controlled, however this matter is still under debate (Vijayalakshm, 2002).

Elution of the target biomolecule from the RPC support is achieved by gradient elution using an organic modifier which breaks the hydrophobic interaction between the support and biomolecules causing them to desorb.

RPC supports are typically composed of porous insoluble materials such as silica or synthetic organic polymers, with covalently attached hydrophobic ligands.

Reversed-Phase liquid Chromatography (RPLC) is a high resolution purification technique, employed both on an analytical scale and large scale for the purification of a variety of biomolecules such as nucleic acids (McNeilly, 2001) and proteins (McNay *et al.,* 2001). Although RPLC is a highly effective chromatography method for the purification of biomolecules, it has not been used extensively because there is a possibility of protein denaturation due to the solvents and surfaces employed (Purcell *et al*., 1989). Additionally complex retention behaviour has also been reported for some biomolecules (Guo *et al.,* 1986).

1.3 Evolution of target products

Over twenty years ago, the commercial launch of recombinant insulin, marked the launch of the first biotechnology derived drug (Berg *et al*., 2002). These initial biopharmaceutical products were much less complex in comparison to today's sophisticated biotherapeutics.

The concentration of these early biologics was significantly lower than their microbiologically expressed successors, and therefore the purification problems experienced with these initial bioproducts was a lot different to what is experienced today (Curling, 2007).

Research into more effective methods for the purification of insulin products was lead by companies such as Eli Lilly & Co and Novo Nordisk, who developed a large scale chromatography step for the purification of insulin using Sephadex G-50 (Lasagna, 1987). Over the next fifteen years (1980-1994) twenty nine new therapeutic products were approved including ten new recombinant drugs (http://www.bio.org). Along with production of these recombinant products came advancements in both bacterial and mammalian cell fermentations. The production of new recombinant products lead to most purification processes experiencing problems, with either the removal endotoxin levels from *E.coli* fermentations or the reduction of host cell proteins and DNA from CHO cell culture. Biotechnology processes now required a more systematic approach in order to obtain therapeutic products that satisfied regulatory body specifications, new process development focused on process economics, hygiene, regulatory issues, and validation (Jungbauer & Boschetti, 1994). It was the employment of Chromatography as a

purification tool which solved many of the purification problems at the time, and presently column chromatography is the only technique that can produce the impurity clearance required by FDA for plasmid DNA (pDNA)(Diogo *et al*., 2005).

The majority of biotechnology products (including a selection of vaccines, hormones, and growth factors) that were produced up until the mid 1990s required very small quantities to be purified (Skukla *et al*., 2007). However, as the 1990s came and went with an ever increasing variety of target products to be purified (Walsh, 2003), the decade seemed to have little to show in improvements or alternations to the design of chromatography supports for the purification of a specific biomolecule (i.e. proteins, antibodies, viruses & pDNA) (Lyddiatt & O'Sullivan, 1998). Subsequently increasing product titres caused major technical challenges downstream as chromatography struggled to deal with these high expression levels (Low *et al*., 2007). From the year 2000 onwards, typical expression levels in mammalian cell culture was measured to be hundreds of milligrams per litre, and predictions for the next decade to be in the range of 10g/L (Langer, 2006).

Presently, the advancements of modern science have lead to the continuous identification of functional genes for modern medical treatments like genetic vaccination or gene therapy (Voβ *et al*., 2003). Gene therapy is a therapeutic treatment in which a nucleic acid is transferred into a human cell hence modifying the cells genetic properties for therapeutic applications (Prazeres *et al.*, 2001). The demand for gene therapy vectors is predicted to rise continuously over the next few years, with the market for these products expected to reach US $45 billion by 2010 (Ferreira *et al*., 2000).

1.4 Downstream Innovation

1.4.1 Alternatives to chromatography

Although chromatography is renowned as one of the most effective purification techniques, it now becoming more notorious for been one of the most costly techniques in a biotechnology process (Przybycien *et al*., 2004). Due to the problems associated with the use of chromatography supports for the purification of nano-sized products, many alternative techniques have been created. These include: membrane filtration; aqueous two phase extraction; three phase partitioning; precipitation, and membrane chromatography (Lydiatt, 2002).

Aqueous Two phase systems (ATPS) are a liquid-liquid extraction method that has been used for the primary recovery and partial purification of a variety of biological products (Benavides *et al*., 2008). The main advantages of this technique include: ease of scaling up; process integration capability, and biocompatibility (Fernandes *et al.*, 2001).

ATPS two phase systems are formed when two different polymers, or a polymer and salt, are mixed over a certain concentration in water. The separation between certain biomolecules within the two phases is controlled by both the properties of the biomolecules and the phase system components (Albertsson, 1987). It is reported that the location of a biomolecule within a particular phase is influenced by factors such as: the molecular mass of the phase forming polymers; types of salts employed, and the pH of the system (Sebastiao *et al.*, 1997).

Researchers have identified numerous two phase system conditions for the purification of specific biomolecules (Diamond & HSU, 1990; Benavides *et al*., 2008; Helfrich *et al*.,

2005). Recently ATRPS has been employed in the recovery and partial purification of double layered Rotavirus-like Particles (DLRLP), this was achieved by using a PEG-Potassium Phosphate two phase system. The author of this work reports, yields of 85%, and a purification factor greater than 50 (Benavides *et al*., 2008). Helfrich and co workers (2005) have also shown that PEG-dextran ATPS can be used for the fractionation, assembly, and recovery of bionanoparticulates.

Three-phase partitioning (TPP)

Three-phase partitioning is an extension of the two phase systems described above, it enables the partition of biomolecules within three different phases (Hartmann *et al*., 1974). The third phase in the system is a precipitation phase between an organic solvent layer and an aqueous phase. The organic solvent employed is typically butanol and the third phase is usually made up of salts, for example ammonium sulfate (Przybycien *et al*., 2004). It can be used as a purification tool for a variety of large biomolecules (Przybycien *et al*., 2004).

TPP has also proved to be very useful technique when employed at the isolation stage of a process, due to the fact that cell debris will locate in the top organic layer and nucleic acids will partition in the middle salt phase (Przybycien *et al*., 2004). It has been shown that the optimisation of separation conditions in TPP can be achieved by introducing more selective ligands into the system. Gutpa *et al*. (2002) improved the selectivity of TPP by incorporating affinity components such as divalent metal ions.

Precipitation

Precipitation can used to separate nanaparticules from contaminants present in the process stream (Galaev *et al.,* 2004). It can be employed as a pre-chromatography column separation technique by introducing: solvent; salts, and polymer into the process stream. Recent scientific developments have shown that precipitation can be used as a selective purification technique (Freitag *et al*., 2001; Galaev *et al.* 2004; Morgan *et al.,* 2005).

Freitag and co workers (2001) developed a precipitation method for the purification of plasmid DNA. The authors report that this technique can obtain yields as high as 70% to 90%. This method was performed by linking DNA to a thermoresponsive polymer via an oligonucleotide. Below the critical temperature of the thermoresponsive polymer (40°C), the polymer-oligonucleotide forms a complex with the plasmid in solution. The temperature is then raised above the polymers critical temperature and the formed polymer-oligonucleotide-plasmid complex precipitates (Freitag *et al*., 2001).

Other precipitation conditions developed by Galaev *et al.* (2004), showed that plasmid DNA can be purified from a clarified alkaline lysate by the addition of a polycation (poly N,N-dimethyldiallyl-ammonium chloride PDMDAC), it is reported from this work that the polycation and the plasmid formed an insoluble complex and 80% of the plasmid was recovered in a highly concentrated form.

Morgan and co workers (2002) have reported on selective precipitation of viruses; this method allowed for the purification and concentration of viruses by employing both anionic polyelectrolyte and cationic polyelectrolyte, followed by centrifugation (Morgan *et al.,* 2005).

Membrane filtration

Membrane filtration or **high performance tangential flow filtration (HPTFF)** as it otherwise known can be incorporated into a process as an alternative to chromatography in the polish purification step (Van Reis & Zyndey., 2001). It separates on basis of electrostatic interactions between the biomolecules in solution and a charged membrane. The pH and ionic strength of the mobile phase can be altered, so that the biomolecules possess different charge properties, and can be separated on the basis of charge rather than size (Przybycien *et al*., 2004).

In a recent study the use of membrane filtration for the recovery and purification of virus particles proved to be effective in not only concentrating virus particles, but also purifying them by removing contaminants such as host cell proteins and DNA (Grzenia *et al*., 2008).

1.4.2 Modernisation of process chromatography

As previously discussed in Section 1.3, with the production of new recombinant products throughout the 1990's came the need for changes in the manufacturing process of biotherapeutics. There was now urgency for more systematic methods for process development which lead on to most industrial processes evolving around the following issues: process design; automation; process economics; validation; hygiene, and regulatory affairs.

The reduction of endotoxin levels from fermentations and other contaminants were the key factors in approaching process design, with process chromatography the only technique that could successfully remove all the impurities from a process stream (Diogo,

2005). The biotechnology industry then went on to focus on viral clearance, with the improvements of process chromatography directed towards eliminating animal derived products from the process stream, and thus improving the safety of biotherapeutics. The requirement for process chromatography was now that it delivered a recombinant protein, which satisfied the high standards set by regulatory bodies, falling under the categories of: homogeneity; purity; consistency, and potency (Jungbauer & Boschetti., 1994). Process Chromatography was performed under stringent and highly validated conditions, chromatography columns and supports were more robust and had a greater tolerance to alkaline cleaning reagents, which enabled regeneration over many cycles (Jungbauer & Boschetti, 1994). During this decade automated computerized control took over from manual technologies, which enhanced the control of large scale chromatography and reduced process error (Londo *et al.,* 1996). Today high speed chromatography processes are complimented with precise automated instrumentation.

During this 1990s **expanded bed adsorption** (EBA) was created as an alternative purification method to packed bed chromatography. It operates similar to a fluidized bed; firstly liquid buffer is pumped upward through the column at a suitable flow-rate until a stable fluidized bed is established. The expansion of the adsorbent bed creates a distance between the adsorbent beads, resulting in an increase of void volume fraction, allowing for unhindered passage of cells, cell-debris and other particulates during application of crude feed to the column. EBA adsorption behaviour is dominated by mass transfer diffusion mechanisms; therefore the breakthrough capacity of smaller particles is higher than that of larger particles, due to the shorter diffusion paths (Karau *et al.,* 1997). However, small particles used in complex process environments induce inter-particle cross linking which can result in collapse of the bed (Karau *et al.*, 1997). Subsequently,

one of the major hindrances for EBA advancement is that current commercially available adsorbents, exhibit low binding capacities for large biomolecules and are too closely related to packed bed matrices, therefore similar problems exist for both types of support.

Today the purification of antibodies has dominated the development of process chromatography (Shukla *et al*., 2007). Most processes to date have involved the use of Protein A affinity chromatography, as it is highly selective for MAbs, achieving over 95% purity in a single step (Shukla *et al*., 2007). The process chromatography steps for larger biomolecules (pDNA & viruses) follow a different sequence of steps, with anion exchange and size exclusion chromatography been dominate in most processes. However, as previously discussed, chromatography still fails to solve many of the problems associated with the purification of nanoparticulates, yet it is still the most utilised application in industrial bioprocesses (Lyddiatt, 2002).

1.5 References

Adrados B.P., Galaev Y., Nilsson K., Mattiasson B. (2001) Size exclusion behaviour of hydroxypropylcellulose beads with temperature-dependent porosity. *J. Chromatogr. A* **930:** 73-78.

Afeyan N.B., Gordon N.F., Mazsaroff I., Varady L., Fulton SP., Yang Y.B., Regnier F.E. (1990) Flow-through particles for the high-performance liquid chromatographic separation of biomolecules: perfusion chromatography. *J. Chromatogr*. *A* **519**: 1-29.

Albertsson P.A., Cajarville A., Brookes D.E., Tjerneld F. (1987) Partition of proteins in aqueous polymer two phase systems and the effect of molecular weight polymer. *Biochem. Biophys*. **926**: 87-96.

Axen R., Porath J., Ernback S. (1967) Chemical coupling of peptides and proteins to polysaccharides by means of cyanogens halides. *Nature* **214**: 1302-1304.

Benavides J., Aguiler O., Lapizcao-Encinas B.H., Rito-Palomares M. (2008) Extraction and purification of bioproducts and nanoparticles using Aqueous Two-phase systems strategies. *Chem. Eng. Technol.* **31**: 838-845.

Berg C. (2002) The evolution of Biotech. *Drug* Discovery **1**: 845-846.

Borath H.G., Mori S. (1999) Size exclusion chromatography. 1st edition Springer publishing: 6.

Bruch T., Graalfs H., Jacob L., Frech C. (2009) Influence of surface modification on protein retention in ion exchange chromatography evaluation using different retention models. *J. Chromatogr. A* **1216**: 919-925.

Cuatrecasas P., Wilchek M., Anfinsen C.B. (1968) Selective enzyme purification by affinity chromatography. *Proc. Nat. Acad. Sci*. **61**: 636–43.

Chahal P.S., Aucoin M.G., Kamen A. (2007) Primary recovery and chromatographic purification of adeno-associated virus type 2 produced by baculovirus/insect cell system. *J. Virol. Methods* **139**: 61-70.

Culter P. (2004) Protein Purification. 2ND Ed. Humana Press: 125.

Curling J. (2007) Process Chromatography: Five decades of innovation. www.BioPharm International.com.

Diamond A.D., HSU J.T. (1990) Protein partitioning in Peg/Dextran aqueous two phase systems. *AIChEM.* **36:** 1017-1023.

Diogo M.M., Queiroz J.A., Prazeres D.M.F. (2005) Chromatography of plasmid DNA. *J. Chromatogr. A* **1069**: 3-22.

Diogo M.M., Queiroz J.A., Prazeres D.M.F. (2003) Assessment of purity and quantification of plasmid DNA in process solutions using high performance hydrophobic interaction chromatography. *J. Chromatgr. A* **998**: 109-117.

Ettre L.S. (2000) Chromatography:The separation technique of the 20th century. *Chromatographia* **51**: 7-17.

Eon-Duval A., Burke G. (2004) Purification of pharmaceutical-grade plasmid DNA by anion-exchange chromatography in an RNase-free process. *J. Chromatogr. B* **804**: 327–335.

Fanget B. (1999) Method for purifying viruses by chromatography. International patent number 6008036.

Ferreira N.M.G., Monterio G.A., Prazeres M.F. (2000) Downstream processing of plasmid DNA for gene therapy and DNA vaccine applications. *Trends Biotechnol.* **18**: 380-388.

Fernandes S., Johansson G., Hatti-Kaul R. (2001) Purification of recombinant cutinase by extraction in an aqueous two phase system facilitated by a fatty acid substrate. *Curr. Opin. Biotechnol.* ***15***: 469-479.

Firestone D. (1994) Gel-permeation liquid-chromatographic method for determination of polymerized triglycerides in oils and fats - summary of collaborative study. *J. Assoc. Off. Anal. Chem. Int*. **77**: 957-960.

Frechet J.M., Frantisek S., Vladimi S. (1994) Multimodal Chromatographic separation media and process for using same. International patent number 5316680.

Freitag R., Costioli M.D., Fisch I., Garret-Flaudy F., Hilbrig F. (2003) DNA Purification by triple helix affinity precipitation. *Biotechnol. Bioeng.* **81**: 535-545.

Gagnon P., Grund E. (1996) Large-scale process development for hydrophobic interaction chromatography: Part 4 Controlling selectivity. *Biopharm.* **9**: 54- 59.

Galaev Y., Wahlund P.O., Gustavsson P.E., Larsson P.O. (2004) Precipitation by poly-cation as capture step in purification of plasmid DNA from a clarified lysate. *Biotechnol. Bioeng.* **87**: 675-684.

Ghosh R. (2002) Protein separation using membrane chromatography: opportunities and challenges. *J. Chromatogr. A* **952**: 13-27.

Grzenia D.L., Carlson J.O., Wickramasingh R.S. (2008) Tangential flow filtration for virus purification. *J. Membr. Sci.* **321**: 373-380.

Guo D., Mant C.T., Hodges R.S. (1986) Prediction of peptide retention times in reversed-phase high performance liquid chromatography. II. Correlation of observed and predicted peptide retention times and factors influencing the retention times of peptides. *J. Chromatogr. A* **359**: 519–532.

Gupta M.N., Roy I. (2002) Three phase affinity partitioning of protein. *Anal. Biochem.* **300**: 11-14.

Hartmann A., Johansson G., Albertsson P.A. (1974) Partition of proteins in a three phase system. *Eur. J. Biochem*. **79:** 450-456.

Helfrich M.R., Kouedi-Mahnaz E., Etherton M.R., Keating C.D. (2005) Partitioning and assembly of metal particles and their bioconjugates in aqueous two-phase systems. *J. Surf. Colloid Sci*. **21**: 8478-8484.

Hjertén S. (1961) Agarose as an anticonvection agent in zone electrophoresis. *Biochim. Biophys. Acta*. **53**: 514–517.

Hjertén S. (1964) The preparation of agarose spheres for the chromatography of molecules and particles. *Biochim. Biophys. Acta.* **79**: 393–398.

Hjertén S. (1973) Some general aspects of hydrophobic interaction chromatography. *J. Chromatogr. A* **87:** 325–331.

Hood L., Hg W.L., Schummer M., Cirisano F.D., Baldwin R.L., Karlan B.Y. (1996) High throughput plasmid mini preparations facilitated by micro-mixing. *Nucleic Acids Res.* **24**: 5045-5047.

Huber C.G. (1993) High resolution liquid chromatography of DNA fragments on a non-porous poly(styrene-divinylbenzene) particles. *Nucleic Acids Res.* **21**: 1061-1066.

Janson J.C., Hedman P. (1982) Large-scale chromatography of proteins. *Adv. Biochem. Eng*. **25**: 43–99.

Jonsson B., Stahlberg J. (1999) Electrostatic interaction between a charged sphere and an oppositely charge planar surface and its application in protein adsorption. *Colloids Surf. B: Biointerface* **14**: 67-76.

Jungbauer A., Boschetti E. (1994) Manufacture of recombinant proteins with safe and validated chromatographic sorbents. *J. Chromatogr. A* ***662***: 143-179.

Karau A., Benken C., Thommes J., Kula M.R. (1997) The influence of particle size distribution and operating conditions on the adsorption performance in a fluidized bed. *Biotechnol. Bioeng.* **55**: 54-64.

Kopachewicz W., Rounds M.A., Reginer F.E. (1986) Factors contributing to intrinsic loading capacity in silica based packing materials for preparative anion-exchange protein chromatography. *J. Chromatogr. A* **362:** 187-196.

Kubin M. (1975) A model of the mechanism of the separation of macromolecules in gel permeation chromatography on a packing with non homogeneous pores. *J. Chromatogr. A* **108:** 1-12.

Langer E., Ranck J. (2006) Capacity bottleneck squeezed by downstream processes. *BioProcess Int*. **4**: 14–18.

Lederer E. (1972) La renaissance de la method chromatographie de M Twett en 1931. *J. Chromatogr. A* **73**: 361-366.

Londo T., Lynch P., Kehoe T., Meys M., Gordon N. (1998) Accelerated recombinant protein purification process development: Automated, robotics-based integration of chromatographic purification and analysis. *J. Chromatogr. A* **798**: 73-82.

Low D., O' Leary R., Pujar N.S. (2007) Future of antibody purification. *J. Chromatogr. A* **848**: 48-63.

Lute S., Norling L., Hanson M., Emery R., Stinson D., Padua K., Blank G., Chen Q., Brorson K. (2008) Robustness of virus removal by protein A chromatography is independent of media lifetime. *J. Chromatogr. A* **1205**: 17-25.

Lyddiatt A., O'Sullivan D.A. (1998) Biochemical recovery and purification of gene therapy vectors. *Curr. Opin. Biotechnol.* **9**: 177-185.

Lyddiatt A. (2002) Process chromatography: current constraints and future options for the adsorptive recovery and bioproducts. *Curr. Opin. Biotechnol.* **13**: 95-103.

Mallik R., Michelle J.Y., Chen S.Y., Hage D.A. (2008) Studies of verapamil binding to human serum albumin by high performance affinity chromatography. *J. Chromatogr. A.* **876**: 69-75.

Malik D.J., Webb C., Holdich R.G., Ramsden J.J., Warwick G.L., Roche I., Williams D.J., Trochimczuk A.W., Dale J.., Hoenich N.A. (2009) Synthesis and characterisation of size exclusion nano-porous polymeric adsorbents for blood purification. *Sep. Purif. Technol.* **66**: 578-585.

McGreavy C., Junior A., Rajagopal K. (1990) Size exclusion chromatography in pore networks. *Chromatographia* **30:** 639-644.

McNay J.L.M., O'Connell J.P., Fernandez E.J. (2001) Protein unfolding during reversed phase chromatography 11. Role of salt type and ionic strength *Biotechnol. Bioeng.* **70:** 233-240.

McNeilly D. (2001) Method for purifying plasmid DNA and plasmid DNA substantially free of genomic DNA. International patent number 6441160.

Mohr P. (1985) Affinity Chromatography: Practical and Theoretical aspects. 1st Ed. CRC Press: 105.

Morgan J.R., LeDoux J.M., Yarmush M.L.(2005) Selective Precipitation of Viruses with Polymers. International patent number 6884613.

Peterson E.A., Sober H.A. (1954) Chromatography of proteins: Cellulose ion-exchange adsorbents. *J. Am. Chem. Soc*.**76**: 751–755.

Porath J., Flodin P. (1959) Gel filtration: A method for desalting and group separation. *Nature* **183**: 1657-1661.

Porath J., Sundberg L., Fornstedt N., Olsson I. (1973) Salting-out in amphiphilic gels as a new approach to hydrophobia adsorption *Nature* 245:465–466.

Porath J., Carlsson J., Olsson I., Belgrage G. (1975) Metal chelate affinity chromatography, a new approach to protein fractionation. *Nature* **258:** 598–599.

Porath J. (1986) Salt promoted adsorption: recent developments. *J. Chromatogr*. **376**: 331-341.

Prazeres D.M.F., Monteiro G.A., Ferreira G.N.M., Diogo M.M., Ribeiro S.C., Cabral J.M.S. (2001) Purification of plasmids for gene therapy and DNA vaccination. *Biotech. Annu. Rev*. **7:** 1-30.

Przybycien T.M., Pujar S.N., Steel L.M. (2004) Alternative bioseparation operations: life beyond packed-bed chromatography. *Curr. Opin. Biotechnol.* **15**: 469-478.

Purcell A.W., Aguilar M.I., Hearn M.T. (1989) High-performance liquid chromatography of amino acids, peptides, and proteins XCI. The influence of temperature on the chromatographic behavior of peptides related to human growth hormone. *J. Chromatogr. A* **476**: 125–133.

Schleup T., Cooney C.L. (1998) Purification of plasmids by triplex affinity interaction. *Nucleic Acids Res.* **26**: 4524-4528.

Sebastiao M.J., Martel P., Baptista A., Peterson B.S., Cabral M.S., Aires-Barros M.R. (1997). Predicting the partition coefficients of a recombinant cutinase in polyethylene glycol/phosphate aqueous two phase systems. *Biotechnol. Bioeng.* **56**: 248-258.

Shukla A.A., Hubbard B., Tressel T., Guhan S., Low D. (2007) Downstream processing of monoclonal antibodies—Application of platform approaches. *J. Chromatogr. B* **848**: 28-39.

Stadler J., Lemmens R., Nyhammar T. (2004) Plasmid DNA purification. *J. Gene Med*. **6**: 54-59.

Theodossiou I. (2004) Design of scale flexible separation technology for the recovery of DNA. Thesis from Technical University of Denmark :49.

Transfiguration J., Jorio H., Meghrous J., Jacob D., Kamen A. (2007) High yield purification of functional Baculovirus vectors by size exclusion chromatography. *J. Virol. Methods* **142**: 21-28.

Valliere-Douglass J., Wallace A., Balland A. (2008) Separation of populated of antibody variants by fine tuning hydrophobic interaction chromatography operating conditions. *J. Chromatogr*. *A* **1214**: 81-89.

Van Reis R., Zydney A. (2001)Membrane separations in biotechnology. *Curr. Opin. Biotechnol.* **12** : 208-211.

Varley D.L., Hitchcock A.G., Weiss A.M.E., Horler W.A., Cowell R., Peddie L., Sharpe G.S., Thatcher D.R., Hanak J.A J. (1999) Production of plasmid DNA for human gene therapy and expanded bed anion exchange chromatography. *Bioseparation* **8**: 209-217.

Vijayalakshm M.A. (2002) Biochromatography theory and practice. 1ST Edition CRC press. 47.

Voβ C., Schmidt T., Schleef M., Friehs K., Flaschel E. (2003) Production of supercoiled multimeris plasmid DNA for biopharmaceutical application. *J. Biotechnol*. **105**: 205-213.

Walsh G. (2003) Pharmaceutical biotechnology products approved within European Union. *Eur. J. Pharm. Biopharm***. 55**: 3-10.

Woodgate D., Palfrey D.A., Nagel AV., Hine N.K.H. (2002) Protein mediated isolation of plasmid NDA by zinc finger glutathione S-transferase affinity ligand.
*Biotechnol. Bioeng***. 79**: 450-456.

Wurm F.M. (2004) Production of recombinant protein therapeutics in cultivated mammalian cells. *Nature Biotechnol*. **22**: 1393–1398.

Xiao P.Y., Rathore A., O'Connell J.P., Fernandez E.J. (2007) Generalising a two conformation model for describing salt and temperature effects on protein retention and stability in hydrophobic interaction chromatography. *J. Chromatogr. A.* **1157:** 197-206.

Zaidenzaig Y., Er-El Z., Shaltiel S. (1972) Hydrocarbon-coated sepharoses—use in the purification of glycogen phosphorylase. *Biochem. Biophys. Res. Comm.* **49**: 383–390.

2. INTRODUCTION

2.1 Gene Therapy vectors

The number of gene therapy clinical trials approved worldwide has continued to rise since 1989 to the present day (www.wiley.co.uk/genetherapy) and subsequently there is an ever growing demand for purified gene therapy vectors. It is reported that as of 2009, 18 % of all gene therapy clinical trials worldwide utilized non viral pDNA as the vector of choice and 66% of clinical trials employed viral vectors (www.wiley.co.uk/genetherapy/clinical). An overview of the different gene therapy techniques employed in clinical trials is shown on Figure 2.0.

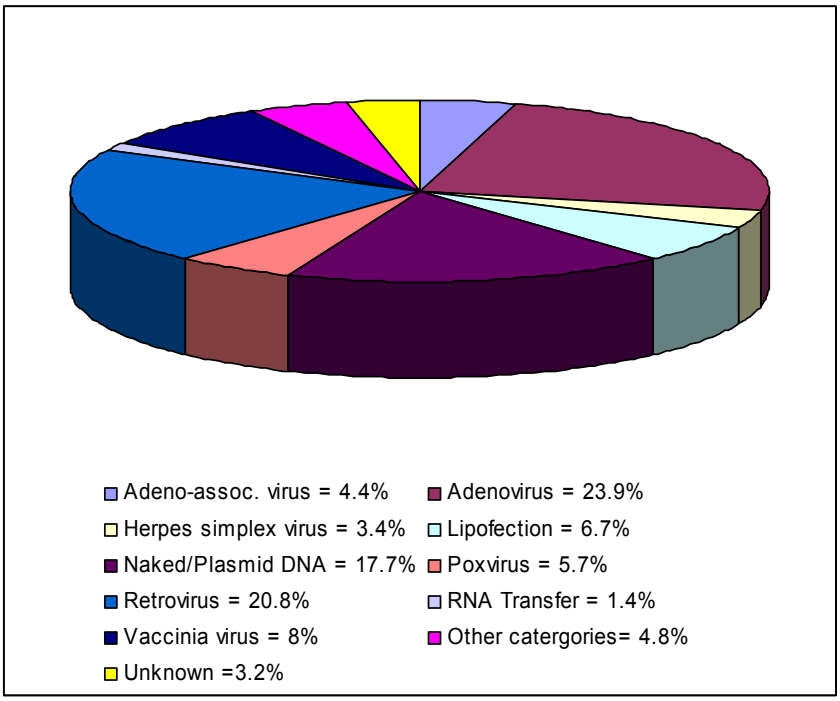

Figure 2.0: Gene therapy vectors employed in clinical trials during 2009 (data from http://www.wiley.co.uk/genetherapy/clinical/)

These vectors are significantly larger than proteins, with viral vectors ranging in size from 30-120 nm and naked plasmid DNA components before formulation in the size range of 200 nm to >1000 nm (Figure 2.1) (Lyddiatt & Sullivan, 1998). Lyddiatt and Sullivan (1998) referred to these large biomolecules as 'nanoparticulates'.

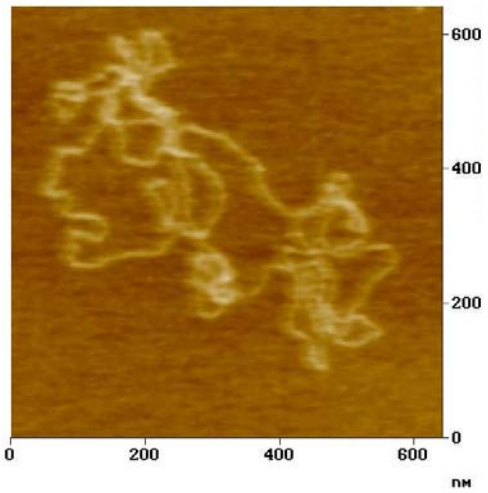

Figure 2.1: Atomic Force Microscopy (AFM) image of plasmid DNA (pAS2: pDNA with green fluorescent protein, 8.5kb=2.8µm) purified by Qiagen® Kit (http://www.nanostructure.de/en.html). Permission to use image granted by Professor W Nellen, Institute of Biology, University of Kassel, Germany.

2.2 The purification of nanoparticulates via packed bed chromatography

Large biotherapeutics such as nanoparticulates presents a range of complications downstream, their large size and shape makes them susceptible to damage, they also produce high viscosity solutions, and impurities with similar properties (Prazeres *et al*., 1999). Another hurdle, in the purification of plasmid DNA, is that it can adopt different structural formations (Figure 2.2), and it is reported that over 90% of the plasmid should be super-coiled for successful gene therapy applications (Prazeres *et al*., 2001).

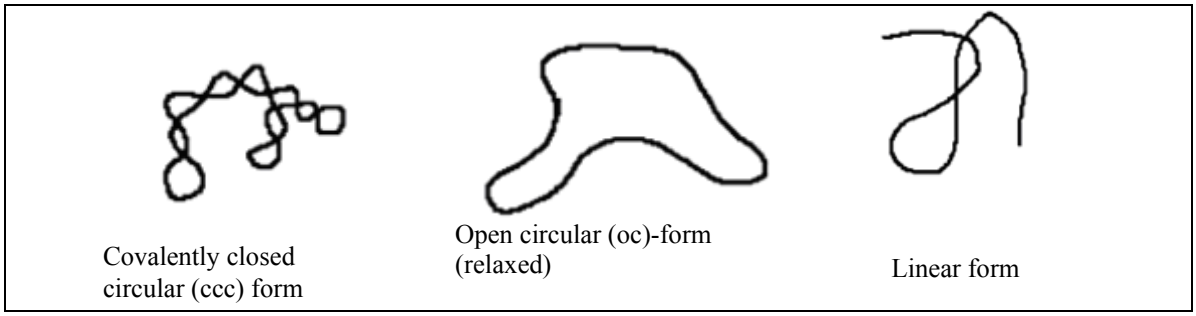

Figure 2.2: Different plasmid conformations (Voβ *et al*., 2003)

Purified pDNA for therapeutic applications also has to be free from host genomic DNA (gDNA (<0.05μg/μg pDNA), host proteins (undetectable) and endotoxins (> 0.1 EU/μg pDNA) (Diogo, 2005). Although alternative purification techniques have proved effective in the purification of nano-sized biomolecules (discussed in Chapter 1, Section 1.4.1) packed bed chromatography is still one of the most effective methods for removing all cellular host components (RNA, proteins, gDNA fragments, & endotoxins) and non supercoiled plasmid DNA formations (Diogo *et al.,* 2005). Many researchers have reported, that by combining different chromatography techniques successful purification of nanoparticulates can be achieved (Varley *et al*., 1999; Fanget *et al.,* 1999). Varley *et al.* (1999) concluded that for the purification of plasmid DNA at least two different chromatography techniques are required to remove all the contaminants and impurities, whereas Fanget and co workers *(*1999) developed a method for purifying viruses by chromatography with three different chromatographic steps (anion exchange, cation exchange, & affinity chromatography). Even with multiple steps the purification of nano-sized bioproducts by chromatography suffers from many problems, most arising from the design of current commercially available media. Many commercially available supports have an average bead size of 50-300 μm and pore diameters of 30-400 nm (Lyddiatt & Sullivan, 1998), the pore size of these supports prohibits the mass transfer of large

biomolecules (Ljunglöf *et al.,* 1999). This is illustrated in Figure 2.3 which shows plasmid DNA concentrated at the surface of anion exchange supports. The plasmid is clearly unable to enter the pores due to its size. Huber *et al.* (1993) showed that the limitations in the mass transfer of large biomolecules generate broad peaks and low recovery.

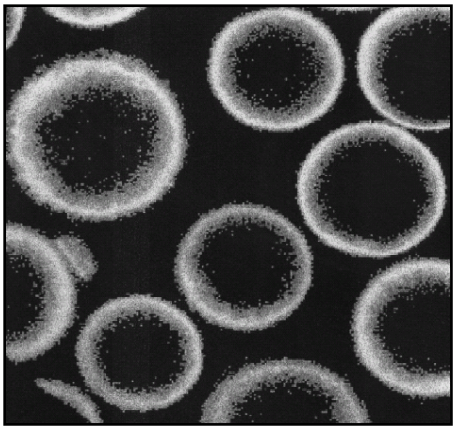

Figure 2.3: Confocal image of Triple Helix Affinity Chromatography (THAC)-media (Ljunglöf *et al.,* 1999) after the saturation with plasmid DNA and visualisation with fluorescent dye YOYO (copyright permission granted)

Another problem that is common to all chromatography techniques is that high molecular weight products generate highly viscous solutions, which can cause significant pressure drops in packed bed columns. It has been suggested that one solution to this problem is to reduce the impurity load prior to chromatography steps (Guilherme *et al*., 1999), however dilution can add to operating costs, due to the fact that an additional process step is required in order to concentrate the product.

The disadvantages of each packed bed chromatography function when employed in the purification of nano-particulates is detailed below, and the principles of chromatography are discussed in detail in chapter 1.

Anion exchange suffers from many problems when purifying large biomolecules, often low binding capacities and co elution of contaminants with the target product are the results (Ljunglöf *et al.,* 1999).

Size Exclusion Chromatography has the ability to purify large nanoparticulates such as plasmid DNA and viruses from lower molecular entities in the same process step. This technique has proved effective in separating super-coiled plasmid DNA (Marquet *et al.,* 1996) and viruses (Transfiguracion *et al*., 2007). Unfortunately this method in the purification of the nano-sized biomolecules suffers from low selectivity, and loss of resolution, which can only be improved by increasing the column length or decreasing the sample load. However this results in longer process times and the product is obtained in a non concentrated solution (Voß, 2008)

Hydrophobic interaction chromatography is a high resolution separation method. Although HIC is a powerful tool in the purification of large nanoparticulates it suffers from many limitations (Diogo *et al*., 2001). Firstly HIC supports generally have very low binding capacities for large biomolecules. Secondly high salt concentrations are required in order to achieve sufficient binding of the target product, these high salt concentrations are associated with high costs and have an environmental impact (Diogo *et al*., 2003).

Table 2.0: Summary of chromatography techniques used for the purification of nano-sized biomolecules. (Adapted from Queiroz *et al*., 2008).

Chromatography Type	Advantages	Disadvantages
SEC	Allows for isolation of target products from smaller molecules. Effective as a final polishing step.	Low resolution achieved. High dilution required. Long process times.
AEC	Can be used for preparative and analytical scales. Separates sc and oc pDNA conformations. Does not require organic solvents.	Co elution of target products with contaminants resulting in low resolution. Low binding capacities are observed.
HIC	Can be used for preparative, analytical and industrial scales. Results in efficient separation of pDNA from endotoxins.	Elution at high salt concentrations. Low binding capacities observed.

Affinity Chromatography is a highly effective one step purification method for the purification of nanoparticulates (plasmids & viruses) from clarified lysates. Subsequently large volumes of lysate can be processed at one time, resulting in collected fractions containing a high concentration of the target product. There are a variety of different types of AC, such as: Immoblised metal-ion affinity chromatography (IMAC); Triple helix affinity chromatography, and Polymyxin B. The main drawbacks to AC as a technique for purifying larger biomolecules are that it results in co elution of all DNA

conformations (IMAC); pDNA in the flowthrough (IMAC); non specific interactions of ligands with target product (Polymyxin B), and poor yields (Polymyxin B) (Queiroz *et al*., 2008).

Triple helix affinity chromatography (**THAC)** is an extension of AC, specifically developed for plasmid DNA purifications. THAC supports consist of pyrimidine oligonucleotide groups covalently linked to a solid support. Plasmid DNA binding occurs through a double stranded target sequence which interacts with the support (Wills *et al*., 1997). One advantage to THAC over AC is that the beads are stable under cleaning in situ with no leakage of the oligonucleotides attached (Schluep & Cooney, 1998), however the authors also report low yields and long chromatographic runs.

Monolith materials have been introduced as an alternative to standard packed bed chromatography supports in an attempt to overcome the limitations of current chromatography beads (Jungbauer *et al*., 2004). This technique has proved successful for separations involving large biomolecules such as viruses (Kramberger *et al*., 2007) and plasmid DNA (Williams *et al.,* 2005). A typical monolith is a continuous bed consisting of a single piece of a highly porous solid material with large channels (pores) of about 700-1000 nm, which allow for the mass transfer and binding of large molecules (Kramberger *et al*., 2007). The surface chemistry of the pores is modified by covalent attachment of ligands such as: ion exchange; hydrophobic interaction, and affinity that interact with the target molecule. The mobile phase is passed though the pores of the stationary phase and separation is on the basis of convective flow and not diffusion controlled mass transfer (Jungbauer *et al*., 2004).

One study that compared the dynamic binding capacity of plasmid DNA on both a monolith (CIM DEAE) and packed bed (Q Ceramic Hyper 20) anion exchange supports showed that a binding capacity of 8.9 mg/mL from the CIM DEAE beads was achieved where as a lower binding capacity of 6.1 mg/mL was observed with the Q Ceramic Hyper (Urthaler *et al.,* 2005). This result shows that one big advantage of monoliths is that higher binding capacities can be achieved for larger biomolecules compared to packed bed supports. It is reported that the main disadvantages to monoliths, are the high cost of the matrices, and in some cases high-pressure drops are still observed (Ghosh, 2002).

Membrane Chromatography has been studied for over a decade as an alternative to conventional packed chromatography. It can exist in a selection of configurations such as: stacked membranes; hollow fibre membranes, and spiral wound membranes. It operates with a variety of chromatographic principles for example: ion exchange; hydrophobic; reversed-phase, and affinity. Adsorptive membranes are similar to monoliths with the interactions between the dissolved molecules and the active sites on the membrane occurring in the convective through-pores rather than in stagnant fluid inside the pores of the adsorbent (Teeters *et al*., 2003). These short wide beds are able to perform at high velocities and operate at high volumetric capacities (Roper & Lightfoot., 1995). It is these properties that produce increased throughputs, short residence times, which therefore reduce the degradation and denaturation of the target products (Roper & Lightfoot., 1995). Membrane chromatography is an attractive alternative for the purification of large particles (Teeters *et al*., 2003). The main advantage to this technique is that it can operate at high flow rates yet enabling the mass transport of larger biomolecules hence high binding capacities are obtained (Endres *et al.,* 2003). Teeters and co workers (2003) demonstrated that plasmid DNA (size 6.1kb) could easily access the ion exchange sites

present in the large convective pores of an adsorptive membrane. The reported disadvantages of this technique are same as that reported for monoliths (Ghosh, 2002).

2.3 Bi-layered packed bed chromatography supports

As previously discussed (Section 2.2) to date all attempts to innovate chromatography supports for the purification of nano-sized biomolecules have been with limited success as purification problems still remain unresolved. Alternative methods have also been created in attempt to solve the problems associated with purifying nano-sized biomolecules with packed bed chromatography however none have been completely successful (Chapter 1, Section 1.4.1:Alternatives to chromatography). Although packed bed chromatography suffers from many drawbacks when used to purify large biomolecules, many authors report it to be an essential step in achieving the purity requirements for gene therapy products (Dunnill *et al*., 2000; Diogo, 2005). The problems experienced with packed bed chromatography supports could be solved with the re-design of chromatography beads for specific task of successfully purifying larger biomolecules. On type of design could be to introduce two different functionalities onto one support i.e. a bi-layered packed bed chromatography bead. The concept behind this bi-layered bead is that it would possess two different chromatographic properties (bi-functional). One example of a bi-layered support is a bead with an anion exchange property in the inner core and a size exclusion property present on the outer surface of bead. This bi-functional bead would allow smaller biomolecules and contaminants (i.e. proteins & RNA) to diffuse into the charged core, whereas larger biomolecules would be prohibited by their size from entering the pores of the support (Figure 2.4)

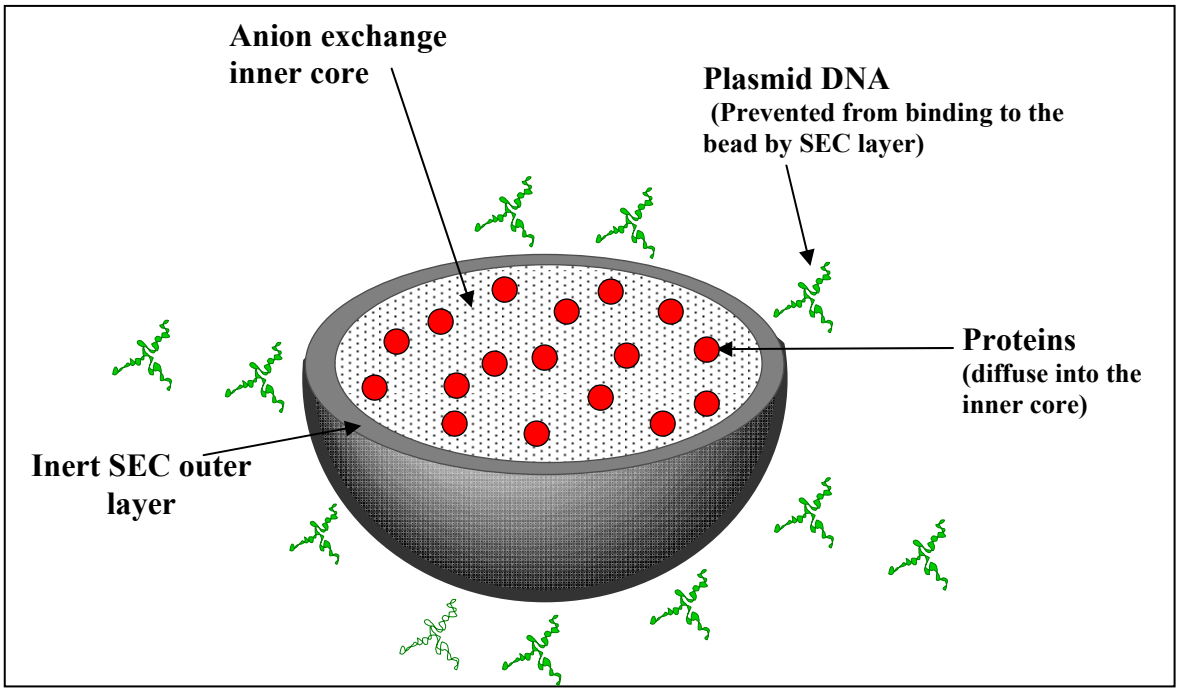

Figure 2.4: Schematic representation of a bi-layered support, consisting of an inert outer layer, which is impermeable to large molecules, such as DNA, and a charged inner core (adapted from Gustavsson *et al*., 2004).

It is reported in literature that the creation of a bi-functional support has already been achieved with various different synthetic chemistry methods (Pinkerton 1991; Dainiak *et al*., 2002; Viloria-Cols *et al*., 2004; Jahanshahi *et al*., 2008; Bergström *et al*., 2002, Gustavsson *et al*., 2004; Kepka *et al*., 2004; Berg *et al.,* 2005)

Pinkerton (1991) reviews in detail 'dual zone chromatography beads' that were created to solve many of the problems associated with high-performance liquid chromatography. The source of the problem is that many biological components possess similar chemical properties making the isolation of smaller molecules from larger macromolecules by HPLC increasingly difficult. The improved bi-layered HPLC supports enable the elution of sample macromolecules with high recovery in one peak, whilst allowing for the

permeation and partitioning of small biomolecules. To date all chemistry synthesises tested to create bi-layered HPLC supports have been done on silica beads and numerous chemistry approaches have been employed. The concept of a bi-functional HPLC support was initially introduced by Hagestam and Pinkerton (1985), in this work a hydrophilic functionality is introduced on to silica beads which have a pore size of 80Å. This hydrophilic layer typically contains diol groups in which various partitioning phases can be introduced i.e. hydrophobic and ion-exchange functions into the inner core of the beads. The supports were then treated with enzymes in order to remove any binding properties from the outer surface of the beads. The enzymes due to their large size could not penetrate the porous supports and diffuse into the inner core. The resulting beads exhibited hydrophobic or ion-exchange properties present in the internal surface and hydrophilic diol groups on the external surface. These beads have proved to be particularly effective in the purification of serum proteins by HPLC, achieving 99% serum protein yields. The serum protein is not adsorbed on the support and is collected whilst smaller biomolecules can diffuse into the pores.

The developments of Hagestam and Pinkerton (1985) were followed by further advancements by Gisch and co-workers (1988) in which another type of bi-layered HPLC bead was created. These supports prevented the adsorption of proteins onto the external surface by an approach referred to as shielded hydrophobic phase (SHP) (Gisch *et al.,* 1988). This bead was produced by firstly activating the silica base matrix with polyethylene oxide and then attaching a hydrophilic polymer (Polyethylene Glycol) throughout the bead. This hydrophilic polymer network also contained hydrophobic phenyl groups. The concept in the design of this HPLC bead was that the hydrophilic PEG system would protect the hydrophobic phenyl groups and therefore prevent certain

proteins from interacting with the hydrophobic phase. Pinkerton (1991) concludes that the high hydrophobic retentive properties of the SHP beads would be most suitable for HPLC applications involving very hydrophilic compounds, which may limit its use. The author also concludes that the effectiveness of SHP supports in separating a variety of biomolecules has yet to be shown. Unfortunately all the approaches discussed above to develop bi-layered supports have only proved useful in small scale HPLC applications, probably because only a limited number of biomolecules that can be separated by these methods.

The early chemistry approaches (Hagestam & Pinkerton, 1985; Gisch *et al*., 1988) that attempted to create a bi-layered chromatography support were typically performed by attaching a hydrophilic polymer on to the surface of the bead and then introducing a second chromatographic functionality throughout the bead. Dainiak and co workers (2002) further advanced the concept of a bi-layered support by developing EBA cell repelling ion exchangers (EBA discussed in detail in Chapter 1: Section 1.4.2). These beads were used for the direct capture of the target product from a fermentation broth. In this study (Dainiak *et al*., 2002) the commercially available EBA supports, Streamline DEAE (GE Healthcare, Uppsala, Sweden) were modified to possess a hydrophilic polymer layer, poly(acrylic acid) (PAA). Highly polymerized PAA was electrostatically attached to the surface of the matrix. This polymer layer acted as a protective barrier preventing the binding of cells and cell debris to the adsorbent whilst allowing proteins to diffuse into the pores of the support. The modified PAA-Streamline supports maintained a high protein binding capacity, whilst effectively reducing the binding of yeast cells to the surface of the adsorbent (not more than 15% bound). Dainiak *et al*. (2002) then applied the same procedure described above to modify Amberlite IRA-401 CL (BDH,

Toronto, Canada) supports to again possess a cross-linked hydrophilic polymer outer layer, poly(acrylic acid) (PAA). The modified beads proved to be effective in the direct capture of shikimic acid and the authors conclude that this technique could be employed for the direct capture of products from cell containing fermentations using fluidized bed adsorption. The methods developed by Dainiak *et al*. (2002) were later applied by Viloria-Cols *et al*. (2004) in which the anion-exchange resin Amberlite IRA-400 (BDH, Toronto, Canada) was coated with agarose followed by cross-linking of the agarose polymer layer. The recovery values for the modified supports showed that 100% of the cells injected were recovered in the flow through, while all the lactic acid was recovered during the elution step (Viloria-Cols *et al*., 2004).

Jahanshahi *et al*. (2008) also coated the EBA anion exchange support Streamline DEAE (GE Healthcare, Uppsala, Sweden) and the EBA cation exchange support CM-Hyper Z (PALL Corporation, New York, USA) with an agarose polymer layer. The researchers tested the beads with complex feedstocks and concluded from this work when comparing both coated and uncoated supports, that the coated (CM-Hyper Z & Streamline DEAE) proved to be more effective in yielding a product in a purer more concentrated form (Jahanshahi *et al*., 2008). These new EBA supports (Dainiak *et al*., 2002; Dainiak *et al*., 2002; Viloria-Cols *et al*., 2004; Jahanshahi *et al*., 2008) could prove useful when incorporated as an intermediate recovery step of a purification process for a gene therapy product (Prazeres & Ferreira, 2004). By employing EBA as a process step it would possible to by-pass clarification and concentration operations therefore increasing process yields (Prazeres & Ferreira, 2004). However a therapeutic product such as a gene therapy vector would still require a final purification stage to obtain a high level of purity. The

purification stage of a process typically involves a combination of packed bed chromatography techniques.

Bergström and co workers (2002) went on to create a synthetic chemistry route that allowed for the fabrication of packed bed chromatography beads that possessed two completely distinct functional layers. In this study Sepharose 6 Fast Flow (FF) (GE Healthcare, Uppsala, Sweden) was firstly activated with allyl glycidyl ether and then limited amounts of bromine were reacted with the allyl groups present on the surface of the bead. The reaction of bromine with allyl groups is extremely fast and this enables the bromine to react at the surface faster than it can diffuse into the pores of the beads. After this reaction is complete the beads have an alkyl bromide layer on the surface whilst a high percentage of allyl groups remain in the inner core. Next the beads were treated with sodium hydroxide that eliminated the bromide groups and resulted in hydroxyl groups present on the outer surface of the beads. This generated a hydrophilic outer layer. The allyl groups in the inner core were then reacted with bromine and finally an anion exchange ligand was attached to the inner core of the beads. The resulting fabricated bi-layered chromatography beads were comprised of a size exclusion outer layer and an anion exchange inner core. The authors report that this bi-layered support proved to be successful in separating smaller proteins (12.4KD) from larger proteins (660 KD) (Bergström *et al*., 2002).

The chemistry methods developed by Bergström and co workers (2002) were later applied by Gustavsson *et al*. (2004) to produce what the authors referred to as the 'lid' bead. In this study the exact same synthetic chemistry route developed by Bergström *et al*. (2002) was employed on the commercially available SEC support Sephacryl S-500

HR (GE Healthcare, Uppsala, Sweden). This bi-layered support had a positively charged core with an inert outer layer (Figure 2.4) and was created specifically for plasmid DNA purifications. The design allowed RNA and proteins to diffuse into the charged inner core, whilst plasmid DNA, due to it large size, could not enter the pores of the support. Thus the inert outer layer prevented plasmid DNA binding from the outer surface of the bead. The author highlighted the need for a thin a SEC outer layer so as not to compromise the binding capacity of the bi-layered support. Gustavsson and co workers (2004) reported that an SEC layer comprising of 10% of the beads diameter reduced approximately 50% of the RNA binding capacity of the bead. The researchers observed that large amounts of bromine resulted in a significant reduction in plasmid DNA binding but at the detriment of the protein binding capacity. They identified that the optimum conditions for the creation of a bi-layered support was an outer layer that was approximately 5% of the beads diameter, typically 2-3 μm thick which reduced about 30% of the binding capacity. After the researchers established optimum reaction conditions for the creation of the 'lid' bead they then integrated the bead in a two column procedure for the purification of plasmid DNA. The first column was packed with the 'lid' bead to remove RNA and proteins from the process stream. The second column was packed with a regular anion exchange (Q Sephacryl S-500 HR) support to bind the plasmid DNA. This study showed that the 'lid 'bead was partially effective in the two column process, recovering between 69-89% of pDNA due to it been adsorbed to the bi-layered support in the first column (Gustavsson *et al*., 2004). Although this chemistry approach did create a bi-layered support, the results show that even a relatively thick outer layer that reduced approximately 30% of the inner core binding capacity, point

charges still remained in the outer layer that prevented a complete recovery of plasmid DNA (69-89%).

Kepka *et al*. (2004) also employed the 'lid' bead in a three step purification process for plasmid DNA. This purification process involved an ultra/diafiltration step, followed by a polymer/polymer aqueous two phase system, and then finally a chromatography column packed with the bi-layered support. The 'lid' beads were prepared exactly as that described above for the work completed by Gustavsson *et al*. (2004), except that the Q ligand was replaced by a different anion exchange ligand (Ethylene Diamine). This increased the charge density of the support as this ligand (Ethylene Diamine) has two positive charges per ligand molecule compared to Q which only has one (Kepka *et al*., 2004). This study revealed that the problems previously experienced by Gustavsson *et al*. (2004) still prevailed. The chromatogram showed that the plasmid DNA peak was completely free from RNA, however the plasmid DNA fraction still contained some contaminating proteins, and the overall plasmid DNA yield from the complete process was 69%. These results indicated that this chemistry approach was not completely successful in creating two distinct layers and that point charges remained in the size exclusion outer layer.

Berg and co workers (2005) fabricated Streamline base matrix (GE Healthcare, Uppsala, Sweden) to possess two functional layers in order to create a bi-layered chromatography support. This synthesis was very similar to that previously developed by Bergström *et al*. (2002). The first step of synthesis involved the activation of the base matrix with allyl glycidyl ether. This chemical reagent introduced double bonds throughout the support. The next step involved a fast chemical reaction with potassium permanganate to oxidise 12% of the double bonds to diol groups. The idea behind this reaction was that the

reagent reacts faster than it diffuses into the pores of the support therefore forming a size exclusion outer layer on surface of the bead. The double bonds remaining in the inner core of the bead are then reacted with bromine and finally the charged anion exchange ligand (Diethylamine) was coupled into the inner core. Cell adsorption experiments were then performed to test the effectiveness of these new bi-layered supports. The results showed that the amount of cells binding to the support was reduced by 87% when compared to the unmodified supports where no outer layer had been created. This chemistry also proved to be only partially successful in producing a bi-layered support as it is apparent from the cell binding results that point charges were still present in the inert layer, which resulted in binding to the outer surface of the bead. Protein binding studies were not conducted in this study, however Gustavsson *et al*. (2004) reported that a 12% reduction in the total bead volume reduces approximately 30% of the binding capacity.

It is apparent that none of the chemistry approaches discussed above were completely successful in creating a bi-layered chromatography support, possessing a thin inert outer layer and charged inner core. All the methods proved to be effective to a certain extent as after the layer was created a reduction in outer surface binding was observed. However, outer surface binding was still a problem as point charges appeared to remain in the size exclusion outer layer compromising the inertness of the layer. Also in order to obtain a significant reduction in surface binding a substantial amount of the inner core binding capacity was also reduced.

2.4 Aim of the thesis

The aim of the thesis was to address the limitations of existing packed bed chromatography supports for the purification of the nanoparticulates. After review of the existing technology (Chapter 1) a bi-layered packed bed chromatography support was considered a promising solution to the problems experienced when purifying large biomolecules (Chapter 2). The development of this support became the primary goal of the study. The focus of the scientific work was on developing chemistry methods that resulted in a SEC-IEC packed bed support, where both chromatographic functionalities were present in two distinct layers. This bi-layered SEC-IEC bead design would allow for:

1. Successful and gentle separation of nanoparticulates from smaller chemically similar contaminants – in a 'one-bead one column' process;

2. A possible solution to overcome the main obstacle with EBA operations – by eliminating the occurrence of non specific interactions of cells and cell debris with the adsorbents.

2.5 Outline of thesis

In chapter 1 and 2 the state of existing separation techniques for the purification of large biomolecules have been reviewed and the case for pursuit of a bi-layered chromatography support has been discussed. Chapter 3 describes the chemistry approaches pursued in order to achieve the aim of the project. This study began by examining previously developed chemistry routes. It was viewed as important to investigate previous chemistry approaches in order to gain an understanding into the chemistry methods and to observe

why exactly these methods were unsuccessful. The data obtained from these experiments highlighted how these methods alone were incapable of significantly reducing plasmid binding from the surface of the bead, and that in all cases only a partially inert layer was created which still maintained point charges. Next a new synthetic chemistry route was developed to modify chromatography beads to produce a bi-layered support, yet again the results showed that this chemistry was only partially effective. Microwave technology and different solvent chemistry were then employed to enhance the chemistry already tested, and a positive outcome was observed, in which a further elimination of pDNA binding was achieved without a substantial reduction in the protein binding capacity.

Microwave heating did improve the chemical synthesis of the bi-layered supports however it was viewed as important to analyse the support after microwave heating for any visual or mechanical alterations. In Chapter 4, the data comparing the compatibility of microwave radiation with a variety of chromatography media is presented. In this study both microwaved and unmicrowaved supports were examined using visual, mechanical and size analysis. The visual study was carried out with Light Microscopy and Scanning Electron Microscopy. A Mastersizer was employed for the size analysis and the mechanical properties of the beads were tested using Micromanipulation. The results revealed that only certain types of chromatography supports could undergo microwave heating without experiencing any visual, size and mechanical changes. It showed that some specific bead properties were more susceptible to damage from microwaves than others.

Finally some conclusions are made about the results observed from the study and suggestions are made for future development.

2.6 References

Berg H., Busson P., Carlsson M. (2005) Chromatographic two-layer particles. Patent number 2005/024037.

Bergström J., Berglund R., Soderberg L. (2002) Process for introducing functionality. Patent number 6426315.

Dainiak M., Galaev I.Y., Mattiasson B. (2002) Direct capture of product from fermentation broth using a cell-repelling ion exchanger. *J. Chromatogr. A* **942:** 123-131.

Dainiak M., Galaev I.Y., Mattiasson B. (2002) Polyelectrolyte-Coated Ion Exchangers for Cell-Resistant Expanded Bed Adsorption. *Biotechnol. Prog.* **18:** 815-820.

Diogo M.M., Queiroz J.A., Prazeres D.M.F. (2001) Studies on the retention of plasmid DNA and *Escherichia coli* nucleic acids by hydrophobic interaction chromatography. *Bioseparation* **10**: 211-220.

Diogo M.M., Queiroz J.A., Prazeres D.M.F. (2003) Assessment of purity and quantification of plasmid DNA in process solutions using high-performance hydrophobic interaction chromatography. *J. Chromatogr. A* **998**: 109-117.

Diogo M.M., Queiroz J.A., Prazeres D.M.F. (2005) Chromatography of plasmid DNA. *J. Chromatogr. A* **1069**: 3-22.

Dunnill P., Levy S.M., O' Kennedy R.D., Ayazi-Shamlou P. (2000) Biochemical engineering approaches to the challenges of producing pure plasmid DNA. *Trends Biotecnol.* **18**: 296-305.

Endres H.N., Johnson J.A.C., Ross C.A., Welp J.K., Etzel M.R. (2003) Evaluation of an ion-exchange membrane for the purification of plasmid DNA. *Biotechnol. Appl. Biochem*. **37**: 259-266.

Fanget B. (1999) Method for purifying viruses by chromatography. Patent number 6008036.

Gagnon P., Grund E., Lundbäck T. (1995) Large scale process development for hydrophobic interaction chromatography. Part 2: controlling process variation. *BioPharma* **8**: 21-27.

Ghosh R. (2002) Protein separation using membrane chromatography: opportunities and challenges. *J. Chromatogr. A* **952:** 13-27.

Gisch D.J., Hunter B.T., Feibush B. (1988) Shielded hydrophobic phase: a new contact for direct injection analysis of biological fluids by high performance liquid chromatography. *J. Chromatogr. A* **433:** 264-268.

Guilherme N.M., Ferreira M.M., Cabral J.M.S., Prazeres D.M.F. (1999) Development of process flow sheets for the purification of supercoiled plasmids for Gene Therapy applications. *Biotechnol. Progr*. **15**: 725-731.

Gustavsson P.E., Lemmens R., Nyhammar T., Busson P., Larson P.O. (2005) Purification of plasmid DNA with a new type of anion-exchange beads having a non-charged surface. *J. Chromatogr. A* **1038**: 131-140.

Hagestam H., Pinkerton T. (1985) Internal surface reversed phase silica supports for liquid chromatography. *Anal. Chem*. **57**: 1757-1763.

Huber C.G. (1993) High resolution liquid chromatography of DNA fragments on a non-porous poly(styrene-divinylbenzene) particles. *Nucleic Acids Res.* **21**: 1061-1066.

Jahanshahi M., Partida-Martinez L., Hajizadeh S. (2008) Preparation and evaluation of polymer-coated adsorbents for the expanded bed recovery of protein products from particulate feedstocks. *J. Chromatogr. A* **1203**: 13-20.

Jungbauer A., Vlakh E., Ostryanina N., Tennikova A.T. (2004) Use of monolithic sorbents modified by directly synthesized peptides for affinity separation of recombinant tissue plasminogen activator (t-PA). *J. Biotechnol*. **107**: 275-284.

Kepka C., Lemmens R., Vasai J., Nyhammer T., Gustavsson P.E. (2004) Integrated process for purification of plasmid DNA using aqueous two-phase system combined with membrane filtration and lid bead chromatography. *J. Chromatogr. A* **1057:** 115-123.

Kopachewicz W., Rounds M.A., Reginer F.E. (1986) Factors contributing to intrinsic loading capacity in silica based packing materials for preparative anion-exchange protein chromatography. *J. Chromatogr. A* **362:** 187-196.

Kramberger P., Peterka M., Boben J., Ravnikar M., Štrancar A. (2007) Short monolithic columns—A breakthrough in purification and fast quantification of tomato mosaic virus. *J. Chromatogr. A* **1144**: 143-149.

Kubin M. (1975) A model of the mechanism of the separation of macromolecules in gel permeation chromatography on a packing with non homogeneous pores. *J. Chromatogr. A* **108:** 1-12.

Ljunglöf A., Bergvall P., Bhikhabhai R., Hjorth R. (1999) Direct visualisation of plasmid DNA in individual chromatography adsorbent particles by confocal scanning laser microscopy. *J. Chromatogr. A* **844**: 129-135.

Lyddiatt A., O'Sullivan D.A. (1998) Biochemical recovery and purification of gene therapy vectors. *Curr. Opin. Biotechnol.* **9**: 177-185.

Marquet M. (1996) Production of pharmaceutical grade plasmid DNA. Patent number 5561064.

Pinkerton T.C. (1991) High performance liquid chromatography packing materials for the analysis of small molecules in biological matrices by direct injection. *J. Chromatogr. A* **554**: 13-23.

Prazeres D.M.F., Guilherme N.M., Ferreira G.N.M., Monterio G.A., Cooney C.L., Cabral J.M.S. (1999) Large scale production of pharmaceutical grade plasmid DNA for gene therapy problems and bottle necks. *Trends Biotechnol.* **17**: 169-173.

Prazeres D.M.F., Monteiro G.A., Prazeres D.M.F., Ferreira G.N.M., Diogo M.M, Ribeiro S.C., Cabral J.M.S. (2001) Purification of plasmids for gene therapy and DNA vaccination. *Biotech. Annu. Rev.* **7:** 1-30.

Prazeres D.M.F., Ferreira G.N.M. (2004) Design of flowsheets for the recovery and purification of plasmids for gene therapy and DNA vaccination. *Chem. Eng. Process*. **43**: 615–630.

Queiroz J.A., Sousa F., Prazeres D.M.F. (2008) Affinity chromatography approached to overcome the challenges of purifying plasmid DNA. *Trends Biotechnol.* **26**: 518-525.

Rober R., Lightfoot E.N. (1995) Estimating plate height in stacked bed chromatography by reversed flow. *J. Chromatogr. A* **702**: 69-80.

Schleup T., Cooney C.L. (1998) Purification of plasmids by triplex affinity interaction. *Nucleic Acids Res.* **26**: 4524-4528.

Teeters M.A., Conrardy S.E., Thomas B.L., Root T.W., Lightfoot E.N. (2003) Adsorptive membrane chromatography for purification of plasmid DNA. *J. Chromatogr. A* **989**: 165-173.

Transfiguration J., Jorio H., Meghrous J., Jacob D., Kamen A. (2007) High yield purification of functional Baculovirus vectors by size exclusion chromatography. *J. Virol. Methods* **142**: 21-28.

Urthaler J., Schlegl S., Podgornik A., Strancar A., Jungbauer A., Necina R. (2005) Application of monoliths for plasmid DNA purification: Development and transfer to production. *J. Chromatogr. A* **1065**: 93-106.

Viloria-Cols M.E., Hatti-Kaul R., Mattiasson B. (2004) Agarose-coated anion exchanger prevents cell-adsorbent interactions. *J. Chromatogr. A* **1043**: 195-200.

Varley D.L., Hitchcock A.G., Weiss A.M.E., Horler W.A., Cowell R., Peddie L., Sharpe G.S., Thatcher D.R., Hanak J.A.J. (1999) Production of plasmid DNA for human gene therapy using modified alkaline cell lysis and expanded bed anion exchange chromatography. *Bioseparation* **8**: 209-217.

Voβ C., Schmidt T., Schleef M., Friehs K., Flaschel E. (2003) Production of supercoiled multimeris plasmid DNA for biopharmaceutical application. *J. Biotechnol*. **105**: 205-213.

Voβ C. (2008) Downstream Processing of Plasmid DNA for Gene Therapy and Genetic Vaccination. *Chem. Eng. Technol.* **31**: 858-863.

Williams S.L., Eccleston M.E., Slater K.H. (2005) Affinity capture of biotinylated retrovirus on macroporous monolithic adsorbents: Towards a rapid single step purification process. *Biotechnol. Bioeng.* **89**: 783-787.

Wills P., Escriou V., Warnery A., Lacroix F., Lagneaux D., Ollivier M., Crouzet J., Mayauz J.F., Schermann D. (1997) Efficient purification of plasmid DNA for gene transfer using triple-helix affinity chromatography. *Gene Ther.* **4**: 323-330.

3. PREPARATION AND CHARACTERISATION OF BI-LAYERED CHROMATOGRAPHY SUPPORTS

3.1 Abstract

In this work the design, manufacture and initial testing of bi-layered 'size exclusion - ion exchange' hybrid matrices is described. These materials promise efficient and gentle separation of 'nanoplex' bioproducts from smaller chemically similar contaminants in a 'one column – one bead' process. These beaded materials comprise of positively charged inner cores surrounded by thin inert outer layers. The charged core is accessible to globular proteins and low to medium molecular weight RNA; however the inert outer layer is designed to act as a size exclusion barrier preventing the access of larger charged molecules to the positively charged interior. These bi-layered chromatography supports were developed via three main synthetic chemistry routes employing microwaves and different solvents. The first synthetic route involved: (i) activating Sepharose CL-6B with allyl glycidyl ether (AGE); (ii) partial bromination of the introduced allyl functions; (iii) hydrolysis of the resulting layer of bromo-alkyl groups in an attempt to create an inert outer layer; (iv) full bromination of the support; and finally (v) coupling of the charged quaternary amine ligand, trimethylamine, to the support's inner core. The second synthesis was analogous to the first approach with the exception that the partial bromination step was replaced with a partial oxidation step. The third synthetic route involved: (i) activation of Sepharose CL-6B with epichlorohydrin (ECH); (ii) partial hydrolysis of the three membered epoxide rings introduced into the supports so as to create an inert outer layer of diol groups; and finally (iii) coupling of trimethylamine to generate a positively charged core.

None of chemistry approaches described above created two distinct layers in the modified supports. It was apparent from the plasmid DNA binding results, that the diffusion of the chemical into the pores of the support was faster than reaction taking place on the surface of the bead, resulting in only a partially inert outer layer. The employment of microwave heating in all three chemical syntheses greatly enhanced the reaction taking place on the surface of the bead, producing a distinct SEC outer layer. These new bi-layered chromatography beads were subsequently characterised (in terms the thickness and degree of inertness of the outer layer) and tested under static binding conditions using BSA and plasmid DNA.

3.2 Introduction

Although downstream processing technologies have progressed significantly since the first approval for a gene therapy clinical trial in the 1990, many purification problems remain unsolved (see Chapter 2, Section 2.2). There is still a need for fast, simple, and inexpensive downstream processing techniques to purify both viral and non viral vectors for gene therapy applications (Morenweiser, 2005). Furthermore, it is predicted that increasing amounts of purified vectors will be required to satisfy the demand for gene therapy clinical trials worldwide (Wu & Ataai, 2000). Packed bed chromatography is viewed as a key technique for the purification of large biomolecules such as plasmid DNA and viruses (Dunnill *et al*., 2000; Diogo, 2005), however it suffers from many inadequacies when purifying these larger entities. The main problems associated with packed bed chromatography in the purification of nanoparticulates are: low binding capacities; co elution of target product with contaminants; long process times, and loss of resolution (Queiroz *et al*., 2008; Gustavsson *et al*., 2004). A bi-layered packed bed chromatography support could reduce many of the problems associated with the

downstream processing of large bioproducts. This bi-functional bead could be employed at the capture or polishing stages in a one column process for the purification of a nanoplex product, possibly: reducing the required number of process steps thus increasing yields and enabling the collection of the required product in a more purified form.

Previously published work reported (see Chapter 2, Section 2.3) on different chemistry approaches for the creation of a bi-layered support, however none were completely successful in creating a bi-layered support possessing two completely distinct functional layers, and where the biding capacity of the support was not compromised (Bergström *et al*., 2002, Gustavsson *et al*., 2004; Kepka *et al*., 2004; Berg *et al.,* 2005).

This study begins by examining a previously published method that attempted to generate a bi-layered bead (Gustavsson *et al.,* 2004). It was viewed important to begin the study experimenting with already tested chemistry in order to: gain an understanding into the methods employed; to identify why this method was unsuccessful, and finally to investigate reaction conditions that would modify the method to make it more effective.

This chapter will begin by discussing the different synthetic chemistry routes employed in this study to create a bi-layered packed bed chromatography bead, with particular focus on the chemistry previously published by Gustavsson *et al.* (2004). The testing and characterisation of the bi-layered supports created will then be explained in detail and the results observed for each assay discussed. Next microwave chemical synthesis will be introduced and its beneficial effects explained on the modification of the supports. Finally the chapter will conclude by discussing the best possible reaction conditions and synthetic chemistry route in creating a bi-layered support and suggest what should be done in future experimental work.

In this work plasmid DNA is used as a probe to test for outer layer inertness, because of its large size it will not penetrate the pores of the support and will only bind to the outer surface if there is charge present. Bovine Serum Albumin (BSA) is the protein used to test the binding capacity of the supports. All the chemistry performed in each synthetic step was monitored using an assay for specific functional groups. This provided a method to test if the reaction taking place on the support had been a success and also revealed how much of the reagent had reacted during the reaction. The effect of microwave heating on each chemical synthesis was investigated in an attempt to further enhance the chemistry already tested in creating a bi-layered chromatography support.

3.2.1 Microwave Theory

3.2.1.1 Microwaves

Microwaves are electromagnetic waves that have a frequency range of between 0.3 to 300 GHz and have wavelengths in the electromagnetic spectrum from 1 mm to 1 m (Brimicombe, 1990). Typically industrial and domestic microwaves are only authorized to operate at either 915 MHz or 2.45 GHz to avoid interfering with radar and telecommunication frequencies (Zhang & Hayward, 2006).

Microwave appliances are composed of three main components: the source, the transmission lines and the applicator (Thostenson & Chou, 1999). The source of radiation in a microwave is from a magnetron tude and this introduces the electromagnetic radiation into the heating chamber. Co axial transmission lines transport the electromagnetic energy from the source to the applicator. The applicator then transfers the microwave energy to the material. Laboratory and domestic

microwave applicators are typically multimode (microwaves with temperature detectors and controllers), and are capable of maintaining a number of high order modes at one time (Thostenson & Chou, 1999). The theory behind the operation of all three microwave components is predicted from the most general form of Maxwell equations (equations 3.0 & 3.1) (Oliveira & Franca, 2002).

Equation 3.0 $$\nabla \times E = \frac{\partial B}{\partial t}, \qquad \nabla . B = 0,$$

Equation 3.1 $$\nabla \times H = \frac{\partial D}{\partial t} + I, \quad \nabla . D = \rho$$

Where, E is the electric field density, H, corresponds to the magnetic field intensity, D, the electric displacement, B, the magnetic induction and ρ the charge density (Oliveira & Franca, 2002). It is the Maxwell equations that explain how electromagnetic fields vary over time (Thostenson & Chou, 1999).

3.2.1.2 Mechanisms of dielectric heating

In order for a material to be able in interact with microwave irradiation and transmit heat, there are certain criteria that have to be fulfilled. The two main mechanisms for heat generation from microwaves are the dipolar mechanism and the conduction mechanism, provided the heated substances possess either dipolar or ionic species (Wathey *et al*., 2002).

The dipolar polarisation mechanism involves the initial interaction of the electric field with the material. This mechanism is based on the fact that in order for a material to produce heat by microwaves the material must possess a dipole moment (Lidström *et al*., 2005). Microwave energy is introduced into the material and the dipoles attempt to align themselves with the electric field by rotating (Figure 3.0). As the electric field oscillates and the dipoles try to realign with the already changing electric field, a phase difference is created between the dipoles and the alternating electric field. This phase difference results in energy loss from the dipole by molecular friction and molecular collisions, therefore producing dielectric heating (Kappe & Standler, 2005). The generation of heat is not only dependent on the dipole but also on the frequency of the radiation applied. If the frequency is too high the dipole will not have time to align with the alternating electric field before the field changes direction and no heat will be produced, the same result is observed if the dipole aligns perfectly with electric field and moves with field fluctuations (Wathey *et al*., 2002).

Figure 3.0: Dipolar molecules which try to align with an oscillating electric field; image taken from Lidström *et al*. (2005).

The conduction mechanism is another important interaction between the electric field and ions present in the material. The oscillating electric field causes the ions present to move back and forth, these ions then collide with adjacent molecules, causing an overall motion of molecules throughout the material. It is this motion of the molecules that also generates heat. It is reported that the movement of ions in a material caused by the

interaction with electromagnetic radiation is a much greater producer of heat than the corresponding movement of dipoles (Wathey *et al*., 2002). Consequently, ionic substances heat up extremely fast when they interact with microwaves.

3.2.1.3 Loss Tangent (Tan δ)

As mentioned above it is essential that a substance contains dipolar or ionic properties in order to convert electromagnetic energy into heat. The dielectric properties of a material can predict how it will perform under microwave radiation. The loss of tangent is used as an expression to describe how it will respond to the electromagnetic energy from microwaves and generate heat. These values (Tan δ) can prove very useful when identifying how different chemicals will respond to microwaves and help in establishing optimum reaction conditions for a microwave chemical synthesis. Typically in order for effective heating to be achieved with microwaves, materials should possess a high loss of tangent value. In general, solvents can be classified as high (Tan δ >0.5), medium (Tan δ = 0.1-0.5), and low microwave absorbing (Tan δ <0.1) (Kappe, 2004). The loss of tangent is expressed as:

Equation 3.2

$$\text{Tan}\,\delta = \frac{\varepsilon''}{\varepsilon'}$$

Where, ε" is the loss factor which represents the efficiency of the material to convert the transferred energy into heat; and ε' is the dielectric constant of the material.

The loss of tangent as a description for the conversion of electromagnetic energy into to heat, comes from the fact that for dielectric materials to produce heat from microwave, a phase difference between the dipoles and the electric field must be created. As

mentioned previously, at high frequencies the dipoles are restricted from moving with the alternating field, and a phase difference between the dipoles and the electric field is generated. The phase difference (δ) produces a component *I Sinδ* (Figure 3.1) which is in phase with the electric field (Mingos *et al*., 1998). As dipoles try realign with the alternating electric field there will be a displacement of charge which is equivalent to the electric current (Maxwell's displacement current) (Mingos *et al*., 1998). This phenomenon describes how energy from the electric field is consumed by a dielectric object and converted into heat.

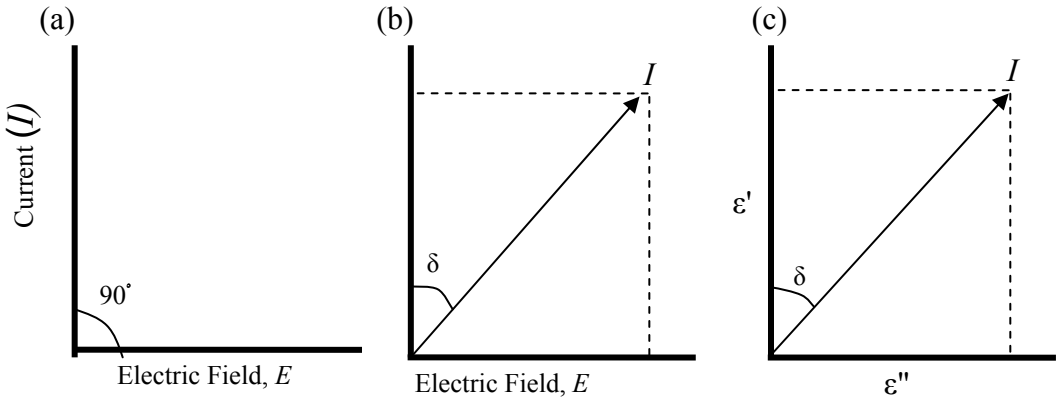

Figure 3.1: Phase diagrams for (a) an ideal dielectric where the energy is transmitted without loss; (b) where there is a phase difference (δ) and the current acquires a component ISinδ in phase with the voltage and consequently there is a dissipation of energy; (c) the relationship between ε' and ε" is displayed as Tan δ= ε"/ ε'.
Adapted from Mingos *et al*. (1998).

The Tan δ is basically a trigonometric function (Figure 3.1c), for more complex theory behind the loss tangent the reader is referred to Mingos *et al*. (1998).

3.3 Materials and Methods

3.3.1 Materials

Sephacryl S-500 High Resolution, Sepharose CL-6B, and Sephadex G-50 were obtained from GE Healthcare Bio-Sciences AB (Uppsala, Sweden). Bicinchoninic acid (BCA) protein assay kit was supplied by Pierce Biotechnology (Rockford, IL, USA). The QIAFilter plasmid purification kit was purchased from Qiagen GmbH (Hilden, Germany). The *E. coli* DH5α strain containing the plasmid pOCI (high copy plasmid; 10 KB) was kindly provided by Professor Chris Thomas (School of Biosciences, University of Birmingham, Edgbaston, UK). The *E. coli* DH1α strain containing the plasmid pSJC901 (High copy number, 3.5 Kb, Amp Vector) was supplied by Dr. Tim Overton (School of Biochemical engineering, University of Birmingham, Birmingham, UK). Blue dextran 2000 (2,000,000 mw), sodium borohydride ($NaBH_4$, 99%), trimethylamine hydrochloride, allyl glycidyl ether (AGE), epichlorohydrin, bromine, 'unacidified dilute' bromine water (potassium bromide-potassium bromate), and bovine serum albumin (BSA, fraction V, 96-99% albumin) were obtained from Sigma-Aldrich Company Ltd (St. Louis, MO, USA), as were all other chemicals used in this study (all of AnalaR grade). Deionised water was used to make all the solutions unless otherwise stated. This water was obtained from a Millipore ion exchange laboratory system.

3.3.2 Methods

3.3.2.1 Synthetic route 1a (adapted from Gutavsson *et al*., 2004; Soderberg *et al.,* 2002)

Step 1a. Allylation of Sepharose CL-6B (synthetic routes 1a)

Objective: Activation step, allyl groups introduced throughout the bead.

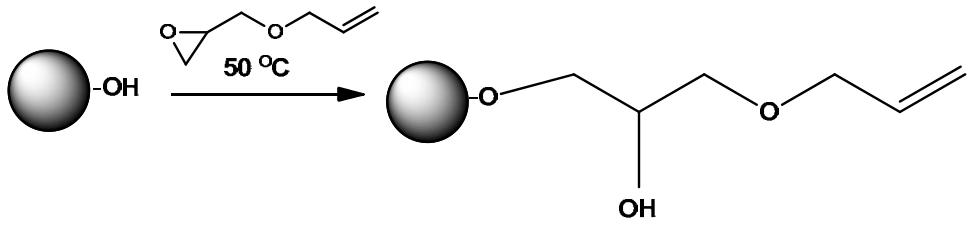

Sixty millilitres of sedimented Sepharose CL-6B was washed with copious quantities of water under vacuum using a sintered glass Buchner filter funnel. The supports were subsequently transferred to a 250 mL conical flask using 24 mL of sodium hydroxide solution (50% w/v), and then 0.25 g $NaBH_4$ and 6.7 g sodium sulphate were added under manual stirring. The flask was immediately immersed in a 50°C water bath fitted with a reciprocating shaker (model OLS 200; Grant Instruments (Cambridge) Ltd, Shepreth, UK) and shaken at 150 rpm for 1 h. The temperature of the water bath was then lowered to 40°C and 51 mL of 100% AGE was added to the flask; the reaction was allowed to proceed overnight (15 h) under vigorous shaking (170 rpm). At the end of the reaction the support was washed sequentially with water, 70% ethanol, and then water again, before storing in 20% ethanol at 4°C. The allyl group content of the support was determined using a bromine based assay (Methods section 3.3.2.11).

Step 2a. Bromination of allylated Sepharose CL-6B (synthetic route 1a)

Objective: Bromination of allyl groups present on the surface of the bead to initiate the creation of an SEC outer layer

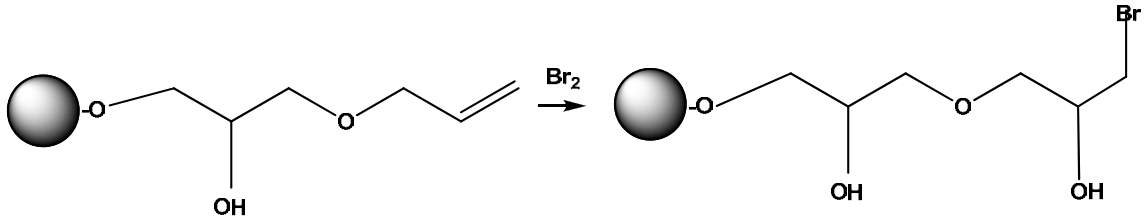

A 25 mL portion of the 'allylated' support from Step 1 was transferred to a 250 mL conical flask containing 20 mL concentrated sucrose solution (2 g/mL). Sodium acetate (0.55 g) and 40 g of sucrose were further added to the flask under gentle mixing (150 rpm) using an orbital shaker (model SO1; Stuart Scientific, Stone, UK). After the sucrose was completely dissolved, the stirrer speed was increased to 200 rpm. Meanwhile, a calculated amount of bromine was added to a tube containing 10 mL of concentrated sucrose solution. The tube was tightly sealed and shaken vigorously before adding this bromine-sucrose mixture, to the conical flask containing the reaction mixture. The support was removed from the shaker when the yellow colour had disappeared, due to the bromine reacting. The supports were then washed subsequently on a glass filter funnel with copious amounts of water, before transferring to a fresh conical flask containing 25 mL of water.

The experimental procedure described above was then repeated two more times under the following conditions prior to the addition of the bromine: (a) heating the support in a

commercial microwave oven (950 W; model ST44; Micro-Chef Ltd, Solva, UK) for 6 s; and (b) incubating the support in a water bath for 24 h at 56°C.

Step 3a. Sodium hydroxide reacted with the brominated outer layer of Sepharose CL-6B (synthetic route 1a)

Objective: Reaction of sodium hydroxide with the brominated bead to produce completely inert outer layer

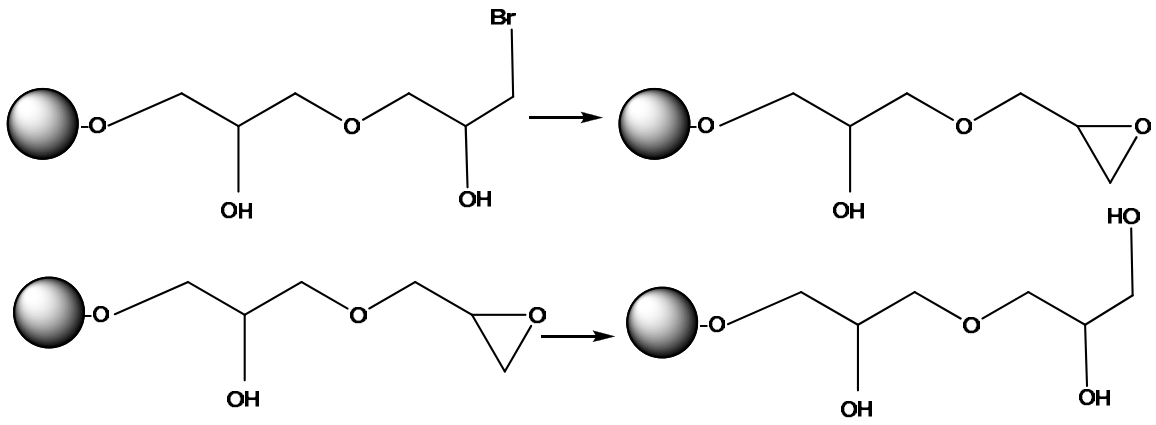

A solution of NaOH (2.3 g in 2.3 mL of water) was prepared and added with 0.1 g of $NaBH_4$ to the reaction flask containing the brominated supports from Steps 2 & 3, and hydrolysis of the immobilised alkyl bromide groups was achieved by incubation in a shaking water bath at 40°C for 15 h (overnight). Subsequently, the supports were washed with copious amounts of water with the aid of a sintered glass Buchner filter under vacuum.

Step 4a. Coupling of trimethylamine chloride to the modified supports (synthetic route 1a)

Objective: Coupling of the charged ligand to the inner core of the bead.

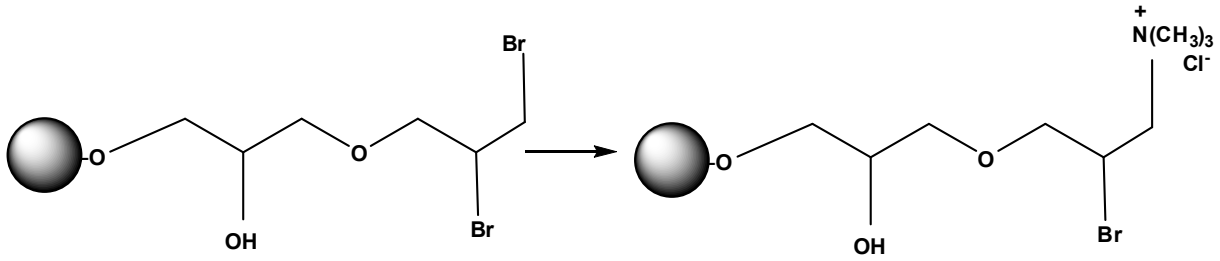

Twenty three millilitres of the brominated support prepared by synthetic Steps 1-4 were transferred to clean 250 mL conical flasks containing 10 mL of water. Next 1.1g of sodium acetate was added to each reaction flask, and the flasks were placed on an orbital shaker (model S01, Stuart Scientific, Stone, UK) and shaken at 150 rpm for approximately 300 s until all the sodium acetate had dissolved. The supports were then fully brominated by adding sufficient amounts of bromine to give a permanent yellow colour to the solution. The supports were subsequently washed with water (using a sintered glass Buchner filter under vacuum) until the filtrate turned colourless, transferred to clean conical flasks with 10 mL of water, and the following reagents were added: 15 mL of 65 % (w/v) trimethylamine chloride; 3.9 mL of 1 g/mL NaOH; and 0.1 g of $NaBH_4$. The reaction was left to proceed at room temperature for 15 h with shaking at 150 rpm, and finally the supports were washed with: water; 1 M NaCl, and then water once again.

3.3.2.2 Synthetic route 1b

Step 1b. Allylation of Sepharose CL-6B (synthetic route 1b)

Objective: Activation step, allyl groups introduced throughout the bead.

Methods performed exactly as that described for Synthetic route 1a: Step 1a

Step 2b. Bromination of allylated Sepharose CL-6B (synthetic route 1b)

Objective: Bromination of allyl groups present on the surface of the bead to initiate the creation of an SEC outer layer

Methods performed exactly as that described for Synthetic route 1a: Step 2a

Step 3b. Coupling of blue dextran to the outer surface of the partially brominated Sepharose CL-6B (synthetic route 1b)

Objective: Attachment of Dextran tentacles to the outer surface of the bead to further prohibit plasmid DNA binding

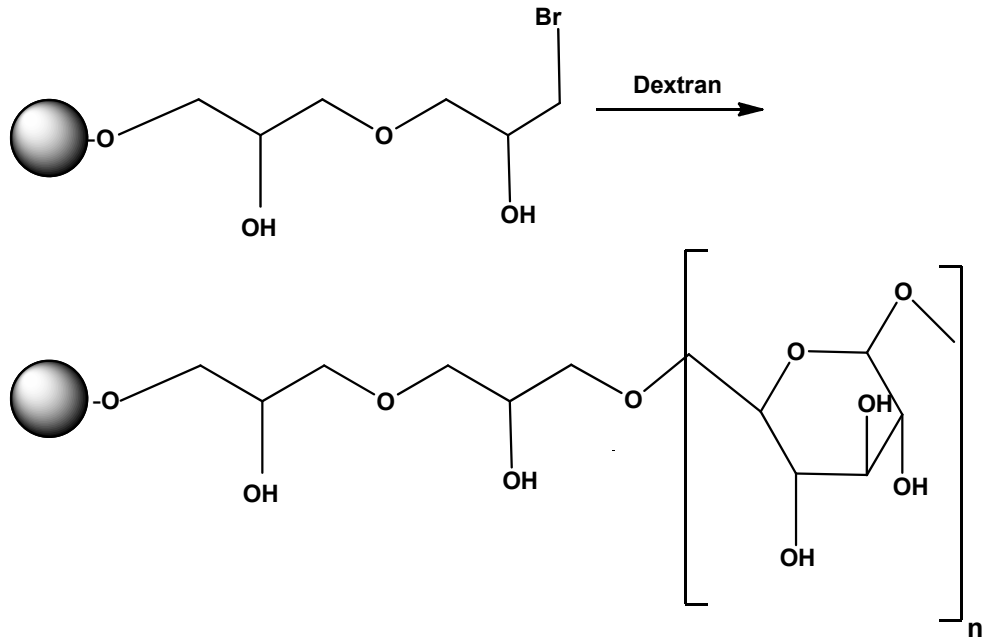

An 8 mL portion of the partially brominated support described in Step 2 was transferred to a conical flask containing 9.2 mL of blue dextran (100 mg/mL), and was left to mix gently at room temperature for 1 h in order to obtain a homogeneous solution. The coupling reaction was initiated by adding an aqueous solution of NaOH (1.168 g in 3.64 mL) and $NaBH_4$ (0.03 g), and was left to shake (190 rpm) at 50°C. The reaction was stopped, after approximately 16 h, by supplementing glacial acetic acid until a pH of 5 was reached. The modified support was then washed thoroughly with water, before continuing with the hydrolysis (Step 4) and ligand coupling (Step 5).

Step 4b. Sodium hydroxide reacted with the brominated outer layer of Sepharose CL-6B (synthetic route 1b)

Objective: Reaction of sodium hydroxide with the brominated bead to produce completely inert outer layer

Methods performed exactly as that described for Synthetic route 1a: Step 3a

Step 5b. Coupling of trimethylamine chloride to the modified supports (synthetic route 1b)

Objective: Coupling of the charged ligand to the inner core of the bead.

This step was carried out the same as step 5 described above, except 9.2 mL of the dextran activated supports were placed in a conical flask (150 mL) and the amount of each reagent added was adjusted accordingly.

3.3.2.3 Synthetic route 1c

Step 1c. Allylation of Sepharose CL-6B (synthetic route 1c)

Objective: Activation step, allyl groups introduced throughout the bead.

Methods performed exactly as that described for Synthetic route 1a: Step 1a

Step 2c. Partial bromination of allylated Sepharose CL-6B) (synthetic routes 1c)

Objective: Bromination of allyl groups present on the surface of the bead to initiate the creation of an SEC outer layer

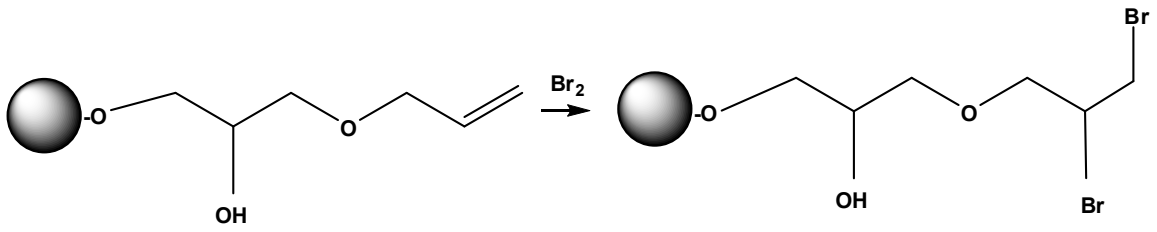

One millilitre of suction drained 'allylated' support from Step 1 was transferred to a 20 mL conical flask containing 22 mg of sodium acetate. Next 1 mL of DMSO was added to the reaction flask. Then a calculated amount of bromine was added to the reaction, and the solution was mixed on a vortex mixer (Chiltern Scientific, Auckland, New Zealand) for approximately 60 s until the yellow colour indicating the presence of the bromine had disappeared. The support was subsequently washed with water using a glass filter funnel, before transferring it to a fresh conical flask.

Step 3c. Sodium hydroxide reacted with the brominated outer layer of Sepharose CL-6B (synthetic route 1c)

Objective: Reaction of sodium hydroxide with the brominated bead to produce completely inert outer layer

Methods performed exactly as that described for Synthetic route 1a: Step 3a

Step 4c. Coupling of trimethylamine chloride to the modified supports (synthetic route 1c)

Objective: Coupling of the charged ligand to the inner core of the bead.

This step was performed as that described for Synthetic route 1a: step 4a

3.3.2.4 Synthetic route 2

Step 1. Allylation of Sepharose CL-6B

Objective: Activation step, allyl groups introduced throughout the bead.

This step was carried out exactly as described previously (Section 3.3.2.1 – Step 1).

Step 2. Partial oxidation of allylated Sepharose CL-6B, method 1 (Saegebarth & Wilberg, 1956).

Objective: Oxidation of the allyl groups present on the surface of the bead to create an inert outer layer

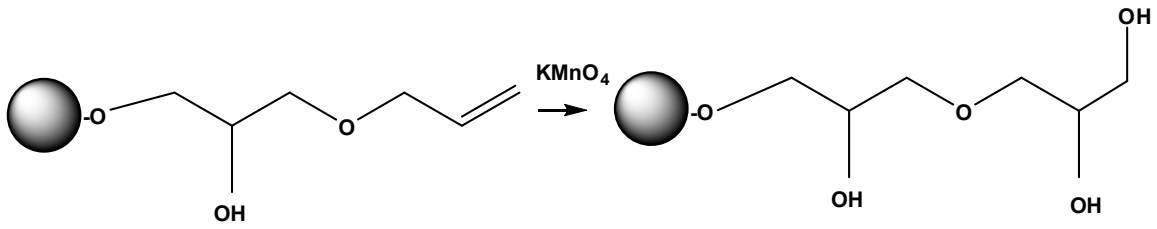

A 5 mL portion of the allylated support from Step 1 was placed in a 50 mL conical flask and then placed on ice. Next the following solutions were made and kept on ice: solution (1) - 1 g NaOH dissolved in 100 mL water at room temperature, and further diluted with 800 mL of iced water; solution (2) - 0.8 g potassium permanganate in 80 mL of water. Solutions (1 and 2) were then added to the reaction flask. The required volumes were determined by the results from the bromide assay, which indicated the number of allyl groups present on the support. From the calculated amount of allyl

groups present on the support the amount of potassium permanganate was added to create the outer layer, while still maintaining allyl groups in the inner core

In these experiments increasing volumes of solutions (1) & (2) were added to the different reaction flasks. The flasks were then shaken manually for approximately 180 s until the purple colour, due to potassium permanganate, completely disappeared and a brown-green colour was observed (indicating the reduction of manganate ions to manganate VII, which is green, and manganate IV which is brown). The flask was then placed on ice for 1 h. The supports were then washed copiously with 25 mM HCl and water.

***Step 2. Oxidation of allylated Sepharose CL-6B, method 2 (Berg et al.,* 2005)**

Objective: Oxidation of the allyl groups present on the surface of the bead to create an inert outer layer

A 1 mL portion of the allylated support from Step 1 was added to a 20 mL conical flask. Next 1 mL of a dextran T500 solution (10 % w/v) was added to the flask. This was added to increase the viscosity of the solution and therefore reduce the diffusion of the potassium permanganate. The flask was allowed to stir for 0.25 h at 150 rpm on an orbital shaker (model S01, Stuart Scientific, Stone, UK).

A calculated amount of potassium permanganate ($KMnO_4$) was added to the reaction flask under continuous stirring. The reaction was allowed to proceed for 0.25 h at room temperature. A 2.5 mL volume of a NaOH (50% W/V) solution was added to the flask, the reaction mixture turned brown instantly, indicating the formation of permanganate dioxide aggregates. The reaction was again allowed to proceed at room temperature for

1 h. A concentrated volume of acetic acid was added to the reaction flask (approximately 200 μL) until the pH reached 5. The beads were then placed on a glass filter, and washed with aqueous H_2O_2 (30% in water), on order to remove any residual potassium permanganate. Then the beads were washed with distilled water (50 mL).

Step 3. Reduction reaction of Carboxylic acid groups to alcohols (Dapurkar et al., 2003) on the surface of the bead.

Objective: Reduction of carboxylic acid groups (or aldehyde groups) that may have formed during the oxidation step therefore, ensuring that the charged amine ligand cannot react at the outer layer.

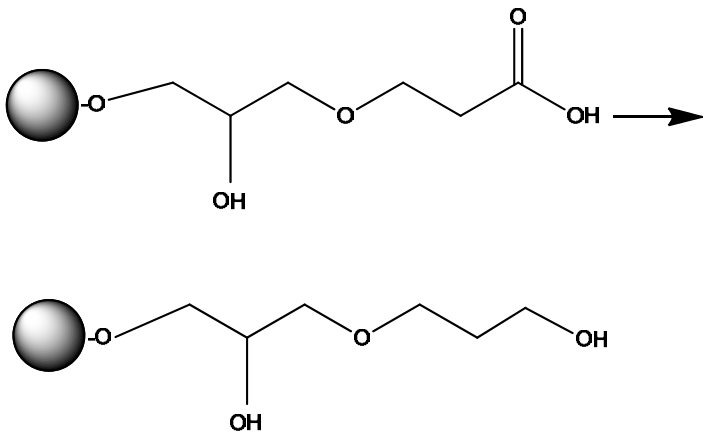

A reaction flask containing: 1 mL suction drained partially oxidised support; 6 mg sodium borohydride in 1 mL THF; 8 mg sodium sulphate; and 8 mmols of boronic acid, was left to mix at 150 rpm on a orbital shaker (model S01, Stuart Scientific, Stone, UK) at room temperature for 15 h, before the beads were washed with copious amounts of water using a sintered glass funnel.

Step 4. Coupling of trimethylamine chloride to 'modified' supports.

Objective: Coupling of the charged ligand to the inner core of the bead.

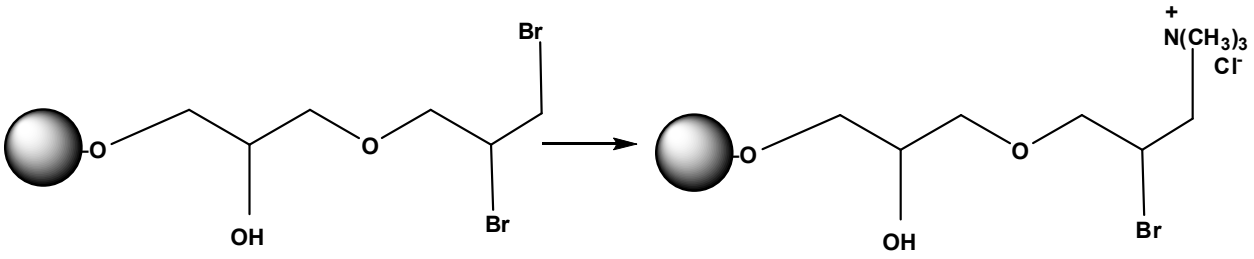

Five milliliters of beads were transferred to clean 150 mL conical flasks containing 2 mL of water. The flasks were placed on an orbital shaker (Stuart Scientific, Stone, UK) and 240 mg of sodium acetate was added. The flasks were shaken at 150 rpm for approximately 300 s until all the sodium acetate had dissolved, followed by addition of sufficient amount of bromine to give a permanent yellow colour to the solution. The supports were subsequently washed with water (using a sintered glass Buchner filter under vacuum) until no more yellow colour was detected in the filtrate, and placed in a clean conical flask with 2 mL of water, before adding 3.2 mL of 65 % (w/v) trimethylamine chloride solution; 848 μL of 1 g/mL NaOH; and 22mg of $NaBH_4$.

The reaction flask was then placed on an orbital shaker (model S01, Stuart Scientific, Stone, UK), the reaction was left to proceed at room temperature for 15 h, with continuous shaking at 150 rpm. The supports were subsequently washed with: water, 1M NaCl, and finally with water once again.

3.3.2.5 Synthetic route 3a

Step 1a. Epichlorohydrin activation of Sepharose CL-6B (Synthetic route 3a) (Matsumoto et al., 1979)

Objective: Activation step, epoxide groups are introduced throughout the bead

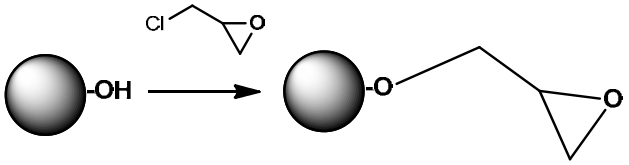

Sepharose CL-6B (30% v/v) was suspended in a solution containing 0.4 M NaOH. Five millilitres of (5 % v/v) epichlorohydrin (ECH) was added to the mixture and the reaction was allowed to proceed on an orbital shaker at 150 rpm (model S01, Stuart Scientific, Stone, UK) for 24 h at room temperature. The support was then washed with copious amounts of 1 M NaOH and water.

Step 2a. Partial hydrolysis (under acidic conditions) of epichlorohydrin activated Sepharose CL-6B (Synthetic route 3a)

Objective: Hydrolysis of the epoxide groups present on the surface of the bead to create an inert outer layer

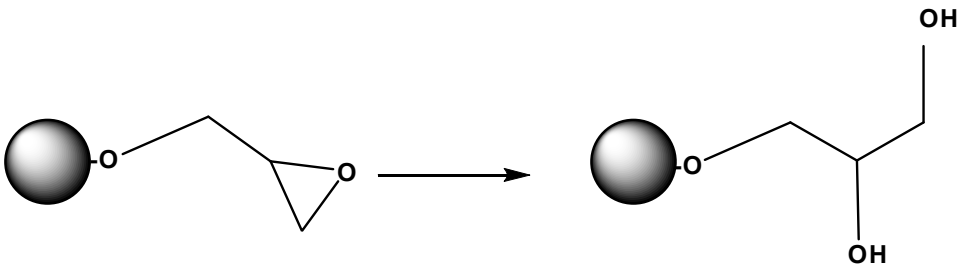

Hydrolysis (elimination of 5-20% of the epoxide groups) of the epichlorohydrin activated Sepharose CL-6B from Step 1 was performed under acidic conditions by adding various volumes of 25 mM HCl solution to a series of conical flasks containing 1 mL of the support under vigorous shaking. A calculated amount of acid was added to each reaction flask, and the solutions were mixed on a vortex mixer (Chiltern Scientific, Auckland, New Zealand) for approximately 120 s. The experiment was repeated under the same reaction conditions, but was immediately preceded by brief (6 s) heating in a domestic microwave oven at full power (950 W; model ST44; Micro-Chef Ltd, Solva, UK). All supports were then washed with copious amounts of water using a sintered glass funnel.

Step 3a. Coupling of trimethylamine to epichlorohydrin activated Sepharose CL-6B (Synthetic route3a) (Ikeda et al., 1996)

Objective: Coupling of charged amine ligand to the inner core.

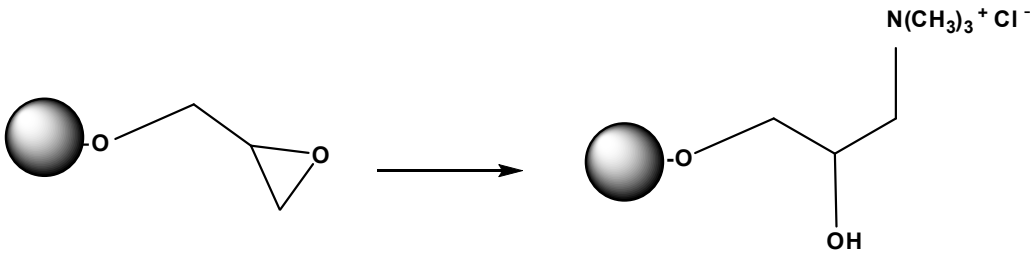

Twenty three millilitres of the two types of supports prepared by synthetic Steps 1-2 were transferred to clean 250 mL conical flasks containing 10 mL of water. Next 15 mL of 65 % (w/v) trimethylamine hydrochloride chloride; and 3.9 mL of 1 g/mL NaOH solution were added to the reaction flasks. The flask was then placed on an orbital shaker (model S01, Stuart Scientific, Stone, UK) and the reaction was left to proceed at

room temperature for 15 h, with shaking at 150 rpm. The supports were subsequently washed with: water, 1 M NaCl and finally with water once again.

3.3.2.6 Synthetic route 3b

Step 1b. Epichlorohydrin activation of Sepharose CL-6B (Synthetic route 3b) (Matsumoto et al., 1979)

Objective: Activation step, epoxide groups are introduced throughout the bead

Methods performed exactly as that described for synthetic route 3a: Step 1a

Step 2b. Hydrolysis (under basic conditions) of epichlorohydrin activated Sepharose CL-6B (Synthetic route 3b)

Objective: Hydrolysis of the epoxide groups present on the surface of the bead to create to an inert outer layer.

Partial hydrolyses of epichlorohydrin activated Sepharose CL-6B was also carried out under basic conditions by replacing the 25 mM HCl solution with 25 mM NaOH. A calculated amount of base was added to the reaction flask, and the solution was mixed on a vortex mixer (Chiltern Scientific, Auckland, New Zealand) for approximately 120s. The rest of the experiment was completed exactly as that described in Step 2a.

Step 3b. Coupling of trimethylamine to epichlorohydrin activated Sepharose CL-6B (Synthetic route 3b) (Ikeda & Kida, 1996)

Objective: Coupling of the charged amine ligand to the inner core.

Methods performed exactly as that described for synthetic route 3a: Step 3a

3.3.2.7 Synthetic route 3c

Step 1c. Epichlorohydrin activation of Sepharose CL-6B (Synthetic route 3c) (Matsumoto et al., 1979)

Objective: Activation step, epoxide groups are introduced throughout the bead

Methods performed exactly as that described for synthetic route 3a: Step 1a

Step 2c. Hydrolysis (under acidic & methanol conditions) of epichlorohydrin activated Sepharose CL-6B

Objective: Hydrolysis of the epoxide groups present on the surface of the bead to create an inert outer layer (Synthetic route 3c)

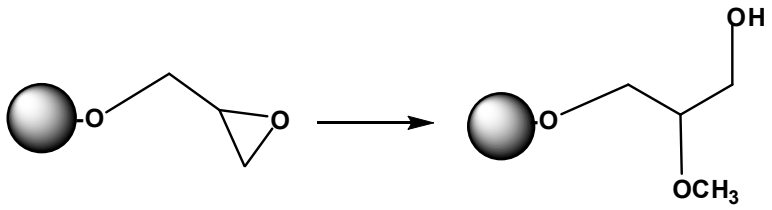

Hydrolysis of epichlorohydrin activated Sepharose CL-6B was also performed under acidic - methanol conditions by following exactly the same protocol as the one described in Synthetic route1a-Step 2a by replacing the 1 mL of water with 99.9% (v/v) methanol. The rest of the experiment was carried out exactly as that described in Step 2a.

Step 3c. Coupling of trimethylamine to epichlorohydrin activated Sepharose CL-6B (Synthetic route 3c)(Ikeda & Kida, 1996)

Objective: Coupling of the charged amine ligand to the inner core.

Methods performed exactly as that described for synthetic route 3a: Step 3a

3.3.2.8 Synthetic route 3d

Step 1d. Epichlorohydrin activation of Sepharose CL-6B (Synthetic route 3d) (Matsumoto et al., 1979)

Objective: Activation step, epoxide groups are introduced throughout the bead

Methods performed exactly as that described for synthetic route 3a: Step 1a

Step 2d. Hydrolysis (under basic & methanol conditions) of epichlorohydrin activated Sepharose CL-6B (Synthetic route 3d)

Objective: Hydrolysis of the epoxide groups present on the surface of the bead to create an inert outer layer

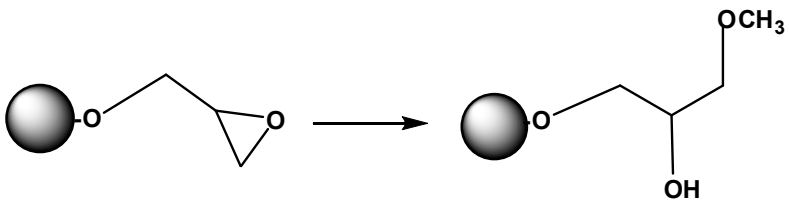

Hydrolysis of epichlorohydrin activated Sepharose CL-6B were also performed under basic-methanol reaction conditions by following exactly the same protocol as the one

described in Synthetic route1a -Step 2a by replacing the 1 mL of water with 99.9% (v/v) methanol. The rest of the experiment was carried out exactly as that described in Step 2a.

Step 3d. Coupling of trimethylamine to epichlorohydrin activated Sepharose CL-6B (Synthetic route 3d) (Ikeda & Kida, 1996)

Objective: Coupling of the charged amine ligand to the inner core to introduce anion exchange properties.

Methods performed exactly as that described for synthetic route 3a: Step 3a

3.3.2.9 Protein static binding studies

Portions of suction drained anion exchange supports (0.050 g) were equilibrated with 1.5 mL of 50 mM Tris-HCl pH 7.5 for 0.5 h on a rotary mutltimixer (model IKA vibrax VXR, Denley Instruments Ltd, West Sussex, UK) at 75 rpm. After settling, the supernatants were removed and 1.5 mL of 50 mM Tris-HCl pH 7.5 was added. Following a second equilibration period (0.5 h with gentle mixing), the supports were again allowed to settle, and the supernatants were poured off. Next 1.5 mL aliquots of BSA (1.0 mg per mL of 50 mM Tris-HCl, pH 7.5) were added and the supports were then transferred to fresh 10 mL screw-cap plastic Sarstedt tubes. A further 6 mL of 1.0 mg/mL BSA solution were added to each tube, and the resulting mixtures were incubated at room temperature for 15 h with gentle mixing at 75 rpm on a rotary multimixer (model IKA vibrax VXR, Denley Instruments Ltd, West Sussex, UK). The

supernatants were subsequently analysed for residual protein content using the commercially available Pierce BCA protein assay.

3.3.2.10 DNA binding studies

Preparation of plasmid DNA feedstock

E. coli DH5α cells containing the plasmid pOCI (stored in 20% glycerol at -80°C) were plated out on LB agar plates supplemented with 100 μg/mL ampicillin and allowed to grow for 24 h at 37°C. Starting cultures were prepared by inoculating 40 mL aliquots of sterile Luria Bertani (LB) broth containing 100 μg/mL ampicillin with a fresh single colony of *E. coli* DH5α/pOCI and shaking overnight at 37°C and 200 rpm (shaker model Innova 43, New Brunswick Scientific, Herefordshire, UK). The above inoculum culture was then added to a sterile conical flask containing 400 mL of LB broth supplemented with 100 μg/mL ampicillin and the contents were shaken in an orbital shaker (shaker model innova 43, New Brunswick Scientific, Herefordshire, UK) at 200 rpm for 16 h at 37°C. The cells were harvested by centrifugation (4°C for 0.25 h at 6,000 g_{av}; model J2-J1, rotor JA-20, Beckmann Coulter, Buckinghamshire, UK), and the plasmid was purified using the QIAFilter Giga purification kit. The final plasmid concentration obtained was 0.5 μg/mL in 50 mM Tris-HCl, pH 7.5.

Static binding studies

Suction drained anion exchange supports (0.1 g) were equilibrated twice with 1.5 mL of 50 mM Tris-HCl, pH 8 for 0.5 h with shaking at 150 rpm on a orbital shaker (model SO1; Stuart Scientific, Stone, UK). Following equilibration, the supports were

incubated with 1.5 ml of 25 μg/mL plasmid DNA stock solution for 20 s at room temperature with manual mixing, followed by centrifugation (Microcentaur, model 5415D, MSE, London UK) for 20 s. The supernatants were analysed for residual DNA content by absorbance measurements at 260 nm (model 922 Unikon spectrophotometer, Kantron instruments, Chichester, UK). The amount of bound material was calculated by the difference between the concentration in the initial plasmid DNA solution and the supernatant obtained from the sample, assuming that one A_{260nm} unit corresponds to a DNA concentration of 50 μg/mL.

3.3.2.11 Analysis – BCA; pDNA; Bromine assay; ionic capacity, and epoxide assays

Assay for protein

The concentration of the protein in solution before and after binding was measured by the bicinchoninic acid assay (BCA assay). Protein samples of 100 μL were added to 2 mL of BCA reagent and left at room temperature for 2 h. The BCA reagent was prepared from mixing 50 parts of reagent A (sodium carbonate, sodium bicarbonate, bicinchoninic acid and sodium tatrate in 0.1 M sodium hydroxide) and with one part of reagent B (4% cupric sulfate in 25 mL). The solution developed a purple colour and the absorbance was measured at 562 nm. Protein concentrations were then calculated by comparing with a calibration curve of bovine serum albumin standards (Appendix; Section 6.8). The 50 mM Tris-HCl binding buffer was used as the blank for the spectrophotometer readings.

Assay of for pDNA

The concentration of the plasmid before and after binding was measured by taken the absorbance of the plasmid DNA solution at 260 nm. The amount of DNA in solution

was calculated from the absorbance readings (based on the assumption that one A_{260nm} unit corresponded to a DNA concentration of 50 μg/mL).

Assay for Allyl groups to determine the amount of double bonds present on the support (bromine assay)

An 'acidified bromine stock solution' was prepared by adding 0.5 M H_2SO_4 to a standard solution of potassium-bromide: potassium-bromate (2:1 (v/v). Next 1.5 mL of this bromine solution was added to 100 mg of suction drained AGE activated supports. After brief manual shaking (~10 s), the sample was centrifuged for 10 s at 13,000 rpm (Microcentaur, model 5415D, MSE, London UK) and the absorbance of the supernatant was read immediately at 410 nm using a Unikon 922 spectrophotometer (Kantron instruments, Chichester, UK). The number of moles of the bromine that reacted was calculated, which corresponds to the number of allyl groups present on the support.

Assay for Epoxide (Oxirane ring) groups (Porath & Sundburg, 1974)

The assay calculates the number of epoxide groups present on the adsorbent by a ring opening reaction of the epoxide by sodium thiosulphate (see schematic below).

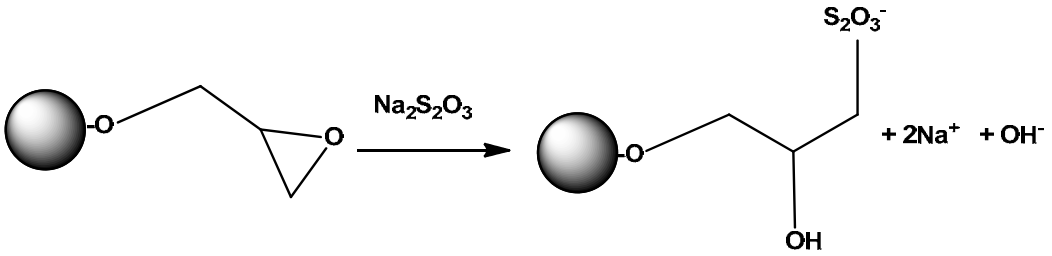

Epoxide groups on the activated supports was determined by mixing 0.5 g of suction drained beads with 1.5 mL of 1.3 M sodium thiosulphate solution (pH 7), and shaking at 75 rpm on a rotary multimixer (model IKA vibrax VXR Denley Instruments Ltd,

West Sussex, UK) for 1.3 h. The supports were allowed to settle, the pH of the solution was measured and then the solution was titrated with 0.1 M HCl. The moles of epoxide present on the support were calculated from the amount of acid needed in order to maintain neutrality.

Ionic capacity (Pitfield, 1992)

The anion exchangers (300 mg) were incubated with 50 mL of 2 M NaCl for 1.5 h to convert them into the quaternary ammonium chloride form. Excess acid was then removed from the supports by washing three times on a glass sinter with 50 mL aliquots of water, before transferring the suction drained materials to 100 mL bottles containing 50 mL of 0.1 M NaOH and mixing at 150 rpm for 24 h on an orbital shaker (model S01, Stuart Scientific, Stone, UK). Following settling of the support, 1 mL aliquots of the liquid phases were mixed vigorously on a rotary multimixer (model IKA vibrax VXR, Denley Instruments Ltd, West Sussex, UK) for 600 s at room temperature with 100 µL of 0.25 M ammonium iron (III) sulphate in 9 M nitric acid and 100 µL of a saturated solution of mercury (III) thiocyanate in 96% ethanol.

The chloride ion contents were determined from absorbance measurements at 460 nm (model 922,Unikon spectrophotometer, Kantron instruments, Chichester, UK).

Determination of extents of partial bromination, oxidation and hydrolysis

The extent of partial bromination, partial oxidation and partial hydrolysis achieved in each reaction was estimated in two ways: (i) from the drop in measured allyl or epoxide contents compared to the untreated allylated or epoxy activated supports; (ii) from the decrease in ionic capacity of finished supports compared to appropriate controls, for

example supports that had not received a partial bromination (Appendix; Section 6.10;), oxidation (Appendix; Section 6.11) or hydrolysis treatment (Appendix ;Section 6.12).

3.4 Results and Discussion

In this study, three main synthetic chemistry routes were employed in an attempt to create a bi-layered chromatography adsorbent. This bi-layered bead would be comprised of both anion exchange and size exclusion chromatographic principles, present in two distinct layers. This bi-functional support could be employed in the purification of plasmid DNA[1] and viruses, solving many of the problems associated with purifying these large biomolecules with chromatography. Bi-layered packed bed chromatography supports are discussed in more detail in Chapter 2.

The size exclusion bead Sepharose CL-6B was the support employed as the base matrix for all the chemical synthesises described in this study. It is a commercially available adsorbent, chemically stable and readily modified with various chemical reagents. Also the pores of this support had to be within a certain size range so as to allow the diffusion of proteins into the pores of the support whilst prohibiting plasmid DNA from entering the pores. The average pore size of Sepharose CL-6B is approximately 35 nm (Bosma *et al*., 1998), whereas large biomolecules are typically greater than 0.2 μm in size. Therefore mass transfer of the plasmid into the pores of the support would be much slower in comparison to proteins[2] or RNA.

[1] Plasmids differ hugely in size (e.g. from as little as 3 to greater than 100 kilobases). Their size also changes dramatically in response to pH and esp. ionic strength. Naked plasmid DNA before formulation can be 200 to >1000 nm (Lyddiatt & O'Sullivan, 1998)
[2] Protein BSA is 3.59 nm (Stokes radius) (Zhang & Sun, 2002)

3.4.1 Introduction to Synthetic routes 1, 2 & 3

Three different synthetic chemistry routes were employed in the preparation of this new type of bi-layered support and the chemistry schemes are presented in Figures: 3.1; 3.4; 3.5, & 3.6.

3.4.1.1 Synthetic route 1

The starting point of this scientific study began by experimenting with a synthesis (**Synthetic route 1a**) adapted from a paper by Gustavsson and co workers (2004) in which a bi-layered support was created. The results from this work showed that this chemistry approach was not that successful in creating a bi-layered support (see Chapter 2), however it was viewed as important to start the study repeating previously published work, to gain an understanding into the chemistry methods and to establish why this chemistry was ineffective. In order to provide an accurate comparison with the published results, Sodium Borohydride was added to the supports one hour prior to the addition of the reagent, therefore copying the method of Gustavsson *et al*. (2004). Sodium Borohydride does not take part in the chemical reaction, however it is a reducing reagent and the addition of it to the supports would reduce any aldehyde groups present to alcohols groups therefore increasing the number of activation sites present on the supports.

The chemistry synthesis employed by Gustavsson *et al*. (2004) is displayed in Figure 3.2. In first step of synthetic route 1 (Step1), the supports were activated with Allyl Glycidyl Ether (AGE) in order to introduce double bonds throughout the bead. The extent of activation with AGE was determined using the assay for allyl groups described

in Section 3.3.2.11. The allylated chromatography matrix was then reacted with limited amounts of Bromine (Step 2). The amount of bromine reacted was estimated from the number of allyl groups on the support. The concept behind the partial bromination step was that the reaction of bromine with the allyl groups would occur faster than the chemical diffuses into the pores of the support. When a limited number of moles of bromine are added these will react with the allyl groups present on the surface of the bead therefore leaving unreacted allyl groups present in the inner core, and creating a brominated outer layer. This brominated layer must be as thin as possible. The thicker the outer layer the greater the loss in the protein binding capacity of the bead. From the results obtained it was shown that with increasing bromine additions shrinking core behaviour was evident (Figure 3.8). Next sodium hydroxide was reacted (Step 4) with the brominated layer to replace any remaining bromide groups present on the surface of the bead with hydroxide groups. The supports were subsequently treated with excess bromine (Step 5), which reacts with the remaining allyl groups present in the inner bead core. Finally the addition of trimethylamine hydrochloride introduces the positively charged amine ligand into the inner core. The chemistry approach adapted by Gustavsson *et al*. (2004) was unsuccessful in creating a complete inert outer layer on the surface of the bead. From the results obtained it was shown that with increasing bromine additions shrinking core behaviour was evident, a 9% reduction in ally groups to create outer layer resulted in an 7% reduction in the protein binding capacity whereas doubling the number of allyl eliminated to 18% produced more than a 5 fold decrease in the protein binding capacity (Table 3.1 & Figure 3.8). A substantial elimination of pDNA binding was only achieved with significant reductions in the protein binding capacity and even when a thick outer layer was created it still maintained point charges.

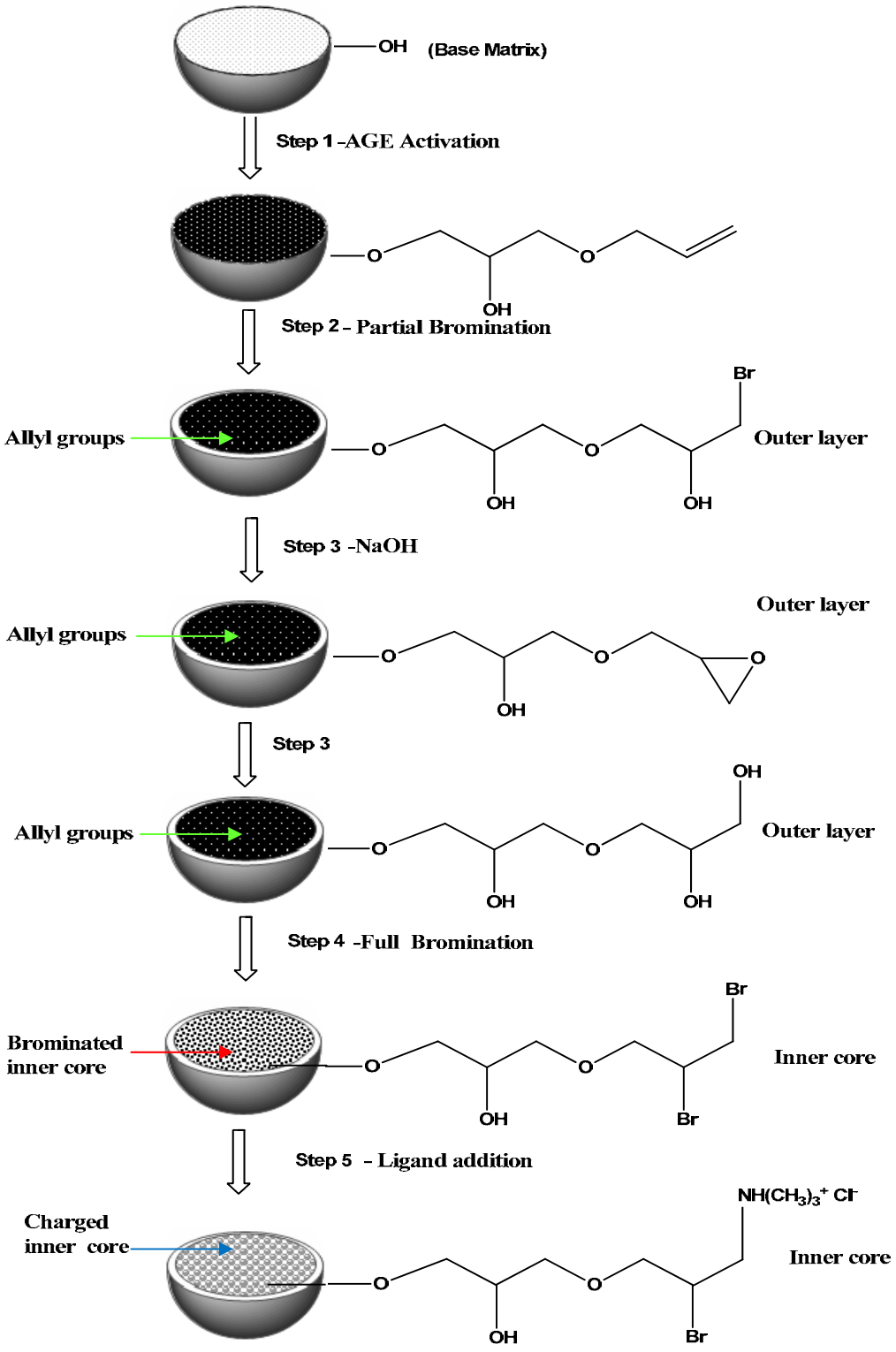

Figure 3.2: Synthetic scheme 1a for the preparation of SEC-AEC Sepharose CL-6B chromatography supports (Gustavsson *et al.,* 2004): (step 1) NaOH, $NaBH_4$, Na_2SO_4, AGE, 50°C, 24 h.(step 2) Sucrose, H_20, Sodium Acetate, Br_2, 60 s.(Step 3) NaOH, $NaBH_4$, 40°C. (step 4) H_20, Br_2, Sodium Acetate. (step 5) $N(CH_3)_3$.HCl, NaOH, $NaBH_4$, 24 h.

There are a variety of reasons as to why this chemical approach adapted from Gustavsson *et al,* (2004) was not effective in creating two distinct functional layers within the fabricated bead. One possibility is that it may be due to the formation of bromohydrin products (major and minor) during the bromination of the allyl groups present on the surface of the bead (Figure 3.3). This bromination reaction is performed in water so it can be assumed that a hydroxyl group reacts at the carbon site where the majority of charge is located (ending up at the more substituted carbon), forming the major bromohydrin product. However it is also possible that the hydroxide will react at the other carbon site creating a minor bromohydrin product (Clayden *et al*., 2001).

At alkaline pH, bromohydrins are converted to epoxides; the addition of sodium hydroxide will result in the conversion of these bromohydrin products to three membered epoxide rings by an intramolecular etherification (Lang *et al*., 1998; Honda *et al*., 1987). However, a three membered epoxide ring is a strained structured and a bulky functional group, it could be the case due to steric effects that not all bromohydrins are converted to a epoxides and that bromide groups may still be present in the outer layer. These bromide groups would then allow for the introduction of the charged ligand, therefore jeopardizing the inertness of the outer layer.

Due to the fact that sodium hydroxide is added in excess any three membered epoxide rings created should then be hydrolysed and converted to diols. One concern with hydrolysis of epoxides with sodium hydroxide is that it is reportedly a slow reaction, and can take up to 24 hours at room temperature. Patel and co workers (1999) previously showed that only 30% of the epoxide groups were hydrolysed under basic conditions after a period of 24 hours. If epoxide groups remain in the layer the charged

amine ligand can react with these groups and introduce charge into the outer layer. The explanations discussed above maybe why this chemistry was not that effective in creating an 'inert' outer layer. An additional factor could be that this supposedly 'very fast' chemical reaction is just not fast enough, and that some of the chemical diffuses into the pores of the support faster than it can react at the surface of the bead.

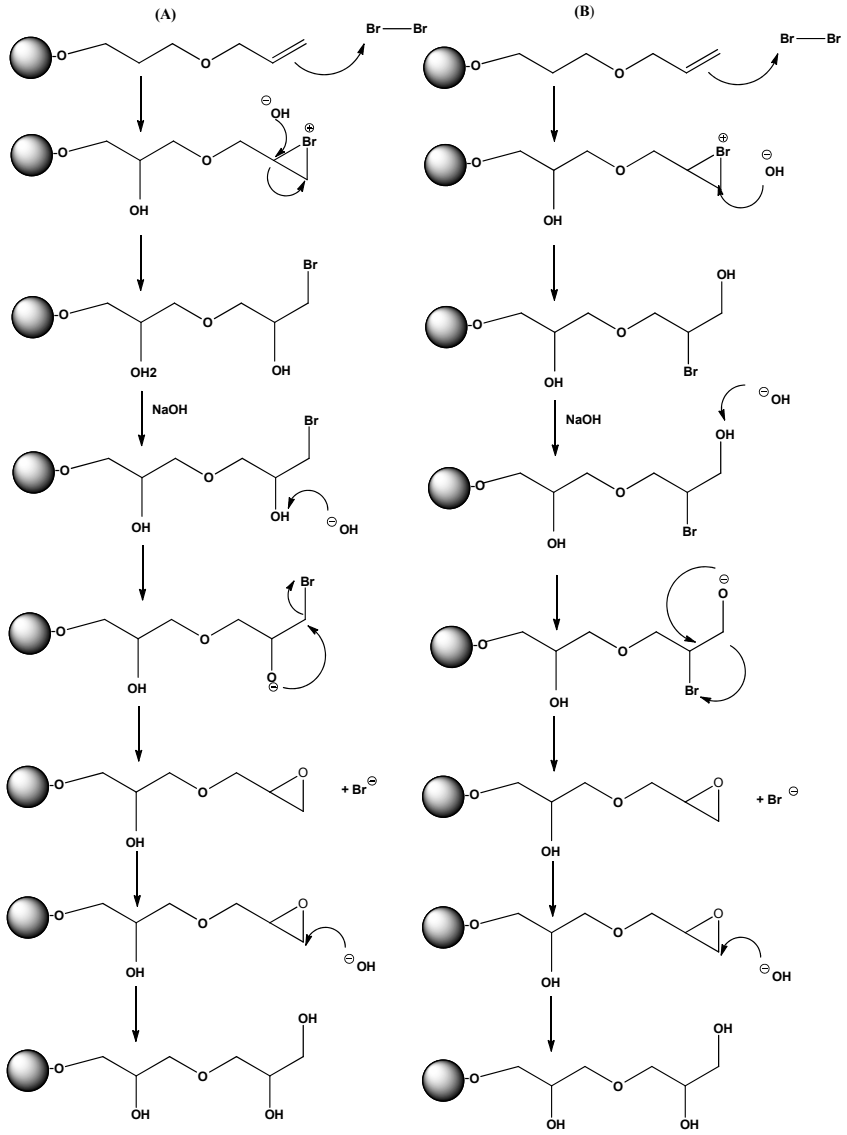

Figure 3.3: The mechanism of (a) Major Bromohydrin & (b) Minor Bromohydrin products on the outer layer of the bead during the partial bromination and hydrolysis step.

In this study the reaction conditions employed by Gustavsson *et al*. (2004) were further developed by experimenting with the attachment of dextran tentacles to the outer layer. Dextran is a very large hydrophilic polymer. Due to its large size (2,000,000 mw) it cannot penetrate the pores of the support (fractionation limit 10,000-1,000,000). The immobilisation of dextran tentacles at the exterior surface should create an additional barrier preventing the binding of large nucleic acid molecules. Successful dextran coupling was evident by the change of support colour from white to blue (Figure 3.4). The dextran supports were created under the exact same reaction conditions as that previously described for synthetic route 1a with an additional step in the synthesis involved the coupling of Dextran to the outer surface of the support. This step was introduced after step 2 in the synthesis (**Synthetic route 1b**) where, dextran was reacted with the brominated outer layer. The rest of the synthesis followed the exact series of steps as previously described for synthetic route 1a.

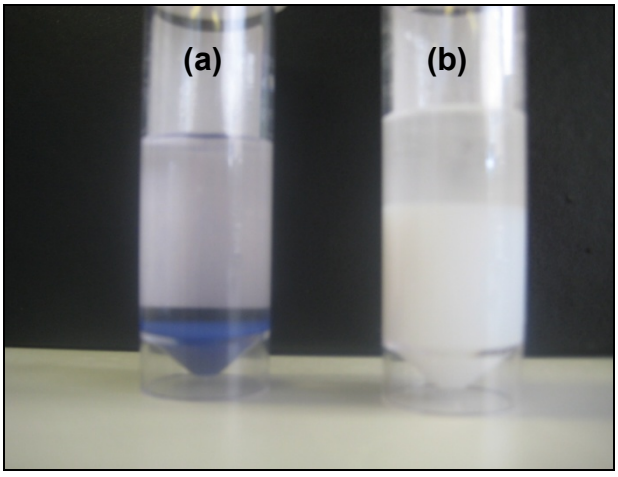

Figure 3.4: Photograph of (a) Blue dextran linked beads after the hydrolysis step in synthesis 1b & (b) Beads with no dextran attached.

3.4.1.2 Synthetic route 2

Synthetic route 2 (Figure 3.5) differed from route 1 during Step 2 only. Here the partial bromination step was substituted with a partial oxidation step using potassium permanganate. The concept behind replacing the bromination step (Figure 3.2; synthetic route 1a) with an oxidation step was that by oxidising the allyl groups present on the surface of the bead the possibility of mixed bromohydrin products would be eliminated. Allyl groups are easily oxidised to diols with potassium permanganate. It is this partial oxidation step that creates a SEC layer on the outer surface of the bead. It was thought that this chemistry approach might prove more effective. The results for synthetic route 2 are displayed in Table 3.2.

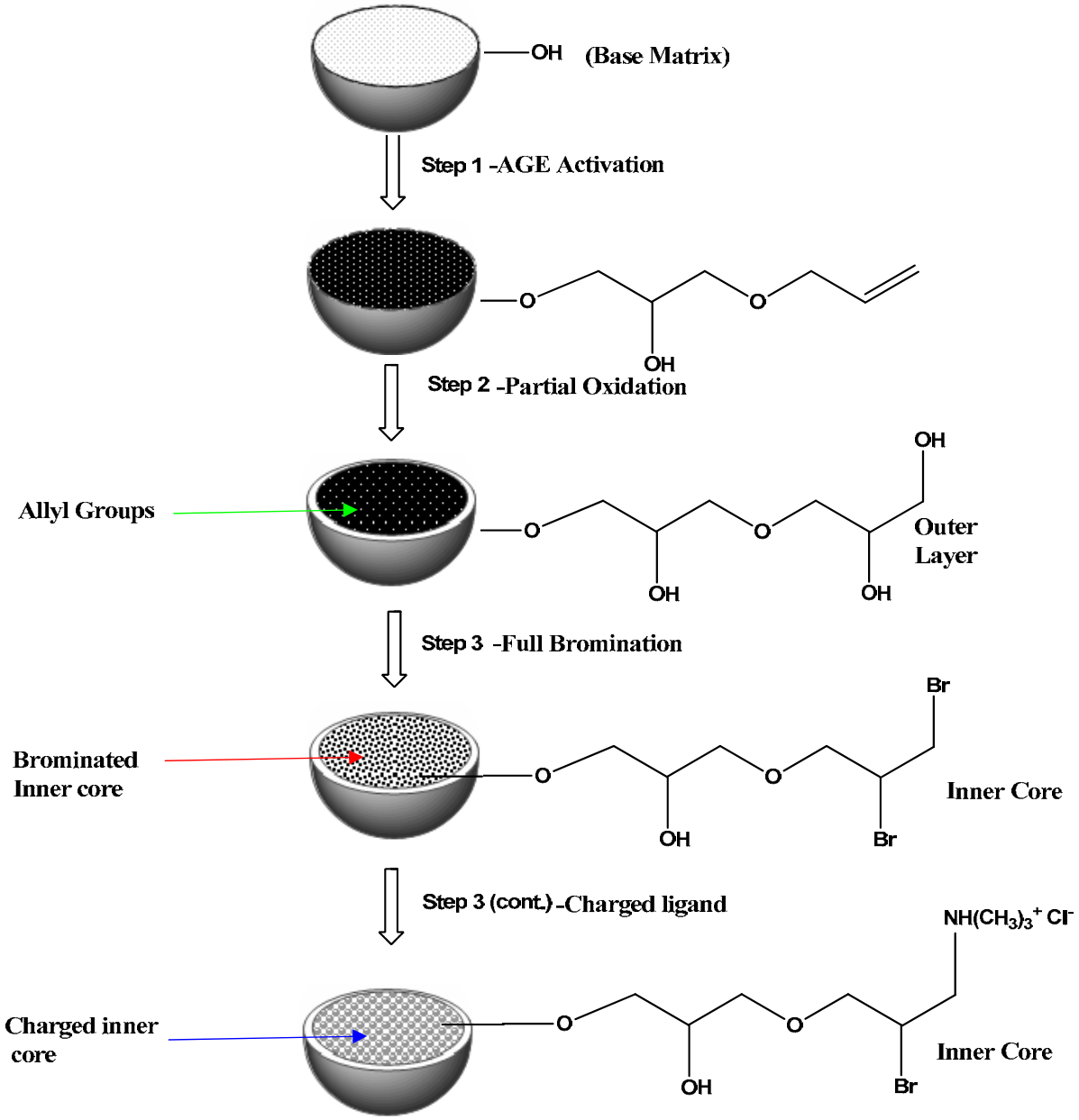

Figure 3.5: Preparation of SEC-AEC Sepharose CL-6B supports via Synthetic route 2. (step 1) NaOH, $NaBH_4$, Na_2SO_4, AGE, 50°C, 24 h.(step 2: method1) NaOH, $KMnO_4$, HCl, -4 °C, 1h, .(step 2: method 2) Dextran T500, $KMnO_4$, NaOH, Acetic acid, H_20_2 (step 3) Br_2, $N(CH_3)_3$.HCl, NaOH, $NaBH_4$, 24 h.

3.4.1.3 Synthetic route 3

Synthetic route 3 begins with the support been activated throughout with ECH (Figure 3.6). ECH reacts with hydroxyl groups present on the support, thereby introducing three membered epoxide rings throughout the bead. This is in contrast to synthetic chemistry routes 1 and 2, where the supports were initially activated with AGE. After the activation of the supports with ECH, the number of moles of ECH reacted with the support was determined by the epoxide assay (see Materials & Methods, Section 3.3.2.11). This allowed for calculation of the number of moles of acid or alkali required for the partial hydrolysis step (Step 2). The epoxide groups present on the surface of the bead are then hydrolysed (under basic or acid conditions) (Step 2) to create an SEC layer on the surface of the bead. In the last step of the synthesis the amine ligand is attached to the support, which introduces charge throughout the interior of the bead.

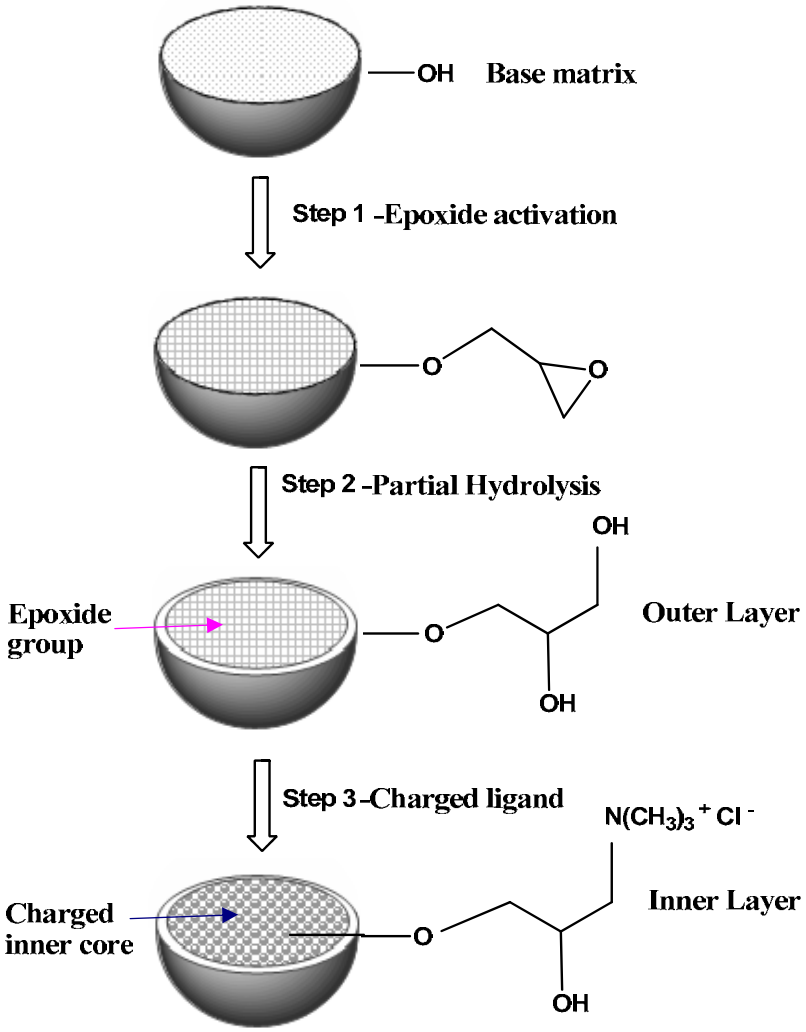

Figure 3.6: Preparation of SEC-AEC Sepharose CL-6B supports **via Synthetic route 3a.**(Step 1) NaOH, $NaBH_4$, ECH, RT., 24 h,(Step 2a) HCl, H_20 RT, 60s,(Step 2b) NaOH, H_20,RT, 60s (Step 3) EtOH, NaOH, $N(CH_3)_3$.HCl, 24 h, RT.

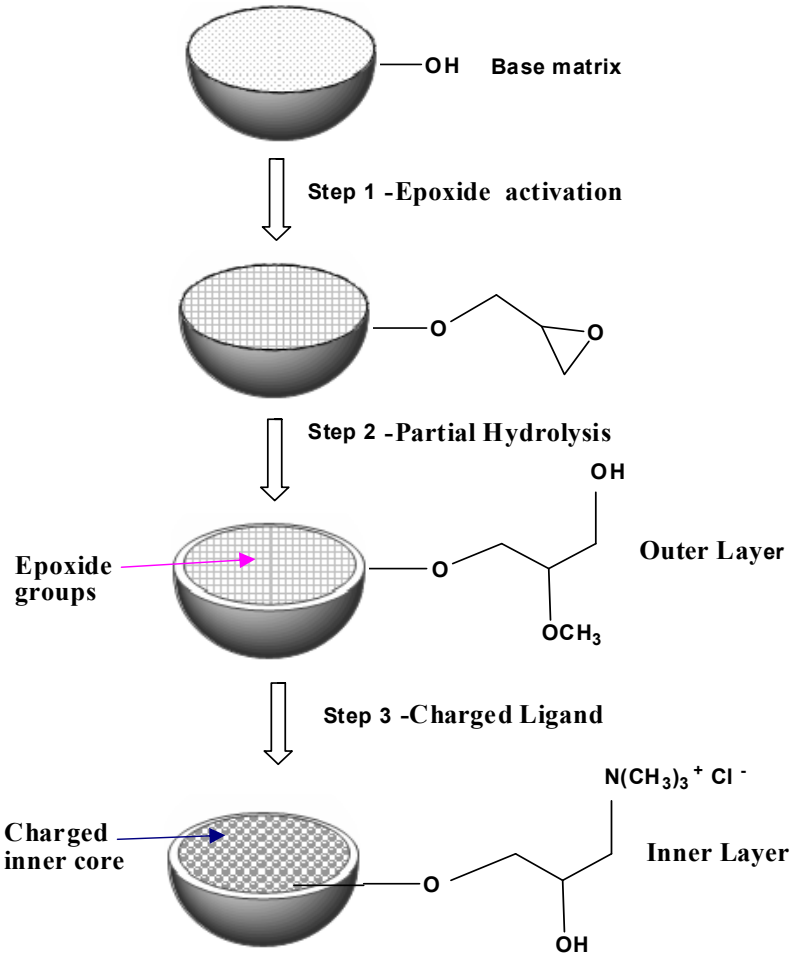

Figure 3.7: (a) Preparation of SEC-AEC Sepharose CL-6B supports via **Synthetic routes 3c & 3d**. (Step 1) NaOH, $NaBH_4$, ECH, RT, 24 h,(Step 2) [3] HCl, MeOH, RT, 60s, (Step 3) EtOH, $N(CH_3)_3$.HCl, NaOH 24 h, RT.

[3] Under basic condition the base reacts at the least substituted site on the epoxide ring

3.4.2 Characterisation and testing of supports created by synthetic routes 1, 2 & 3 at room temperature

The characterisation of the bi-layered supports was achieved by using a variety of chemical and biological assays. Firstly, allyl or epoxide group density measurements provided a way to control the thickness of the outer layer (Tables 3.1, 3.2, & 3.3). The ionic capacity assay verifies how much of the charged amine ligand reacted with the support and secondly indicates to what extent the ionic capacity of the modified supports was reduced.

3.4.2.1 Characterisation and testing of synthetic route 1

The assay results obtained for synthetic chemistry route 1 are tabulated in Table 3.1. The allyl group assay gives a indication of how many moles of AGE reacted in the activation step (step 1), and this value is then used as a control to measure exactly how many moles (%) should be reacted in the partial brominatation step in order to fabricate a layer on the outer surface of the support. However, from the results displayed in Table 3.1, it is apparent that there are discrepancies with the % estimated amount of bromine for the reaction and the actual amount that does react. For example the estimated 5% partial bromination eliminated 9.7% of the allyl groups, whereas an estimated 20% partial bromination corresponded to 18.6% loss in allyl groups. One reason for these results maybe due to errors in the assay for allyl groups, also bromine has a high density which makes it a very difficult chemical to pipette accurately. In all cases the aim was to achieve a value equivalent to theoretical required modification, but it is evident from the results that there are some discrepancies between the different assays. However, by combining all assay results a clear conclusion of the chemistry effects can be drawn.

Table 3.1: Allyl group density, ionic capacity, static protein and DNA binding capacities for supports prepared via Synthetic route 1a & 1b (Figure 3.0, Results from synthesis adapted from Gustavsson *et al*., 2004)

Support no	**Reaction conditions**	**Allyl groups (mmol/mL)**	**% Bromination (based on loss of allyl groups)**	**Ionic capacity (mmol Cl^-/mL)**	**% bromination (based on loss in ionic capacity**	**% bromination (mean)**	**Protein binding capacity (mg BSA/mL)**	**% reduction in protein binding**	**DNA binding capacity (µg plasmid/mL)**	**% reduction in pDNA binding**
1-1	Control	0.145	0	0.14	0	0	123	0	210	0
1a-1	5% bromination & blue dextran coupling	0.131	9.7	0.10	28.6	19.2	107	13.0	123	41.4
1b-1	5% bromination	0.133	8.3	0.13	7.1	7.7	118	4	196	6.7
1b-2	10% bromination	0.127	12.4	0.12	14.3	13.4	107	13.1	138	34.3
1b-3	15% bromination	0.123	15.2	0.09	35.7	25.5	95	22.8	116	44.8
1b-4	20% bromination	0.118	18.6	0.09	35.7	27.2	77	37.4	76	63.8

It is evident from the allyl groups/ionic capacity results (Table 3.1) that the reaction of allyl groups with bromine was achieved during **synthetic route 1a**. An increasing reduction in allyl groups/ionic capacity was observed with increasing additions of the bromine. The results displayed in Table 3.1 also show that the AGE/ partial bromination chemistry was not effective in creating an SEC-AEC bead. At 20% partial bromination, 64% of plasmid DNA binding was eliminated. Unfortunately it was shown that 37% of the protein binding capacity was also reduced.

In synthetic route 1b the attachment of dextran within the SEC layer slightly enhanced the effectiveness of the outer layer, acting as a protective barrier against DNA binding. The results (Table 3.1) for the dextran support revealed only 42% of plasmid DNA binding was eliminated with 13% of the protein binding capacity erased. This result was a slight improvement on the results obtained for synthetic route 1a, but these results show that neither synthetic routes 1a or 1b are successful in creating a bi-layered chromatography bead. As previously mentioned, the size exclusion layer must be as thin but as inert as possible so as to not compromise the protein binding capacity. However, it is evident from the results (Table 3.1) that the even when a thick size exclusion layer is created it is not completely inert, and plasmid DNA can bind to the outer surface. This is a clear indication that most of the bromine is diffusing into the pores of the support faster than it can react at the surface. It is however apparent that a certain amount of bromine is reacting at the surface of the bead, and with increasing volumes of bromine an increasing reduction is plasmid DNA binding is observed (Figure 3.8). The thickness of the brominated layer created on the surface, increased with increasing volumes of bromine, coinciding with decreasing protein binding (Shrinking core

behaviour). Reasons as to why this chemistry approach (synthetic route 1a; Gustavsson *et al*., 2004 & synthetic route 1b) was not effective in creating a thin inert outer layer on the surface of the bead have previously been discussed in more detail in Section 3.4.1.

3.4.2.2 Characterisation and testing of synthetic route 2

From the results displayed in Table 3.2 it is evident that **synthetic route 2** was unsuccessful in creating a bi-layered chromatography bead. It apparent from the results that the potassium permanganate did react with the allyl groups present on the support, as a reduction in the allyl groups and ionic capacity are observed after the partial oxidation step. However, plasmid DNA binding and allyl group results indicate there were two competing factors: the rate of reaction at the surface of the bead and the diffusion of the potassium permanganate into the pores of the support. The result show that the oxidation reaction eliminated 15% of the allyl groups which should have resulted in a thick SEC outer layer however this result only reduced 33% of the plasmid DNA binding. The low reduction in plasmid DNA binding highlights the fact that most of the potassium permanganate did not react at the surface of the bead but diffused into the inner core prior to reacting.

3.4.2.3 Characterisation and testing of synthetic route 3

The epichlorohydrin hydrolysis in **synthetic route 3** was again ineffective in developing a bi-layered chromatography support. This synthesis appears to be more susceptible to error than synthetic routes 1 and 2, with bigger deviations observed with epoxide hydrolysis step (Table 3.3). This could be due to the lower values obtained with epoxide activations therefore the assays are more prone to error at this very low

detection range. The greatest differences from the theoretical modifications are observed from the ionic capacity assay results. There are inconsistencies for all sets of data obtained from the ionic capacity assay (Tables 3.1-3.3), however by combining all the assay results it is possible to identify the effects that the chemistry had on modifying the support.

From the epoxide assay results (Table 3.3) the acid did react with the epoxide groups, as a decrease in epoxide groups is observed with increasing volumes of acid. It is apparent from the results (Table 3.3) that the rate of diffusion of the reagent into the pores is competing with the rate of reaction at the surface of the bead. Evidence for this statement is supported by both epoxide assay results/protein binding and plasmid DNA binding results. From the epoxide assay results it is apparent that all of the acid that was added reacted with the epoxide groups on the support, however the plasmid DNA binding results highlight the fact the only some of the chemical reacts at the surface of the bead. The 20% partial hydrolysis step eliminated 33% of the epoxide group content, indicating that the all the reagent added reacted with the support. However, only 62% of the plasmid DNA binding was reduced in the 20% partial hydrolysis step. The results for this synthesis are displayed in Figure 3.8.

Table 3.2: Allyl group density, ionic capacity, static protein and DNA binding capacities for supports prepared via Synthetic route 2 (Figure 3.4)

Support no	**Reaction conditions**	**Allyl groups (mmol/mL)**	**% oxidation (based on loss of allyl groups)**	**Ionic capacity (mmol Cl⁻/mL)**	**% oxidation (based on loss in ionic capacity**	**% oxidation (mean)**	**Protein binding capacity (mg BSA/mL)**	**% reduction in protein binding**	**DNA binding capacity (µg plasmid/mL)**	**% reduction in pDNA binding**
2-1	Control	0.145	0	0.14	0	0	123	0	210	0
2-2	5% oxidation	0.139	4	0.13	7	5.5	97	21	180	14
2-3	10% oxidiation	0.131	10	0.12	14	19	86	30	163	22
2-4	15% oxidation	0.123	15	0.10	28	21	78	36	142	32

Table 3.3: Epoxide group density, ionic capacity and static protein and DNA binding capacities for supports prepared via Synthetic route 3a (Figure 3.5 & 3.6)

Support no	**Reaction conditions**	**Epoxide groups (µmol/mL)**	**% hydrolysis (based on loss of epoxide groups)**	**Ionic capacity (mmol Cl⁻/mL)**	**% hydrolysis (based on loss in ionic capacity**	**% hydrolysis (mean)**	**Protein binding capacity (mg BSA/mL)**	**% reduction in protein binding**	**DNA binding capacity (µg plasmid/mL)**	**% reduction in pDNA binding**
3-1	Control	30	0	0.11	0	0	53	0	161	0
3-2	5% hydrolysis (H^+)	27	10	0.10	9	9.5	48	7	141	12
3-3	10% Hydrolysis (H^+)	25	17	0.09	18	17.5	42	27	135	16
.];p3-4	15% Hydrolysis (H^+)	23	23	0.07	36	29.5	37	30	98	39
3-5	20% Hydrolysis (H^+)	20	33	0.05	54	43.5	35	34	60	62

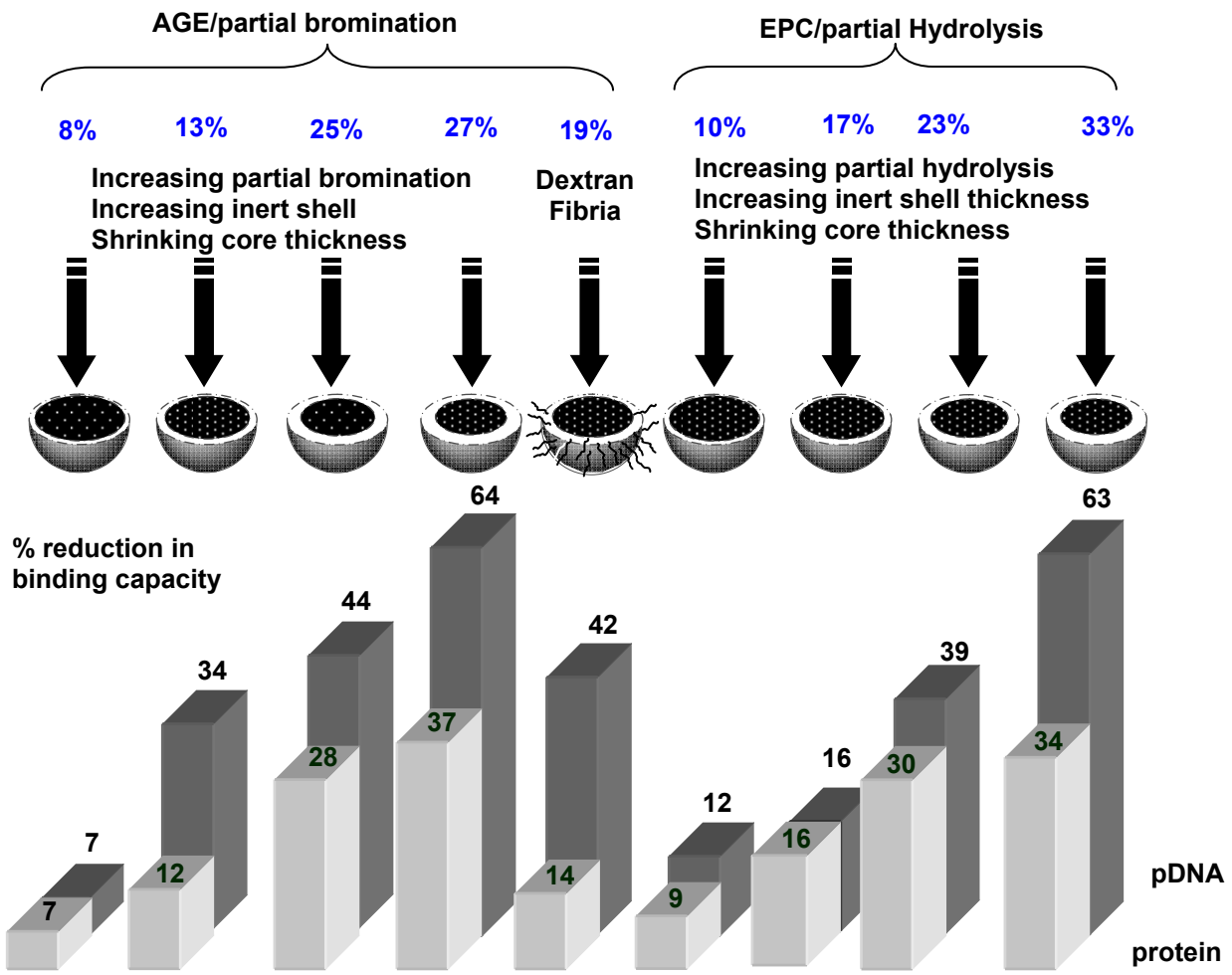

Figure 3.8: Impact of partial bromination (route 1a) and partial hydrolysis (route 3a) modifications (performed in aqueous solvents) on the reduction in static protein and plasmid DNA binding capacities of selected supports.

Table 3.4: Summary of all three synthetic routes tested (1a, 1b, 2, & 3a)

Synthetic route	Reaction conditions	Best result	Conclusion
1a	AGE activation ,bromine, H_20, bromination & Q coupling.	64% reduction in plasmid binding, 37 % protein binding reduced.	Not that effective in creating a bi-layered support. High protein binding losses observed with plasmid binding reductions.
1b	AGE activation, bromine H_20, Dextran tentacles attached , bromination & Q coupling.	42% reduction in plasmid, 14% protein binding reduced.	The attachment of dextran tentacles did slightly improved synthetic route 1.
2	AGE activation, (oxidation) potassium permanganate, bromination & Q coupling.	42% reduction in plasmid binding, 23% protein binding reduced.	Not as effective as synthetic route 1b in creating a bi-layered support. Least of successful of all chemistry routes tested.
3a	EPC activation , Hydrolysis (HCl in H_20), Q coupling.	63% reduction on plasmid binding, 34% protein binding reduced.	Not that successful in creating a bi-layered support. High protein binding losses observed with reductions in plasmid DNA binding. Similar result to synthetic route 1a, however lower protein binding (mg/mL) achieved overall with this synthesis .

To summarise Table 3.1-3.4 show that all of the synthetic routes (1-3) tested were successful, to varying degrees, at reducing plasmid DNA binding from the surface of the bead. Significant reduction in plasmid DNA binding was only achieved with high losses from the inner core (Figure 3.8). Synthetic route 1b was most successful maintaining protein binding whilst still achieving a reduction in plasmid DNA binding. It could be concluded that synthetic route 1b was the most effective route, but the 42% reduction in plasmid DNA was disappointing. As with all three routes employed the synthesis did not result in a support possessing two distinct layers because the SEC outer layer still

maintained point charges which permitted plasmid DNA binding. One reason why all these reactions did not produce a completely inert outer layer, was thought to be a result of the chemical reagent diffusing into the pores of the support faster than it could react at the surface of the bead. Another possible explanation with synthetic route 1 is due to the formation of mixed bromohydrin products during the bromination step.

Considerations of how to improve the rate of reaction at the surface of the bead, lead to investigating the already tested synthetic chemistry (synthetic routes 1-3) under different solvents conditions and the application of microwave technology. It was thought that the solvents in some cases may increase the rate of reaction, and also produce more effective chemical synthesis.

So far all the results for the reactions that were conducted at room temperature show that the diffusion rate is similar in magnitude to the rate of reaction at the surface of the bead. It was purposed that heating the mixture during the synthetic step for the creation of the outer layer might increase the rate of reaction relative to rate of diffusion. Recently, microwave heating has become an established technique in synthetic chemistry producing: faster; cleaner and more energy efficient processes (Kappe, 2003). The idea behind employing microwave heating in this study was that it could significantly increase the rate of reaction at the surface of the bead. Recent publications on the employment of microwave technology in the synthesis of chromatographic materials highlight the beneficial effects of microwave radiation in bioseparation support chemical synthesis (Gupta *et al*., 2007; Zhang e*t al*., 2007; Zhao *et al*., 2008).

The rate constant of a chemical reaction is described by the Arrhenius equation.

Equation 3.4

$$k = Ae^{-Ea/RT}$$

Where: k is the rate constant for a chemical reaction; A is the pre-exponential factor; T is the temperature; R is the gas constant, and Ea is the activation energy. From the Arrhenius equation (**Equation 3.4)** it is apparent an increase in temperature increases the rate constant and therefore increases the rate of the reaction. This phenomenon can be explained using collision theory as increased temperature produces a higher frequency of collisions between the reacting particles. Some authors think that in addition to increasing temperature microwave heating can also influence the pre-exponential factor and the activation energy (Adnadevic & Jovanovic, 2007). As previously described (Section 3.2.1) the alternating electromagnetic field from the microwave causes the molecules to collide and vibrate, it has been proposed that the pre-exponential factor and the activation energy are significantly lower with microwave heating than with conventional heating methods (Adnadevic & Jovanovic, 2007). This could be due to the effects of microwave on the orientation of the reacting molecules and therefore increasing the number of collisions resulting in reactions. In comparing microwave heating with traditional heating methods, a large number of chemical synthesises proved to be much more effective under microwave heating (Lidström *et al*., 2001; Adnadevic & Jovanovic, 2007; Heller *et al*., 2009).

3.4.3 Different Solvents and Microwave Synthesis

Prior to introducing microwave heating to the synthesis of modified supports the heating properties of numerous solvents were explored in a domestic microwave oven. These experiments were performed to gain information into how each solvent responded to

microwave heating over time, and to identify which solvents would be the most suitable for microwave chemical synthesis. As previously discussed in Section 3.2.1, dielectric materials absorb microwave energy and convert it to heat and the key parameter influencing a materials response to microwave energy is the loss of tangent. The higher the loss of tangent the greater a solvents ability to covert electromagnetic energy into thermal energy. The loss of tangent values for the different solvents employed in this study are displayed in Table 3.4.

Table 3.4: Tan delta values of different solvents (2.45 GHZ. 20 °C) (adapted from Kappe, 2003).

Solvent	**Tan Delta**
DMSO	0.825
Methanol	0.659
Water	0.123
Hexane	0.02

The experiments were conducted by placing two millilitre samples of each solvent in a microwave for 4 s and the temperature was recorded immediately afterwards. This was then repeated with fresh samples been heated for 8 s, 12 s, 16 s and 20 s. The results for these experiments are displayed in Figure 3.9. It was observed that DMSO heated most readily, followed by methanol, water, and then hexane. The results displayed in Figure 3.9 were as expected based on microwave theory (Section 3.2.1). DMSO, the solvent with the highest tan delta value, reached the highest temperature, whereas Hexane with the lowest tan delta solvent obtained the lowest temperature under microwave heating. The

next stage was to identify how the addition of chromatography supports to the solvents would influence the rate of microwave heating. Sepharose CL-6B was mixed with each of the previously tested solvents and this solvent-support mixture was subjected to the same microwave heating test as the pure solvents. The results for this experiment are presented in Figure 3.10

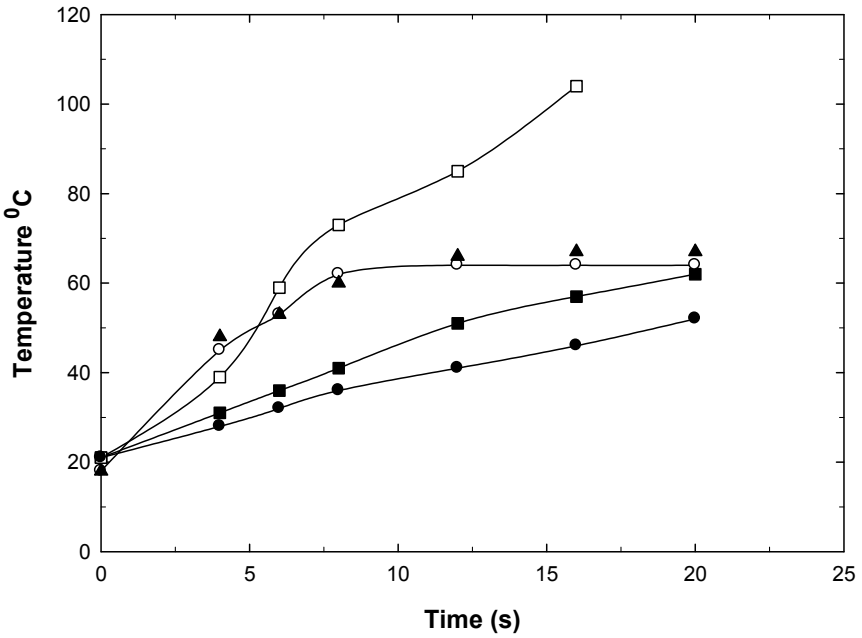

Figure 3.9: Microwave temperature effects of different solvents versus time. Symbols: (■) Water, (□) DMSO (●) Hexane (○) Methanol, & (▲) 72% Methanol 28% water solution.

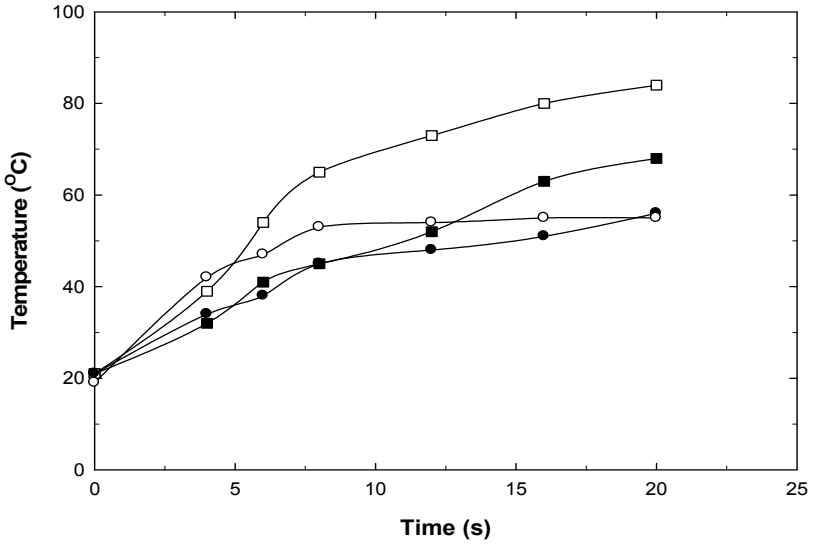

Figure 3.10: Microwave temperature effects of different solvents equilibrated with Sepharose CL-6B versus time. Symbols: (■) Water-support, (□) DMSO-support, (●) Hexane-support, & (○) Methanol- support

The data (Figure 3.10) acquired from the support-solvent heating experiment revealed what temperatures would be reached in the reaction flask during microwave chemical synthesis. Sepharose CL-6B is composed of 6% cross-linked polysaccharide and 94% water, both polysaccharides and water are polar compounds that can easily absorb microwave energy and convert it into heat (M^{c}Carty *et al*., 2002). The DMSO-support experiment reached the highest temperature after 20 s. Two millilitres of pure DMSO was heated in the microwave and the temperature recorded was 105°C after 15 s (Figure 3.9), however when 1 mL of DMSO and 1 mL of support are mixed and heated in the microwave the temperature reached just 82°C after 15 s (Figure 3.10). This is a significant reduction in the rate of heating. There are two factors that will contribute to this, firstly, the mixture of DMSO and support will have a greater mass than the pure DMSO and a higher heat capacity. Therefore the mixture requires more energy for a

given temperature rise than pure DMSO. The second contributing factor is the beads, comprising mainly of water have a lower loss of tangent value than DMSO. Therefore the DMSO solvent mixture would convert less of the microwave energy into heat.

The water-support experiment obtained the second highest temperature, after 15 s it reached a temperature of 60°C (Figure 3.10). The next highest temperature obtained was for the methanol-support, followed by the hexane-support mixtures. It is worth noting that in both experiments the temperature of the methanol reached a plateau. This is likely to arise due to methanol having reached its boiling point of 63°C.

3.4.3.1 Solvent and microwave effects on synthetic route 1

The results for synthetic route 1 with and without the use of microwave and DMSO are shown in Figure 3.11. Changing the solvent from water to DMSO in the partial bromination step at room temperature (Synthetic route 1c), clearly had a beneficial effect in reducing plasmid DNA binding on the surface of the support (Figure 3.11). A further 32% reduction in pDNA binding was observed when the partial bromination reaction was performed in DMSO, while a high protein binding capacity was maintained. The partial DMSO-Bromine reaction can follow two possible mechanisms (Figure 3.12). The first mechanism involves the bromine reacting with the allyl groups present on the surface of the bead, creating a dibromide product. Next the addition of sodium hydroxide can generate a bromohydrin, which is able to undergo an intramolecular etherification reaction with the base and be converted to an epoxide (Lang *et al*., 1998). Sodium hydroxide is added in excess so it was assumed that the epoxide was further hydrolysed to a diol. The reason why this mechanism significantly improved the inertness of the outer SEC may due to stabilisation of the positively charged bromide intermediate, by a dipole

in DMSO. This effect has been reported in literature (Lee *et al*., 2001). The first step in the second mechanism (Figure 3.12) for the DMSO-Bromine reaction consists of Bromine complexing with the DMSO and generating Hydrogen bromide (Aida *et al*., 1976). Hydrogen Bromide will then react with the allyl groups to create an alkyl-Bromide. Next the addition of the sodium hydroxide will convert the alkyl-bromide product to an alcohol (Clayden *et al*., 2001). Both mechanisms are possible, however the second mechanism will occur to a much lesser extent. Experimental results revealed that when DMSO and bromine were mixed together only one sixth of the amount of bromine added reacted with DMSO to generate hydrogen bromide.

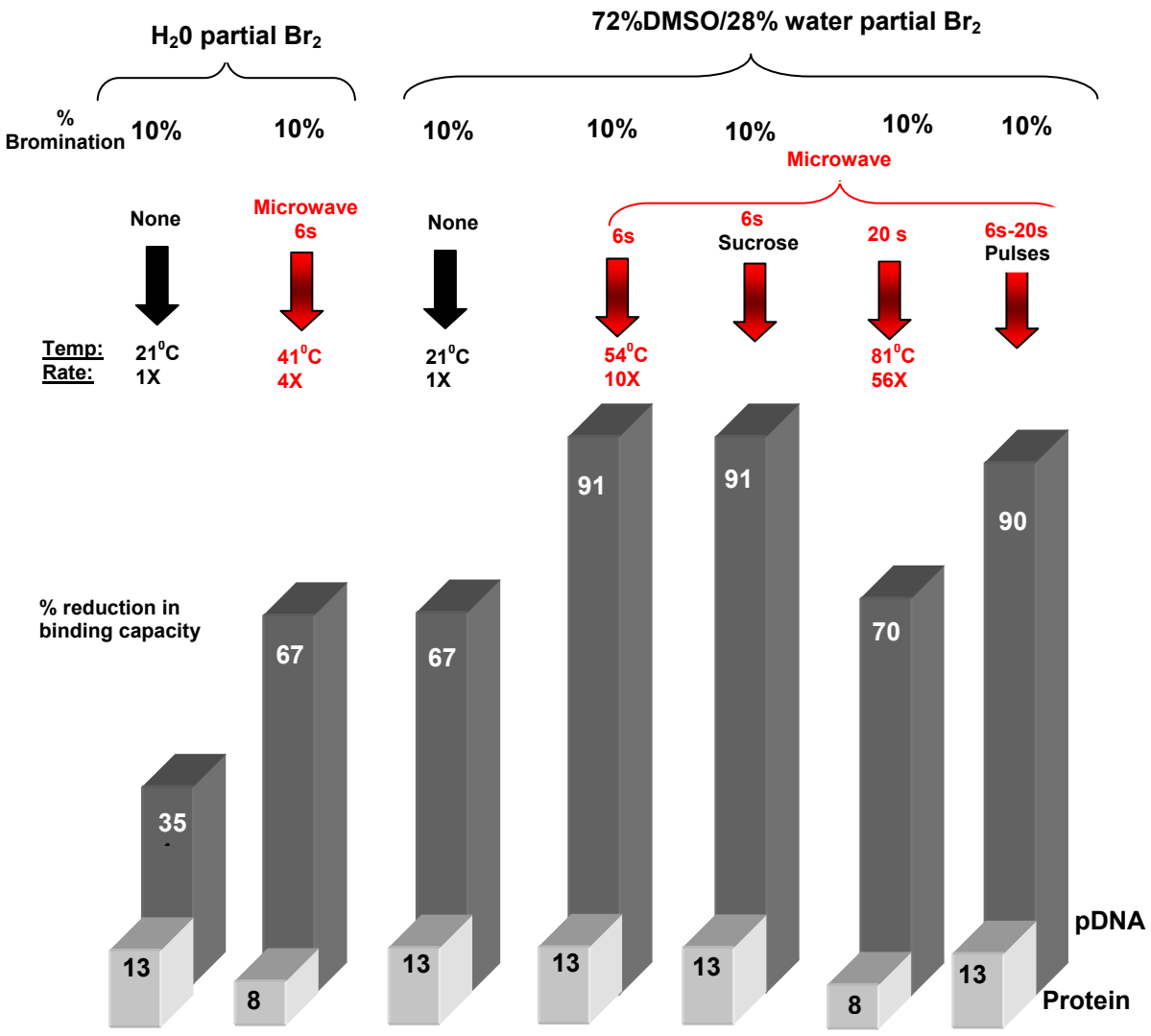

Figure 3.11: Impact of microwave and solvent on the production of pDNA and protein binding of supports modified by AGE synthetic route 1.0. (100% protein binding capacity = 123 mg/mL, & 100% pDNA = 101µg/mL)

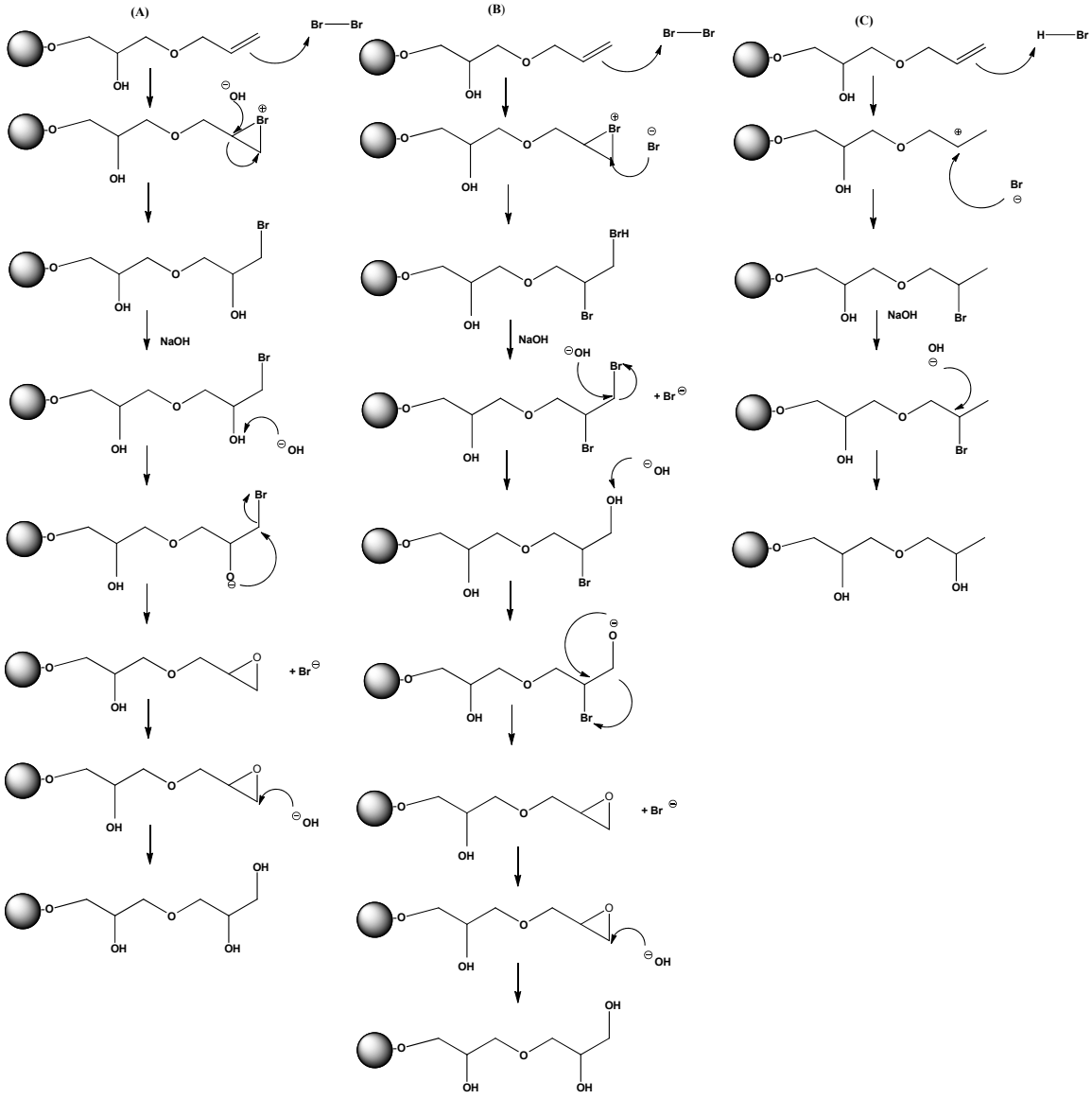

Figure 3.12: Mechanism for bromination and hydrolysis steps for the products formed on the surface of the bead during synthesis 1a and synthesis 1c, (a) t formation of the major bromohydrin product in water, (b) formation of bromide product in DMSO (mechanism 1) & (c) formation of bromide product in DMSO (mechanism 2). (Aida *et al*., 1976; Clayden *et al*., 2001).

The results displayed in Figure 3.11 also show the effects of microwave heating on the bromination reaction. From the results displayed in Figure 3.11, it is evident that microwave technology further increases the rate of reaction on the surface of the bead;

plasmid DNA binding is reduced with the employment of microwave heating while a high protein binding capacity was maintained. Improvements for both the bromination reaction in water and DMSO were observed with microwave heating. DMSO again proved to be the more effective solvent under microwave heating in comparison to water (Figure 3.11). This result would be expected as it was shown that the DMSO-support mixture reached a much higher temperature when compared to the water-support mixture (Figure 3.10). It is reported that for every 10°C rise in temperature the rate of reaction can be expected to double (Kappe, 2003). The temperature reached by the DMSO Sepharose CL-6B microwave experiment is approximately 55°C, so the rate of reaction might be expected to increase 8 times in comparison to if the reaction was performed with no microwave heating (21°C). The protein binding values for experiments performed with and without microwave heating were similar, however the difference in the plasmid DNA binding between the two supports was significant; a further 33% reduction in pDNA binding was achieved with microwave radiation. These results suggest that microwave heating produces a more inert SEC layer on the surface of the bead. Increasing the temperature appears to have increased the rate of reaction at the surface of the bead relative to the rate of diffusion of bromine into the pores of the support. Therefore ensuring all the bromine reacts at the surface, which is crucial for the formation of a complete inert outer layer.

Sucrose was introduced into the reaction conditions and the results are displayed in Figure 3.11. It is evident that same results were obtained for the microwave experiments performed both with and without sucrose. The concept behind saturating the solution with sucrose was to increase the viscosity of the solution in an attempt to slow the rate of the diffusion of bromine into the pores of the support, but this proved to be ineffective.

In order to investigate if the microwave effects were solely due to a rise in temperature, and hence an increase in the rate of reaction taking place on the surface of the bead, comparative experiments were carried out where a reaction flask was heated up to 54 ºC in a water bath. Fifty four degrees is the temperature recorded for a reaction flask containing a DMSO-support mixture after 6 s microwave heating (Figure 3.9). The results from these experiments are displayed in Figure 3.13. This data shows a greater enhancement of the chemistry was achieved by microwave heating, than was obtained using conventional heating. The binding results for the support prepared via microwave chemical synthesis revealed a further 24% decrease in pDNA binding compared with the support heated by the water bath, while similar protein binding capacities were maintained.

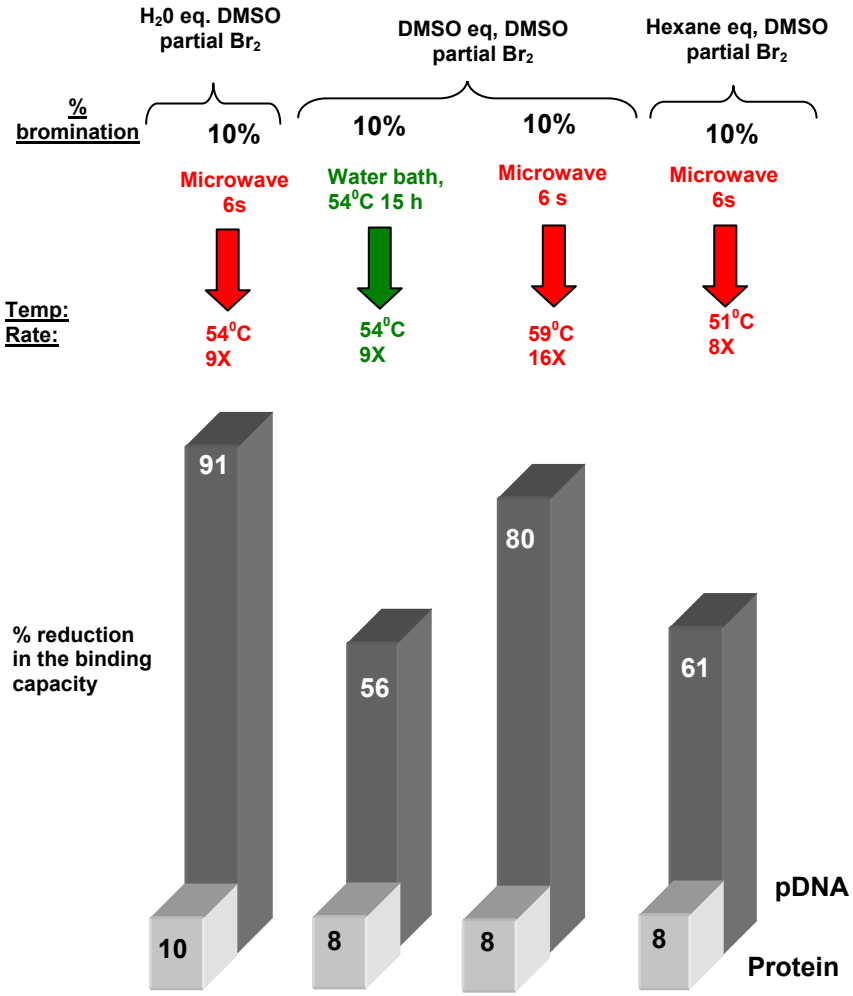

Figure 3.13: Impact of solvent and microwave treatment on the reduction of pDNA and protein binding of supports made by AGE, partial bromination chemistry. (100% protein=105 mg/mL & 100% plasmid DNA = 368 µg/mL)

One explanation for the difference in the results is that although the temperatures measured of the bulk solution were the same for both water bath and microwave heating. The temperature throughout the reaction flask heated in the water bath should have been uniform as it was given 24 hours to reach thermal equilibrium, in contrast, the rapid heating of the microwave sample would result in temperature gradients.

There would be a variety of dielectric properties present in the reaction flask from the DMSO in the bulk solution, water in the pores of the support, and the Sepharose beads. These dielectric properties would determine the temperature reached for each substance

present in the reaction flask under microwave heating and generate temperature gradients. It can be assumed that the water present in the pores of the supports would be cooler than the DMSO bulk solution in which the beads are suspended in. Previous experimental results showed that 2 mL DMSO reached a temperature of 105 ºC after 15 s of microwave exposure while 1 mL of DMSO mixed with 1 mL support (support made up of 94% water) reached a temperature of only 82°C after 15 s (Section 3.4.3). This is clear indication that it is the water in the pores that results in the reduction in the temperature observed, and this also corresponds with the tan delta values for water (Tan $\delta = 0.125$) compared to DMSO (Tan $\delta = 0.825$). It was difficult to determine the exact temperature of the beads and other researchers have reported similar difficulties with achieving accurate temperature measurements from domestic microwave ovens with solid support reactions (Lidström *et al*., 2001). The DMSO could heat the surface of the beads by heat transfer. It could also be the case that the supports due to their dielectric properties would heat up faster than the DMSO in the liquid phase, resulting in a faster reaction at the surface. It is however difficult to obtain data for the exact heat capacity and loss of tangent for cross-linked sepharose beads, to further support this statement. It can be concluded from the results that the mechanism by which heat is delivered by microwave heating proves to be more effective than traditional heating methods at increasing the reaction at the surface of the beads.

Different solvent conditions (Figure 3.13) were also explored in order to identify any experimental advantages of creating temperature gradients at the support/liquid interface. Firstly, the beads were equilibrated in a specific solvent (water, DMSO, and hexane) for 24 hours under gently mixing. Immediately before the reaction flask was placed in the microwave DMSO was added. The flask was heated in the microwave for 6 s. The

objective of this procedure was to have a different solvent in the bulk phase to that inside the pores. It was proposed that the differing response of the two solvents to microwave energy would result in a steep temperature gradient between the inside of the support and its surface. This in turn would increase the rate of the reaction at the surface relative to diffusion of Bromine into the pores.

The results for the reaction in which the beads were equilibrated in water and then reacted in DMSO appears to be slightly more effective, than using just DMSO in the reaction. From the loss of tangent values and specific heat capacities it is expected that the DMSO would heat up faster than the beads, containing a high percentage of water. If the DMSO is hotter than the contents of the beads this could increase the difference between the rate reaction of bromine at the surface compared to its rate of diffusion into the bead.

Comparing the effects of equilibrating supports with Hexane prior to the reaction is currently inconclusive, as the supports placed in hexane formed into clumps, which would have inhibited the bromine from reacting with all the sites present on the surface of the bead (Figure 3.13).

Next the DMSO-support time experiments were carried to investigate the effects of microwave heating the reaction over time. In these experiments five different reaction flasks were prepared under identical reaction conditions, except each flask was microwaved for a different length of time (4s, 8s, 12s, 16s, and 20s). The results for these experiments are displayed in Figure 3.14. The protein binding for the supports prepared in each experiment was the same. The plasmid DNA binding results show the greatest

reduction in binding was observed for the experiments heated for between 10 and 20 seconds.

Although it was identified from the microwave time experiments, that 12 s of microwave (Figure 3.14) radiation appeared to be the most effective. All the experiments further discussed in this study were still heated with the microwave for 6s so that comparisons could be made with previous results.

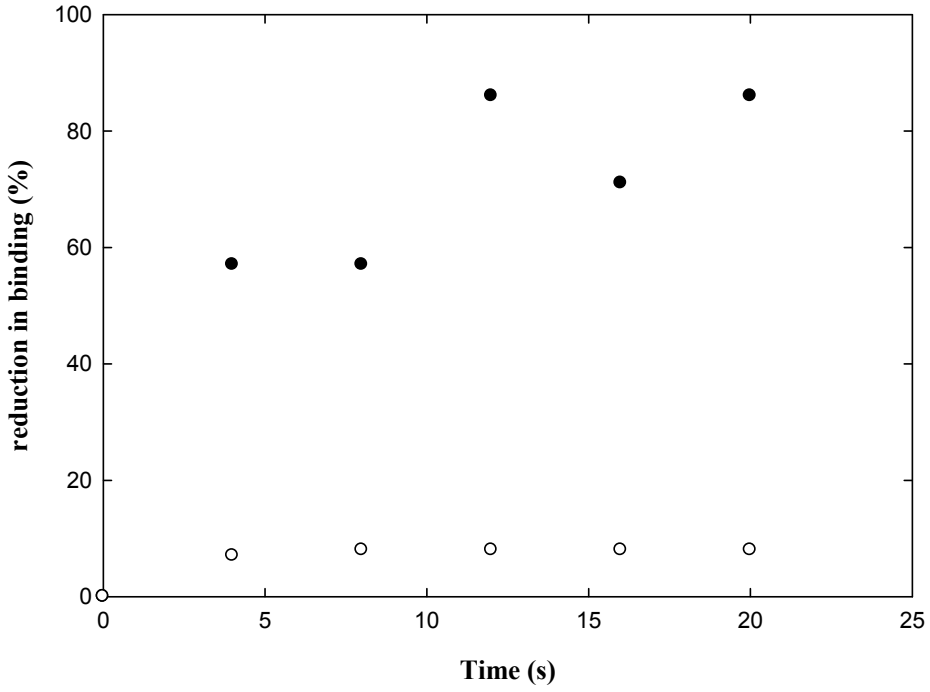

Figure 3.14: Microwave effects the reduction of both plasmid DNA and protein binding capacities over a range to times (0-20s). For SEC-AEC Sepharose CL-6B fabricated via synthetic route 1c. Symbols: (●) % reduction in pDNA, (○) % reduction in protein.

3.4.3.2 Microwave effects on synthetic route 2

To analyse the effect of temperature and the method of heating on synthetic route 2. The oxidation reaction was carried out under a range of temperatures using microwave and conventional heating. The results for these experiments are displayed in Figure 3.15. The reaction conditions for the experiments were the same as that described for the synthesis performed at room temperature. In addition to repeating the synthesis at room temperature the synthesis was also carried out at 41°C using a water bath and then at the same temperature using microwave heating. The experiments carried out at 4°C were prepared with a slightly different experimental method (Material & Methods: Section 3.3.2.4; Step 2, method 1).

The first set of data in Figure 3.15 represents the experimental results for the protein and plasmid DNA binding when the partial oxidation reaction was performed at 4°C. This choice of reaction temperature was taken from a procedure in which the oxidation of allyl groups with potassium permanganate was successfully carried at 4°C (Saegebarth & Wilberg, 1956). The results show that this temperature is not effective in the partial oxidation reaction for creating a bi-layered support.

The concept behind employing the water bath was again to compare traditional heating methods with microwave heating. The water bath experiments were carried out at 41ºC as this was the temperature recorded when an identical water-support mixture was heated in the microwave for 6 s (Figure 3.9). The results obtained from these experiments are displayed in Figure 3.15. The effects of microwave heating are evident, when comparing the three sets of data for the supports reacted under the identical reaction conditions with the exception of the heating methods employed. Firstly when comparing the supports

reacted at room temperature and a water bath at 41ºC there is little difference in the results, however the microwave modified beads appear to have had a similar reduction in the protein binding capacity but eliminating approximately 20 % more plasmid DNA binding. The reason as to why microwave heating proved more effective than conventional heating with a water bath (previously discussed in Section 3.4.3.1) is probably due to the temperature gradients that would be observed in the reaction flask under microwave heating. The water bath would achieve a uniform temperature of 41ºC throughout the reaction flask. Due to the different dielectric properties of the water, reagents, and solid supports, they would each interact differently with the microwave radiation and therefore create a temperature gradient. Experimental results have already shown (Section 3.4.3; Figures 3.8-3.9) that 2 mL of water reached a lower temperature than 2 mL of a water-support mixture when exposed to microwave heating for the same duration of time. This is a clear indication that the supports reach a higher temperature than the water in the bulk solution and the water in the pores of the support. If the supports reach a higher temperature than the water surrounding the supports, this could have increased the rate of reaction occurring at the surface of the beads. This explanation is based upon the fact that the results indicate that microwave heating has increased the rate of reaction relative to rate of diffusion to a greater extent than conventional heating.

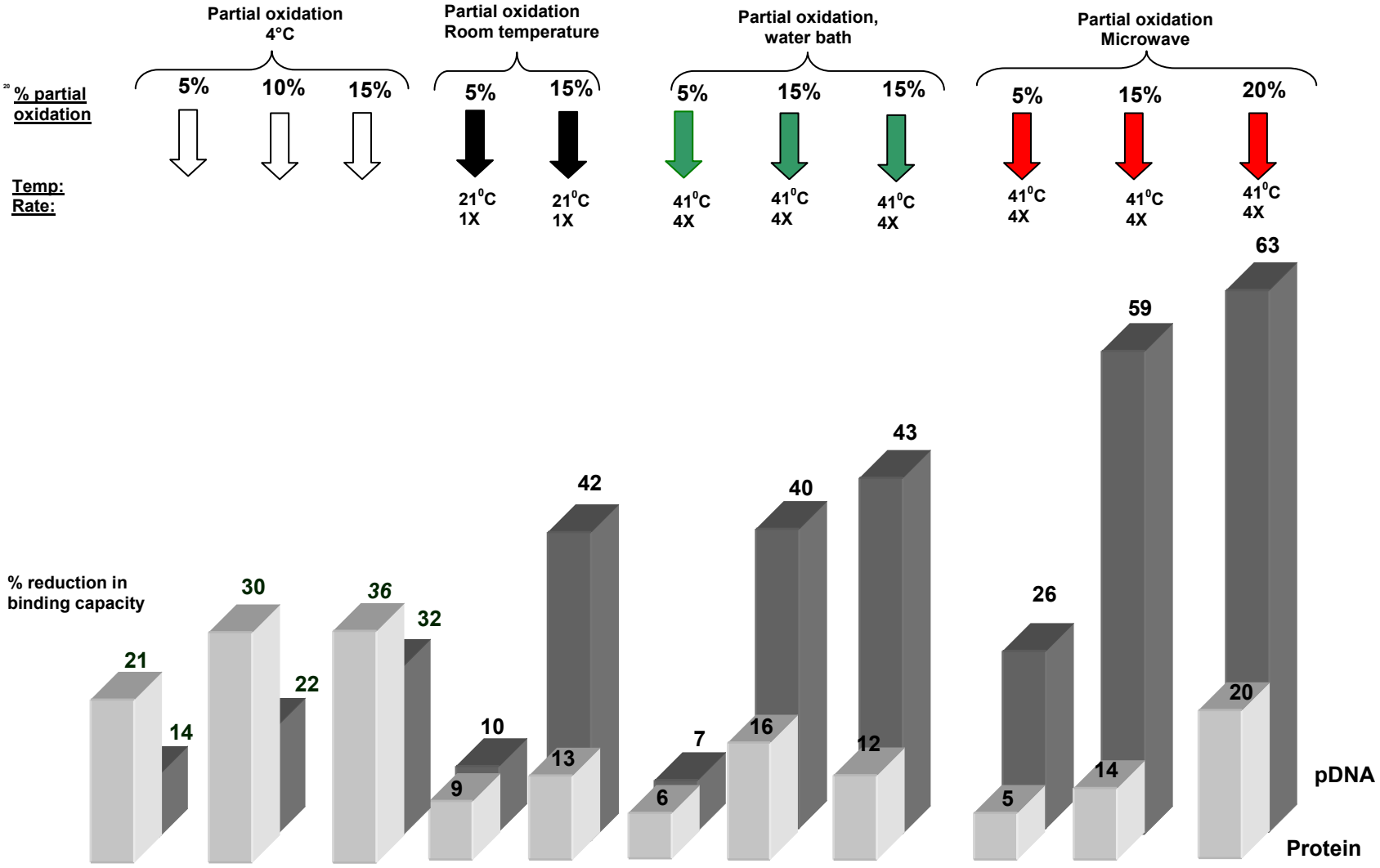

Figure 3.15: Impact of microwave treatment on the reduction of pDNA and protein binding of supports made by AGE, partial oxidation chemistry Supports reacted at 4°C were activated according to partial oxidation method 1, all other supports were activated according to partial oxidation method 2 (100% protein binding capacity = 80 mg/mL, & 100% pDNA = 191 µg/mL).

3.4.3.3 Solvent and microwave effects on synthetic route 3.

Next the Epichlorohydrin activation chemistry was tested under microwave conditions. Synthetic route 3a when carried out at room temperature proved to be unsuccessful in creating a bi-layered SEC-AEC adsorbent (Figure 3.16). The application of microwave technology in this synthesis again proved effective in further increasing the rate of the reaction on the surface of the bead (Figure 3.16) in both basic and acid conditions. A significant decrease in pDNA binding was also observed with supports prepared via microwave synthesis. The results show a 91% reduction in pDNA binding for the supports prepared via microwave heating under acidic conditions (synthetic route 3a) while a limited amount of the protein binding capacity was reduced (14%). This result again supports the fact that microwave heating appears to increase the rate of reaction at the surface of the bead relative to the rate of diffusion. The consequence of this is a support with a size exclusion outer layer that does not significantly reduce the binding capacity of the inner core. The explanation for this effect has been discussed in detail in sections 3.4.3.1 and 3.4.3.2.

The reaction of epoxides with sodium hydroxide is reportedly slow and can take up to 24 hours at room temperature. Patel and co workers (1999) previously showed that only 30% of the epoxide groups were hydrolysed under basic conditions after a period of 24 hours. The results for the synthesis performed with microwave heating and basic conditions show that a 65% reduction in pDNA binding was observed but this was at the expense of 30% reduction of the protein binding capacity. It is clear from the results displayed in Figure 3.16 that the hydrolysis of the epoxides with sodium hydroxide has taken place in a matter of seconds with the assistance of microwave heating. However, although the results (Figure 3.16) in this study show that microwave heating has increased the rate of reaction,

it is evident that the hydrolysis of epoxides with sodium hydroxide would not be suitable for creating a bi-layered support due to the high reduction in protein binding, and that the acid hydrolysis is a better approach.

In previous work completed by Sabitha and co workers (1999), it was reported that the synthesis of epoxides (aminolysis of epoxides) in dry media via microwave technology produced extremely positive results. The researchers obtained higher yields and much faster reaction times were achieved, in comparison to when the reaction was carried out under conventional heating methods (Sabitha *et al*., 1999).

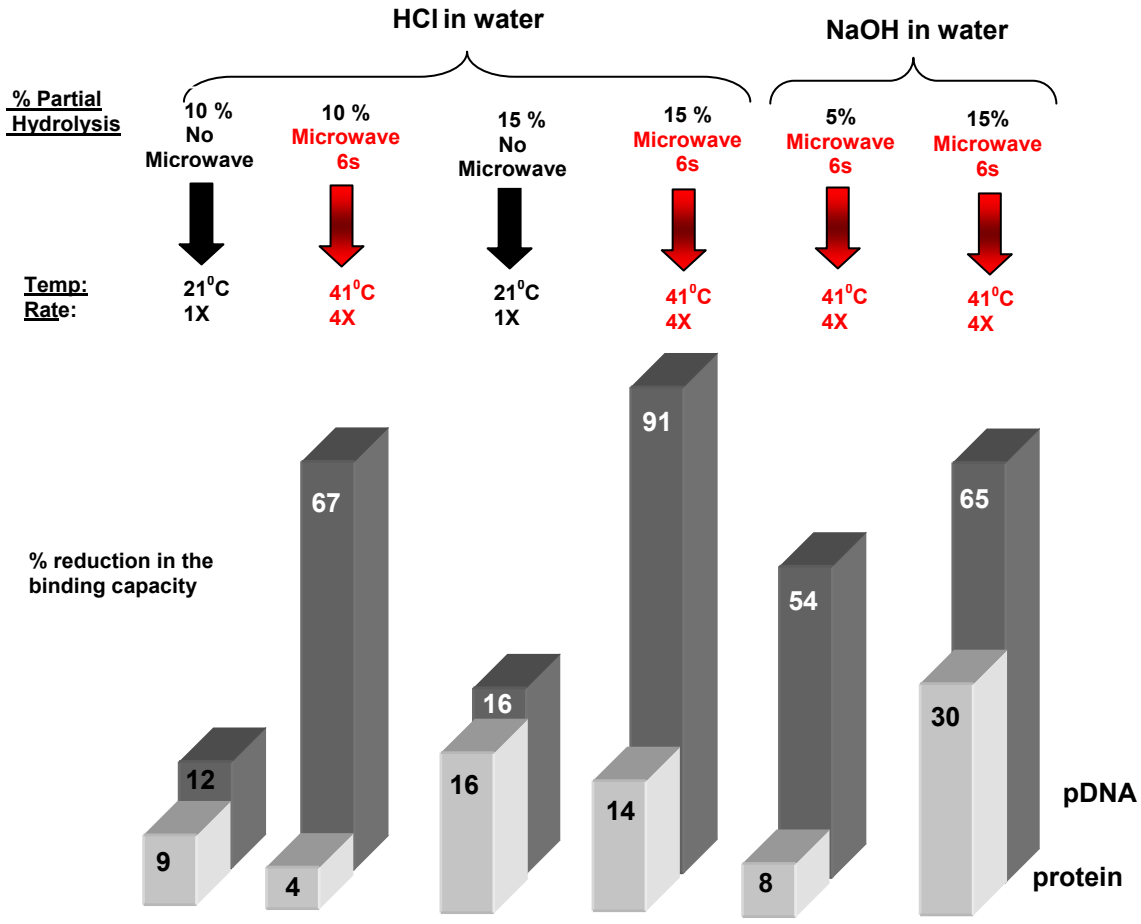

Figure 3.16: Impact of microwave treatment on the reduction of pDNA and protein binding on supports made by EPC, hydrolysis step in synthetic routes 3 & 3. (100% protein binding capacity = 53 mg/ml, & 100% pDNA = 161 µg/ml)

Previously the hydrolysis step in synthetic routes 3a and 3b was carried out in water under both acid and alkali conditions. As already discussed the hydrolysis step under basic conditions was not as successful as under acidic conditions. This section describes the effects of changing the solvent from water to methanol in the hydrolysis step (synthetic routes 3c & 3d). Under acidic conditions using methanol as a solvent yielded large reductions in pDNA binding with only a limited reduction in protein binding at both room temperature and under microwave heating (synthetic route 3c). Under basic (synthetic route 3d) conditions at room temperature the reaction produced a very small

reduction in pDNA however using microwave heating the results with methanol were better than under the same conditions with water as a solvent.

The results for the experiment under acidic conditions in methanol (synthetic route 3c) at room temperature showed a 77% reduction in plasmid DNA binding with high protein binding capacities maintained (14% reduction) (Figure 3.17). This was much better than under the same conditions with water as a solvent. The chemistry under methanol-acid conditions results in the opening of the epoxide ring at the most substituted carbon site, where protonation by the acid on the oxygen produces a positive charged intermediate, and the methoxide then attacks at the carbon where the most positive charge is located. This is in contrast to what occurs under water conditions where, it is an hydroxyl that attacks at this site. The application of microwave heating in synthetic routes 3c produced a slightly improved reduction in pDNA binding along side a smaller reduction in protein binding. Prior experimental results (Figure 3.10) showed that the methanol-support mixture heated up faster than the water-support experiment. Methanol has a higher tan delta value (0.659) than water (0.123) and so this result would be expected. This additional rise in temperature with the methanol experiments seemed to further enhance the rate of reaction on the surface of the bead. It was difficult to determine from prior experiments (Section 3.4.3) if the beads were hotter than the solvent present in the reaction flask due to the fact that the solvent reached boiling point very quickly under microwave heating.

The hydrolysis step under basic conditions in methanol results in the methoxide reacting at the least substituted carbon site, and is slower than when the reaction is performed under acidic conditions. Microwave effects again proved beneficial in synthetic route 3d

where an extra 72% reduction in pDNA binding was observed in comparison to the unmicrowaved synthesised sample and limited amounts of the charged inner core were reduced (Figure 3.17).

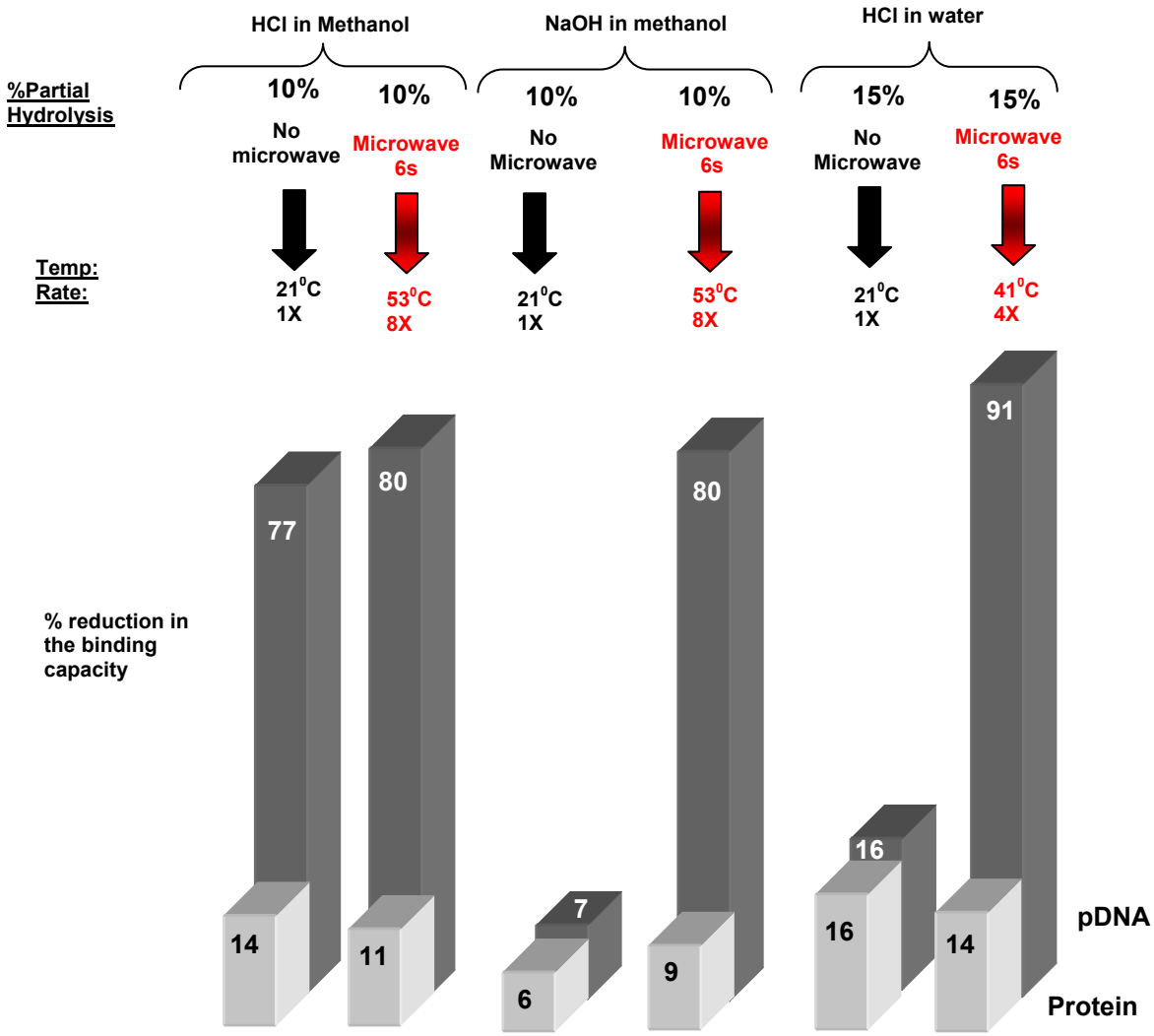

Figure 3.17: Impact of microwave treatment on the reduction of pDNA and protein binding on supports made by EPC, partial hydrolysis synthetic route. (100% protein binding capacity = 53 mg/ml, & 100% pDNA = 159µg/ml).

3.5 Summary of all three synthetic chemistry routes and reaction conditions studied

This study began by initially testing chemistry methods previously published by Gustavsson *et al*. (2004) (**synthetic chemistry route 1**). The results for this synthesis showed that point charges still remained in the SEC layer which allowed for substantial amounts of plasmid DNA binding and that even when a thick inert outer layer was created high levels of plasmid DNA binding was still observed. The effects of dextran tentacles incorporated into outer SEC layer were then investigated. The concept of the dextran tentacles was that they might act as a protective barrier preventing DNA from reaching the surface of the bead. Although the dextran tentacles slightly reduced plasmid DNA binding from the surface of the bead, high levels of plasmid DNA binding were still occurring. Different solvent conditions for the synthesis were then explored, where water present in the bromination step was replaced with DMSO. It was thought that DMSO would eliminate the mixed bromohydrin products forming on the surface of the bead when the bromination step was performed in water. The results for the DMSO-Bromine reaction were positive with a further 32% reduction in plasmid DNA binding while the protein binding capacity remained the same. Microwave heating was then employed in synthetic route 1 to further increase the rate of reaction occurring at the surface of the bead, this again proved to be effective in improving the synthesis. The results showed a further a 24% reduction in plasmid DNA binding in compared to when the synthesis was completed at room temperature whilst protein binding value was similar under both conditions.

Synthetic route 2 is identical to synthetic route 1 with exception that the bromination step is replaced by an oxidation step. This endeavour was again to try and improve on the

results already obtained for synthetic route 1. The results for synthetic route 2 showed that the oxidation reaction did not occur fast enough at the surface of the bead. The synthesis was then tested under different reaction temperature conditions: 4ºC; room temperature; water bath, and microwave, in an effort to improve on the results already observed. Overall the results showed this synthetic approach to be unsuccessful.

Synthetic chemistry route 3 was a completely different to the other two approaches tested (synthetic chemistry routes 1 & 2). This novel chemistry route was created with the aim of further enhancing the results observed from the previously tested chemistry routes. The second step of synthesis was initially performed with water and HCl. This second step in the synthesis is the key to the successfully creating a bi-layered support. When water was used as the solvent the results showed that the reaction conditions were only partially effective in producing the acquired result, with point charges still present in the SEC layer after the synthesis was complete. It was thought that changing the solvent from water to methanol might further improve the synthesis, by increasing the rate of reaction at the surface of the bead. The reaction in methanol produced some very positive results, with 80% of the plasmid DNA binding eliminated and only 11% of the protein binding capacity reduced (reaction conditions-acid hydrolysis in methanol). Microwave heating was again employed in this synthesis in an effort to optimize the results already observed. The results showed in some cases microwave heating appeared to increase the rate of reaction at the surface of the bead when compared to the results from when the reaction was carried out at room temperature. However synthetic route 2 produced lower ligand activation values and therefore lower protein binding capacities were observed in the inner core, making this approach less appealing than synthetic chemistry route 1.

In comparing all three synthetic chemistry routes and reaction conditions tested, synthetic chemistry route 1c using DMSO as a solvent, with microwave heating, proved to be the most effective in creating a bi-layered support. Using these conditions a 91% reduction in plasmid DNA binding with only a 13% reduction in protein binding was achieved. This chemistry approach also produced high ligand coupling values, which enabled a high protein binding capacity (mg/mL) in the inner core after the layer had been created.

3.6 Conclusions and future work

Current commercially available packed bed chromatography supports for the purification of large biomolecules result in many purification problems. These problems are due to the physical properties of these large nanoplex products and the fact that packed bed chromatography supports are not designed to purify nanoparticulates. The results are low binding capacities, poor selectivity, and co elution of the target product with contaminants. A bi-layered packed bed chromatography support could resolve many of the problems discussed above for purification of nanoparticulates.

In this study three different synthetic chemistry approaches were tested in an attempt to create a bi-layered chromatography support. Different solvent chemistries were explored with positive results obtained for both synthetic route 1 and 3. However, all the synthetic chemistry routes performed at room temperature proved ineffective in achieving the experimental goal of creating a ‘restricted access support’ with a thin inert outer layer and charged inner core. With the only exception been the support that was prepared by the partial acid hydrolysis in methanol (synthetic route 3), in which the reaction proved to be very successful at room temperature.

Microwave heating was employed in attempt to increase the rate of reaction at the surface of the bead. Comparing the results obtained from both experiments executed with and without microwave technology, it is obvious that the application of microwave radiation has beneficial effects on the reaction taking place on the surface of the support. In some cases the reaction appeared to be very slow at room temperature however after the application of microwave heating, the reaction rate increased significantly (for example the sodium hydroxide, hydrolysis, in methanol). It was shown from the experimental results that the beads typically reached a higher temperature than the solution surrounding the beads. The experiments that were performed in a solvent with a higher tan delta value produced better results than reactions carried out in a lower tan delta solvent. These results would be expected as according to microwave theory the higher the tan delta value of the solvent the greater the temperature it will reach under microwave heating, and with an increase in temperature the reaction would be expected to increase and occur faster on the surface of the bead. This increase in the rate of reaction ensured that all the reagent reacted at surface of the bead rather than diffusing into the pores of the support, therefore the possibility of point charges been introduced into the layer was reduced and the overall performance of the bead was improved with microwave heating. It was thought that this chemistry synthesis conditions developed in this study maybe useful for other applications requiring a bi-layered support i.e. a bi-layered expanded bed adsorbent and this investigation is discussed in more detail in Chapter 4 and the Appendix.

The microwave procedures completed to date were done in a conventional microwave oven. Repeat experiments will be done in a laboratory microwave in which controlled experimental conditions can be employed. Under these conditions more reproducible results should be obtained and optimisation of the microwave heating process including timing and temperature.

Future work should involve testing the modified supports, identified by this study as been the most successful, under dynamic binding conditions in a packed bed chromatography column.

3.7 References

Aida T., Akasaka T., Furukawa N., Oae S. (1976) Catalytic Reduction of Sulfoxide by bromine-hydrogen bromide system. *B. Chem. Soc. Japan* **49**: 1117-1121.

Adnadevic B., Jovanovic J. (2007) Comparison of the kinetics of conventional and microwave methyl methacrylate polymerisation. *J. Appl. Polym. Sci.* **104**: 1775-1782.

Berg H., Busson P., Carlsson M. (2005) Chromatographic two-layer particles. International patent number US2005/024037.

Bergström J., Berglund R., Soderberg L. (2002) Process for introducing functionality. International patent number WO98/39364.

Bosma J.C., Wesselingh J.A. (1998) pH dependence of ion-exchange equilibrium of proteins. *AIChE. J.* **44**: 2399-2409.

Brimicombe M. (1990) Physics in focus. Nelson and sons publishers 1st edition: 468.

Mingoes P., Camelia G., Gabrial S., Grant E., Halstead B. (1998) Dielectric parameters relevant to microwave dielectric heating. *Chem. Soc. Rev.* **27**: 213-224.

Clayden J., Greeves N., Warren S., Wothers P. (2001) Organic Chemistry. Oxford press 1ST Edition: 513.

Dapurkar S.E., Patel K M., Tale R.H. (2003) An extremely simple, convenient and mild one-pot reduction of carboxylic acid to alcohols using 3, 4, 5-trifluorophenylboronic acid and sodium borohydride. *Tetrahedron Lett.* **44:** 3427-3428.

Diogo M.M., Queiroz J.A., Prazeres D.M.F. (2005) Chromatography of plasmid DNA. *J. Chromatogr. A* **1069**: 3-22.

Dunnill P., Levy S.M., O' Kennedy R.D., Ayazi-Shamlou P. (2000) Biochemical engineering approaches to the challenges of producing pure plasmid DNA. *Trends Biotecnol.* **18**: 296-305.

Gupta N.M., Mondal K ., Solanki K. (2007) Microwave-assisted preparation of affinity medium. *Anal. Biochem.* **360**: 123-129.

Gustavsson P.E., Lemmens R., Nyhammar T., Busson P., Larson P.O. (2004) Purification of plasmid DNA with a new type of anion-exchange beads having a non-charged surface. *J. Chromatogr. A* **1038**: 131-140.

Heller E., Lautenschläger W., Holsgrabe U. (2009) Real time observation of microwave enhanced reaction via fast FTIR spectroscopy. *J. Tetrahedron Lett.* **50**: 1321-1323.

Honda Y., Kataoka Y., Unno M. (1987) Syn-epoxidation of chiral (z)-2-methyl-3-alkenal acetal via stereo-selective bromohydrin formation. *Chem. Lett.* **16:** 2133-2134.

Ikeda I., Kida T., Kim T.S., Nakatsuji Y. (1996) Preparation and properties of multiple ammonium salts quaternized by epichlorohydrin. *Langmuir* **12**: 6304-6308.

Kepka C., Lemmens R., Vasai J., Nyhammer T., Gustavsson P.E. (2004) Integrated process for purification of plasmid DNA using aqueous two-phase system combined with membrane filtration and lid bead chromatography. *J. Chromatogr. A* **1057:** 115-123.

Kappe C.O. (2003) Microwave-enhanced Chemistry-Enabling Technology Revolutionizing Organic Synthesis and Drug Discovery. *Future drug discovery* **43**: 1217-1224.

Kappe C.O. (2004) Controlled Microwave heating in modern Organic synthesis. *Angew. Chem. Int*. **43**: 6250-6284.

Kappe C.O., Standler A. (2005) Microwave in Organic and Medicinal Chemistry. Wiley-VCH publishing, Germany. 1st edition **25**:12.

Lang F., Kassab D.J., Ganern B. (1998) Neighboring group effects in the regioselective cyclization of vicinal *trans*-1, 2-bromohydrins to epoxides. *Tetrahedron Lett.* **39**: 5903-5906.

Lee E.J., Um Hwan I., Jeon S.E. (2001) Contrasting solvent effect profiles for alkaline hydrolyses of Paraoxone and Parathione in DMSO-H_20 mixtures. *Bull. Korean Chem. Soc.* **22**: 1301-1302.

Leffek K.T. (1963) Secondary kinetic isotope effects in biomolecular nucleophilic substituations. *Can. J. Chem.* **42**: 851-859

Lidström P., Tierney J.P. (2005) Microwave assisted organic synthesis. Blackwell publishing CRC Press: 7.

Lyddiatt A., O'Sullivan D.A. (1998) Biochemical recovery and purification of gene therapy vectors. *Curr. Opin. Biotechnol.* **9**: 177-185.

Matsumoto I., Mizuno Y. (1979) Activation of Sepharose with epichlorohydrin and subsequent immobilization of ligand for affinity adsorbent. *J. Biochem*. **85**: 1091-1098.

M^{c}Carty S.P., Korokenyi B. (2002) Microwave-assisted solvent-free or aqueous-based synthesis of biodegradable polymers. *J. Polym. Environ*. **10**: 93-104.

Morenweiser R. (2005) Downstream processing of viral vectors and vaccines. *Gene Ther.* **12**: 103-110.

Oliveira M.E.C., Franca A.S. (2002) Microwave heating of foodstuffs. *J. Food Eng.* **53**: 347-359

Patel N.R., Goswami A., Totleben M.J., Singh A.K. (1999) Stereospecific enzymatic hydrolysis of racemic epoxide: a process for making chiral epoxide. *Tetrahedron-Asymmetr.* **10**: 3167-3175.

Pitfield I.D. (1992) Perfluorocarbon chromatographic supports. PhD Thesis, University of Cambridge, UK.

Porath J., Sundberg L. (1974) Preparation of adsorbents for biospecific affinity chromatography: I. Attachment of group-containing ligands to insoluble polymers by means of bi-functional oxiranes. *J. Chromatogr. A* **90**: 87-98.

Queiroz J.A., Sousa F., Prazeres D.M.F. (2008) Affinity chromatography approached to overcome the challenges of purifying plasmid DNA. *Trends Biotechnol.* **26**: 518-525.

Sabitha G., Reddy B.V., Abraham S., Yadav J.S. (1999) Microwave promoted synthesis of β-aminoalcohols in dry media. *Green Chem.* **1**: 251-252.

Saegebarth K.A., Wiberg K. (1956) The mechanism of Permanganate oxidation IV. *Am. Chem. J.* **79**: 2822-2824.

Seyfried L., Garin F., Marie G., Thiebaut J.M., Roussy G. (1993) Microwave Electromagnetic field effects on reforming catalysts. *J. Catal.* **148**: 281-287.

Thostenson E.T., Chou T.W. (1999) Microwave processing fundamentals and applications. *Composites Part. A* **30:** 1055-1071.

Watley B., Lidström P., Tierney J.P., Westman J. (2001) Microwave assisted organic synthesis- a review. *Tetrahedron* **57**: 9225-9283.

Wu N., Ataai M. (2000) Production of viral vectors for gene therapy applications. *Curr. Opin. Biotechnol*. **11**: 205–208.

Zhang Y.P., Ye X.W., Tien M.K., Qu L.B., Lee K.P. (2007) Novel method to prepare polystyrene-based monolithic columns for chromatographic and electrophorectic separations by microwave radiation. *J. Chromatogr. A* **1188**: 43-49.

Zhang X., Hayward D. (2006) Applications of microwave dielectric heating in environment-related heterogeneous gas-phase catalytic systems. *Inorg. Chim. Acta* **359:** 3421–3433.

Zhang S., Sun Y. (2002) Study of protein adsorption kinetics to a dye-ligand adsorbent by the pore diffusion model. *J. Chromatogr. A* **964**: 35-46.

Zhao Z., Li Z., Xia Q., Xi H., Lin Y. (2008) Fast synthesis of temperature sensitive PNIPAAMm hydrogels by microwave radiation. *Eur. Polym. J*. **44**: 1217-1224.

4. CHROMATOGRAPHY SUPPORTS AND MICROWAVE HEATING

4.1 Abstract

The use of microwaves in the chemical synthesis of materials is gaining importance. Microwave assisted synthesis is: generally faster; can increase yields; reduce side reactions; improve reproducibility, and is more environmentally friendly in comparison with traditional heating methods. The results displayed in chapter 3 show that microwave heating enhanced the rate of the reaction on a chromatography bead. It is therefore highly beneficial to identity which types of chromatography support can with stand microwave radiation. In this study, the effects of microwave heating on numerous bioseparation supports were investigated. After the beads were exposed to microwave heating, they were examined using: image analysis; size distribution, and micromanipulation. Image analysis was achieved by employing light microscopy and scanning electron microscopy. The size measurements of the beads were obtained from a mastersizer and the mechanical properties of selected beads were tested using micromanipulation. It can be concluded from the results obtained that only certain bioseparation supports can undergo microwave heating and therefore can be employed for microwave chemical synthesis.

4.2. Introduction

Microwave irradiation is becoming an increasingly popular technique for heating materials in chemical laboratories, offering a clean, cheap, convenient, selective and instantaneous method of heating (Toukoniitty *et al*., 2005). Using microwaves can reduce chemical reaction times from hours to minutes (Kappe, 2004). It is also known to reduce side

reactions, increase yields, and improve reproducibility (Kappe, 2004). As microwave heating transfers energy directly to the reagents, less energy is lost to the surroundings. It is reported that many top Biotechnology companies are now applying microwave assisted organic synthesis (MAOS), and acknowledge it as a key technique in optimising chemical reactions (Kappe, 2003).

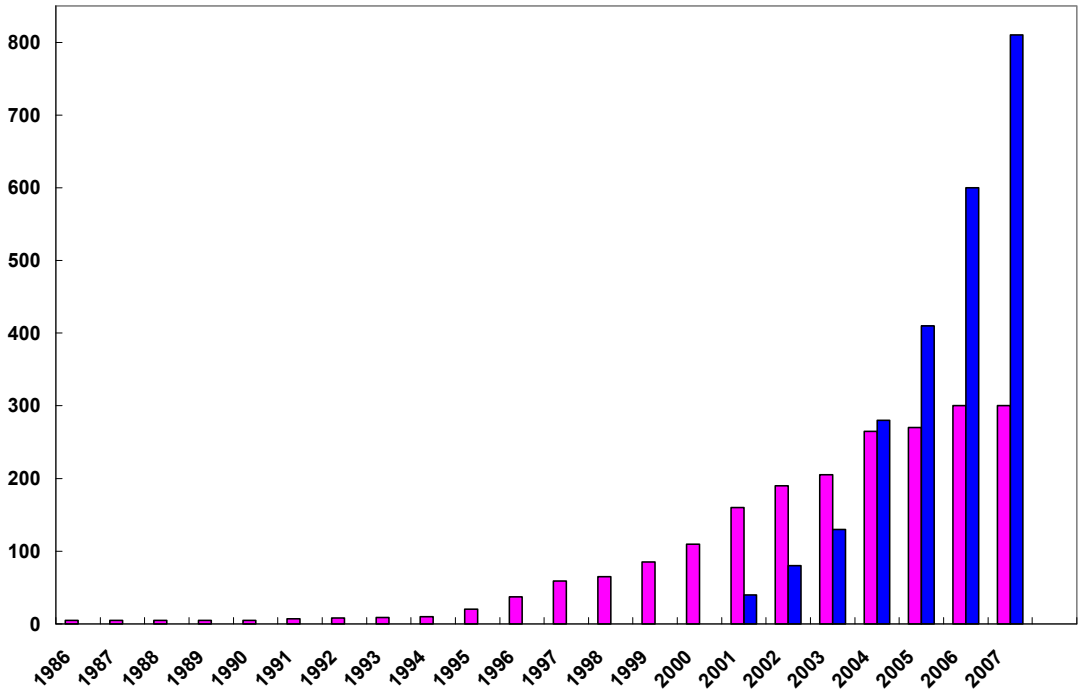

Figure 4.0: Publications on microwave assisted synthesis (1986-2007). Pink bars: number of articles involving MAOS for seven selected synthetic chemistry journals (*J. Org. Chem*., *Org. Lett*., *Tetrahendron*, *Tetrahedron Lett*., *Synth. Commun*., *Synthesis*, *Synlett.*, Scifinder Scholar keyword search on "microwave"). The blue bar represents the number of publications (2001-2007) reporting MAOS experiments in dedicated reactors with adequate process control (50 journals, full text search: microwave). Only those articles dealing with synthetic organic chemistry were selected. (Adapted from Kappe *et al*., 2009).

Microwave heating differs from traditional heating methods by the way the energy is transferred to the material. Under traditional heating the energy is delivered by convection and conduction, whereas microwave energy is transported directly by electromagnetic waves interacting with the molecules of the material (Kappe *et al*., 2009; Thostenson *et al*.,

1999). Microwave heating results in a uniform temperature throughout the reaction vessel whereas traditional heating methods can create temperature gradients that result in decomposition of the product, substrate or reagents (Kappe *et al*., 2008).

4.2.1 Microwave Theory

Microwave theory was previously discussed in detail in Chapter 3; Section 3.2.1. This section is a continuation of microwave theory and focuses mainly on the interaction of microwaves with solid materials.

Materials typically fall into one of three groups with regard to their interaction with to microwaves: (1) microwave reflectors (typically bulk metals and alloys); (2) transmitters which are transparent to microwaves, for example quartz; and (3) absorbers, which are the most important group for microwave synthesis.

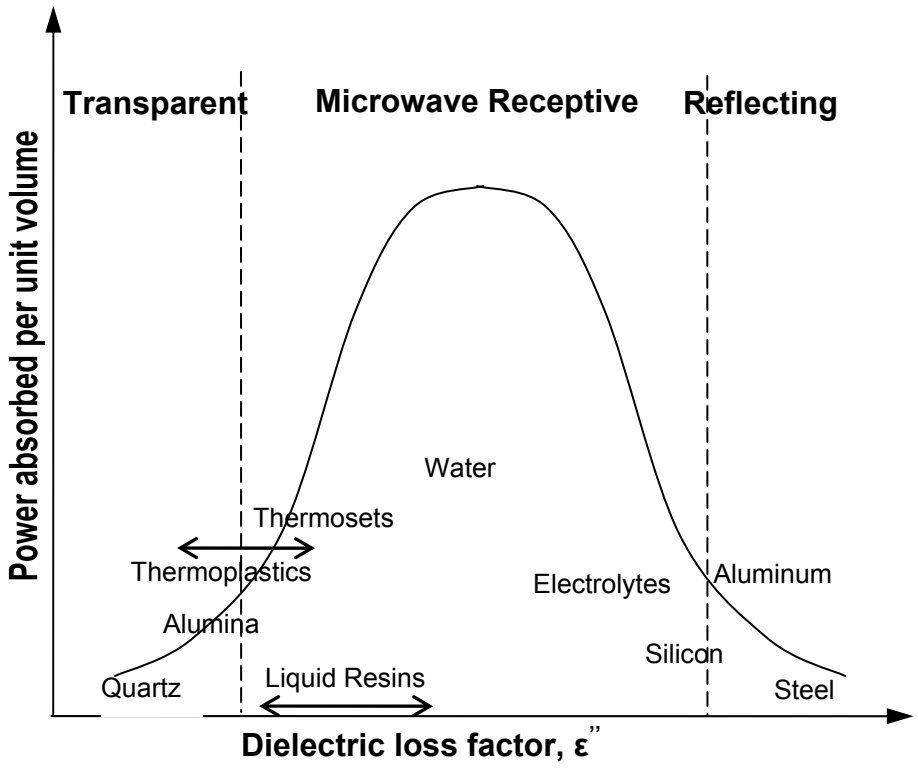

Figure 4.1: Power absorption versus dielectric loss factor for some materials. (Figure adapted from Thostenson *et al*., 1999).

The dielectric loss factor is dependent on the properties of the materials been microwaved and can indicate how effective microwave heating will be for a particular material (Basak, 2007). Generally, a material that possesses a high dielectric loss factor will adsorb microwave energy and covert it to heat, however as it is shown in Figure 4.1, some materials are microwave reflectors and will only slightly adsorb microwave energy. The dielectric loss factor can be calculated for different materials as it is the only variable factor with microwave heating, typically the field strength (E) and the frequency (2.45 GHz) remain constant (Fung, 1999). The measurable properties that allow for the calculation of the dielectric loss factor are the dielectric constant of the material and the loss tangent (Tan δ). The loss of tangent (Tan δ) is the term used to describe a materials ability to convert microwave energy into thermal energy (Fung, 1999).

Equation 4.0 $$\text{Tan}\,\delta = \frac{\varepsilon''}{\varepsilon'}$$

Where: *ε' is* a measure of a materials ability be polarised by an external electric field (dielectric constant); and ε" represents the dielectric loss factor.

It is reported, that many mechanisms contribute to the dielectric response of materials to microwaves (Thostenson *et al*., 1999). However, at microwave frequencies dipole polarization is believed to be the most important mechanism for energy transfer at a molecular level (Thostenson *et al*., 1999).

4.2.1.1 Material Behavior under microwave radiation

Many materials can be synthesized by microwave heating, however it is reported in literature that some materials when subjected to microwave heating have inverted temperature profiles which produces selective heating (Xiaofeng, 2002). These localized high temperature areas are commonly called 'hot spots'. Thermal runaway effect is the phenomenon that refers to a 'hot spot' created by microwave irradiation that leads to uncontrollable heating and damage of the material (Kriegmann, 1991). Ceramics are one type of material which is particularly susceptible to producing temperature gradients under microwave heating. Most ceramics are transparent to microwaves at room temperature, however when heated above a critical temperature, they rapidly couple to microwave energy (Yarlagadda & Tai Soon, 1998). This phenomenon can lead to an uneven temperature distribution (hot spots), as discussed above.

4.2.2 Micromanipulation Theory

A material can be deformed by applying a stress on it, and this stress (σ) can be represented by dividing the force (the implemented force) by the cross sectional area of the material (Müller *et al*., 2005).

Equation 4.1

$$\sigma = \frac{F}{A_0}$$

Where, F is the applied force, and A_0 is the cross sectional area of the material.

The extent of deformation (ε; strain) imposed on the material, can be estimated from looking at the length of the material before (l_0) and after deformation (l).

Equation 4.2

$$\varepsilon = \frac{l_0 - l}{l_0} = \frac{\Delta l}{l_0}$$

Chromatographic materials are typically porous spherical beads which can be composed of a variety of different materials: silica; polystyrene; agarose; cellulose; methacrylates, and acrylamides. These beads are generally composed of 50-96% water and 50-10% polymer. (Müller *et al*., 2005). In previous studies (Yan *et al*., 2009; Müller *et al*., 2005) it was shown that polymer beads in wet state exhibit visco-elastic properties at high deformations (up to 60%). The response of visco-elastic materials to strain is displayed in Figure 4.2, after a certain stress is exerted on the material it reaches a point of irreversible deformation, this term is known as the failure strength of the material.

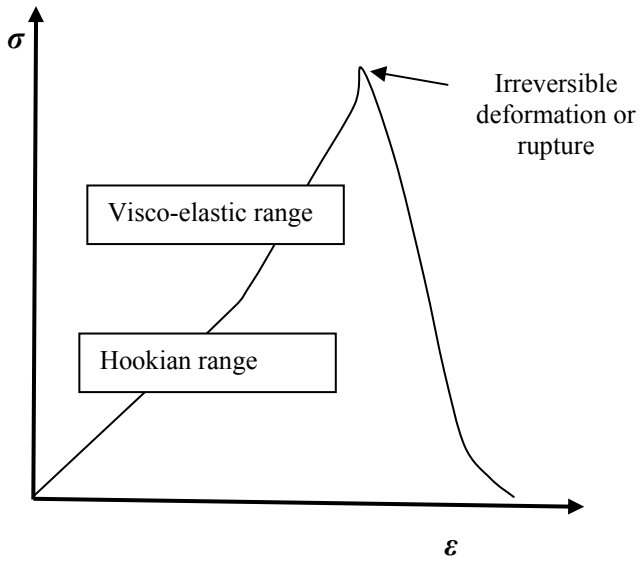

Figure 4.2: Stress versus strain curve for a polymer material, showing linear Hookian range; visco- elastic range, and particle rupture (adapted from Müller *et al.,* 2005).

There are two possible theories which can be applied when investigating the mechanical properties of materials. Firstly, the Hertz theory (Equation 4.3) can be employed for elastic spheres (non porous) which are compressed between two flat rigid surfaces (developed by Hertz & Reine) in 1896.

The Hertz theory is however only valid up to 10% deformation (Yan *et al*., 2009).

Equation 4.3

$$F = \left[\frac{4}{3} \frac{R_p^{0.5}}{2^{3/2}} \frac{E}{1-\mu^2} \right] h^{3/2}$$

Where: F is the force; R_p is the radius of the particle; E is Young's modulus of a sphere; h is the deformation by compression, and μ is Poisson's ratio of 0.5. At higher deformations (>10%), the Tatara Theory (Equations 4.4 & 4.5) is applied which is an extension of the Hertz theory (Tatara.1991; Ping *et al*., 2007).

Equation 4.4 $$F = ah^{3/2} + bh^3 + ch$$

Where *a, b*, and *c* are arbitrary constants determined experimentally, and *a* is a coefficient of the Hertz equation.

Equation 4.5 $$a = \left[\frac{4}{3} \frac{R_p^{0.5}}{2^{3/2}} \frac{E}{1-\mu^2} \right]$$

4.2.3 The theory of size analysis by light scattering

The measurement of particle size is usually obtained by a light scattering instrument (e.g. Mastersizer, Malvern instruments, UK; LS 13 320™, Beckmann Coulter, UK). A Mastersizer (Figure 4.3) is comprised: of a laser to illuminate the particles; an optical system to widen the light beam; a sample cell; a Fourier lens to collect the diffracted light, and a ring detector system to detect the created light scattering pattern (Keck & Müller, 2008).

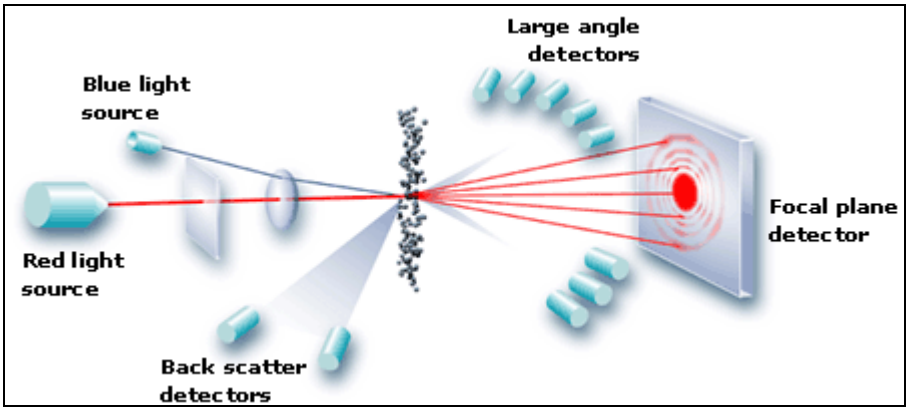

Figure 4.3: Physical components of a mastersizer (http://www.malvern.com).

The system starts the analysis with light from the laser illuminating the particles present in the sample cell. After the light strikes the particles it can be: reflected; refracted; adsorbed,

or re-radiated, depending on the physical property of the particles been analysed. The light scattering pattern produced is based on the ratio of the particle size relative to the wavelength of the light source (d/λ) (Beckmann Coulter, 2009). Depending on this ratio (d/λ) there are usually three types of the light scattering pattern observed: Fraunhofer scattering; Mie scattering, and Rayleigh (Renliang, 2002). Fraunhofer scattering is produced if the size of the particles is much larger than the set wavelength, if the particle size is significantly smaller than the wavelength then Rayleigh scattering is observed, and Mie scattering is generated for particles whose size is relatively close to the wavelength. It reported that the Fraunhofer approximation is applied for all instruments operating at 633 nm (e.g. Mastersizer 2000, Malvern Instruments, UK) for particles no smaller than 3.8µm (Kreck & Müller, 2008). If the particles been analyzed at 633 nm are smaller than 3.8µm then the more complex Mie formula is applied and the optical parameters of the particles is required for an accurate size analysis. In this study the size of all of the particles tested fell within the range covered by the Fraunhofer approximation.

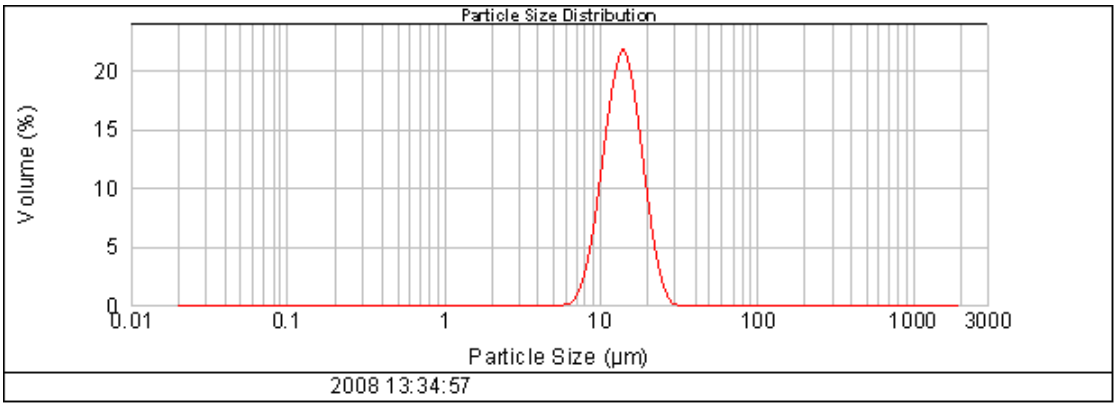

Figure 4.4: Mastersizer results for chromatography beads Source 15Q

The light scattering pattern is then measured by the ring detector system and undergoes mathematical analysis by applying a complex algorithm (Beckmann Coulter, 2009). The

collected data is finally processed by computer software which produces the observed result. The particle size distribution results are displayed as % volume versus particle size (Figure 4.4).

4. 3. Material and Methods

4.3.1. Materials

Sephacryl S-500 High Resolution, Sephacryl S-400 High Resolution, Sepharose 6B Sepharose CL-6B, Sepharose 6 FF, Q Sepharose FF, CM Sepharose FF, DEA Sepharose FF, Phenyl Sepharose CL 4B, Streamline, Stream Q XL, Streamline SP, Sephadex G-50, Sephadex G-25, Superdex 200 prep, Superdex 75 prep, Source 15 Q, Capto Q, Capto S. were bought from GE Healthcare Bio-Sciences AB (Uppsala, Sweden). UFC glass (100-300µm), UFC steel (20-40µm), UFC PEI steel (20-40µm), was purchased from UPFRONT Chromatography AS (Copenhagen, Denmark). Toyopearl HW 40C and Toyopearl HW 75 F were purchased from Tosoh Bioscience LLC (Grove city, USA). CM Hyper Z, Q Hyper Z, Q Hyper DF, S Hyper DF, HEA, PPA, QMA SPHEROSIL LS, SP SPHERODEX LS, were obtained from Pall (Portsmouth, UK). Fractogel EMD was acquired from Merck KGaA (Darmstadt, Germany). Zirconia Beads were bought from Glen Creston (Stanmore, UK).

4.3.2 Methods

4.3.2.1 Microwave heating

One gram of suction drained beads was placed into a 20 mL conical flask with 1 mL of distilled water. The flask was then positioned on the centre of a rotating plate in a domestic microwave oven (950 W; Model ST44; Micro-Chef Ltd, Solva, UK) for 6 s.

After the supports were exposed to microwave irradiation image analysis was carried out using both Light Microscopy (Model B150, Olympus optical Co, Hamburg, Germany) and SEM (XL-30 FEG ESEM, Oxford Inca 300 EDS systems, UK). Size distribution measurements were obtained from a mastersizer (model hydro 2000, Malvern instruments, Worcestershire, UK)

4.3.2.2 Scanning Electron Microscopy

Scanning electron microscopy (XL-30 FEG ESEM, Oxford Inca 300 EDS systems, UK) was performed on suction dried media. Firstly the beads were stuck onto a slide and placed in liquid Nitrogen slush. They were then put into the cryo chamber and etched under vacuum at 90°C for 300 s to remove ice crystals. Finally the sample was sputter coated with gold for 60 s and transferred to the microscope chamber.

4.3.2.3 Micromanipulation

The mechanical strength of the supports was tested using micromanipulation. Micromanipulation technique imposes a compression force on a single bead and the data is measured by a micromanipulation rig (Figures 4.5a & 4.5b). The sample is placed on a glass slide and a single bead is compressed by a probe which is connected to a transducer (Aurora Scientific inc., Canada). The slide is mounted on the stage of an inverted microscope (Micro instruments Ltd., Oxon, UK.) As the particle is squeezed at a pre-set speed of 20μm/s, the stress being imposed on it is measured simultaneously by a PC-30D data acquisition board (Amplicon Liveline, Brighton, UK). The experiments were conducted at room temperature. Ten particles were compressed for each experimental result.

Further details of this technique are explained explicitly in previous published work by Zhang and co workers, (1999).

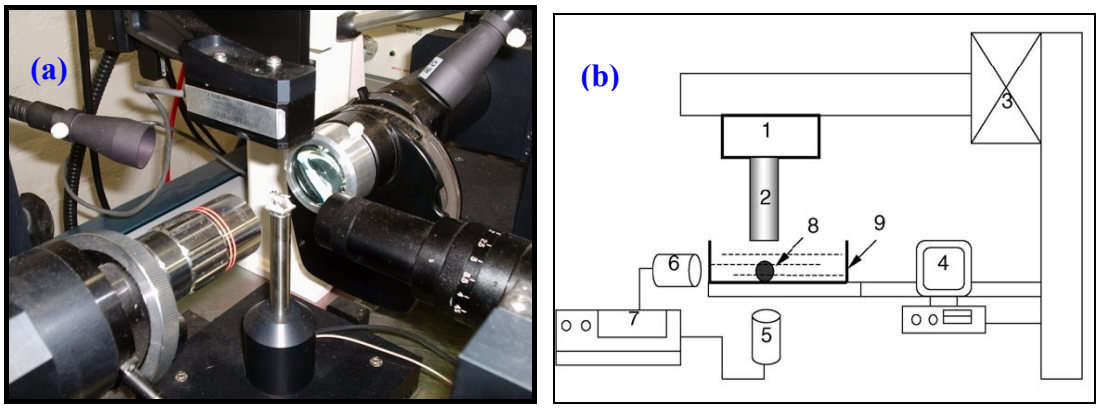

Figure 4.5: (a) Photograph of micromanipulation rig, (b) schematic diagram of the micromanipulation rig, Figure adapted from reference Zhang *et al*. (1999): (1) force transducer, (2) probe, (3) stepping motor, (4) computer with a data acquisition board, (5) bottom-view microscope, (6) side-view microscope, (7) video recorder, (8) resin particle in water and (9) glass chamber.

4.3.2.4 Bead size analysis

All size distribution measurements were performed by a mastersizer (Model 2000, Malvern instruments, UK). A 400 mg sample of suctioned drained supports were placed in water. A 50 mL sample (supports suspended in water) was placed in the sample cell. The sample was then mixed to ensure homogeneity. Water was used as the blank for the measurements.

The mastersizer used low angle light scattering for the particle size analysis. The light source was a He-He laser operating at 633 nm. This laser interacted with the supports and the light scattering pattern was then collected by the silicon detectors. The response of the

detectors to the scattering pattern was processed using the Mastersizer computer software to generate the % volume versus particle size (μm) graph.

4.4 Results and Discussion

In this study after the beads were exposed to microwave heating they were analysed by a variety of different techniques: image analysis; size distribution, and micromanipulation. The control sample is a bead that has not under gone any microwave heating. The results obtained from post heating analysis for each chromatography bead of a specific composition have been tabulated accordingly to help identify possible trends in the beads ability to withstand microwave heating. From the results it is evident that the composition, structure, and ligand attached to the matrix influence the effects of microwave heating.

Possible explanations for the damage of each type of bead have been discussed in detail but the response of the bead to heating is thought to have been dependent upon four key properties: the dielectric response; the heat capacity; the thermal expansion co-efficient, and the brittleness/ductility of the material. For beads comprised of composite materials there are additional considerations.

The first result column in each table represents the observations recorded during the actual heating process. A popping sound was heard while some beads were undergoing microwave heating. This popping noise was probably a result of the beads cracking or breaking due to a thermal stress weakening mechanism. From the results a definite trend was observed, where with nearly all examples if a popping noise was observed during microwave heating, SEM images revealed that the beads were damaged. In these cases it

can be concluded that the microwave induced thermal expansion of the beads material resulting in a stress that exceeded the failure stress of the material.

Table 4.0: Possible Mechanism for damage caused to beads from microwave heating.

Microwave energy absorbed by the bead ⇩	Depends upon the dielectric property of the material and it's ability couple with the electromagnetic wave (loss of tangent), further reading see Sections 3.2.1 & 4.2.1
Temperature rise in material ⇩	Dependent on the heat capacity of the material. (JK^{-1} Kg^{-1})
Thermal Expansion ⇩	Dependent on thermal expansion coefficient of the material (K^{-1}).
Damage	Depends on how ductile/brittle the materials tested are and the materials ultimate tensile strength (MPa).

There are two other complications to consider; firstly the uneven absorption of microwaves which can subsequently result in isolated thermal stresses, leading to hot spots and localized failure. Secondly the water within the pores will also absorb microwave energy, heat up and expand. The subsequent expansion of the water within pores will put additional localized stress on the bead which could also cause damage.

After the supports had undergone microwave heating they were visually analyzed by Light Microscopy (All light micrographs are displayed in the Appendix) and Scanning Electron Microscopy (SEM). By comparing both unmicrowaved beads (control) with microwaved beads for each chromatography support, it was easy to visually identify which beads had been affected by microwave exposure. These results revealed information into which type of a chromatography matrix was unable to under go microwave heating.

Some supports appeared unaffected under the light microscope, however when further inspected using SEM, previously unidentified damage was exposed. Next the size of the supports before and after microwave was investigated by employing a mastersizer. Size distribution results disclosed if the beads were unchanged, amalgamated or fragmented due to microwave exposure.

Finally, the mechanical properties of some selected supports were studied by micromanipulation, this analytical technique disclosed if there was any alternation to the network structure of a support after it was exposed to microwave irradiation. Sepharose CL-6B was of the most important support in this study to undergo micromanipulation as it was the matrix employed in all three chemical synthesises discussed in Chapter 3. Although the support appeared completely unchanged under visual analysis it was essential to obtain data from micromanipulation in order to conclude if this support had changed mechanically due to microwave heating. A previously conducted scientific study completed by Gropper and co workers (1998) reported structural changes in a gel network after microwave heating which would alter the mechanical strength of the gel.

4.4.1 Polymer Beads

It is apparent from the results that nearly all Sepharose supports tested (Table 4.1) could withstand microwave heating, the results show that the supports remained intact after microwave irradiation except when the bead is positively charged. Sepharose is the cross-linked beaded form of agaorse, a polysaccharide polymer. Some polymers are poor absorbers of microwaves up to a critical temperature; this characteristic of polymers may cause processing difficulties (Thostenson *et al*., 1999). However, successful chemical synthesis on polysaccharides via microwave irradiation is extensively reviewed in

literature (Haucai *et al*., 2005). Gupta and co workers (2006) reported successful activation of Sepharose via microwave irradiation to create an affinity matrix. No popping noise was heard during the microwave heating of Sepharose based beads except during the heating of DEAE Sepharose FF, indicating that this support may have been damaged by microwave exposure.

Light micrographs showed that Sepharose beads were undamaged after microwave irradiation, also it is evident from SEM images that the surface morphology of Sepharose beads after microwave exposure remain unscathed (Figures 4.7- 4.13) again with exception of DEAE Sepharose FF.

Table 4.1: Description of supports employed in this study and summary of both audible and visual observations during and after microwave treatment

Support	**Immobilised ligand**	**Description of base matrix**	**Manufacturer**	**Popping sound during heating**	**Difference in appearance after microwave irradiation**			
					Naked eye	**Light microscope**	**SEM**	**Size distribution**
Sepharose 6B	none	45-165 µm (av 90 µm), non-crosslinked bead of agarose, Agarose content 6%. SEC	GE Healthcare, Uppsala, Sweden.	No	Beads formed transparent gel.	No change	No change	Beads appear to have stuck together as microwaved sample appears bigger than control.
Sepharose CL-6B	none	45-165 µm (av 90 µm), crosslinked agarose bead. Agarose content 6 %. SEC	GE Healthcare Uppsala, Sweden	No	No change	No change	No change	Slight change; control is approx.20µm bigger than microwaved sample
Sepharose CL-6B, AGE Activated.	none	45-165 µm (av 90 µm), crosslinked agarose bead. Activated with Allyl Glycidyl Ether. Agarose content 6 %	GE Healthcare Uppsala, Sweden	No	No change	No change	No change	Slight change; control is approx 5µm bigger than microwaved sample
Sepharose CL-6B, EPC activated.	none	45-165 µm (av 90 µm), crosslinked agarose bead. Activated with Epichlorohydrin. Agarose content 6 %	GE Healthcare Uppsala, Sweden	No	No change	No change	No change	Slight change; control is approx.5µm bigger than microwaved sample
CM Sepharose FF	Carboxymethyl ligand (0.09-0.13 mmol (H^+)/mL)	45-165 µm (av 90 µm), crosslinked agarose bead. Agarose content 6 %. IEC	GE Healthcare Uppsala, Sweden	No	No change	No change	No change	Slight change; control is approx. 5µm bigger than microwaved sample
DEAE Sepharose FF	Diethylaminoethyl 0.11-0.16mmol (Cl^-)/mL	45-165 µm (av 90 µm), crosslinked agarose bead. Agarose content 6 %. IEC	GE Healthcare Uppsala, Sweden	Yes	No change	Beads appear broken and damaged	Beads appear cracked.	Slight change; control is approx. 20µm bigger than microwaved sample
Phenyl Sepharose CL-4B	Phenyl group (40 µmol/mL)	45-165 µm (av 90 µm), crosslinked agarose bead. Agarose content 4 %. HIC	GE Healthcare Uppsala, Sweden	No	No change	No change	No change	Slight change; control is approx. 5µm bigger than microwaved sample

DEAE Sepharose 6 FF was the only sepharose based support which appeared to be visually damaged by microwave heating. This bead is an anion exchanger, which has positively charged amine groups located throughout. A charged group on a support affects how it interacts with the electromagnetic field of microwaves, and charge can enhance the dielectric properties desirable for microwave coupling (Basak *et al*., 2007). It could be the case that when Sepharose has a positive charge it has a greater response to microwaves, resulting in temperature hot spots. This could cause localized thermal runaway effects that may have produced stresses that were high enough to fracture the beads. SEM images exposed the surface of DEAE Sepharose FF beads to be fractured and cracked after microwave irradiation (Figure 4.13). The size distribution data showed that the microwaved sample was 50 μm smaller than the control.

Although most Sepharose supports tested appeared to be visually unchanged after microwave heating, Size distribution data did indicate slight changes for all Sepharose beads after microwave treatment where microwaved samples appeared smaller than the control by a size difference of between 5-20 μm., with the exception of Sepharose 6B which changed significantly in size after microwave heating (Figure 4.12).

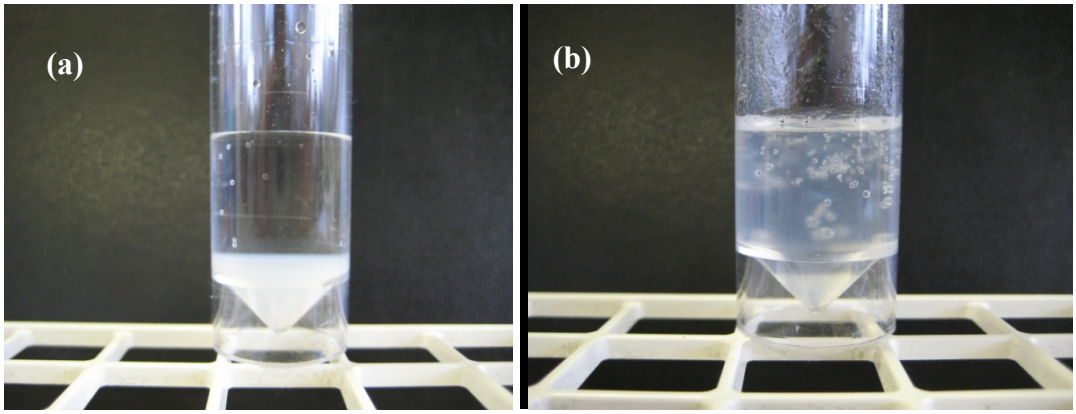

Figure 4.6: Photographs (a) of unmicrowaved Sepharose 6B & (b) microwaved Sepharose 6B.

Sepharose 6B is the un-crosslinked form of Sepharose CL-6B, the cross-linked property of the support seemed to influence microwave heating effects, as Sepharose 6B beads become a transparent gel after microwave exposure (Figure 4.6). In a previous study Zong and co workers (2004), showed that the dielectric constant (ε') and loss factor (ε'') for cross-linked epoxy resins was dependent on the degree of the cross-linking. Resins with the lowest percentage cross-linking had the largest dielectric property and therefore higher temperatures were recorded after microwave heating, when compared to resins with a higher percentage cross-linking. This result is probably due to the fact that with a lesser degree of cross-linking there is a greater freedom for the dipoles to rotate and interact with the electromagnetic wave from the microwave. Size comparisons of the control and microwaved sample for Sepharose 6B showed that the microwaved beads appeared approximately seven times bigger indicating that the beads have agglomerated, however visual analysis with light microscopy and SEM (Figure 4.12) showed that there was no obvious change in shape or surface morphology of the microwaved sample when compared to the control. These results indicate that the beads after microwave are still in there normal beaded form besides the fact that they are stuck together.

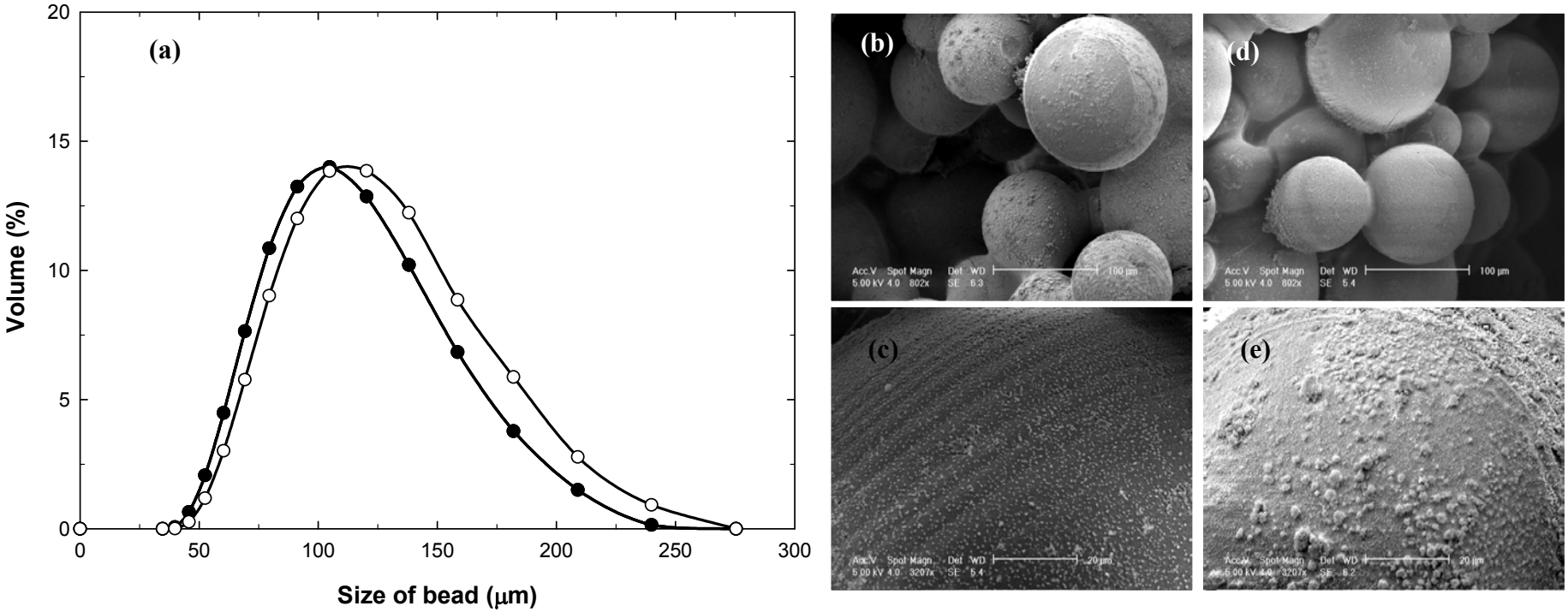

Figure 4.7: (a) Size distribution graph of Sepharose CL-6B: Symbols ●= microwaved sample & ○ = control sample. SEM images of (b) Sepharose CL-6B; (c) surface Sepharose CL-6B; (d) microwaved Sepharose CL-6B, & (e) microwaved surface Sepharose CL-6B.

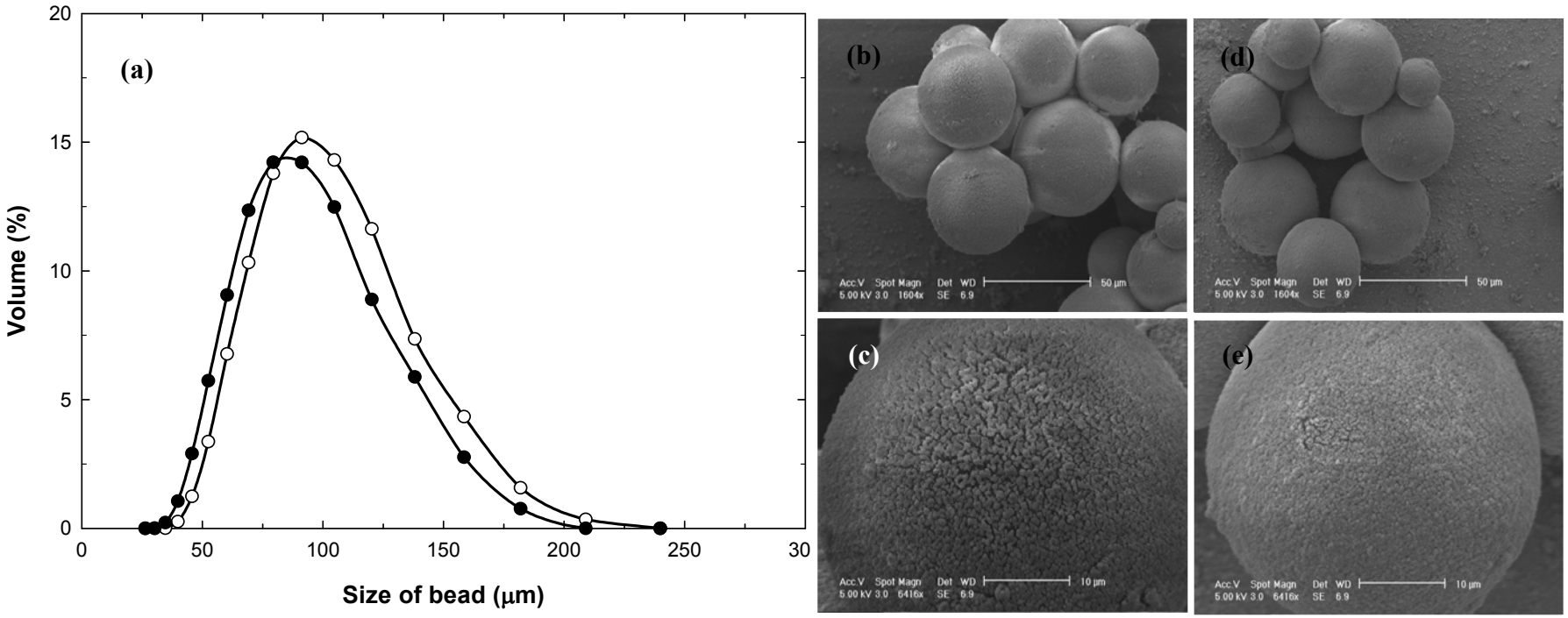

Figure 4.8 :(a) Size distribution graph of Sepharose CM FF: Symbols ●= microwaved sample & ○ = control sample. SEM images of (b) CM Sepharose FF; (c) surface CM Sepharose FF; (d) microwaved CM Sepharose FF; & (e) surface microwaved CM Sepharose FF

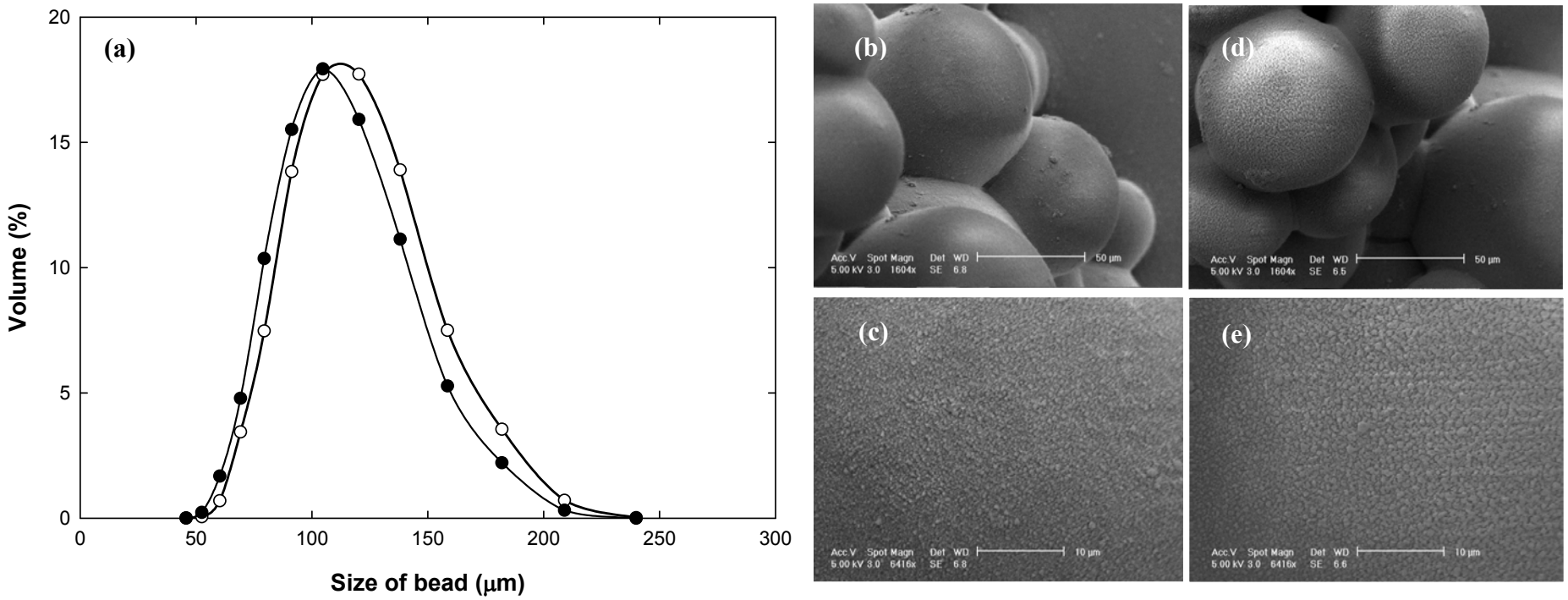

Figure 4.9 :(a) Size distribution graph of Phenyl Sepharose CL-4B: Symbols ●= microwaved sample & ○ = control sample. SEM images of (b) Phenyl Sepharose CL-4B; (c) surface Phenyl Sepharose CL 4B; (d) microwaved Phenyl Sepharose CL-4B, & (e) microwaved surface Phenyl Sepharose CL-4B.

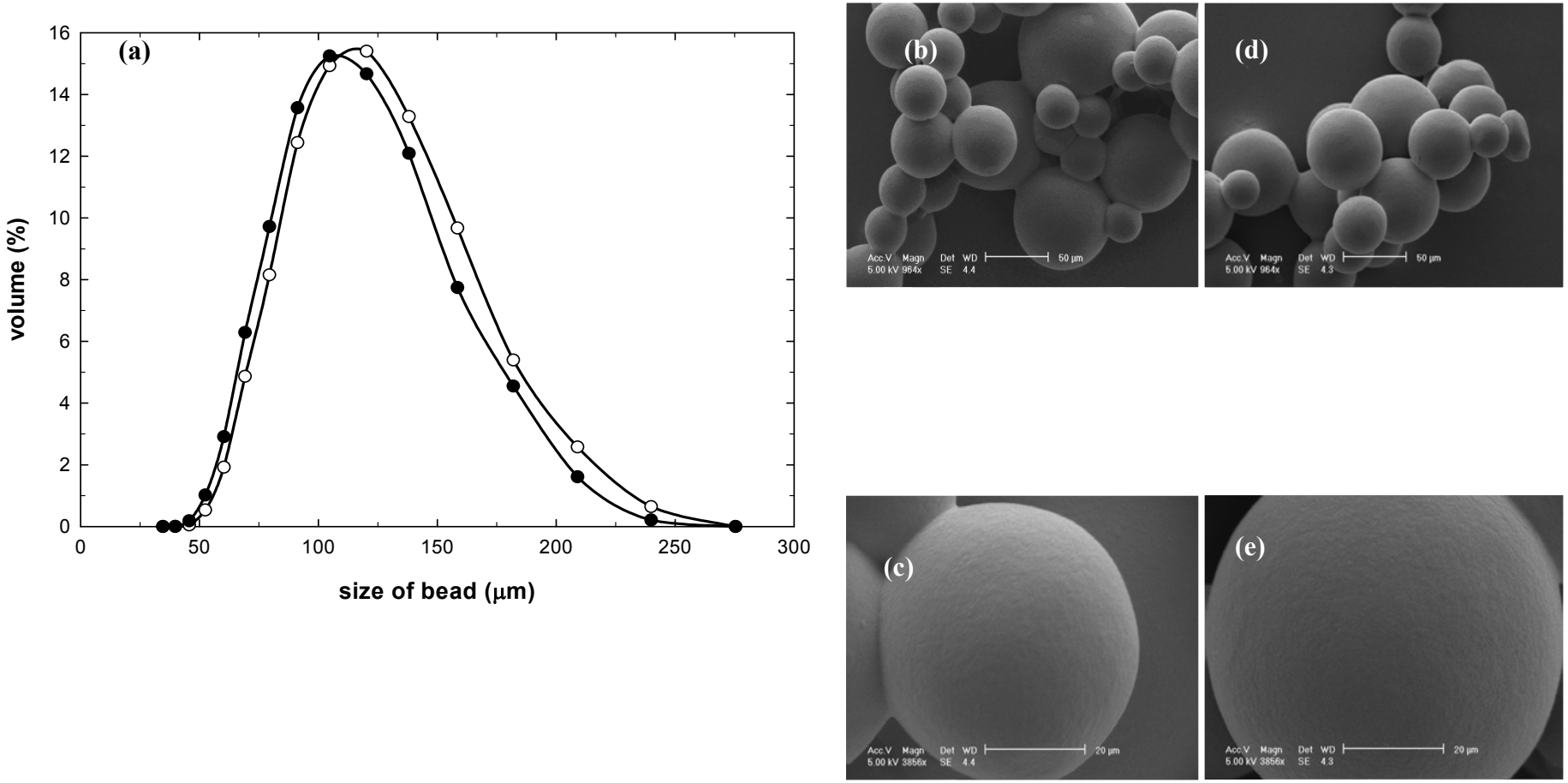

Figure 4.10 :(a) Size distribution graph of AGE activated Sepharose CL-6B: Symbols ●= microwaved sample, & ○ = control sample. SEM images of (b) AGE activated Sepharose CL-6B; (c) surface Activated AGE Sepharose CL-6B; (d) microwaved AGE activated Sepharose CL-6B, & (e) microwaved surface AGE activated Sepharose CL-6B.

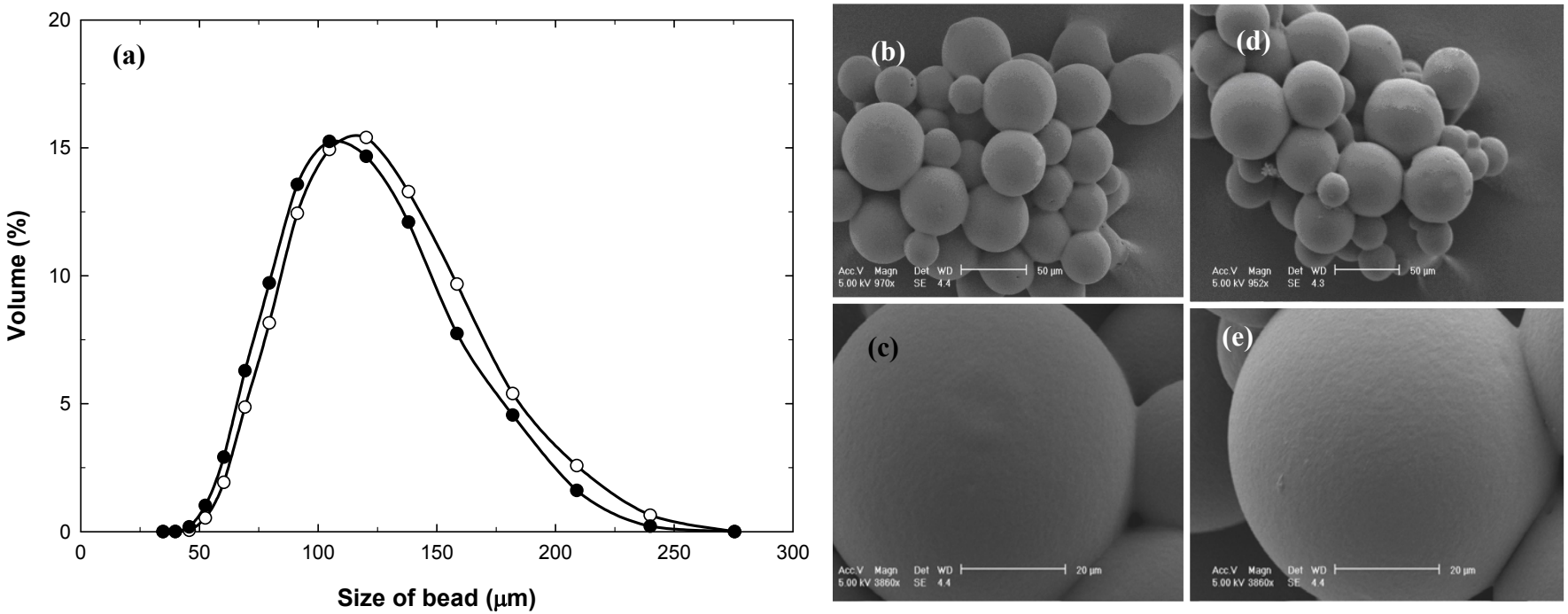

Figure 4.11: (a) Size distribution graph of EPC activated Sepharose CL-6B: Symbols ●= microwaved sample & ○ = control sample. SEM images of (b) EPC activated Sepharose CL-6B ;(c) surface Activated EPC Sepharose CL -6B; (d) microwaved EPC activated Sepharose CL-6B, & (e) microwaved surface EPC activated Sepharose CL- 6B

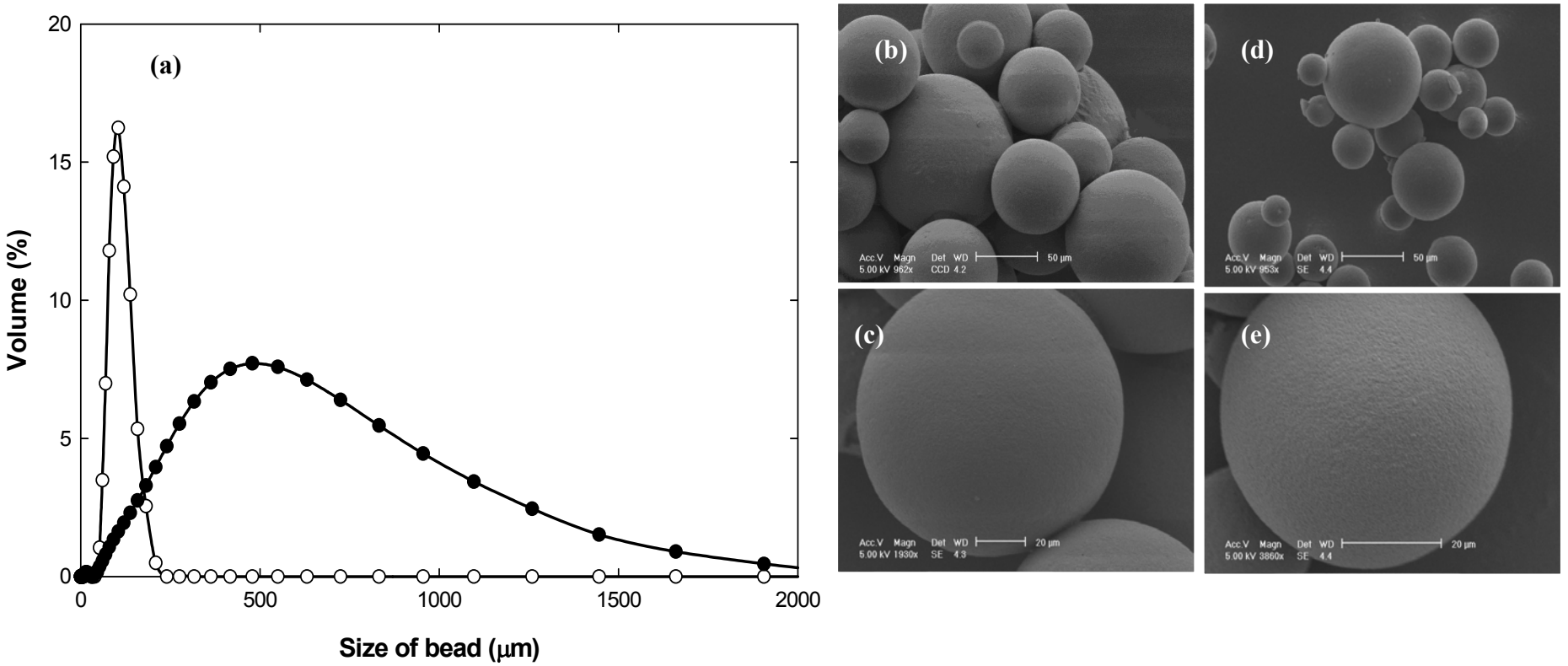

Figure 4.12 :(a) Size distribution graph of Sepharose 6B: Symbols, ●= microwaved sample & ○ = control sample. SEM images of (b) Sepharose 6B; (c) surface of Sepharose 6B; (d) microwaved Sepharose 6B, & (e) microwaved surface of Sepharose 6B.

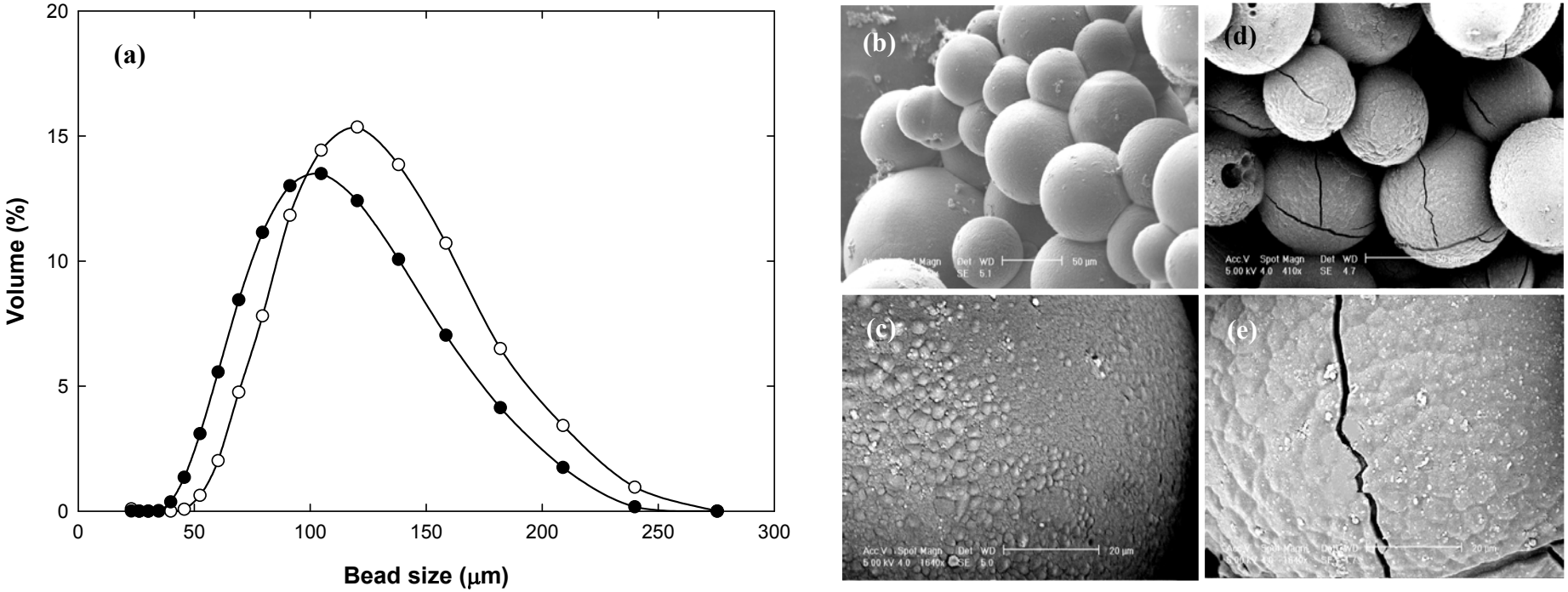

Figure 4.13:(a) Size distribution graph of DEAE Sepharose FF; Symbols, ●= microwaved sample, & ○ = control sample :SEM images of (b) DEAE Sepharose FF; (c) surface of DEAE Sepharose FF; (d) microwaved DEAE Sepharose FF, & (e) microwaved surface of DEAE Sepharose FF.

4.4.1.1 Micromanipulation of Sepharose beads

The mechanical property of Sepharose beads was studied using micromanipulation. This technique would reveal if there was any change in the mechanical property of supports after microwave heating.

The pseudo-stress deformation curve (Figure 4.14) gives a clear representation of the mechanical properties to the beads before and after microwave heating. The pseudo-stress is the force divided by the cross sectional area ($1/4\pi d^2$) where d is the diameter of the bead, and the percentage deformation is obtained by dividing the displacement by the diameter of the bead. Ten particles were compressed for each experimental result (Materials & Methods; Section 4.3.2.2) and the curve in each graph represents the average data for ten particles. The reason ten particles were chosen was to guarantee a clear representation of mechanical properties, it is suggested that a minimum of 10 particles be investigated for each micromanipulation result in order to get statistical data close to Gaussian distribution (α=95%) (Ping *et al*., 2008).

The results obtained from the micromanipulation analysis of Sepharose CL-6B (Figure 4.14) show that up to 35% deformation both samples are mechanically similar, however after 35% deformation a greater stress of approximately between 0.02-0.05MPa was required to compress the microwaved sample in comparison with the control (unmicrowaved sample). These results indicate that microwave irradiation had changed the visco-elastic properties of the beads. This observed change in the visco-elastic properties of the microwaved beads, is probably a result of the bead shrinking approximately 20 μm.

These mechanical changes may not pose a problem as it reported in literature, that the highest deformation in a chromatographic process column caused by flow rate is not greater than 10-15% deformation (Müller *et al*., 2005).

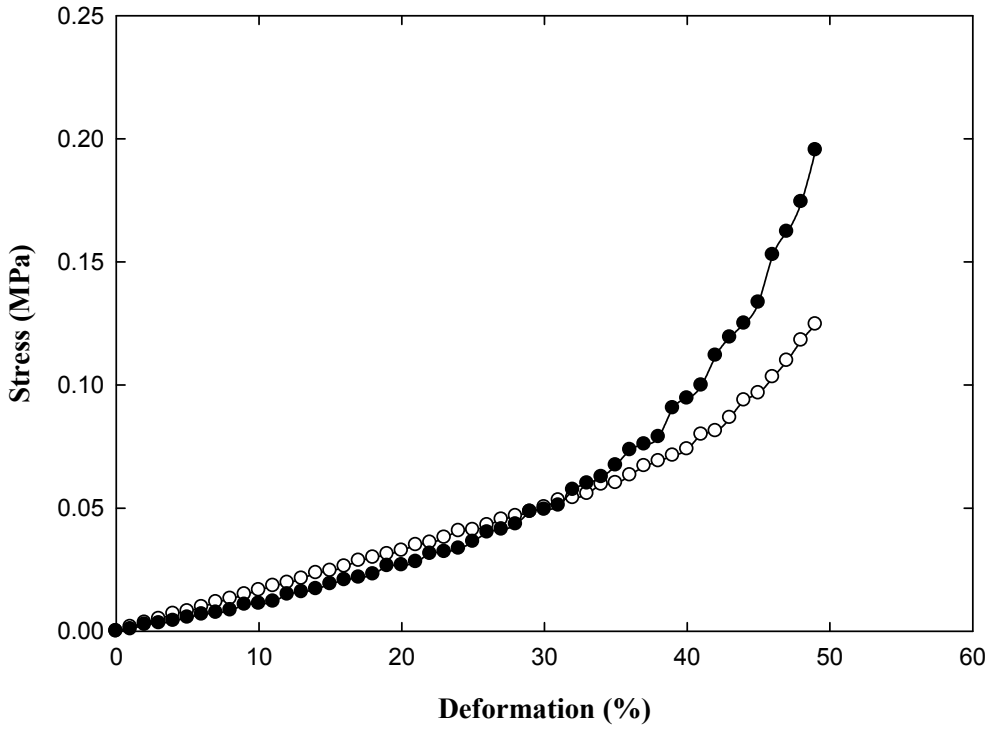

Figure 4.14: Stress/deformation curves for both microwaved and control samples of Sepharose CL-6B: Symbols ●= microwaved sample & ○ = control sample (mean data for 10 particles).

The hysteresis experiments were performed by compressing the beads from both samples multiple times (x5) (Figure 4.15). On the second compression (Figure 4.15b) the control sample displayed similar properties to the microwaved sample up 15% deformation. After 15% up to 39% deformation much higher stress differences were observed (0.05-2.7 MP). It is only after the third compression that the control and microwaved sample differ at a deformation of less than 15% (Figure 4.15d & e).

The loss of water from the beads after each compression may also influence the results, however this effect should be apparent for both samples. From the results it appears that the microwave sample is either more mechanically stable than the control after numerous compressions or is not experiencing the same water losses as the control. It is reported that water softens polymeric porous materials and that the water content in a resin plays an important role on it's mechanical stability (Andrei *et al*., 1996) also the force required to compress chromatography beads in dry state is much higher in comparison to beads in wet state (Müller *et al*., 2005).

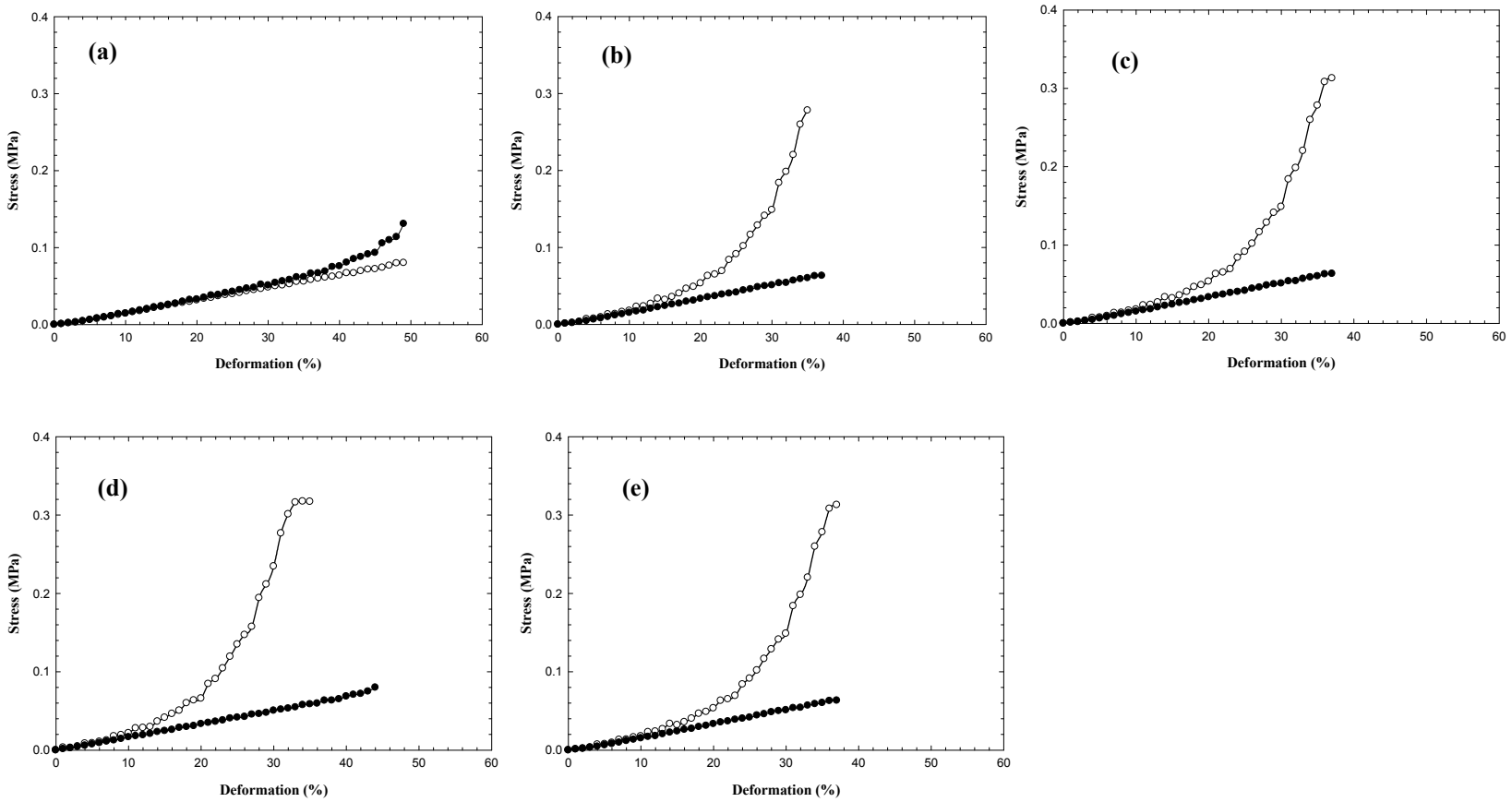

Figure 4.15: Stress/deformation curves of both microwaved and control samples of Sepharose CL-6B from hysteresis experiments: Symbols ●= microwaved sample & ○ = control sample;(a) 1st compression; (b) 2nd compression; (c) 3rd compression; (d) 4th compression, & (e) 5th compression (each line represents data for 10 particles)

The Young's module (E) was calculated using the Hertz equation (Equation 4.3) in the linear region below 10% deformation. Young's modulus is a function of size, the average bead size for each result is the same, also to guarantee a clear representation of mechanical properties a minimum of 10 particles were investigated, and the standard error was calculated.

From the Young's modulus results the mechanical properties of both Sepharose CL-6B samples (Table 4.2) appear to be very similar, other than slight changes in the Young's modulus were observed with each compression, again this could be due to water. These Young's Modulus results compliment the results displayed in the stress versus deformation graphs (Figures 4.14 & 4.15), which also show very slight changes in the mechanical properties of both the microwaved and control samples at deformations less than 10%.

Table 4.2: Young's modules for Sepharose CL-6B hysteresis micromanipulation experiments (mean data for 10 particles)

Sample	***E* (wet state) (MPa)**
Sepharose CL-6B 1st compression	2.9± 0.31
Sepharose CL-6B 2nd compression	5.5±0.62
Sepharose CL-6B 3rd compression	5.7±0.60
Sepharose CL-6B 4thrd compression	5.1±0.51
Sepharose CL-6B 5thrd compression	5.1±0.59
Microwaved Sepharose CL-6B 1st compression	4.5±0.13
Microwaved Sepharose CL-6B 2nd compression	4.0±0.14
Microwaved Sepharose CL-6B 3rd compression	4.2±0.30
Microwaved Sepharose CL-6B 4th compression	4.6±0.51
Microwaved Sepharose CL-6B 5th compression	4.8±0.45

It was thought that the micromanipulation data for Sepharose 6B would complete this data set, and allow for mechanical property comparisons between cross-linked Sepharose and non cross-linked Sepharose after microwave heating. However, it was not possible to perform micromanipulation on the microwaved sample of Sepharose 6B. As previously discussed, the beads of Sepharose 6B appeared to have amalgamated after microwave heating (Figure 4.12) and the probe from the micromanipulation rig was unable to single out individual beads as they were stuck together.

Image analysis for both AGE-Sepharose CL-6B (Figure 4.10) and EPC-Sepharose CL-6B (Figure 4.11) showed both supports to be undamaged after microwave heating, the size distribution data did reveal the beads had shrunk approximately 20 μm after microwave irradiation. The mechanical properties of AGE-Sepharose CL-6B supports remained unchanged after microwave heating. The stresses required to compress both control and microwaved samples were the same (Figure 4.16). Young's modulus values (Table 3.4) are within close range of each other indicating that mechanical properties of the beads are unchanged after microwave heating at deformations less than 10%.

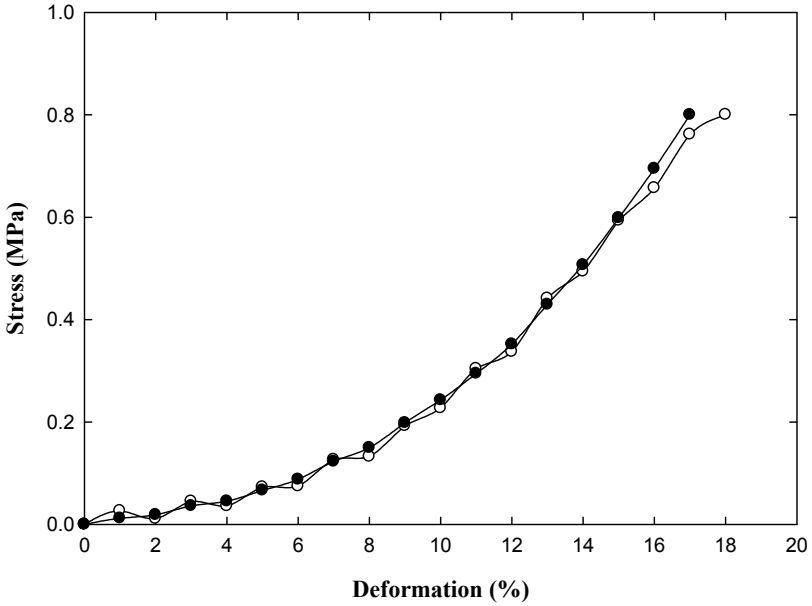

Figure 4.16: Stress/deformation curves of AGE activated Sepharose CL-6B microwaved and control samples; Symbols ●= microwaved sample & ○ = control sample (mean data for 10 particles)

Table 4.3: Young's modules for Activated Sepharose CL-6B micromanipulation experiments (10 particles)

Sample	***E* (wet state) (MPa)**
AGE activated Sepharose CL-6B	35±3.3
Microwaved AGE activated Sepharose CL-6B	40±3.0
EPC activated Sepharose CL-6B	38±3.6
Microwaved EPC activated Sepharose CL-6B	35±3.1

The mechanical properties of EPC-Sepharose CL-6B (Figure 4.17) are the similar up to 16% deformation (Table 4.3). At higher deformations of between 17-20%, a greater stress is required to compress the microwaved sample (0.1-0.4 MPa), indicating that

there is a change in the visco-elastic properties of this support after microwave irradiation.

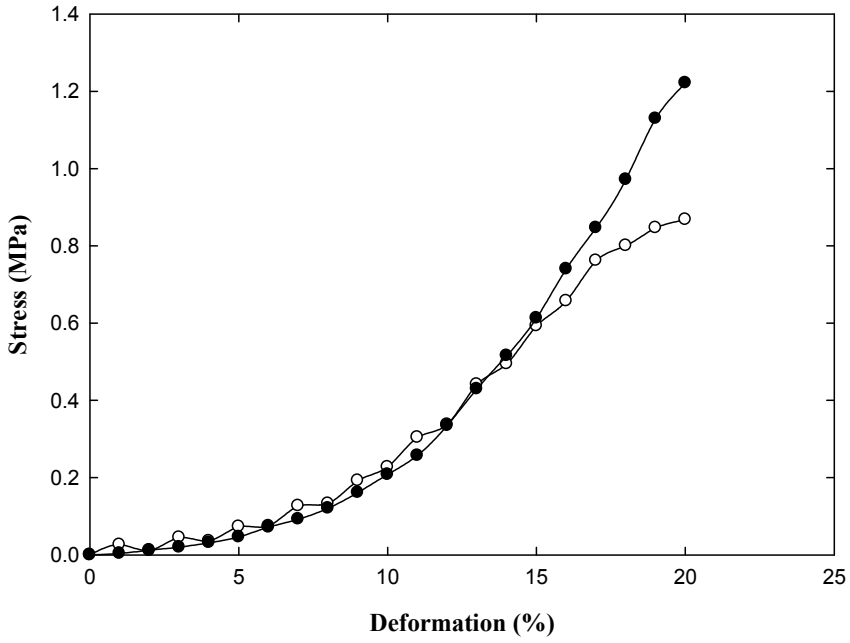

Figure 4.17: Stress/deformation curves of EPC activated Sepharose CL-6B microwaved and control samples. Symbols ●= microwaved sample & ○ = control sample (mean data for 10 particles)

Phenyl Sepharose CL-4B beads appeared visually unchanged after microwave exposure. Size distribution analysis showed that the microwaved sample had shrunk by approximately 10 μm when compared to the control (Figure 4.9). The stress versus deformation graph (Figure 4.18) revealed that there were slight differences with the mechanical properties of both samples. The maximum stress difference of 0.02MPa was observed at approximately 15% deformation. The Young's Modulus values revealed significant changes in the mechanical properties (Table 4.4) of the beads after

microwave heating, with the microwaved sample having a Young's Modulus value 12 MPa greater than the control.

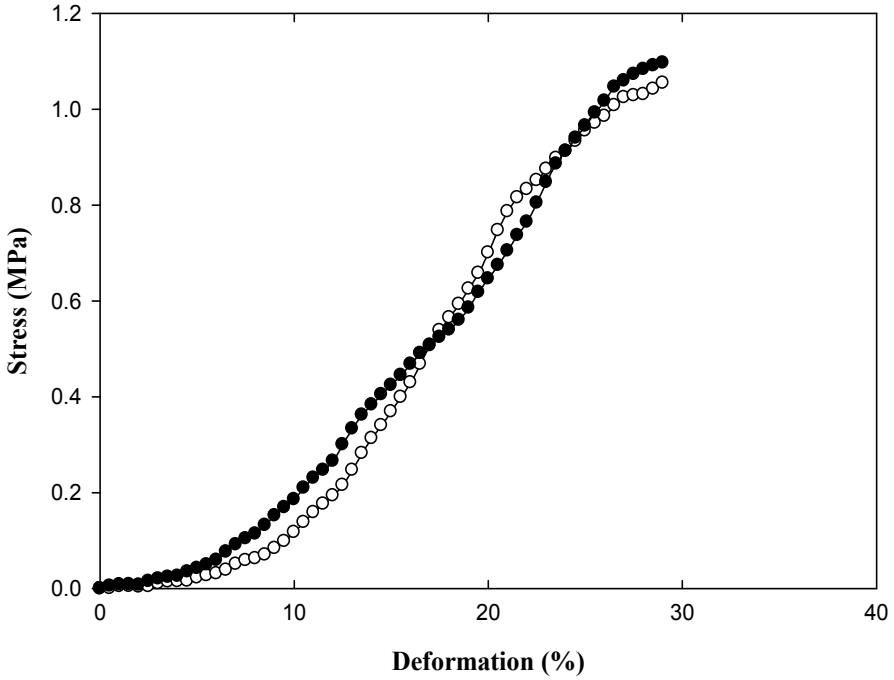

Figure 4.18: Stress/deformation curves of microwaved and control samples of Phenyl Sepharose CL-4B, Symbols ●= microwaved sample & ○ = control sample (mean data for 10 particles).

Table 4.4: Young's modules for Phenyl Sepharose CL-4B micromanipulation experiments (mean data for 10 particles)

Sample	*E* (wet state) (MPa)
Phenyl Sepharose CL-4B	19±1.2
Microwaved Phenyl Sepharose CL-4B	31±2.5

4.4.2 Cellulose Beads

Cellulose is a natural polymer. Antova and co workers previously reported on the successful synthesis of cellulose via microwave technology (Antova *et al*., 2004). A pooping noise was heard during microwave heating of Cellulose based supports a

(Table 4.5) and although light micrographs (Appendix; Figure 6.9) showed no visual change to the beads, SEM images (Figures 4.19 & 4.20) confirmed that surface of cellulose beads was slightly courser after microwave irradiation. Making these supports the exception in this study as with every other support when a popping noise was heard the beads appeared cracked, broken, or deformed after microwave exposure. Size distribution results showed that there was no change in the size of the beads after microwave heating One explanation as to why this support seemed to be able to ensure microwave heating is probably due to its material properties, (heat capacity of ~ 1400 JK^{-1} Kg^{-1} & tensile strength ~120 MPa). The heat capacity of cellulose is very high in comparison to other materials and it requires a large energy input to heat up by one Kelvin. These beads are also highly cross-linked and as previously mentioned this would reduce the free rotation of the molecules which would limit the rise in temperature. It is possible that subsequent damage could however be observed with increasing the microwave exposure time above 6 s.

Table 4.5: Description of Cellulose employed in this study and summary of both audible and visual observations during and after microwave treatment

Support	**Immobilised ligand**	**Description of base matrix**	**Manufacturer**	**Popping sound during heating**	**Difference in appearance after microwave irradiation**			
					Naked eye	**Light microscope**	**SEM**	**Size distribution**
HEA	HEA hyper cell: n-hexyl Ligand (Hexylamine). (50 µmol/mL)	80-100 µm av. Highly porous cross-linked cellulose beads. HIC mixed modal interaction mechanism	Pall, Portsmouth, Hampshire, UK	Yes	No change	No change	Surface appears slightly rougher	No change
PPA	HEA hyper cell: n-phenylpropyl Ligand (Phenylpropylamine) .(50 µmol/mL	80-100 µm av. Highly porous cross-linked cellulose beads. HIC mixed modal interaction mechanism	Pall, Portsmouth, Hampshire, UK	Yes	No change	No change	Surface appears slightly rougher	No change

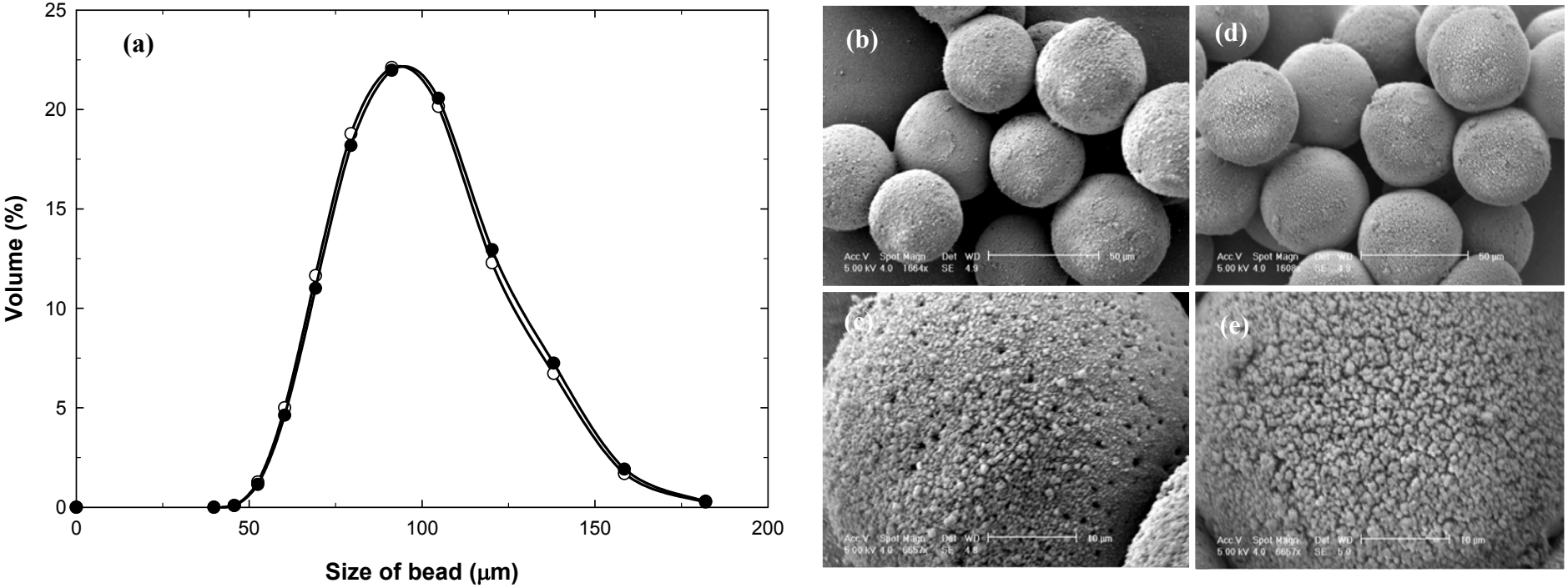

Figure 4.19: (a) Size distribution graph of HEA: Symbols ●= microwaved sample, & ○ = control sample. SEM images of (b) HEA ;(c) surface of HEA ;(d) microwaved HEA; (e) microwaved surface of HEA.

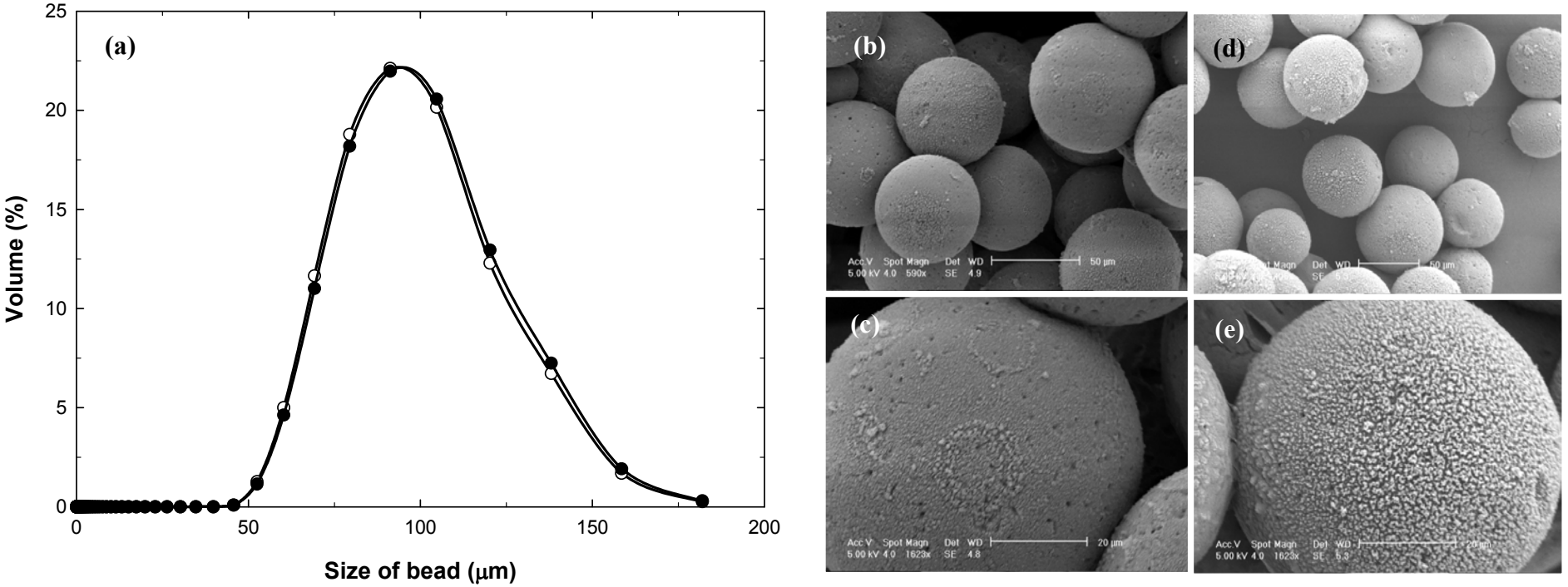

Figure 4.20: (a) Size distribution graph of PPA: Symbols ●= microwaved sample & ○ = control sample. SEM images of (b) PPA, (c) surface of PPA ;(d) microwaved PPA, & (e) microwaved surface of PPA.

4.4.3 Dextran-Polymer Beads

No popping noise was experienced during the microwave heating of all dextran-polymer based supports (Table 4.6), indicating the beads may have remained unchanged after microwave treatment. Light micrographs (Appendix; Figures 6.10-6.11) and SEM images (Figures 4.21-4.28) revealed that the morphology of all the beads tested remained undamaged after microwave treatment. The chemistry of each polymer within the beads would possess different dielectric properties and therefore interact separately with the electromagnetic wave. It can be assumed that there would be temperature gradients present throughout these supports when exposed to microwave heating. However, from the results there was no apparent damage to the beads, it could be the case that for longer lengths of microwave exposure damage could transpire.

Size distribution measurements (Figures 4.26 & 4.24) showed slight changes in the size of Superdex 75 and Sephacryl S-500 HR, where the microwaved samples of both supports were approximately 5 μm bigger then than the controls. Capto Q (Figure 4.27) displayed a much greater change in size after microwave heating where the microwaved sample appeared to be about 50 μm bigger than the control. This support has a positively charged amine group distributed throughout, which may have a greater affinity for the electromagnetic wave generating temperature hotspots throughout the support, which would lead to uneven thermal expansion of the material. Although visually no damage is evident, indicating that the thermal expansion did not create a stress large enough to fracture the material, the thermal stress may have been greater then the ultimate tensile strength of the material. This would have resulted in an irreversible expansion.

Table 4.6: Description of polymer-dextran supports employed in this study and summary of both audible and visual observations during and after microwave treatment

Support	**Immobilised ligand**	**Description of base matrix**	**Manufacturer**	**Popping sound during heating**	**Difference in appearance after microwave irradiation**			
					Naked eye	**Light microscope**	**SEM**	**Size distribution**
Sephadex G-25 Medium	None	85-260 µm av. A highly rigid bead of sepharose cross linked with dextran. SEC	GE Healthcare, Uppsala, Sweden.	No	No change.	No change	No change	No change
Sephadex G-50 Medium	None	50-200 µm av. A highly rigid bead of sepharose cross linked with dextran. SEC	GE Healthcare Uppsala, Sweden	No	No change	No change	No change	No change
Superdex 200 prep grade	None	34 µm av. composite of cross-linked agarose and dextran. SEC	GE Healthcare Uppsala, Sweden	No	No change	No change	No change	No change
Superdex 75 prep grade	None	34 µm av. composite of cross-linked agarose and dextran. SEC	GE Healthcare Uppsala, Sweden	No	No change	No change	No change	Slight change, microwaved sample aprox. 5µm bigger than control
Sephacryl S-400 HR	None	50 µm av. Allyl dextran and N, N'-methylenebisacrylamide. SEC	GE Healthcare Uppsala, Sweden	No	No change	No change	No change	No change
Sephacryl S-500 HR	None	50 µm av. Allyl dextran and N, N'-methylenebisacrylamide. SEC	GE Healthcare Uppsala, Sweden	No	No change	No change	No change	Slight change, microwaved sample aprox. 5µm bigger than control
Capto Q	Amine ligand (anion exchanger), (0.16-0.22 mmol Cl^-/mL)	90µm av. High flow agarose with dextran surface extenders. IEC	GE Healthcare Uppsala, Sweden	No	No change	No change	No change	Microwaved sample aprox. 50µm bigger than control
Capto S	Sulphate ligand (cation exchanger), (0.11-0.14 mmol Na^+/mL)	90µm av. High flow agarose with dextran surface extenders. IEC	GE Healthcare Uppsala, Sweden	No	No change	No change	No change	No change

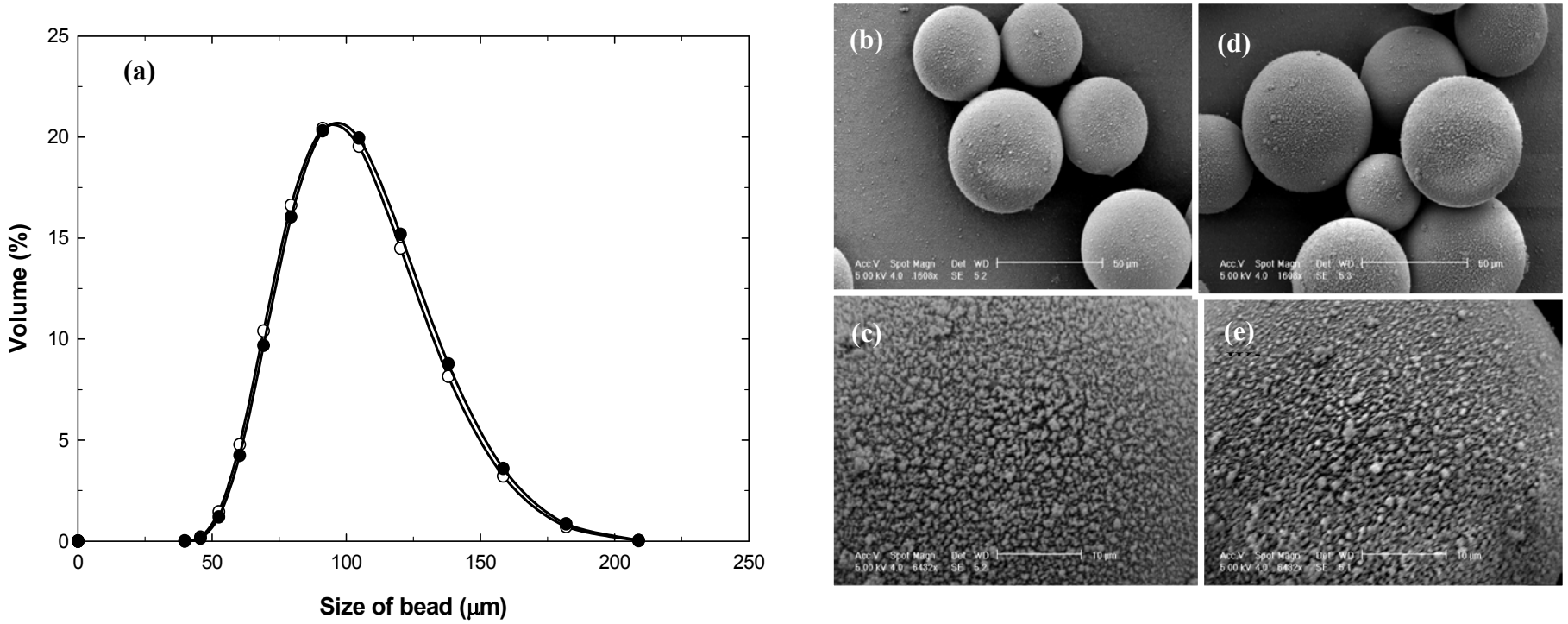

Figure 4.21: (a) Size distribution graph of Sephadex G-25: Symbols ●= microwaved sample, & ○ = control sample. SEM images of (b) Sephadex G-25; (c) surface of Sephadex G-25; (d) microwaved Sephadex G-25, & (e) microwaved surface of Sephadex G-25.

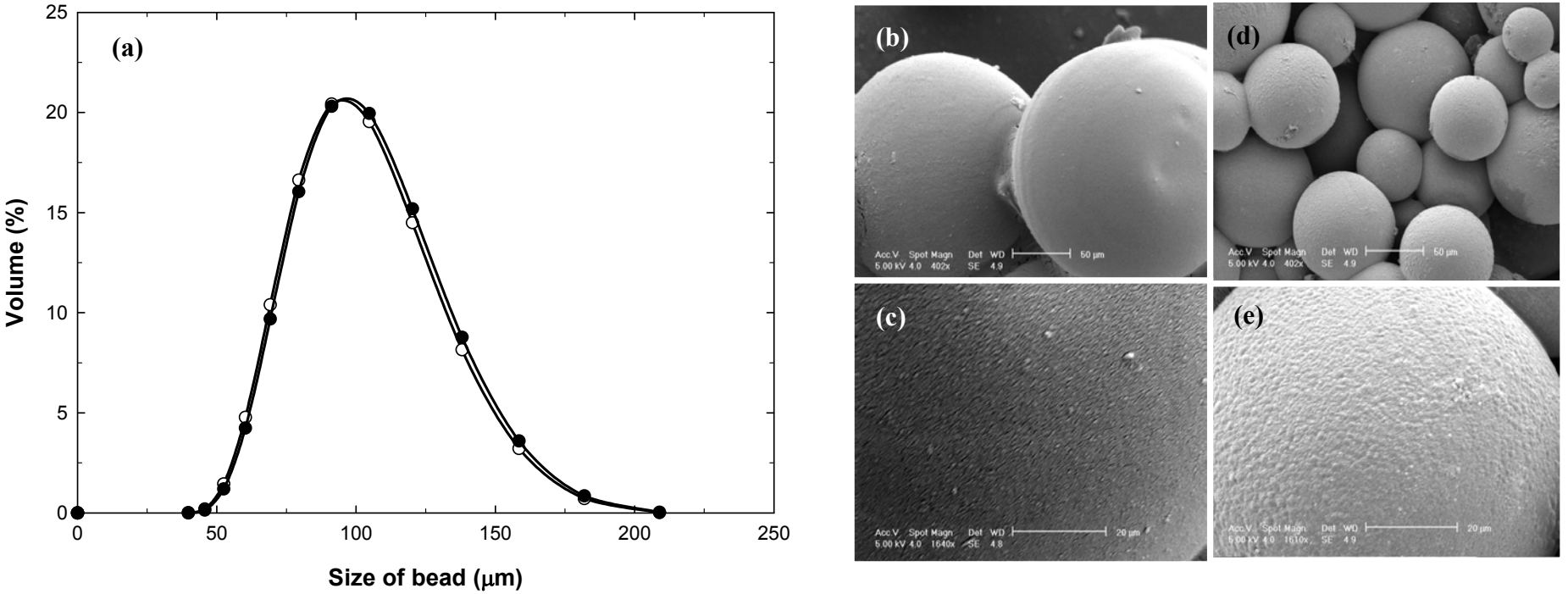

Figure 4.22: (a) Size distribution graph of Sephadex G-50: Symbols ●= microwaved sample, & ○ = control sample. SEM images of (b) Sephadex G-50; (c) surface of Sephadex G-50; (d) microwaved Sephadex G-50, & (e) microwaved surface of Sephadex G-50

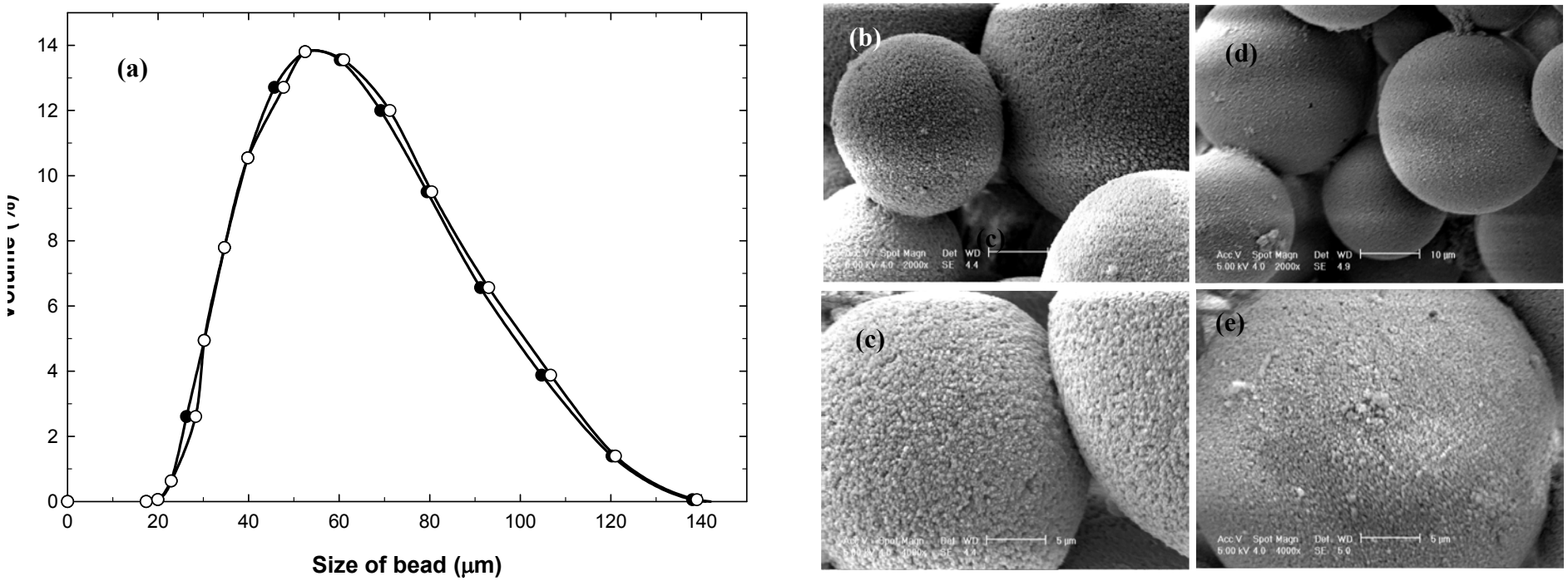

Figure 4.23: (a) Size distribution graph of Sephacryl S-400 HR: symbols ●= microwaved sample, & ○ = control sample. SEM images of (b) Sephacryl S-400 HR; (c) surface of Sephacryl S-400 HR;(d) microwaved Sephacryl S-400 HR, & (e) microwaved surface of Sephacryl S-400 HR.

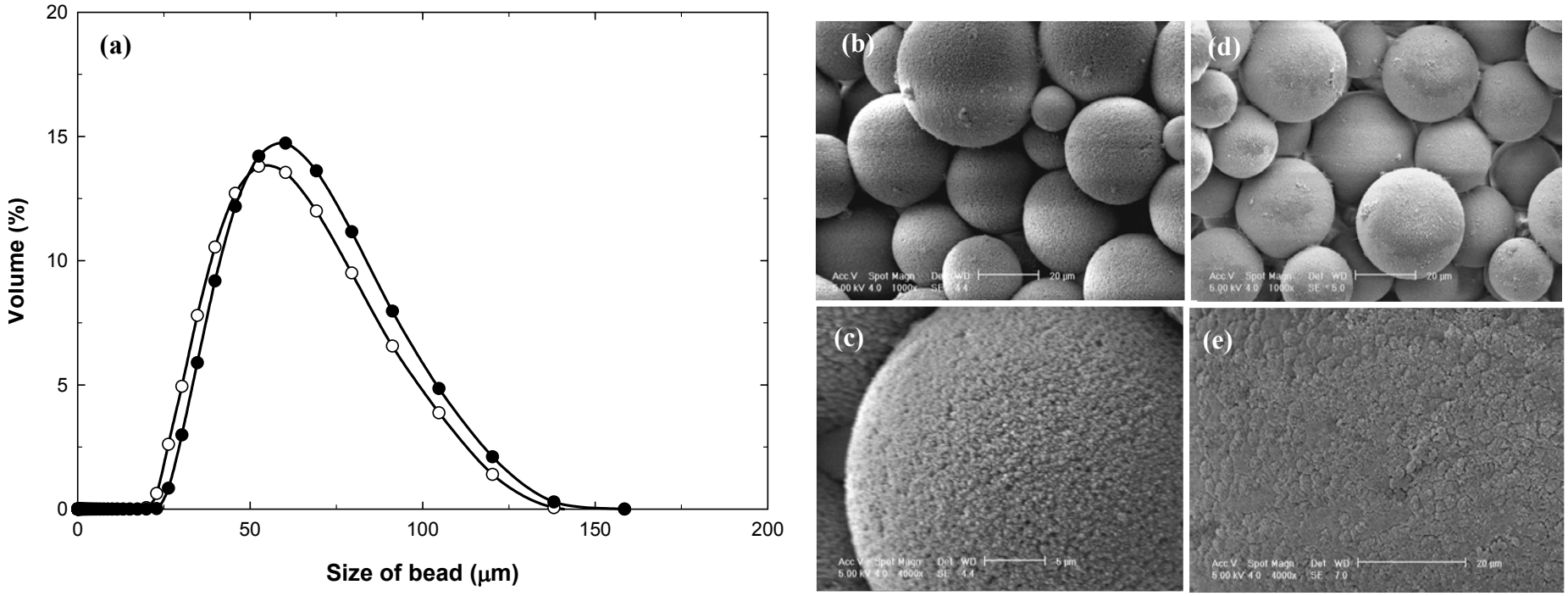

Figure 4.24 : (a) Size distribution graph of Sephacryl S-500 HR: symbols ●= microwaved sample, & ○ = control sample. SEM images of (b) Sephacryl S-500 HR; (c) surface of Sephacryl S-500 HR; (d) microwaved Sephacryl S-500 HR, & (e) microwaved surface of Sephacryl S-500 HR.

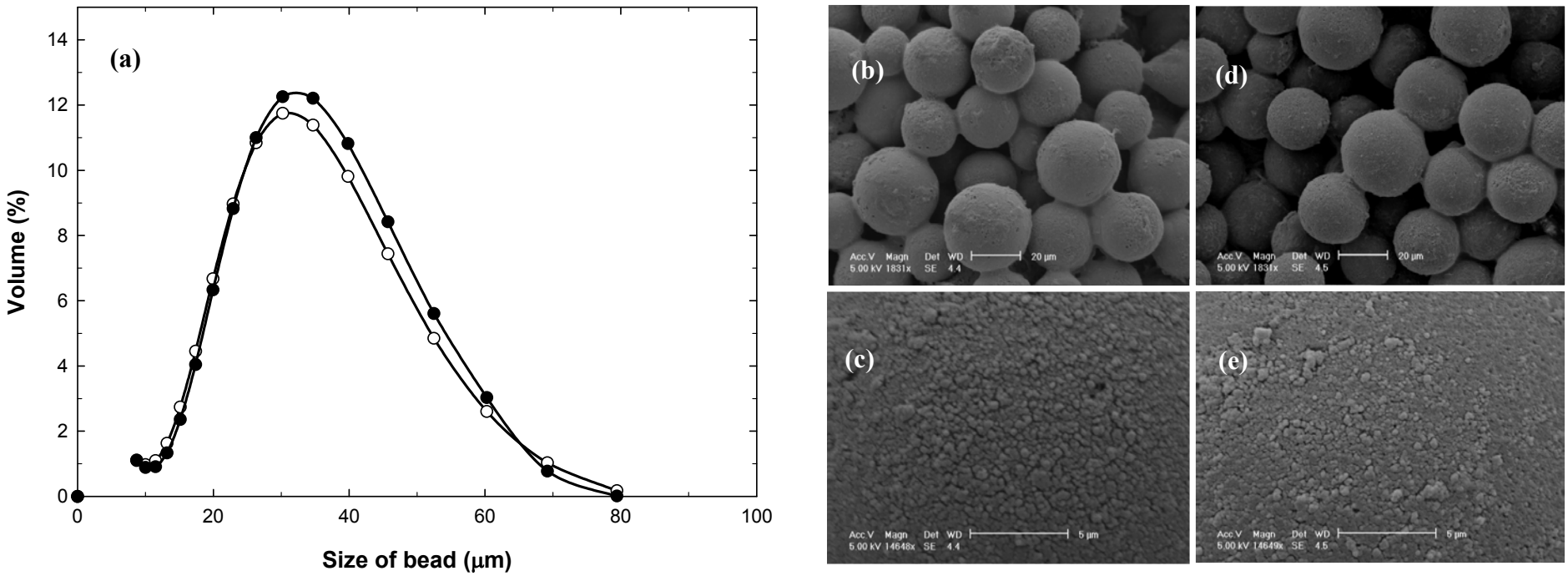

Figure 4.25: (a) Size distribution graph of Superdex 200: symbols ●= microwaved sample & ○ = control sample. SEM images of (b) Superdex 200, (c) surface of Superdex 200; (d) microwaved Superdex 200, & (e) microwaved surface of Superdex 200.

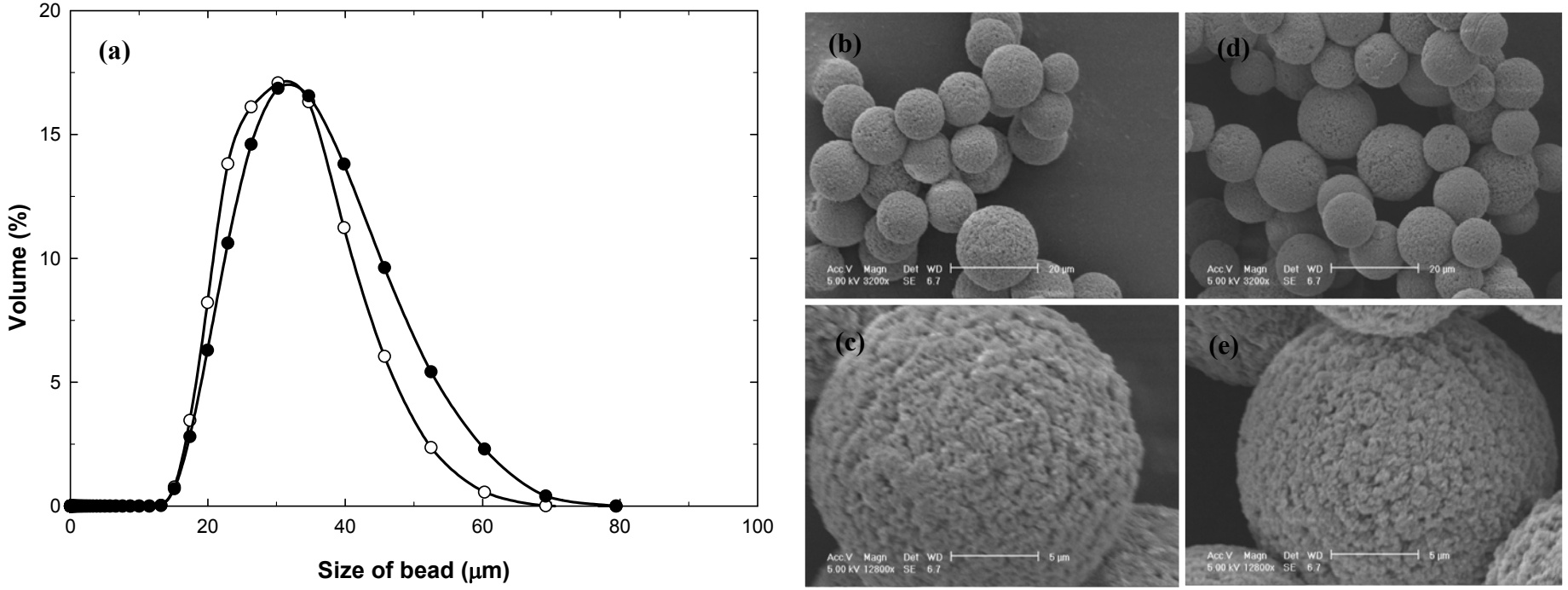

Figure 4.26: (a) Size distribution graph of Superdex 75: symbols ●= microwaved sample, & ○ = control sample. SEM images of (b) Superdex 75; (c) surface of Superdex 75; (d) microwaved Superdex 75, & (e) microwaved surface of Superdex 75.

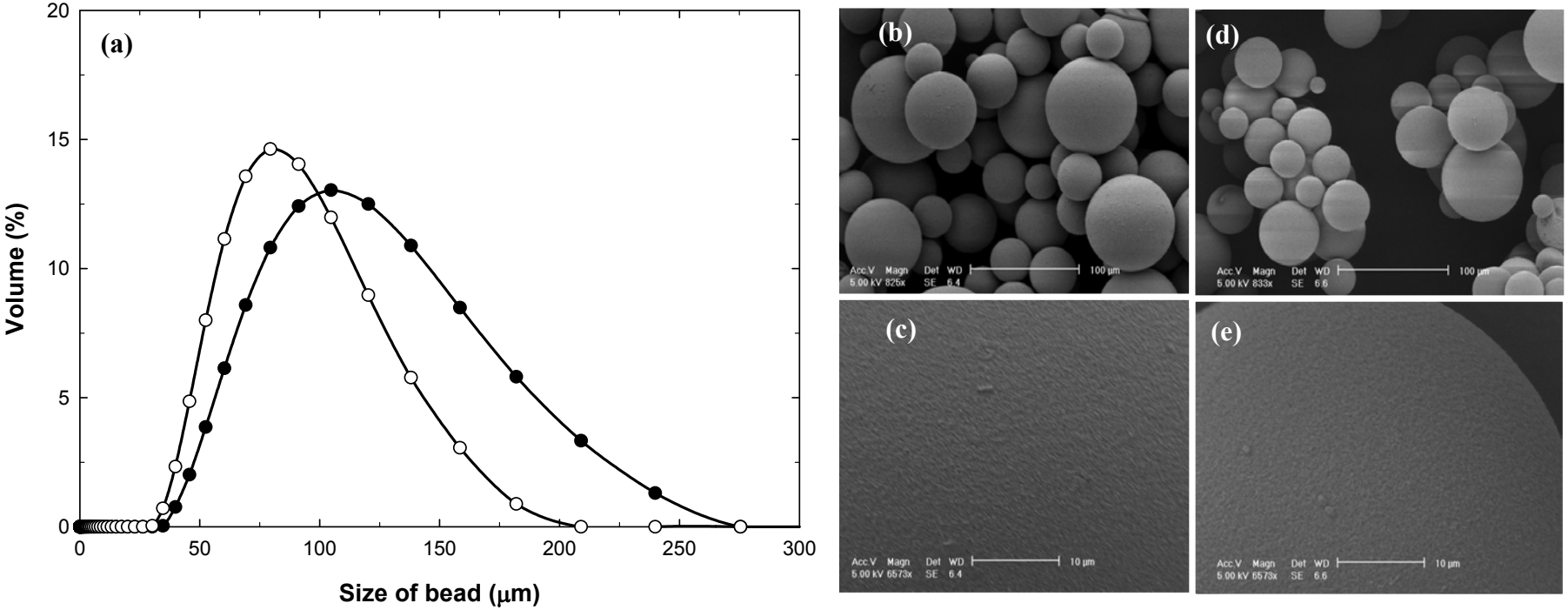

Figure 4.27: (a) Size distribution graph of Capto Q: symbols ●= microwaved sample & ○ = control. SEM images of (b) Capto Q, (c) surface of Capto Q; (d) microwaved Capto Q, & (e) microwaved surface of Capto Q.

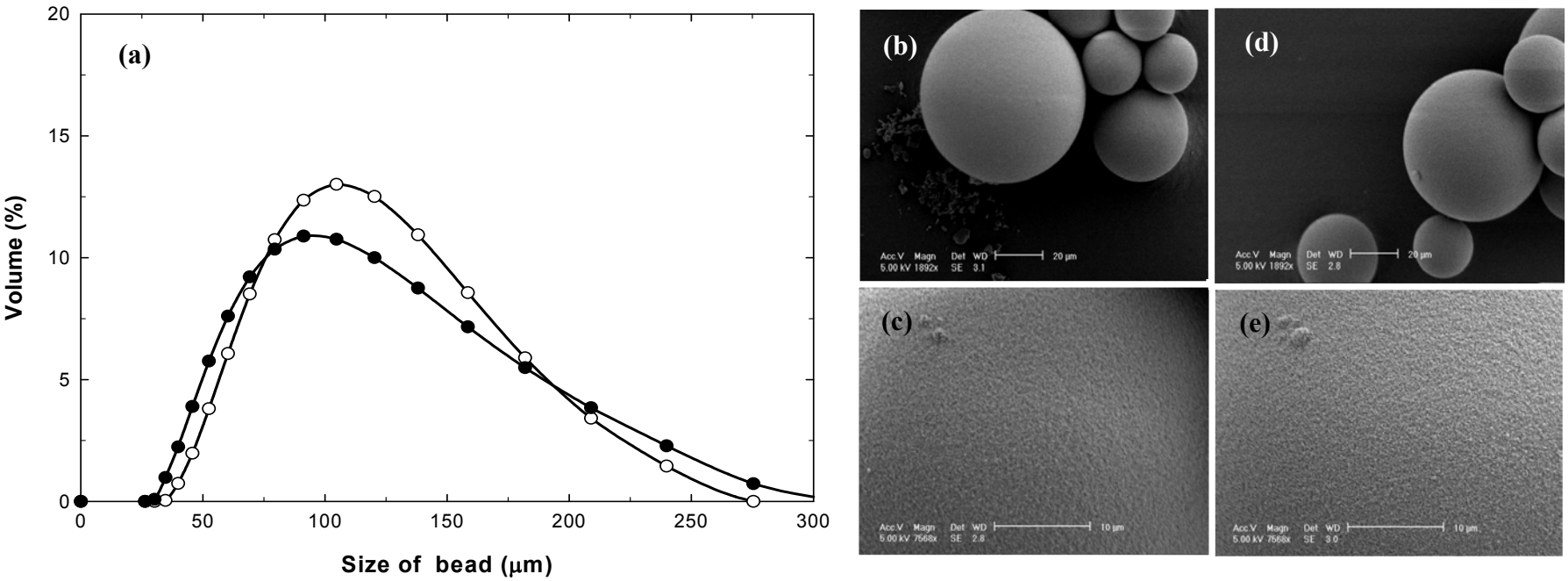

Figure 4.28: (a) Size distribution graph of Capto S: symbols ●= microwaved sample, & ○ = control. SEM images of (b) Capto S; (c) surface of Capto S; (d)microwaved Capto S, & (e) microwaved surface of Capto S.

4.4.3.1 Micromanipulation of Capto S.

Image analysis of Capto S displayed no visual damage after microwave heating (Figure 4.26). Size distribution data did show slight alterations, with the microwaved sample appearing to have expanded by approximately 25 μm (Figure 4.28). The mechanical properties of the both beads (microwaved and unmicrowaved) were very similar up to 28% deformation (Figure 4.29). The young's modulus for both samples is the same, this would be expected as up to 10% deformation there is no significant change in the mechanical properties of the beads (Figure 4.29)

Table 4.7: Young's modules for Capto S micromanipulation experiments

Sample	***E* (MPa) wet state**
Capto S	8.1±2.2
Microwaved Capto S	8.1± 1.5

After 28% deformation the microwaved sample requires a greater stress than to the control with a maximum stress difference (0.2MPa) observed at 40% deformation. The results displayed in Figure 4.29 are a clear indication that the visco-elastic properties of the beads are altered after microwave exposure.

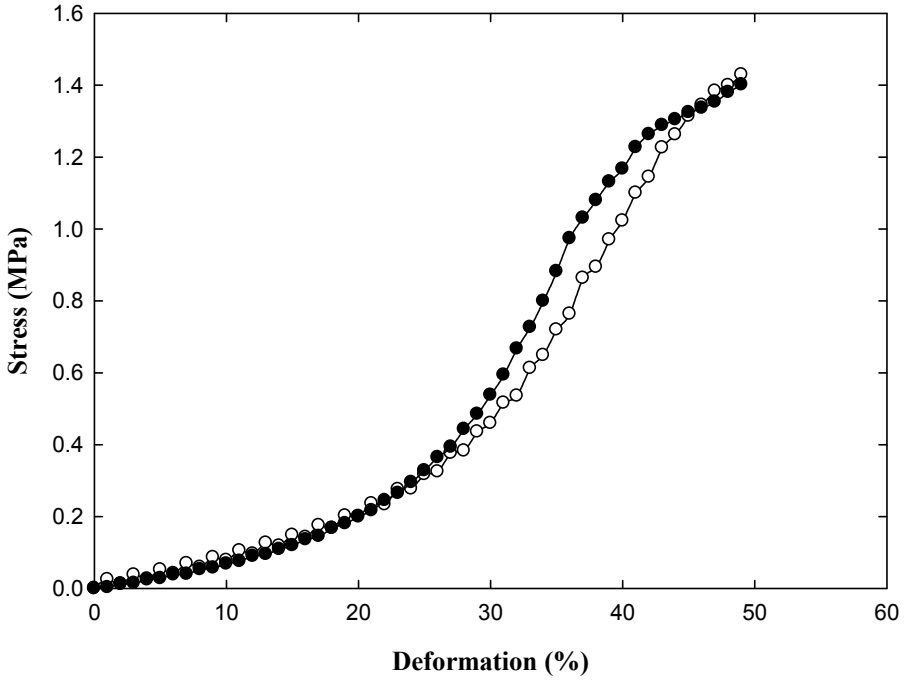

Figure 4.29: Stress/deformation curves of Capto S microwaved and control samples. Symbols ●= microwaved sample & ○ = control sample (each line represents data for 10 particles)

4.4.4 Polystyrene Beads

Source 15 Q is composed of a Polystyrene (specific heat capacity of 1200 J K^{-1} Kg^{-1}, thermal expansion coefficient of 30-210 x 10^{-6} K^{-1} & tensile strength 30-100 MPa) Divinylbenzene, and has a Quaternary amine ligand distributed throughout (Table 4.8). It is reported in literature that standard Polystyrene Merrifield resin under microwave exposure shows thermal stability up to 2200°C without any degradation of the micro-molecular structure of the polymer backbone (Kappe, 2004). The data obtained from audible observation, image analysis, and size distribution showed no damage to Source 15 Q after microwave radiation (Figure 4.30). It can be assumed that temperature gradients would have developed throughout bead as it exposed to microwaves due to the fact that

this support is of mixed chemical composition. Each component possesses a different of dielectric constant and this would interact differently with the electromagnetic wave. It may be useful to investigate the impact of longer microwave exposure times on these beads as under these conditions 'hot spot' may develop due to the mixed composition.

Table: 4.8: Description of polystyrene supports employed in this study and summary of both audible and visual observations during and after microwave treatment

Support	**Immobilised ligand**	**Description of base matrix**	**Manufacturer**	**Popping sound during heating**	**Difference in appearance after microwave irradiation**			
					Naked eye	**Light microscope**	**SEM**	**Size distribution**
Source 15 Q	Quaternary ammonium (Anion exchange).	15 µm av. Rigid, monodispersed, spherical particles of Polystyrene divinylbenzene with controlled pore-size. IEC	GE Healthcare, Uppsala, Sweden.	No	No change	No change	No change	No change

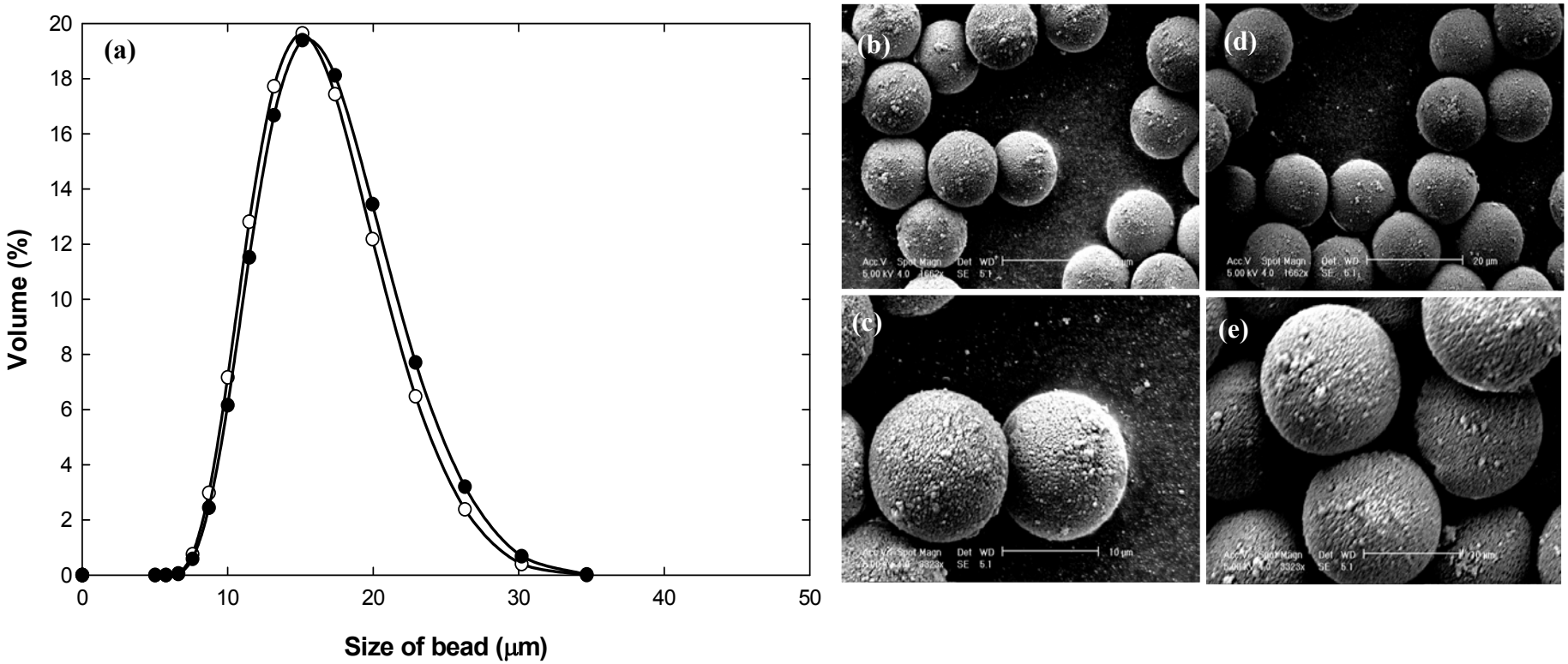

Figure 4.30: (a) Size distribution graph of Source 15 Q: symbols ●= microwaved sample & ○ = control. SEM images of (b) Source 15 Q, (c) surface of Source 15 Q; (d) microwaved Source 15 Q, & (e) microwaved surface of Source 15 Q.

4.4.5 Methacrylate beads

Three different methacrylate based supports were tested in this study: Toyopearl HW 40C; Toyopearl HW 75F, and Fractogel EMD DEAE (results displayed in Table 4.9). Toyopearl beads are composed of Methacrylate and Fractogel EMD is constructed of Penterythritol cross-linked with glycidylmethacrylate. No popping sound was heard when the Toyopearl supports were exposed to microwave heating. Toyopearl HW 40C supports were visually intact after microwave heating (Figure 4.31), however Toyopearl HW 75F (Figure 4.32) appeared slightly defected after microwave exposure. The only differences between the two matrices is pore size and bead diameter; Toyopearl HW 40C has a pore size of 5 nm and a bead diameter range from 50-100 μm whereas Toyopearl HW 75F has a pore size of 10 nm and a bead diameter range of 30-60 μm. The dielectric heating property of a material with regard to microwave can be influenced by the materials network structure (Martin *et al*., 2004). The results obtained for the Toyopearl beads indicate that a greater temperature gradient was reached for Toyopearl HW 75F, which appears to have slightly damaged the bead. However, size distribution data showed no change to either Toyopearl support tested.

Fractogel EMD DEAE matrix (Table 4.9) appeared disfigured by microwaves, this support is composed of two different materials. A popping noise was heard during microwave treatment of Fractogel EMD DEAE indicating the beads may have been affected. Light micrographs (Appendix; Figure 6.13) and SEM images (Figure 4.33) further confirmed that the microwaved sample had changed; SEM images showed that the microwaved beads were cracked. Size distribution data revealed the control sample to be slightly bigger than the microwaved beads. As previously explained (Section 4.2.1.1), the microwave damage observed may have been caused by localized heating

('hotspots'), due to each material present interacting differently with the electromagnetic wave, resulting in thermal induced localised stresses that surpassed the ultimate materials tensile stress.

Table 4.9: Description of Methacylate beads employed in this study and summary of both audible and visual observations during and after microwave treatment

Support	**Immobilised ligand**	**Description of base matrix**	**Manufacturer**	**Popping sound during heating**	**Difference in appearance after microwave irradiation**			
					Naked eye	**Light microscope**	**SEM**	**Size distribution**
Toyopearl HW 40C	None	50-100µm. Hydroxylated methacrylic polymer based bead. Exclusion limit 50 Å. SEC	TOSOH Biosep. CA, USA.	No	No change.	No change	No change	No change
Toyopearl HW 75F	None	50 µm av. Hydroxylated methacrylic polymer based bead. Exclusion limit 1000Å. SEC	TOSOH Biosep CA, USA	No	No change	No change	No change	No change
Fractogel EMD DEAE (650M)	Diethylaminoethyl group (DEAE). Anion exchange.	40-90µm. Pentaerythritol cross linked glycidylmethacrylate beads. Exclusion limit 800Å.IEC	Merck KGaA, Darmstadt. Germany	Yes	No change	Slightly damaged	Damaged	Slightly changed, Control 5µm bigger then microwaved sample

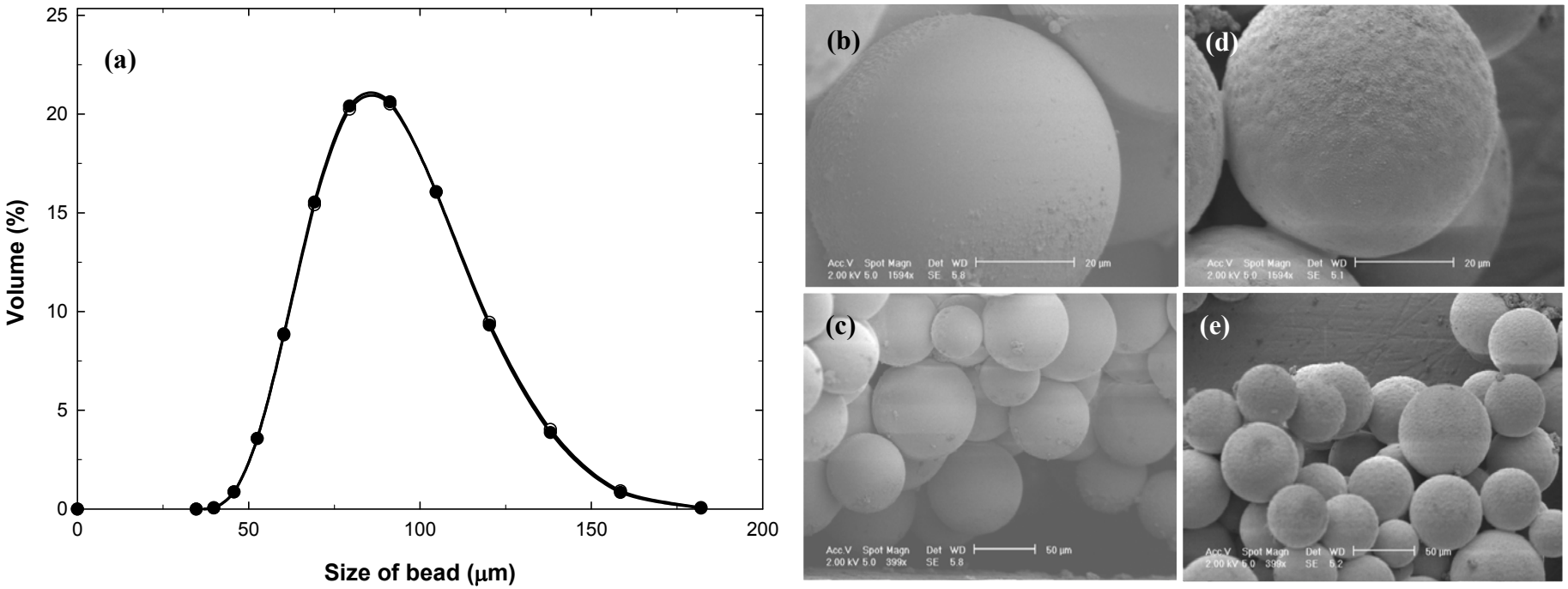

Figure 4.31: (a) Size distribution graph of Toyopearl HW 40C: symbols ●= microwaved sample & ○ = control. SEM images of (b) Toyopearl HW 40C; (c) surface of Toyopearl HW 40C; (d)microwaved Toyopearl HW 40C, & (e) microwaved surface of Toyopearl HW 40C.

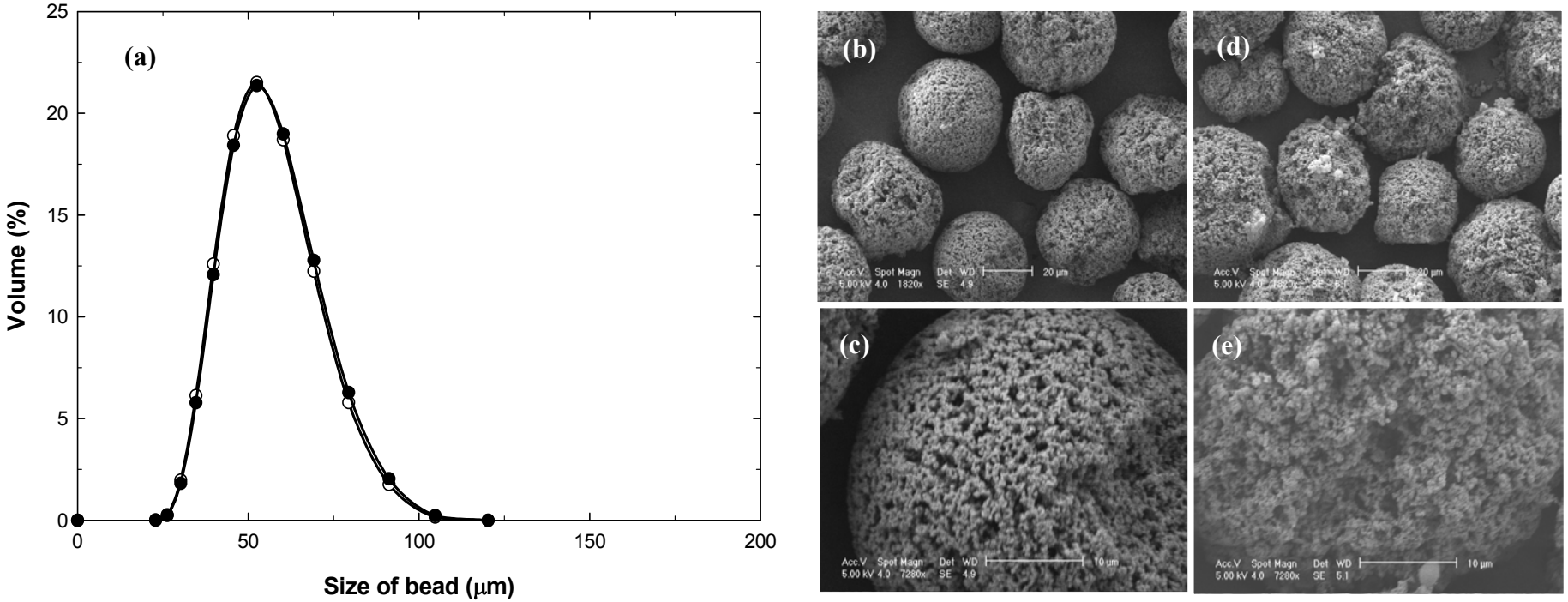

Figure 4.32: (a) Size distribution graph of Toyopearl HW 75 F: symbols ●= microwaved sample, & ○ = control. SEM images of (b) Toyopearl HW 75 F; (c) surface of Toyopearl HW 75 F; (d)microwaved Toyopearl HW 75 F, & (e) microwaved surface of Toyopearl HW 75 F.

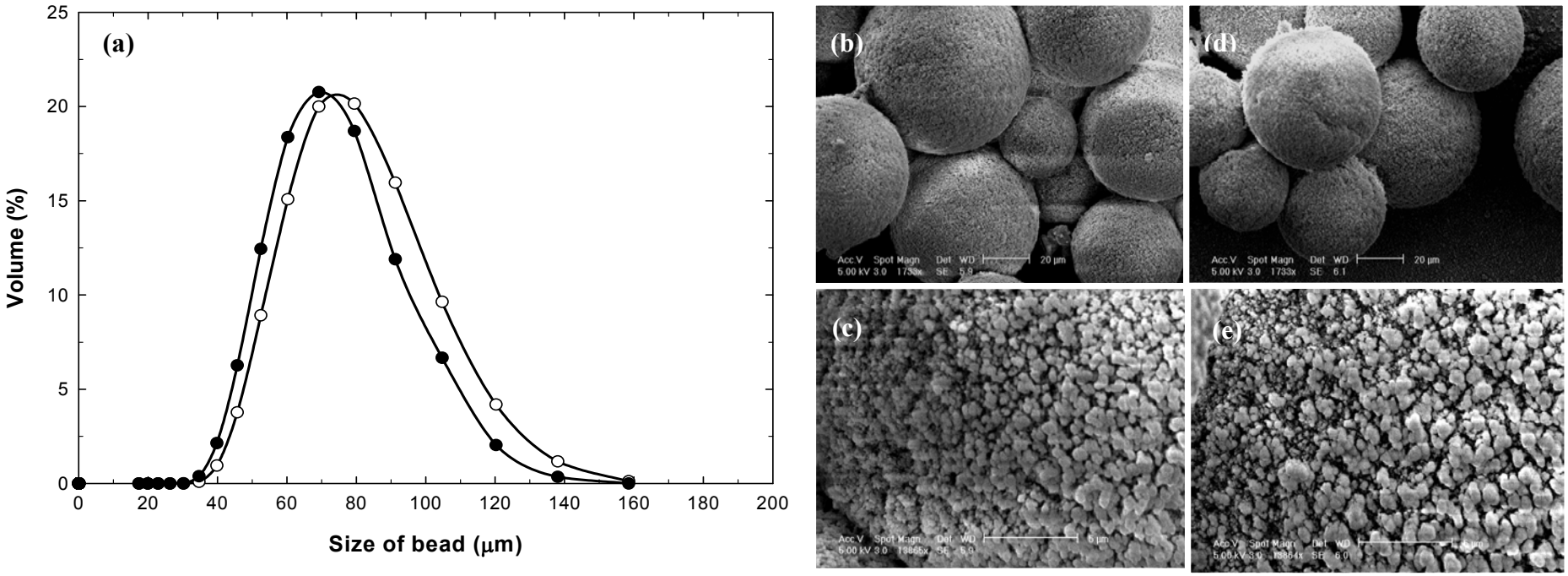

Figure 4.33 : (a) Size distribution graph of Fractogel EMD DEAE: symbols ●= microwaved sample, & ○ = control . SEM images of (b) Fractogel EMD DEAE; (c) surface of Fractogel EMD DEAE; (d) microwaved Fractogel EMD DEAE, & (e) microwaved surface of Fractogel EMD DEAE.

4.4.6 Polymer-inorganic supports

All Streamline beads were unable to endure microwaves; a popping sound was heard for all supports during heating. Visual analysis from light micrographs (Appendix; Figure 6.16) and SEM images showed that the beads were deformed after microwave exposure (Figures 4.34-4.36). These supports are composed of agarose with quartz fragments present in the core. Quartz is a microwave transmitter which is transparent to microwaves, it would therefore not absorb microwave radiation. It could however be heated through conduction from the agarose producing a thermal expansion. Agarose is a microwave absorber so the heat would be generated on the agarose regions of the beads, causing it to expand around the quartz. One explanation for the deformation of Streamline supports may be due to the expansion of agarose at a different rate to the quartz. The thermal expansion coefficient for quartz is 1.77×10^{-6} K^{-1}, it is reported that polymers have a thermal expansion coefficient approximately ten times greater than quartz (www.glassproperties.com). The microwave induced thermal expansion on the agarose resulted in a stress that exceeded the ultimate tensile strength of the material and therefore the beads appear irreversibly deformed. The size distribution data showed that both streamline base matrix and streamline SP (Figures 4.34 & 4.36) were unchanged after microwave heating, however streamline QXL (Figure 4.34) beads appeared to have doubled in size after microwave treatment. Streamline QXL has a positively charged ligand attached to the matrix. The additional damage observed is probably due to the charged ligand which resulted in temperature gradients throughout the support.

Table 4.10: Description of Streamline beads employed in this study and summary of both audible and visual observations during and after microwave.

Support	**Immobilised ligand**	**Description of base matrix**	**Manufacturer**	**Popping sound during heating**	**Difference in appearance after microwave irradiation**			
					Naked eye	**Light microscope**	**SEM**	**Size distribution**
Streamline base matrix	None	100-300µm. Cross linked Agarose bead, agarose content 6% - quartz segments present in the core. SEC	GE Healthcare, Uppsala, Sweden	Yes	No change.	Damaged	Beads appear malformed	No change
Streamline Q XL	Quaternary amine ligand, (Q) (anion exchange)	100-300 µm. Cross linked bead Agarose bead , agarose content 6%, dextran (brush), quartz segments present in the core. IEC	GE Healthcare, Uppsala, Sweden	Yes	No change	Damaged	Beads appear malformed	Microwaved sample appears much bigger than control
Streamline SP	Sulfonpropyl ligand, (S) (cation exchange)	100-300µm. Agarose (6% Cross linked) - quartz core. IEC	GE Healthcare, Uppsala, Sweden	Yes	No change	No change	Beads appear malformed	No change

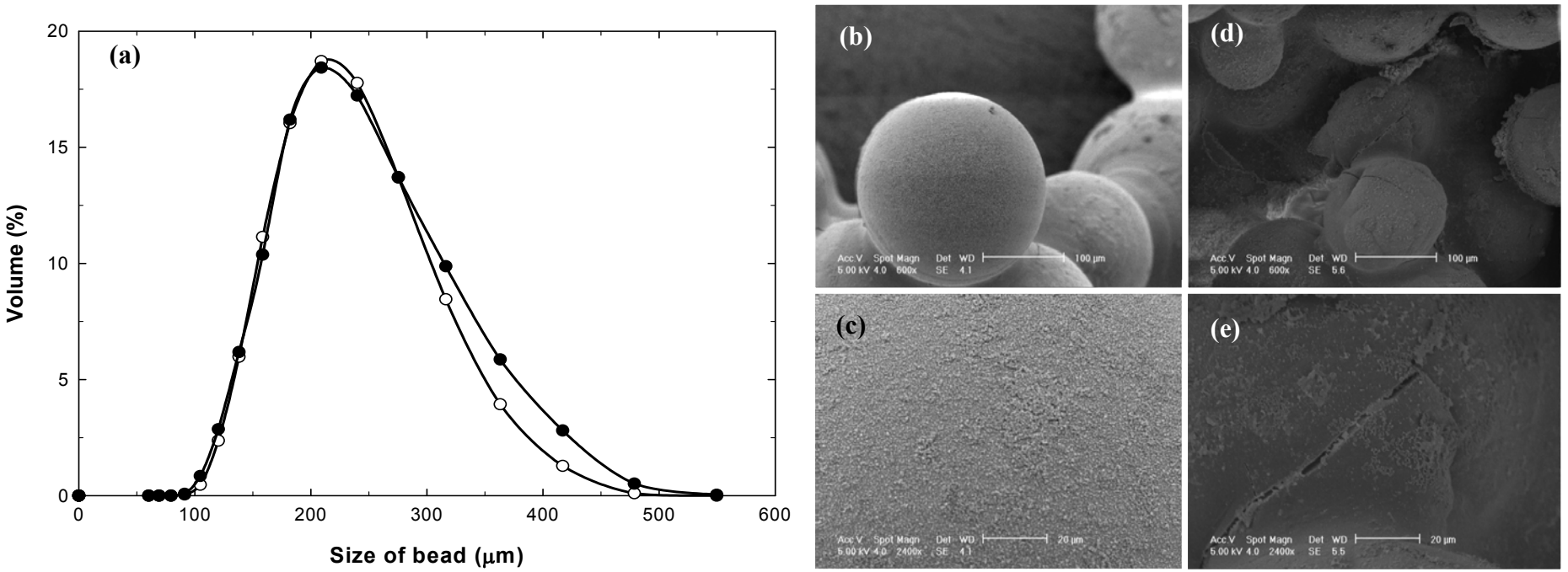

Figure 4.34: (a) Size distribution graph of Streamline base matrix: symbols ●= microwaved sample & ○ = control. SEM images of (b) Streamline base matrix; (c) surface of Streamline base matrix; (d) microwaved Streamline base matrix, & (e) microwaved surface of Streamline base matrix.

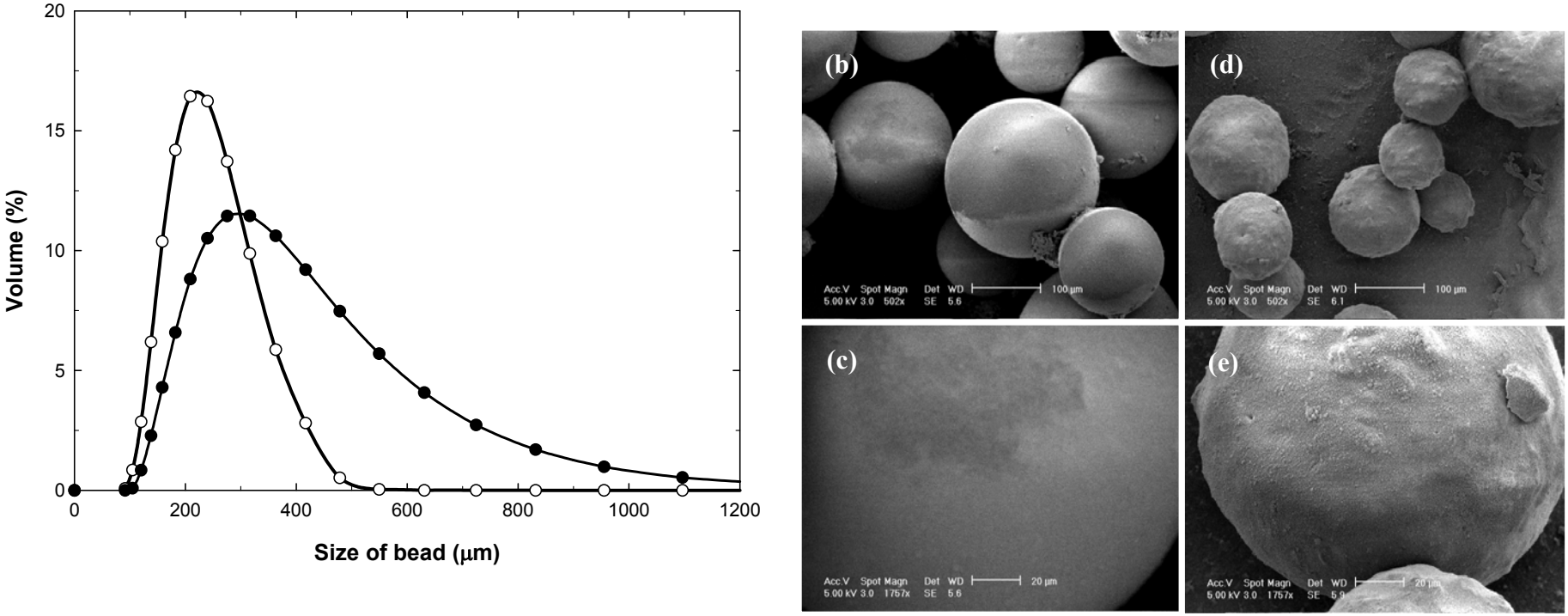

Figure 4.35 : (a) Size distribution graph of Streamline QXL: symbols ●= microwaved sample & ○ = control .SEM images of (b) Streamline QXL; (c) surface of Streamline QXL; (d) microwaved Streamline QXL, & (e) microwaved surface of Streamline QXL.

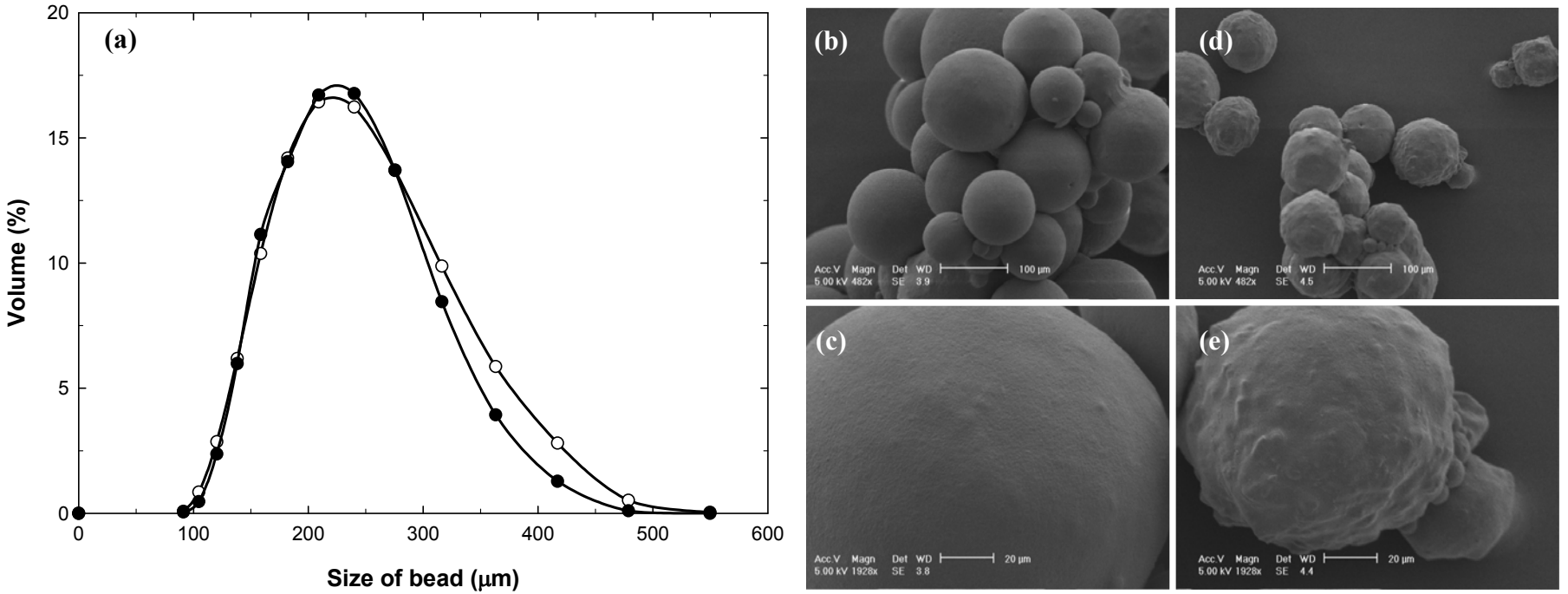

Figure 4.36: (a) Size distribution graph of Streamline SP : symbols ●= microwaved sample & ○ = control : SEM images of (b) Streamline SP;(c) surface of Streamline SP; (d) microwaved Streamline SP, & (e) microwaved surface of Streamline SP.

4.4.6.1 Micromanipulation of Streamline base matrix

SEM images revealed that Streamline base matrix was completely deformed after microwave irradiation: the agarose surrounding the quartz core seemed to have melted and the surface morphology of the microwaved sample is transfigured significantly (Figures 4.34-4.36).

Table 4.11: Young's modules for Streamline base matrix

Bead	***E* (wet state) (MPa)**
Streamline base matrix	1.6± 0.11
Streamline base matrix microwaved	1.6± 0.12

The Young's modules were calculated using the Hertz equation in the linear range below 10% deformation. The mechanical properties of both samples appear to be similar from the Young's modulus results in this deformation range, however the stress versus deformation graph showed significant mechanical differences between the two samples at higher deformations. The microwaved sample required a much higher stress than the control sample with a maximum stress difference of 0.013 MPa at 50% deformation (Figure 4.37). A change in pore size can be assumed from the microwaved beads as the agarose appears to have expanded and cooled around the quartz center, and there is probably no longer a defined porous structure. This observation may explain why a greater stress was required to compress the microwaved streamline sample when compared to the control.

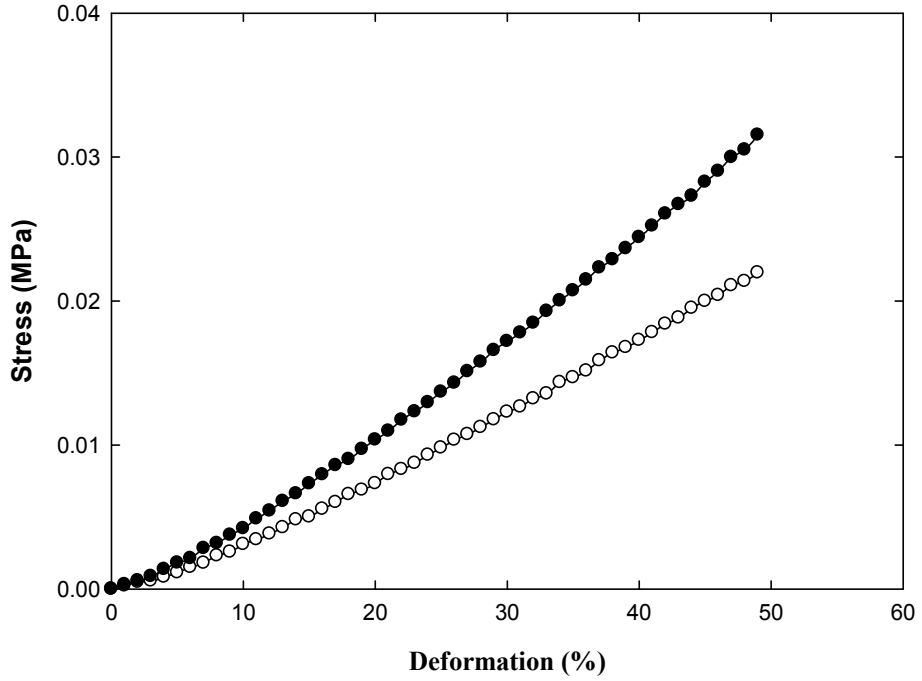

Figure 4.37: Stress/deformation curves of microwaved and control samples of Streamline base matrix, Symbols ●= microwaved sample & ○ = control sample (each line represents mean data for 10 particles).

4.4.7 UFC beads

No popping noise was heard during the microwave heating of all UFC supports (Table 4.12), however visual analysis from light micrographs (Appendix; Figure 6.17) and SEM images (Figures 4.38-4.40) exposed damaged supports after microwave heating.

The UFC steel supports amalgamated after interacting with microwaves (Figure 4.38). These beads are constructed to contain a stainless steel core with an agarose outer layer, agarose is a microwave absorber whereas steel is a microwave reflector. The microwave interacts with the steel causing the electrons near the surface to move, due to the fact that there are so many electrons compacted on the surface as they connect with the electromagnetic wave there is limited side to side movement, thus prohibiting the electric

wave from entering the metal (shielding effect) therefore the wave is reflected. The abnormal rapid movement of the electrons in the metal caused by the strong electric wave can generate heat (Kriegsmann, 1991). Light micrographs (Appendix Figure 6.17) showed that the steel part of the beads was not melted by microwaves; however it was apparent from SEM images and size distribution results (Figure 4.38) that the supports had adhered into sticky clumps and the beads were completely deformed. During heating agarose would have expanded around the steel core, furthermore the rapid generation of heat from the steel would have caused additional expansion of the agarose. It is apparent from the results that the thermal expansion enforced was greater than the tensile strength of the material. Size distribution data confirmed that the UFC steel supports had clustered together after microwave exposure and appear to be at least five times bigger in size when compared to the unmicrowaved sample.

UFC glass supports were all damaged after interacting with microwaves (Table 4.12). Light micrographs (Appendix; Figure 6.17) and SEM images revealed chipped cracked beads after microwave exposure (Figures 4.39 & 4.40). These beads are constructed to contain a glass core with an agarose outer layer. The agarose outer layer is a microwave absorber whereas the glass is a microwave transmitter which is transparent to microwaves. The glass would not generate heat from the microwaves; however it could absorb heat via heat transfer from the surrounding agarose and therefore expand slightly. The inconsistent thermal expansion of the two materials may have resulted in the contortion of the beads, where the stress enforced on the agarose was greater than the ultimate tensile strength of the material. The difference in the chemical composition for UFC glass and UFC PEI would result in individual dielectric properties for the two supports and therefore these beads would respond differently to electromagnetic wave.

This is evident from both SEM images and size distribution data obtained. Firstly the SEM images for both supports disclose that they are both irreversibly changed due to microwave heating, yet the type of damage is distinct for each support. Visually UFC glass appears to be chipped after microwave exposure; this is also confirmed by the size distribution graph where the microwave supports appear to be fragmented. SEM results for UFC PEI showed that the beads were deformed after microwave irradiation; the size distribution graph for this sample verified that the microwaved beads were approximately 200 μm bigger than the control.

Table 4.12: Description of UFC beads employed in this study and summary of both audible and visual observations during and after microwave

Support	**Immobilised ligand**	**Description of base matrix**	**Manufacturer**	**Popping sound during heating**	**Difference in appearance after microwave irradiation**			
					Naked eye	**Light microscope**	**SEM**	**Size distribution**
UFC Glass	None	A bead composed of a glass core surrounded with an agarose layer. SEC	Upfront Chromatography A/S, Copenhagen, Denmark	No	No change.	Slightly damaged	Damaged	Microwaved sample appears much smaller than control indicating that the beads may have fragmented due to microwave heating
UFC Steel	None	A bead composed of a stainless steel core surrounded with a thin agarose layer. Agarose content 6%, thin layer. SEC	Upfront Chromatography A/S, Copenhagen, Denmark	No	Clumped	Sticky	Beads appear to have collapsed	Microwaved sample appears to be much bigger than control, indicating that the microwaved beads may have stuck together due to melting of agarose
UFC Steel PEI	Polyethyleneimine ligand (PEI). Anion exchange	A bead composed of a stainless steel core surrounded with a thin agarose layer. Agarose content 6%, thin layer. IEC	Upfront Chromatography A/S, Copenhagen, Denmark	No	Clumped	Sticky	Damaged	Microwaved sample appears to be much bigger than control, indicating that the microwaved beads may have stuck together due to melting of agarose

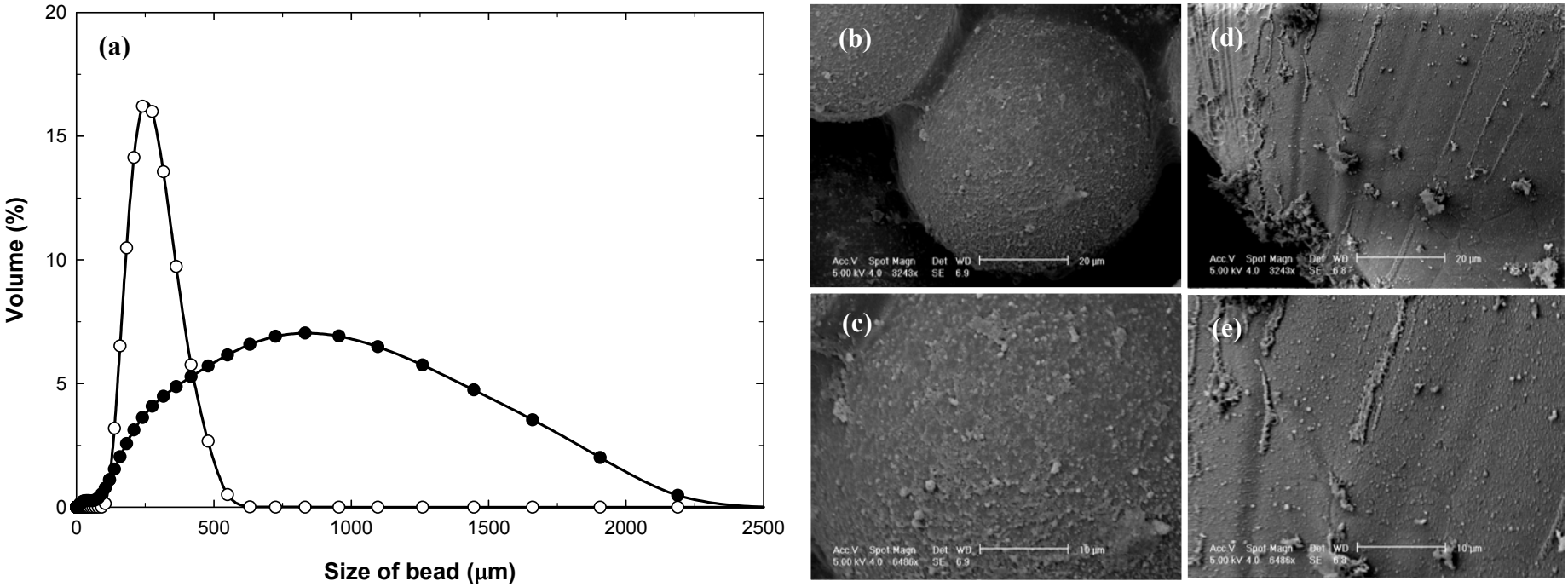

Figure 4.38: (a) Size distribution graph of UFC Steel: symbols ●= microwaved sample & ○ = control. SEM images of (b)UFC Steel; (c) surface of UFC Steel; (d) microwaved UFC Steel, & (e) microwaved surface of UFC Steel

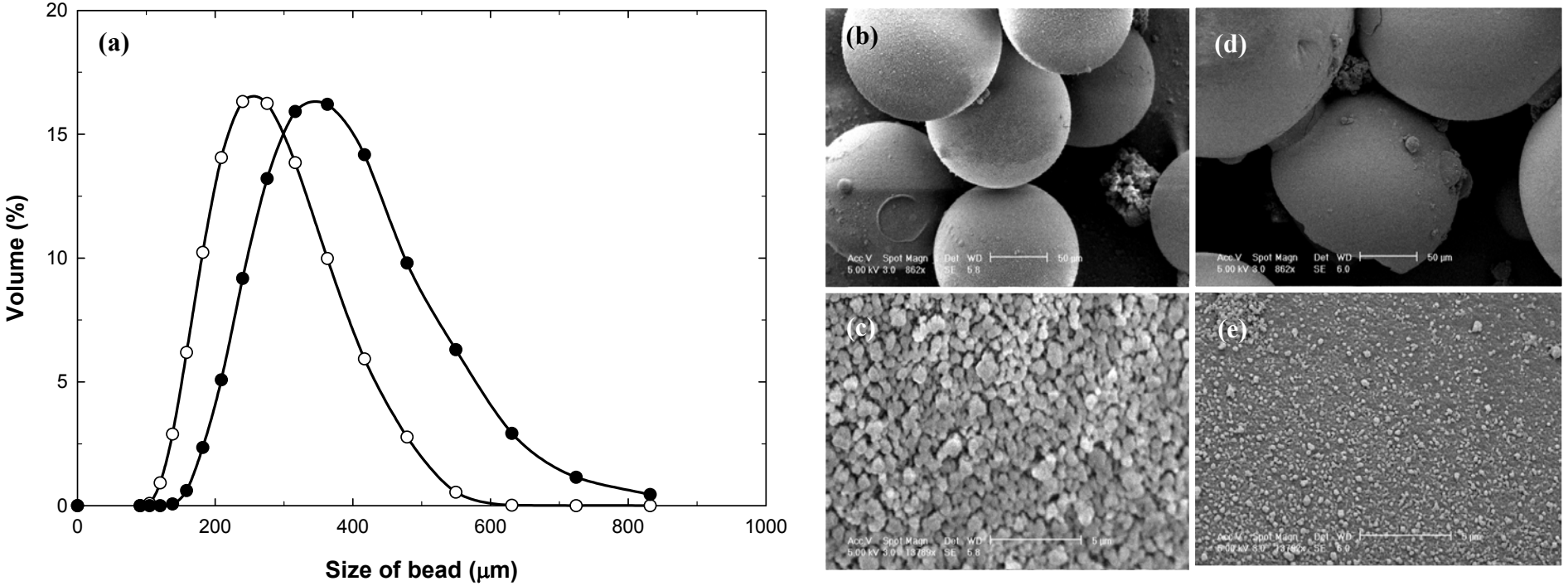

Figure 4.39 : (a) Size distribution graph of UFC PEI : symbols ●= microwaved sample & ○ = control .SEM images of (b)UFC PEI ;(c) surface of UFC PEI; (d) microwaved UFC PEI, & (e) microwaved surface of UFC PEI

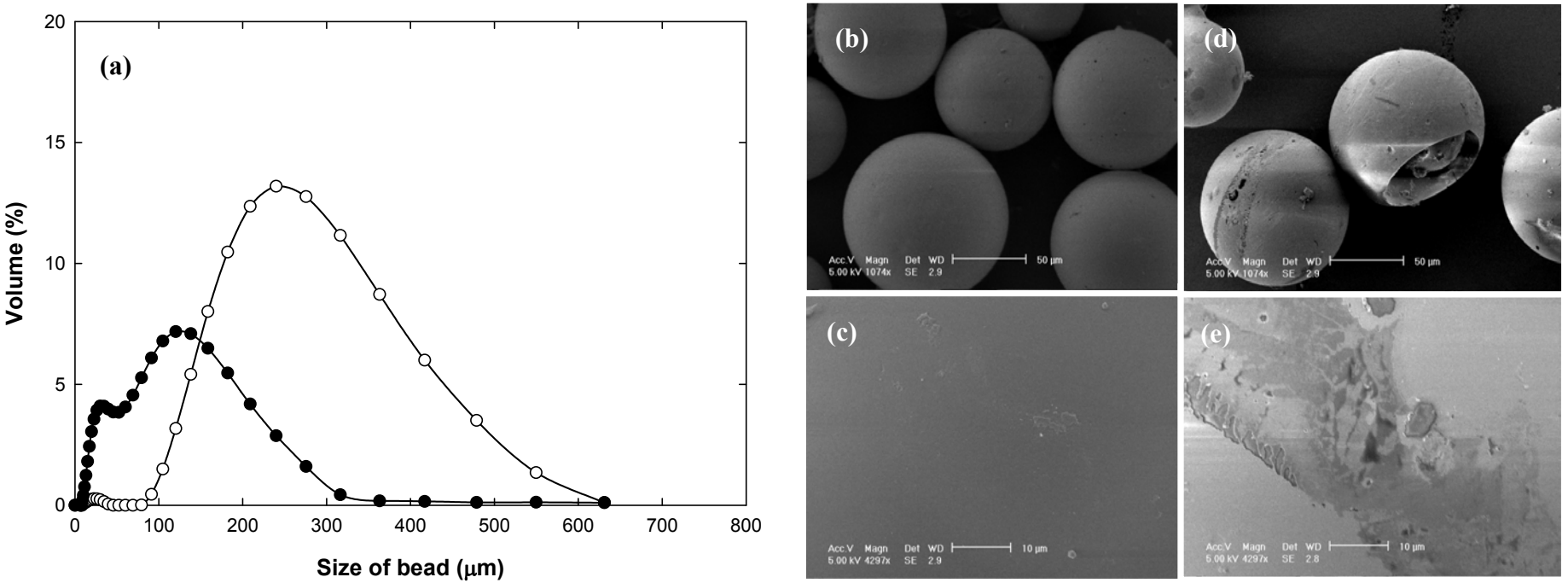

Figure 4.40: (a) Size distribution graph of UFC glass: symbols ●= microwaved sample & ○ = control. SEM images of (b) UFC glass;(c) surface of UFC glass; (d) microwaved UFC glass, & (e) microwaved surface of UFC glass

4.4.8 Ceramic supports

During microwave heating a popping noise was observed for all Zirconia based supports (Table 4.13), except for CM hyper Z, indicating that these beads may not have been damaged. Image analysis (Light microscope & SEM) showed that all Zirconia based matrices were all affected by microwave irradiation. SEM images (Figures 4.41-4.48) showed these supports to be cracked and broken after microwave heating. Zirconia is a ceramic material; as previously discussed most ceramics are transparent to microwaves at room temperature (Section 4.2.1.1). However, when heated above a critical temperature ceramics can rapidly interact with microwave energy (Yamanaka *et al*., 1990; Vriezinga, 1998). If limited areas of the material reach the critical temperature first, then those areas begin to heat more rapidly. This localized thermal runaway can cause stresses that are high enough to splinter the material.

Size distribution results showed no change in the size for Zirconia based matrices after microwave heating.

The silica based supports tested were: QMA Spherosil; DEAE Spherodex LS, and SP Spherodex beads. The Spherodex beads are composed of silica and are cross-linked with Dextran (Table 4.13). QMA Spherosil and DEAE Spherodex LS are anion exchange supports; where as SP Spherodex LS is a cation exchange support. There are numerous publications available on the successful synthesis of silica via microwaves (Min-Zhi *et al*., 2006; Simoes *et al*., 2008; Ramesh *et al*., 2008). It is also reported that many ceramics are poor absorbers of microwaves up to a critical temperature, above this temperature the dielectric loss factor starts to increase, and the material interacts

with microwaves (Vriezinga, 1998). In this study both light microscope and scanning electron microscopy experimental analysis (Figures 4.46-4.48) disclosed all silica based matrices to be damaged after microwave treatment. The damage caused to the silica beads is probably due to the distribution of charge throughout the support; this charge would create varying dielectric properties throughout the silica matrix. It is reported that charge can enhance microwave coupling (Caddick, 1995). It can be assumed that the ligand would therefore have a greater affinity for the electromagnetic wave due to the fact that it is reported that ceramics have poor coupling properties with electromagnetic waves. These areas of localized thermal expansion (hot-spots) induced strains greater than the ultimate tensile strength of the material causing breakage.

There was no change in size for SP Spherodex LS after it endured microwave heating, however slight size changes were observed for QMA Spherosil and DEAE Spherodex LS with a size difference of between 10-20 μm compared to the control sample. As previously explained this may be due to the positive charge located throughout the matrices which seems to further enhance the interaction with microwaves.

Table 4.13: Description of ceramic beads employed in this study, summary of both audible and visual observations during and after microwave

Support	Immobilised ligand	Description of base matrix	Manufacturer	Popping sound during heating	Difference in appearance after microwave irradiation			
					Naked eye	Light microscope	SEM	Size distribution
Zirconia Bead (Glen Creston)	None	Beads composed of Zirconium Dioxide.	Glen Creston, London, UK.	Yes	No change.	Damaged	Damaged, microwaved beads appear cracked.	No change
CM hyper Z	Carboxymethyl ligand (cm), 100-180µmol/mL (cation ion exchange)	40-105µm, 75µm av. A high density bead composed of Zirconium oxide. IEC/EBA	Pall, Portsmouth, Hampshire, UK	No	No change	Damaged	Damaged, microwaved beads appear deformed	No change
Q hyper Z	Quaternary amine ligand (Q), 100-180µmol/mL (Anion exchange)	40-105µm, 75µm av. A high density bead composed of Zirconium oxide. IEC/EBA	Pall, Portsmouth, Hampshire, UK	Yes	No change	Slightly damaged	Damaged, beads appear cracked.	No change
Q hyper DF	Quaternary amine ligand (Q), 250≥ µmol/mL (Anion exchange)	50µm av. Ceramic Media (silica) coated with polyacrylamide. IEC	Pall, Portsmouth, Hampshire, UK	Yes	No change	Slightly damaged	Damaged, microwaved beads appear cracked.	No change
S hyper DF	Methyl Sulphonate Ligand (MS), 150≥ µmol/mL (cation exchange)	50µm av. Ceramic Media (silica) coated with l. IEC.	Pall, Portsmouth, Hampshire, UK	Yes	No change	Slightly damaged	Damaged, microwaved beads appear deformed and cracked.	No change
QMA SPHEROSIL LS	Quaternary amine ligand (Q), 300≥ µmol/mL (Anion exchange)	100-300µm, Polymer grafted silica bead. IEC	Pall, Portsmouth, Hampshire, UK	No	No change	Damaged	Damaged, microwaved beads appear deformed.	Microwaved beads appear to be aprox. 20 µm bigger than control.
SP SPHEROSIL	Sulfopropyl ligand (SP) 300≥ µmol/mL (cation exchange)	100-300µm, Polymer grafted silica bead. IEC.	Pall, Portsmouth, Hampshire, UK	No	No change	Damaged	Damaged, microwaved beads appear deformed.	No change
DEAE Spherodex LS	Diethylaminoethyl group (DEAE). Ligand density 100µmol/mL. Anion exchange	100-300µm, Dextran grafted silica bead. IEC	Pall, Portsmouth, Hampshire, UK	No	No change	No change	Damaged, microwaved beads appear deformed.	Control beads appear to be 10 µm bigger than microwaved beads

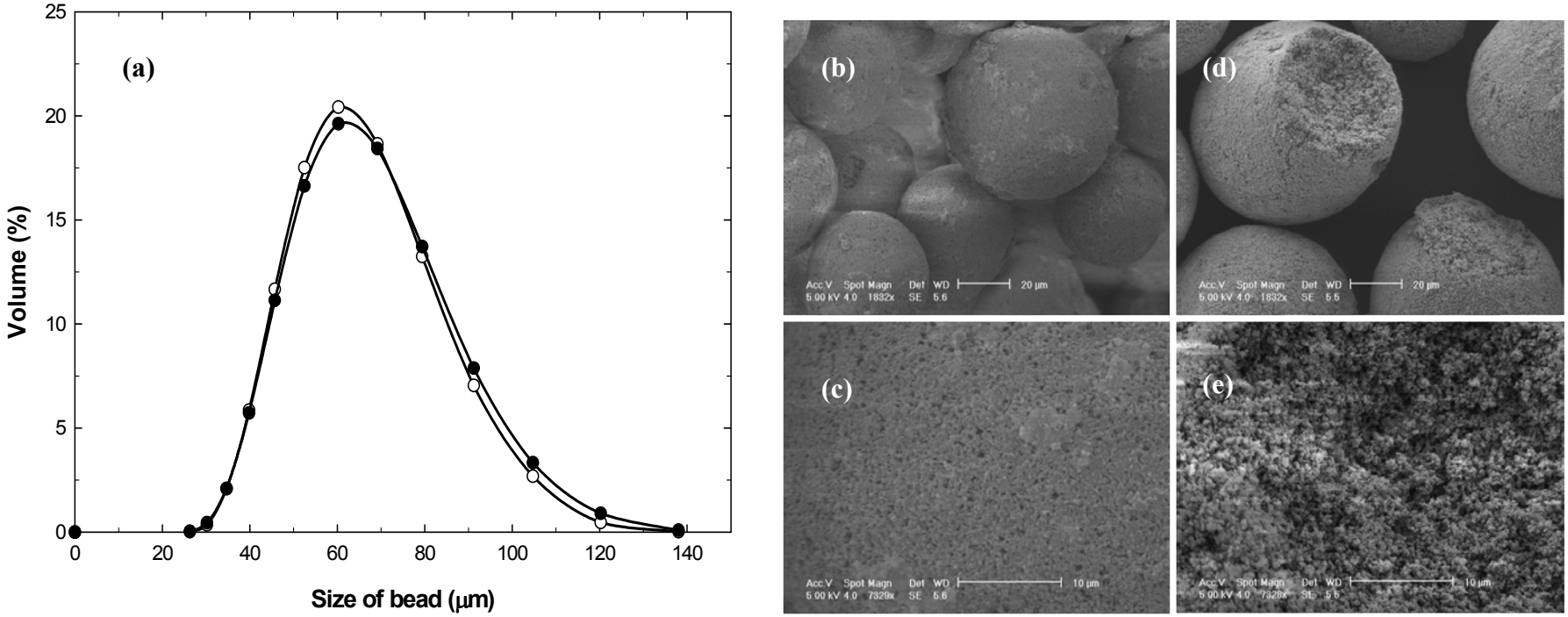

Figure 4.41: (a) Size distribution graph of Q Hyper Z: symbols ●= microwaved sample & ○ = control. SEM images of (b) Q hyper Z (c) surface of Q Hyper Z ;(d) microwaved Q Hyper Z, & (e) microwaved surface of Q Hyper Z.

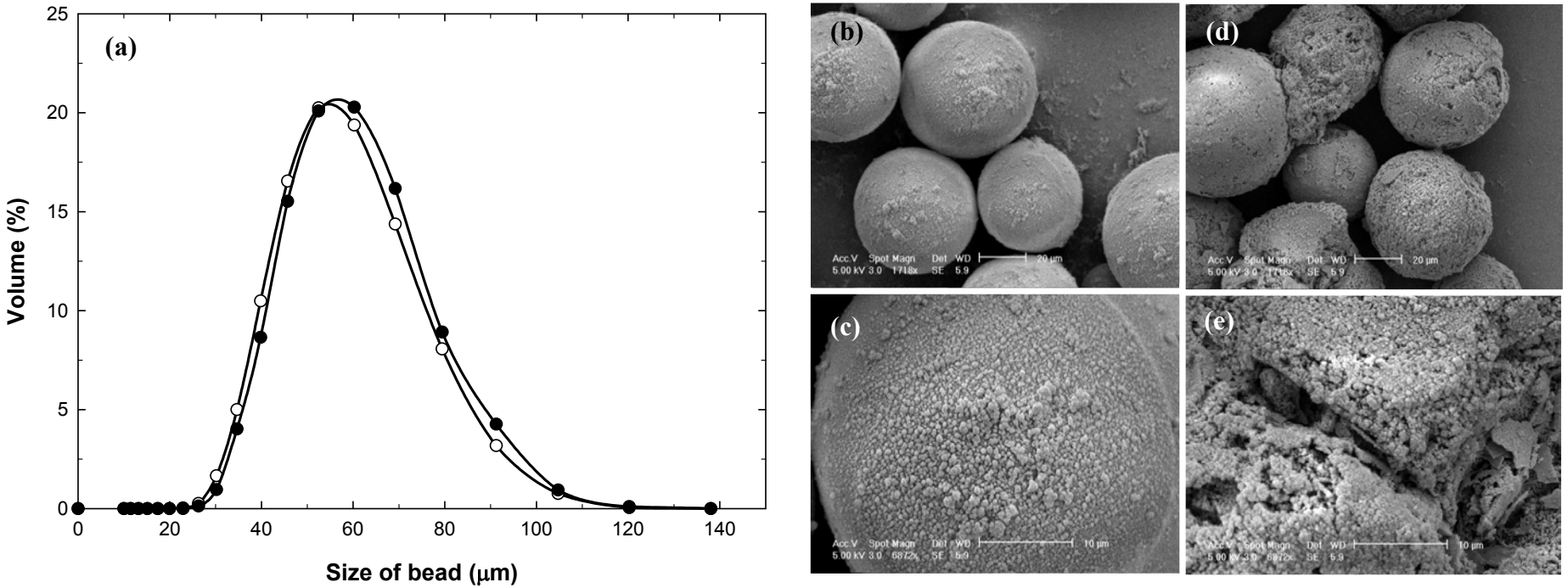

Figure 4.42: (a) Size distribution graph of Zirconia Bead: symbols ●= microwaved sample & ○ = control. SEM images of (b) Zirconia Bead; (c) surface of Zirconia Bead; (d) microwaved Zirconia Bead, & (e) microwaved surface of Zirconia Bead.

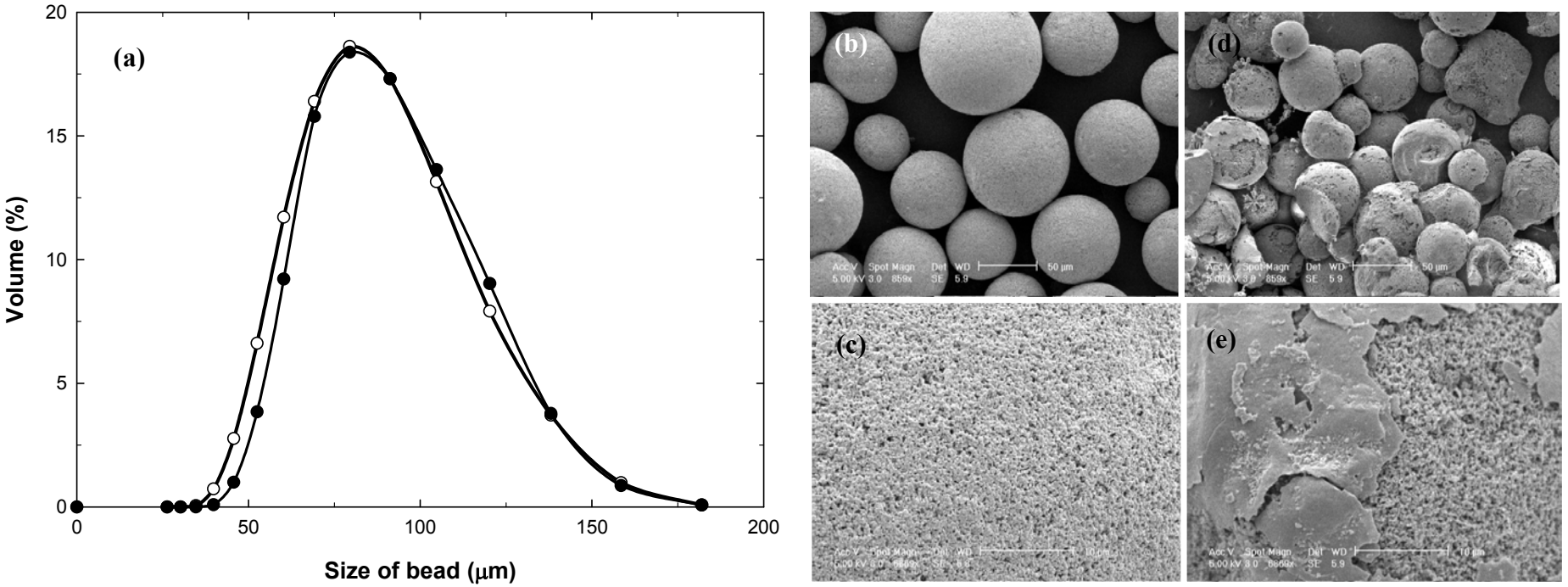

Figure 4.43: (a) Size distribution graph of CM Hyper Z: symbols ●= microwaved sample & ○ = control :SEM images of (b) CM Hyper Z Bead ; (c) surface of CM Hyper Z; (d) microwaved CM Hyper Z, & (e) microwaved surface of CM Hyper Z.

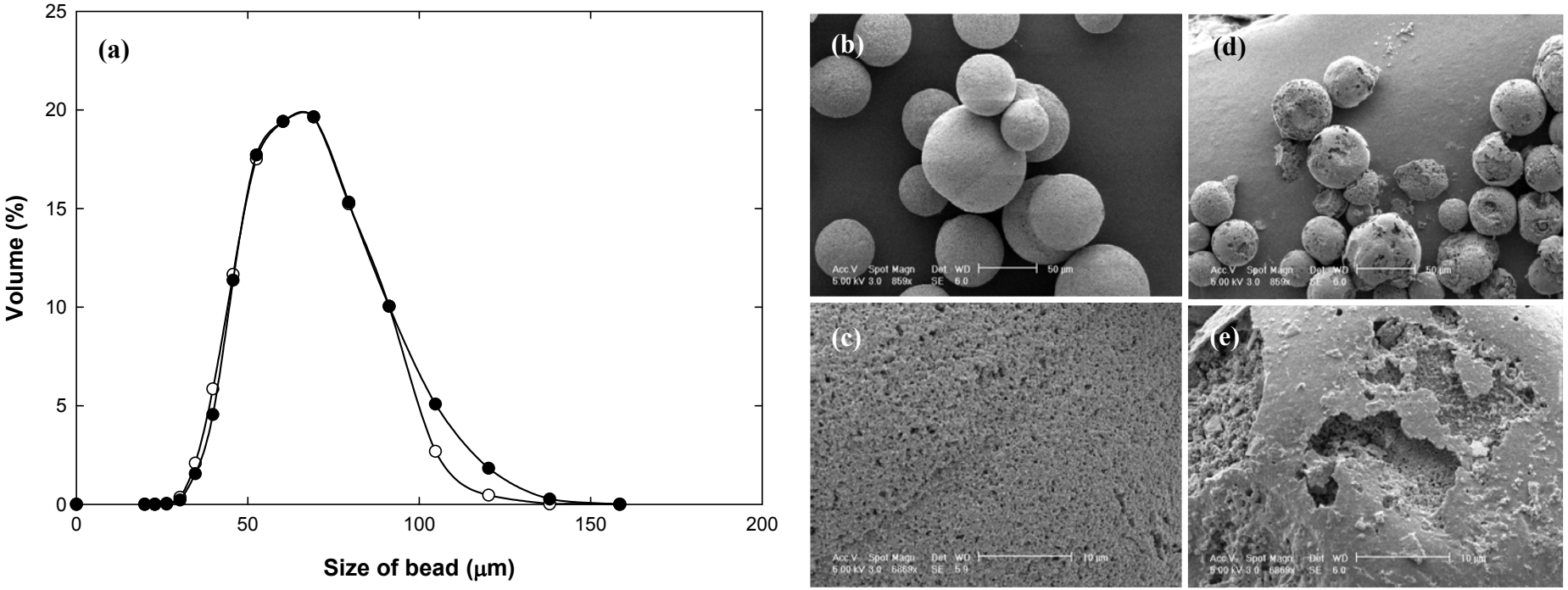

Figure 4.44: (a) Size distribution graph of Q Hyper DF :symbols ●= microwaved sample & ○ = control. SEM images of (b) Q Hyper DF Bead (c) surface of Q Hyper DF; (d) microwaved Q Hyper DF, & (e) microwaved surface of Q Hyper DF

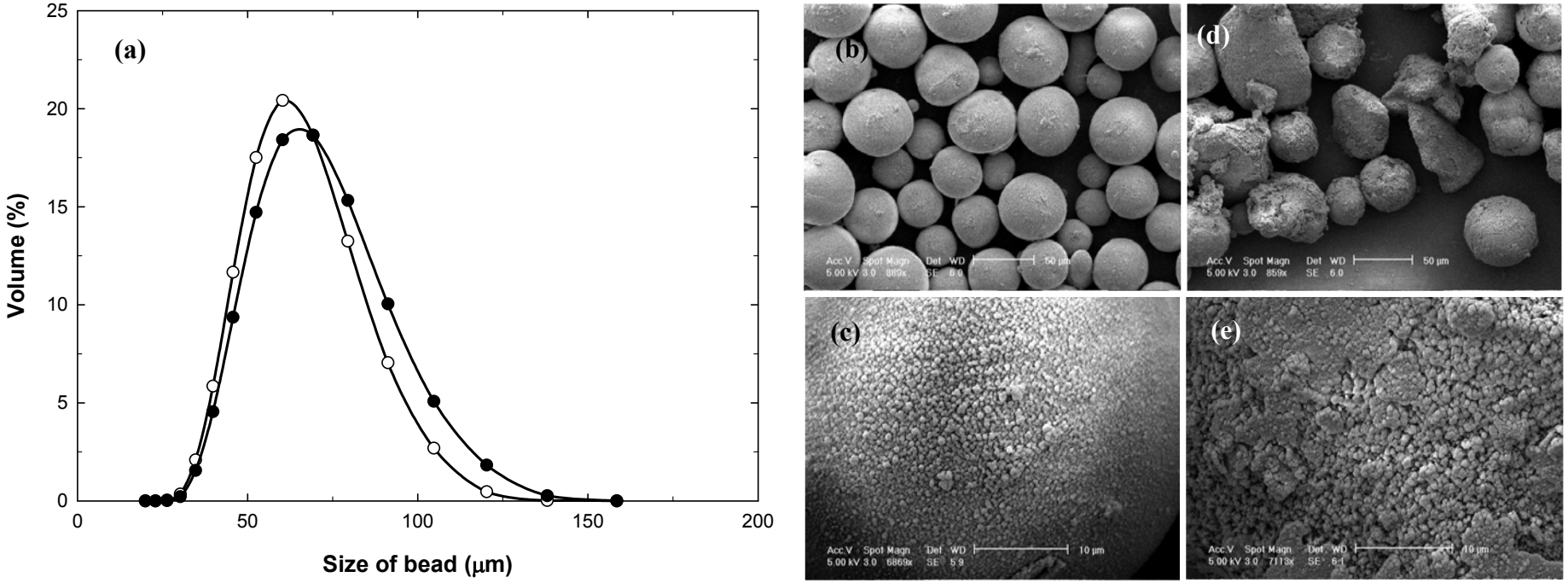

Figure 4.45: (a) Size distribution graph of S Hyper DF: symbols ●= microwaved sample & ○ = control. SEM images of (b) S Hyper DF Bead ; (c) surface of S Hyper DF ;(d) microwaved S Hyper DF, & (e) microwaved surface of S Hyper DF.

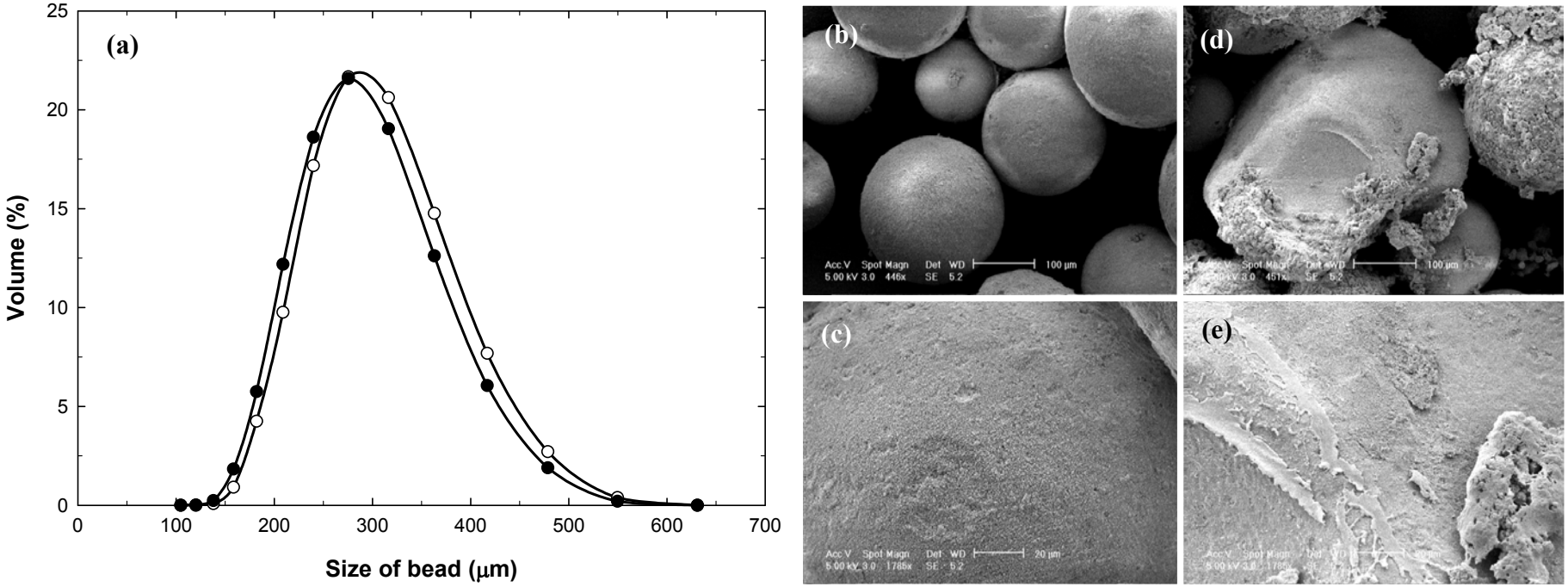

Figure 4.46: (a) Size distribution graph of DEAE Spherodex LS, symbols ●= microwaved sample & ○ = control. SEM images of (b) DEAE Spherodex LS; (c) surface of DEAE Spherodex LS; (d) microwaved DEAE Spherodex LS, & (e) microwaved surface of DEAE Spherodex LS .

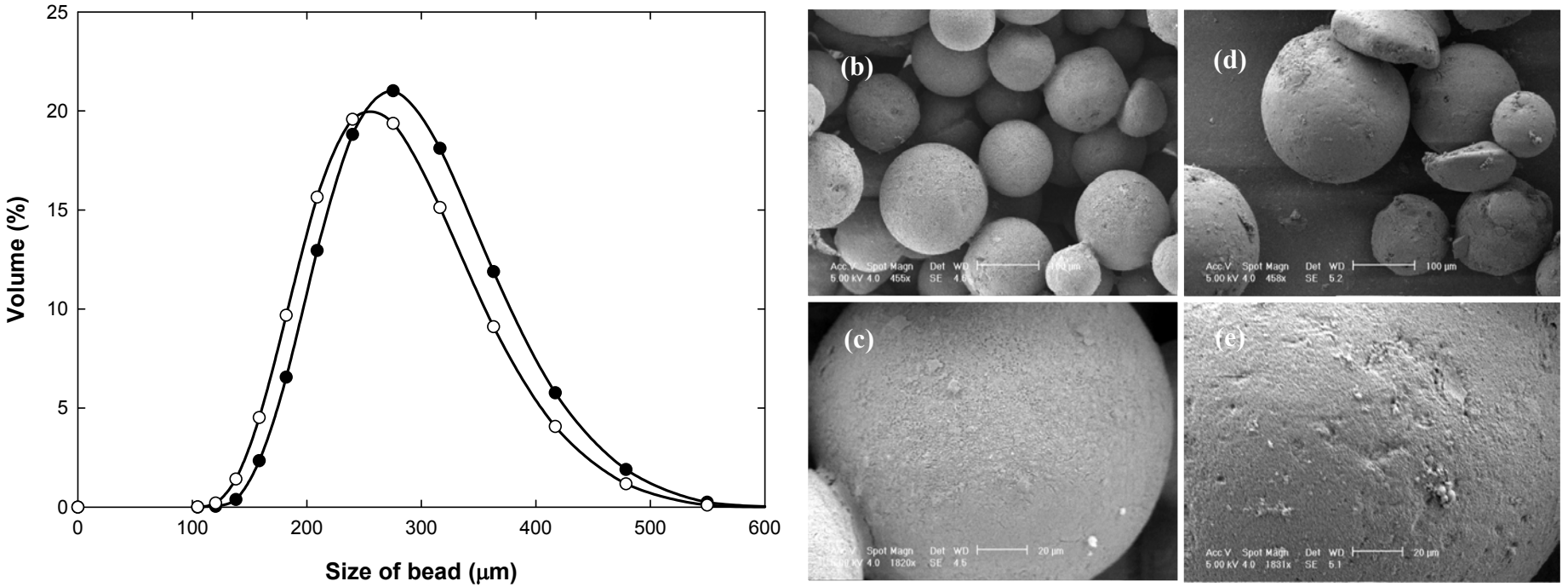

Figure 4.47 : (a) Size distribution graph of QMA SPHEROSIL LS: symbols ●= microwaved sample & ○ = control. SEM images of (b) QMA SPHEROSIL LS; (c) surface of QMA SPHEROSIL LS; (d) microwaved QMA SPHEROSIL LS, & (e) microwaved surface of QMA SPHEROSIL LS.

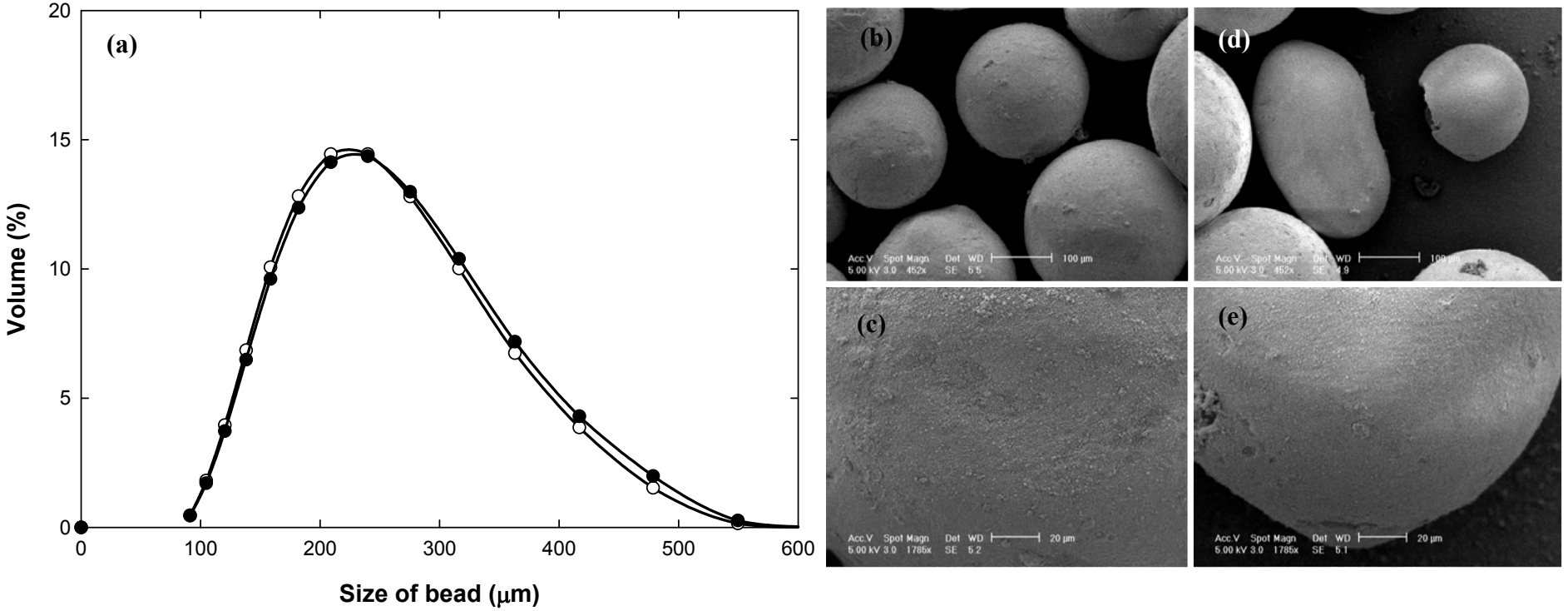

Figure 4.48 : (a) Size distribution graph of SP SPHEROSIL LS :symbols ●= microwaved sample & ○ = control .SEM images of (b) SP SPHEROSIL LS; (c) surface of SP SPHEROSIL LS; (d) microwaved SP SPHEROSIL LS, & (e) microwaved surface of SP SPHEROSIL LS

4.5 Conclusion

In this comprehensive study numerous bioseparation supports were exposed to microwave irradiation, they were then examined using; a light microscope, scanning electron microscopy; size distribution, and in some cases micromanipulation.

Table 4.14: Summary of results for microwave effects on the different types of supports tested

NO DAMAGE	DAMAGED
PACKED BED SUPPORTS	**PACKED BED SUPPORTS**
Base matrices	**Base matrices**
Sephadex G-25	Sepharose 6B
Sephadex G-50	**Functionalized**
Sephacryl S-500 HR	DEAE Sepharose FF
Sephacryl S-400 HR	Fractogel EMD DEAE (650 M)
Sepharose CL-6B	Q Hyper DF
Superdex 75	S Hyper DF
Superdex 200	DEAE Spherodex LS
Toyopearl HW 40C	SP Spherosil LS
Toyopearl HW 75 F	QMA Spherosil LS
Activated	**EXPANDED BED SUPPORTS**
ECH-Sepharose CL-6B	**Base matrices**
AGE- Sepharose CL-6B	Streamline
Functionalized	UFC glass
Phenyl Sepharose CL-4B	UFC steel
CM Sepharose FF	**Functionalized**
Capto Q	Streamline QXL
HEA Hypercel	Streamline SP
PPA Hypercel	UFC PEI (Steel)
Source 15Q	Q Hyper Z
	CM Hyper Z

It can be concluded from the results (Table 4.14) obtained that only certain bioseparation supports can withstand go microwave heating. It appears that most supports composed of a single polymer matrix structure can endure microwave heating. All Sepharose based media tested can undergo microwave treatment, except when it has an anion exchange ligand attached. This study exposed the incompatibility of the bioseparation supports which contain both a polymer and an inorganic material with microwave irradiation; all streamline and Hyper Z beads tested were completely malformed after microwave exposure.

Ceramic based beads tested were all damaged after microwave exposure. Ceramic materials are especially susceptible to thermal runway behavior which can cause fractures in the material. It is apparent from the results that ceramic porous media is not suitable to microwave heating.

4.6 References

Andrei D.C., Briscoe B.J., Luckham P.F., Williams D.R. (1996) The deformation of microscopic gel particles. *J. Chem. Phys.* **93**: 960–976.

Ahmed A., Siomes E. (2001) Microwave joining of 48% alumina-32% zirconia-20% silica ceramics. *J. Mater. Process. Technol*. **118**: 88-94.

Antova G., Vavasova P., Zlatanov M. (2004) Studies upon the synthesis of cellulose stearate microwave heating. *Carbohydr. Polym*. **57**: 131-134.

Basak T. (2007) Role of metallic, ceramic and composite plates on microwave processing of composite dielectric materials. *Mater. Sci. Eng*. *A* **457**: 261-274.

Beckmann-Coulter. (2009) Particle Size Analysis-ISO 13320-1. Data sheet. Beckman-Coulter instruments.

Caddick S. (1995) Microwave assisted Organic Reactions. *Tetrahedron* **51**: 10403-10432.

Fung Y.C. (1999) Microwave Science and Technology. Wiley Encyclopedia of food science and technology 2nd edition: 16.

Gropper M., Ramon O., Kopelman J., Mizrahi S. (1998) Effects of microwave reheating on surimi gel texture. *Food Res. Int.* **30:** 761-768.

Gupta N., Solanki K., Mondal K. (2006) Microwave-assisted preparation of affinity medium. *Anal. Biochem*. **360**: 123-129.

Haucai G., Wan P., Dengke L. (2005) Graft copolymerization of chitosan with acrylic acid under microwave irradiation and its water absorbency. *Carbohydr. Polym*. **66**: 372-378.

Kappe C.O., Dallinger D., Murphree S. (2009) Practical Microwave synthesis for Organic Chemists-Strategies, Instruments, and Protocols. Wiley-VCH Press 1st edition: **19**. 1-7.

Kappe C.O. (2004) Controlled Microwave heating in modern Organic synthesis. *Angew. Chem. Int*. **43**: 6250-6284.

Kappe C.O. (2003) Microwave-enhanced Chemistry-Enabling Technology Revolutionizing Organic Synthesis and Drug Discovery. *Business briefing-Future drug discovery* : 43-46.

Keck C.M., Müller R.H. (2008) Size analysis of submicron particles by laser diffractometry-90% of the published measurements are false. *Int. J. Pharm.* **355**: 150-163.

Kriegsmann G.A. (1991) Thermal runaway in microwave heated ceramics. *J. Appl. Phys*. **71**: 1960-1966.

Malvern. (2009) Mastersizer 2000 data sheet Malvern Instruments, UK.

Martin M.T. (2004) Methods and compositions for directed microwave chemistry. International patent US2004/0209303.

Min-Zhi L.I., Fa L. (2006) Synthesis and microwaved dielectric properties of Si/C/B powder. *Trans. Nonferrous Met. Soc. China* **15**: 470-473.

Müller E., Chung J.T., Zhang Z., Sprauer A. (2005) Characterization of the mechanical properties of polymeric chromatographic particles by micromanipulation. *J. Chromatogr. A* **1097**: 116-123.

Ping P., Norton I.T., Zhang Z., Pacek A.W. (2008) Mechanical properties of gelatin rich micro-particles. *J. Food Eng.* **86**: 307-314.

Rao J., Ganguli M., Ramakriskan B.A., Voidhyanathan B. (1999) Synthesis of Inorganic solids using microwaves. *Chem. Mater*. **11**: 882-895.

Ramesh E., Raghunathan R., Vidhya S., Ekambaram R. (2008) Indium Chloride/silica gel supported synthesis of pyrano/thiopyranoquiolines through intramolecular imino Diels-Alder reaction using microwave irradiation. *Tetrahedron Lett.* **49**: 2810-2814.

Renliang X. (2002) Particle characterization light scattering methods. Softcare Press **13**: 113.

Simoes A.Z., Longo E., Varela J.A., Ramirez M.A., Riccardi C.S. (2008) Growth of $SRBi_4Ti_4O_{15}$ thin films in a microwave oven by the polymeric precursor method. *J. Alloys Compd.* **455**: 407-412.

Tatara Y. (1991) On compression of rubber elastic sphere: over a large range of displacements–part 1: theoretical study. *J. Eng. Mater. Technol.* **113**: 285-291.

Toukoniitty B., Mikkola J.P., Eranen K., Salmi T., Murzin A.Y. (2005) Esterification of propionic, acid under microwave irradiation over an ion exchange resin. *Cat. Today* **100**: 431-435.

Thostenson E.T., Chou T.W. (1999) Microwave processing fundamentals and applications. *Composites Part. A* **30:** 1055-1071.

Vriezinga C. (1998) Thermal runaway in microwave heated isothermal slaps cylinders and spheres. *J. Appl. Phys*. **83**:338-442.

Xiaofeng W. (2002) Experimental and theoretical study of microwave heating of thermal runaway materials. *Thesis* **Chapt.2:** 10-15.

Yamanaka T., Matsui M. (1990) Microwave heating of ceramics and its application to joining. *J. Mater. Res*. **5**: 397-405.

Yan Y., Zhang Z., Stokes J.R., Zhou Q-Z., Hui Ma G., Adams M.J. (2009) Mechanical characterization of agarose micro-particles with narrow size distribution. *Powder Technol.* **192**: 122-130.

Yarlagadda P.K.D.V., Tai Soon R.C. (1998) Characterisation of materials behavior in microwave joining of ceramics. *J. Mater. Process. Technol.* **84**: 162-174.

Zhang Z., Thomas C.R., Saunders R. (1999) Mechanical Strength of single microcapsules. *Microencapsulation* **16**: 117-124.

Zong L., Zhou S., Sun R. (2004) Dielectric analysis of a cross-linking epoxy resin at a high Microwave Frequency. *J. Polym. Sci*. **42**: 2871-2877.

5.0 CONCLUDING REMARKS AND FUTURE WORK

Presently, there is an ever increasing demand for purified plasmid DNA and viral vectors for the biotechnology industry. The purity specifications of these so-called 'nanoparticulates' are expected to match or even surpass those demanded of current protein biopharmaceuticals (therapeutic antibodies, hormones and enzymes). The physical property of these nanoplex products differs greatly from smaller biomolecules as they have: larger size; colloidal nature, and a greater surface complexity. These properties create a variety of difficulties during purification processes, including: increased process stream viscosities; low binding capacities; low selectivity, and co elution with contaminants. Currently, packed bed chromatography is the only technique that can achieve the purity specifications set by the regulatory bodies for these bioproducts. Two of the most commonly used chromatography techniques for the purification of 'nanoplex' products are anion exchange and size exclusion. Even though anion exchange is a commonly utilised method, many commercially available adsorbents are not engineered to purify large nanoparticulates, and the small pore size of these supports results in low binding capacities. Size exclusion chromatography allows for the separation of the large biomolecules from smaller contaminating species, nevertheless it is still not an ideal purification technique suffering from poor resolution and the target product is obtained in a diluted solution. The work presented in this thesis attempts to advance the design of current packed bed chromatography beads in order to address some of the problems discussed above.

In Chapter 1 the history and development of packed bed chromatography supports, the evolution of target products and the limitations of existing alternative technologies is

described. It was concluded that no other separation technique other than packed bed chromatography produced the purification requirements set be the FDA for plasmid DNA and viruses.

In Chapter 2 the problems associated with packed bed chromatography for the purification of large nano-sized biomolecules are discussed. A bi-layered packed bed chromatography support was proposed as a solution to many of these problems. Previous attempts by researchers to create a bi-layered bead are reviewed, including the work by of Gustavsson *et al*. (2004), which was recognised as one of the most promising approaches.

In Chapter 3 a study to create a bi-layered bead began by repeating the approach previously published by Gustavsson *et al*. (2004). The results obtained from this work showed that although the chemistry was effective in eliminating some binding at the surface of the bead, it still did not result in two distinct layers (Synthetic route 1a). The study then looked at different approaches to creating a bead with a more inert outer layer whilst still maintaining a high protein binding capacity. Firstly the testing of a number of alternative synthetic chemistry routes is discussed (Synthetic route 2 & 3). This was followed by investigating the effects of changing the solvents, temperature, and heating methods. Water was replaced by DMSO and methanol in synthetic routes 1 and 3 respectively. Changing the solvent in each synthesis enhanced the SEC-AEC properties of the modified beads where a greater reduction is outer surface binding was observe whilst a high inner core binding capacity was maintained. However, these fabricated beads still did not completely prohibit surface binding. It was thought that perhaps the fast chemical reactions tested were just not fast

enough. Microwave technology was then employed with the intention of speeding up the chemical reaction taking place on the surface of bead. In comparing beads synthesised at room temperature, heated in a water bath and heated in a microwave, it was shown that microwave heating greatly improved the performance of the beads with regard to protein and plasmid DNA binding.

Although microwave technology significantly increased reaction rates one concern with the application of microwave technology was that it may cause damage to chromatography beads. In order to assess this, chromatography beads described in Chapter 3 were subjected to a variety of analytical techniques including: light microscopy; scanning electron microscopy; size distribution, and micromanipulation. This comprehensive analysis is described in Chapter 4 and it was demonstrated that the mechanical properties of certain chromatography beads were altered after microwave exposure. The concept behind this study was that as it has been shown that microwave technology could prove an extremely useful tool in chromatography material development, and it was therefore important to identify which chromatography beads can withstand microwave heating. The data obtained from these experiments demonstrated that only chromatography materials with specific properties can undergo microwave heating. It was shown that all ceramic based supports tested were damaged by microwave exposure whereas most agarose support remained undamaged after microwave heating.

In the experiments described above the bi-layered supports were tested with a purified protein and purified plasmid DNA, however during a purification process there would be a

variety of biomolecules present. Future work should focus on investigating how these restricted access supports would perform when placed in a column and tested under conditions similar to that of a process stream.

As previously discussed in Chapter 3 future microwave investigations should be carried out in a laboratory microwave rather than a domestic microwave to allow for greater reproducibility of results and facilitate a more rigorous optimisation of the heating conditions.

Furthermore, an extended study employing micromanipulation could be performed on microwaved chromatography beads, to provide a more thorough analysis of changes to the mechanical properties sustained due to microwave heating.

6. APPENDIX

Problem free expanded bed adsorbents

6.1 Abstract

In this study two new types of expanded bed adsorbent were created. The first support was created by modifying Streamline base matrix to possess a charged anion exchange inner core with an inert outer layer. The second support was similar to first one, except that a thermoresponsive polymer was incorporated to the inert outer layer. The concept behind this bead was that the charged inner core would allow for the binding of small biomolecules as they diffuse into the pores of the bead. The inert outer layer would act as a barrier against the binding of large biomolecules, such as plasmid DNA. A thermo-responsive polymer Poly (*N*-Isopropylacrylamide) (PNIPAAm) was attached to introduce a self cleaning mechanism on to the modified support. The synthesis to introduce different functional layers throughout the support was achieved by a fast chemical reaction and atom transfer radical polymerisation (ATRP). A reduction in plasmid DNA (pDNA) binding was observed with both supports, the Anion-exchange-size exclusion support obtained a 43% reduction, where as the support with a thermoresponsive polymer attached eliminated 32% of pDNA binding.

6.2 Introduction

It is reported, that the purification of proteins with packed bed chromatography suffers from many problems. Firstly packed bed chromatography is an expensive separation technique, and secondly it fails to effectively deal with the high titres from upstream (Langer, 2007; Low *et al*., 2007). Expanded bed adsorption is one technique which could

greatly reduce current downstream processing costs, as it enables protein capture in a single operation from crude feed stock resulting in fewer process steps.

EBA is a separation technique invented in the 1990's for the purification of the biomolecules. It operates under the same steps as packed bed chromatography with an equilibration; adsorption; washing; elution, and regeneration (GE Healthcare Handbook, 2008). However, EBA differs from packed bead chromatography by the direction of flow which is introduced at the bottom of the column. This results in an increase of bed voidage as different sized beads reposition within the bed. It is this increased bed voidage that allows for the direct application of solid matter, while enabling the adsorption of soluble biomolecules (Ping *et al*., 2006).

The application of EBA offers numerous advantages over packed bed chromatography such as: higher protein yields; shorter purification times; cheaper maintance, and operating costs *(Anspach et al., 1999).* Despite this technique boasting many benefits it presently has not been incorporated into industrial scale bioprocesses for the purification of biomolecules. This is mainly due the problems associated with current commercially available EBA supports, for example DNA binding to the outer surface of these beads can induce inter-particle cross linking that can cause a collapse of the expanded bed (Karau *et al.*, 1997). Furthermore, the occurrence of fouling by solids and large colloidal biomolecules, present in crude feed stocks can lead to clogging of the pores of the adsorbent (Thommes *et al.*, 1999). The consequence of this is low binding capacities and difficulties in removing the contaminating species (Fernandez-Lahore *et al*., 1999). One of the major hindrances for EBA advancement is current commercially available EBA

adsorbents. The defects of these supports could be overcome by the re-design of EBA supports in order to prevent many of the problems discussed above.

The aim of this study was to development two new expanded bed adsorbents which possess different functionalities present in distinct layers. These beads possess an anion exchange inner core allowing for the binding of proteins, but with a thin inert outer layer that would prevent larger biomolecules from binding to the support. The concept behind these new Bi-layered EBA adsorbents is that they would solve many of the problem currently associated EBA by prohibiting DNA binding to the surface of the bead thus preventing interparticle crosslinking and clogging of the pores.

One bead had the further addition of a thermoresponsive polymer (PNIPPAAm) attached to the outer surface, introducing a self cleaning property. It is reported in literature that PNIPPAAm can change into different conformations above or below it LCST, and it can induce cell release (Okano *et al.,* 2000). In the lower range of its critical temperature (LCST) which is below 32ºC, the polymer exists in its extended hydrated hydrophilic form, above 32ºC the polymer chains collapse and the polymer becomes hydrophobic.

The support activated in this study was Streamline base matrix, the protein employed is Bovine albumin, and plasmid DNA is used as a model to represent large biomolecules present in crude feed stock.

6.3 Materials and Methods

6.3.1 Materials

Streamline Base matrix was obtained from GE Healthcare Bio-Sciences AB (Uppsala, Sweden). Bicinchoninic acid (BCA) protein assay kit was supplied by Pierce Biotechnology (Rockford, IL, USA). The QIAFilter plasmid purification kit was purchased from Qiagen GmbH (Hilden, Germany). The *E. coli* DH5α strain containing the plasmid pOCI (high copy plasmid; 10 KB) was kindly provided by Professor Chris Thomas (School of Biosciences, University of Birmingham, Edgbaston, UK).

Sodium borohydride ($NaBH_4$, 99%); trimethylamine hydrochloride; allyl glycidyl ether (AGE); 'unacidified dilute' bromine water (potassium bromide-potassium bromate); Bromine; Copper bromide; 2-2 Dipyridyl and bovine serum albumin (BSA, fraction V, 96-99% albumin) were obtained from Sigma-Aldrich Company Ltd (St. Louis, MO, USA), as were all other chemicals used in this study (all of AnalaR grade). Distilled water was used to make all the solutions unless stated otherwise.

6.3.2 Methods

6.3.2.1 Synthetic route 1c (adapted from Gutavsson *et al*., 2004; Soderberg *et al.*, 2002)

Step 1c. Allylation of Streamline base matrix (synthetic route 1c)

Objective: Activation step, allyl groups introduced throughout the bead.

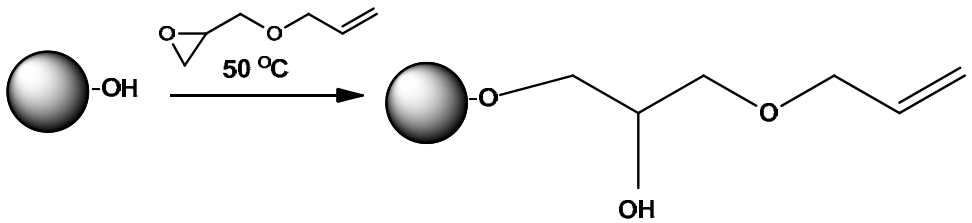

Sixty millilitres of sedimented Streamline base matrix were washed with copious quantities of water under vacuum using a sintered glass Buchner filter funnel. The supports were subsequently transferred to a 250 mL conical flask using 24 mL of sodium hydroxide solution (50% w/v), and then 0.25 g $NaBH_4$ and 6.7 g sodium sulphate were added under manual stirring. The flask was immediately immersed in a 50°C water bath fitted with a reciprocating shaker (model OLS 200; Grant Instruments (Cambridge) Ltd, Shepreth, UK) and was shaken at 150 rpm for 1 h.

The temperature of the water bath was then lowered to 40°C and 51 mL of 100% AGE were added to the flask; the reaction was allowed to proceed (15 h) under vigorous shaking (170 rpm). At the end of the reaction the support was washed sequentially with water, 70% ethanol, and water, before storing it in 20% ethanol at 4°C. The allyl group content of the support was determined using a bromine based assay (methods Section 6.3.2.5).

Step 2c. ***Partial bromination of allylated Streamline base matrix (bromination of the outer support surface via synthetic route 1c)***

Objective: Bromination of allyl groups present on the surface of the bead to initiate the creation of an SEC outer layer.

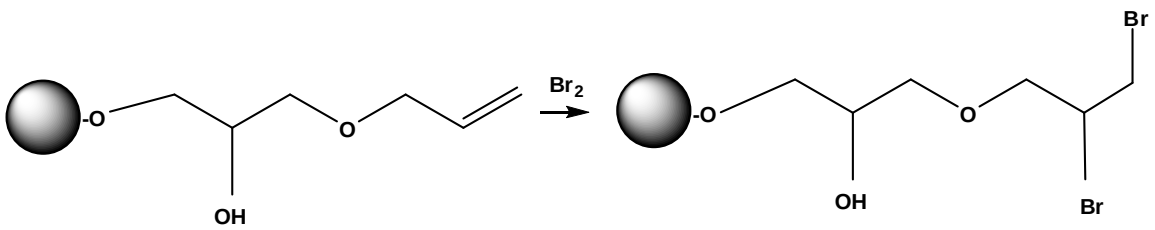

A 25 mL portion of the 'allylated' support from Step 1 was transferred to a 250 mL conical flask containing 25 mL DMSO and sodium acetate (0.55g). Next a calculated amount of bromine was added to the reaction, and the solution was mixed on a vortex mixer (Chiltern Scientific, Auckland, New Zealand) for approximately 60 s until the yellow colour due to the presence of the bromine disappeared. The support was subsequently washed with water using a glass filter funnel, before transferring it to a fresh conical flask. The experimental procedure described above was then repeated with the additional experimental condition of prior to the addition of the bromine, the support were incubated in a water bath for 24 h at 63°C.

Step 3c.Sodium Hydroxide addition to the partially brominated Streamline base matrix (synthetic route 1c)

Objective: Reaction of sodium hydroxide with the brominated bead to produce completely inert outer layer

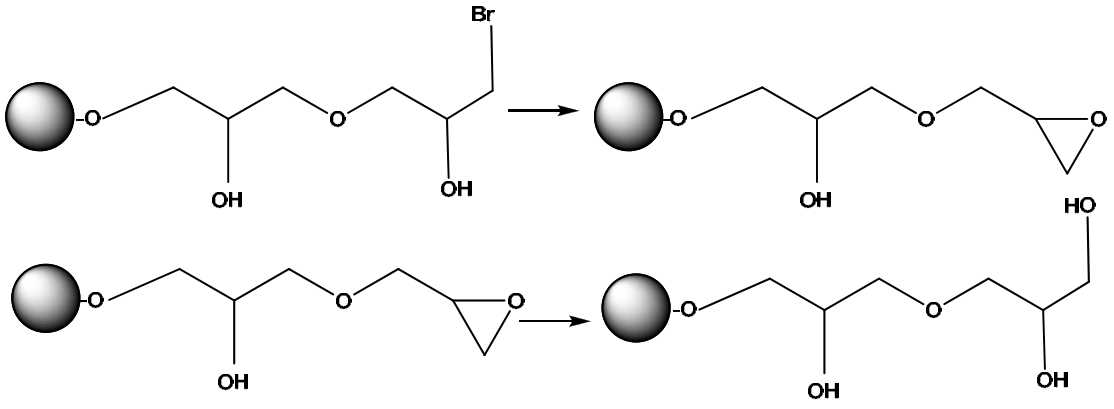

A solution of NaOH (2.3 g in 2.3 mL of water) was prepared and added with 0.1 g of $NaBH_4$ to the reaction flask containing the brominated supports from Steps 2 & 3, and hydrolysis of the

immobilised alkyl bromide groups was achieved by incubation in a shaking water bath at 40°C for 15 h. Subsequently, the supports were washed with copious amounts of water with the aid of a sintered glass Buchner filter under vacuum.

Step 4c.Coupling of trimethylamine chloride to surface modified supports (synthetic route 1c)

Objective: Coupling of the charged ligand to the inner core of the bead.

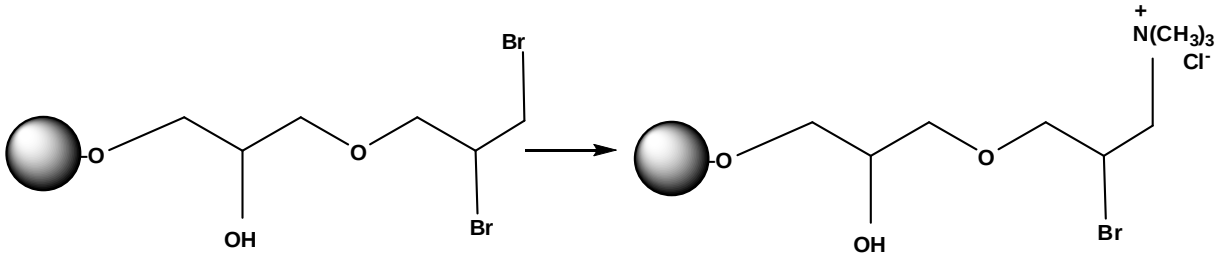

Twenty three millilitres of both the brominated support and the dextran beads prepared by synthetic Steps 1-4 were transferred to clean 250 mL conical flasks containing 10 mL of water. Next 1.1g of sodium acetate was added to each reaction flask, the flasks were placed on an orbital shaker (model S01, Stuart Scientific, Stone, UK) and shaken at 150 rpm for approximately 300s until all the sodium acetate had dissolved. The supports were then fully brominated by sufficient amounts of bromine to give a permanent yellow colour to the solution.

The supports were subsequently washed with water (using a sintered glass Buchner filter under vacuum) until no more yellow colour was detected in the filtrate, transferred to clean conical flasks with 10 mL of water, and the following reagents were added: 15 mL of 65 % (w/v) trimethylamine chloride; 3.9 mL of 1 g/mL NaOH; and 0.1 g of $NaBH_4$. The reaction was left to proceed at room temperature for 15 h with shaking at 150 rpm, anf finally the supports were washed with: water; 1 M NaCl; and then water once again.

6.3.2.2 Synthetic route 1d

Step 1d. Allylation of Streamline base matrix

Objective: Activation step, allyl groups introduced throughout the bead.

The synthesis was carried out exactly as described previously (Section 6.3.2.1 – Step 1c).

Step 2d. partial bromination

Objective: Bromination of allyl groups present on the surface of the bead to initiate the creation of an SEC outer layer.

The synthesis was carried out exactly as described previously (Section 6.3.2.1 – Step 2).

Step 3d. N-Isopropylacrylamide (NIPAAm) attachment on allylated Streamline Base Matrix

Objective: To attach NIPAAm to the outer surface of the bead and introduce an self cleaning mechanism

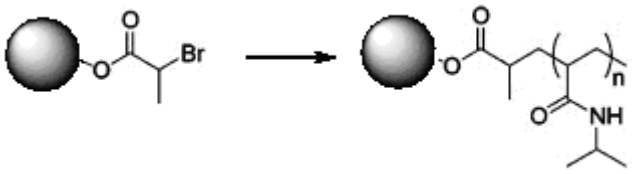

NIPAAm was polymerised on to the allylated partially brominated streamline supports by atomic transfer radical polymerization mechanism. 9 mL of brominated support present in Schlenk flask is mixed with 7.5 g of NIPAAm (38 mmol), 0.096 g of CuBr (0.67 mmol) and 0.211 g 2, 2'-Dipyridyl (0.10 mmol) and the flask content were degassed with vacuum to remove oxygen. 20 mL of degassed water was added to the reaction mixture

and flask was stirred for 5 hours in vacuum conditions. The resultant particles were washed with water and methanol repeatedly.

Step 4d. Hydrolysis of PNIPAAM activated streamline support

Objective: Reaction of sodium hydroxide with the support to produce a completely inert outer layer

The synthesis was carried out exactly as described previously (Section 6.3.2.1 – step 3).

Step 5d. Coupling of trimethylamine chloride to surface modified supports

Objective: Coupling of the charged ligand to the inner core of the bead.

The synthesis was carried out exactly as described previously (Section 6.3.2.1 – step 5).

6.3.2.3 Protein static binding studies

Suction drained anion exchange supports (0.05g) were equilibrated with 1.5 mL of 50 mM Tris-HCl pH 7.5 for 0.5 h on a rotary mutltimixer (model IKA vibrax VXR, Denley Instruments Ltd, West Sussex, UK) at 75 rpm. After settling the supernatants were removed and another 1.5 mL of 50 mM Tris-HCl pH 7.5 was added. After a second equilibration period (0.5 h with gentle mixing), the supports were again allowed to settle, and the supernatants were poured off. Next 1.0 mL of BSA (1.0 mg per mL of 50 mM Tris-HCl, pH 7.5) were added and the supports were then transferred to fresh 10mL screw-cap plastic stardsted tubes Followed by an additional 6 mL of 1.0 mg/mL BSA solution to each tube, and the resulting mixtures were incubated at room temperature for

15 h with gentle mixing at 75 rpm on a rotary multimixer (model IKA vibrax VXR, Denley Instruments Ltd, West Sussex, UK). The supernatants were subsequently analysed for residual protein content using the BCA protein assay. The protein content was determined using a colorimetric assay kit employing the reagent, bicinchoninic acid (BCA), following a protocol recommended by the manufacturer.

6.3.2.4 DNA binding studies

Preparation of plasmid DNA feedstock

E. coli DH5α cells containing the plasmid pOCI (stored in 20% glycerol at -80°C) were plated out on LB agar plates supplemented with 100 μg/mL ampicillin and let to grow for 24 h at 37°C. Starting cultures were prepared by inoculating 40 mL aliquots of sterile Luria Bertani (LB) broth containing 100 μg/mL ampicillin with a fresh single colony of *E. coli* DH5α/pOCI and shaking overnight at 37°C and 200 rpm (shaker model innova 43, New Brunswick Scientific, Herefordshire, UK).The above inoculum culture was then added to a sterile conical flask containing 400 mL LB broth supplemented with 100 μg/mL ampicillin and the contents were shaken in an orbital shaker (shaker model innova 43, New Brunswick Scientific, Herefordshire, UK) at 200 rpm for 16 h at 37°C. The cells were harvested by centrifugation (4°C for 15 min at 6,000 g; model J2-J1, rotor JA-20, Beckmann Coulter, Buckinghamshire, UK), and the plasmid was purified using the QIAFilter Giga purification kit. The final plasmid concentration obtained was 0.5 μg/mL in 50 mM Tris-HCl, pH 7.5.

Static binding studies

Suction drained anion exchange supports (0.1 g) were equilibrated twice with 1.5 mL of 50 mM Tris-HCl, pH 8 for 0.5 h with shaking at 150 rpm on a orbital shaker (model SO1;

Stuart Scientific, Stone, UK). Following equilibration, the supports were incubated with 1.5 ml of 30 μg/mL plasmid DNA stock solution for 20 s at room temperature with manual mixing, followed by centrifugation for 20 s. The supernatants were analysed for residual DNA content by absorbance measurements at 260 nm (model 922 Unikon spectrophotometer, Kantron instruments, Chichester, UK). The amount of bound material was calculated by the difference between the concentration in the initial plasmid DNA solution and the supernatant obtained from the sample, assuming that one A_{260nm} unit corresponds to a DNA concentration of 50 μg/mL.

6.3.2.5 Assay for Allyl groups to determine the amount of double bonds present on the support (bromine assay)

An 'acidified bromine stock solution' was prepared by adding 0.5 M H_2SO_4 to a standard solution of Potassium-bromide Potassium-bromate 2:1 (v/v). Next 1.5 mL of this bromine solution were added to 100 mg of suction drained AGE activated supports. After brief manual shaking (~10 s), the sample was centrifuged for 10 s at 13,000 rpm (Microcentaur, model 5415D, MSE, London UK) and the absorbance of the supernatant was read immediately at 410 nm using a Unikon 922 spectrophotometer (Kantron instruments, Chichester, UK). The number of moles of the bromine that reacted was calculated, which corresponds to the number of allyl groups present on the support.

6.3.2.6 Ionic capacity **(Pitfield, 1992)**

The anion exchangers (300 mg) were incubated with 50 mL of 2 M NaCl for 1.5 h to convert them into the quaternary ammonium chloride form. Excess acid was then removed from the supports by washing three times on a glass sinter with 50 mL aliquots of water, before transferring the suction drained materials to 100 mL bottles containing

50 mL of 0.1 M NaOH and mixing at 150 rpm for 24 h on an orbital shaker (model S01, Stuart Scientific, Stone, UK). Following settling of the supports, 1 mL aliquots of the liquid phases were mixed vigorously on a rotary multimixer (model IKA vibrax VXR, Denley Instruments Ltd, West Sussex, UK) for 600 s at room temperature with 100 μL of 0.25 M ammonium iron (III) sulphate in 9 M HNO_3 and 100 μL of a saturated solution of mercury (III) thiocyanate in 96% ethanol. The chloride ion contents were determined from absorbance measurements at 460 nm (model 922, Unikon spectrophotometer, Kantron instruments, Chichester, UK).

6.3.2.7 Scanning Electron Microscopy

Scanning electron microscopy (XL-30 FEG ESEM, Oxford Inca 300 EDS systems, UK) analysis was performed on suction dried supports. The beads were stuck onto a slide and placed in liquid Nitrogen slush. After this they were then put into the cryo chamber and etched under vacuum at 90°C for 300 s to remove ice crystals. Finally the sample was sputter coated with gold for 60 s and transferred to the microscope chamber.

6.3.2.8 Micromanipulation

The mechanical strength of the supports was tested using micromanipulation. The micromanipulation technique imposes a compression force on a single bead and the data is measured by a micromanipulation rig. The beads are placed on a glass slide and a single bead is compressed by a probe which is connected to a transducer (Aurora Scientific inc., Canada). The slide is mounted on the stage of an inverted microscope (Micro instruments Ltd., Oxon, UK). As the particle is squeezed at a pre-set speed of 20 μm/s, the stress being imposed on it is measured simultaneously by a PC-30D data

acquisition board (Amplicon Liveline, Brighton, UK). Ten particles were compressed for each experimental result.

6.4 Results and Discussion

In this study, two synthetic Chemistry routes were employed in an attempt to create a bi-layered EBA adsorbent, possessing a positively charged inner core, to act as an anion exchanger, surrounded by a thin inert outer layer to introduce a size exclusion property. The concept behind creating a bi-layered EBA bead is that by combining both anion exchange and size exclusion chromatographic principles on one support, many of the problems that currently plague EBA advancement could be resolved.

6.4.1 Synthesis of bi-functional EBA supports

The steps of each synthetic chemistry route employed in the preparation of this new type of bi-layered support are individually presented in Figures 6.0 & 6.1 The first synthesis (Figure 6.0) was adapted from a paper by Gustavsson and co workers (2004), and for the second synthesis the conditions for the addition of the Poly (*N*-isopropylacrylamide (PNIPAAm) to the outer layer was taken from work described by Kim *et al*. (2003). The commercially available EBA adsorbent Streamline base matrix was chosen as the starting matrix for following reasons: it can be activated under the selected chemistry conditions and is already designed specifically for EBA applications.

During the first step (Step 1) of synthetic route 1a, the supports were activated with Allyl Glycidyl Ether (AGE) in order to introduce allyl groups throughout the bead. The extent of activation with AGE was determined using the assay for allyl groups (Section 6.3.2.5). The allylated chromatography matrix then underwent a partial bromination step (Step 2)

with the addition of calculated volumes of bromine, and the amount of bromine reacted was estimated from the number of allyl groups left on the support. In these experiments 10% of the total allyl group content was eliminated to create a brominated outer layer. The idea behind the partial bromination step is that the reaction of bromine with the allyl groups will occur faster than the chemical can diffuse into the pores of the support.

The bromine will react with the allyl groups present on the surface of the bead leaving unreacted allyl groups present in the inner core. In some the experiments the partial bromination reaction was performed at 63°C.

In previous work (Chapter 3: Section 3.3.3.1; Figure 3.13), it was shown that microwave heating can enhance the rate of reaction on the surface bead, however Streamline base matrix was damaged by microwave irradiation (Chapter 4; Section 4.4.6; Figure 4.34). Therefore the supports were heated in a water bath a 63°C to examine if traditional heating could increase the reaction on the surface of the bead.

During the Synthetic route 1a an extra step was introduced (Step 3); the coupling PNIPPAAm onto the beads surface (Figure 6.1). PNIPAAm is thermoresponsive polymer, it can change conformation above and below it critical temperature. In the lower range of its critical temperature (LCST: below 32°C), the polymer exists in its extended hydrated hydrophilic form, above 32°C the polymer chains collapse and the polymer becomes hydrophobic. Next Sodium Hydroxide was added (Step 4) to replace any remaining bromide groups present on the surface of the bead with hydroxide groups. Following ATRP polymerization it is essential in this synthesis that the end terminal be hydrolysed to remove the bromide groups present at the PNIPAAm chain. The supports

were subsequently treated with excess bromine (Step 5), which reacts with the remaining allyl groups present in the inner bead core, before the addition of trimethylamine hydrochloride which introduces the positively charged amine ligand.

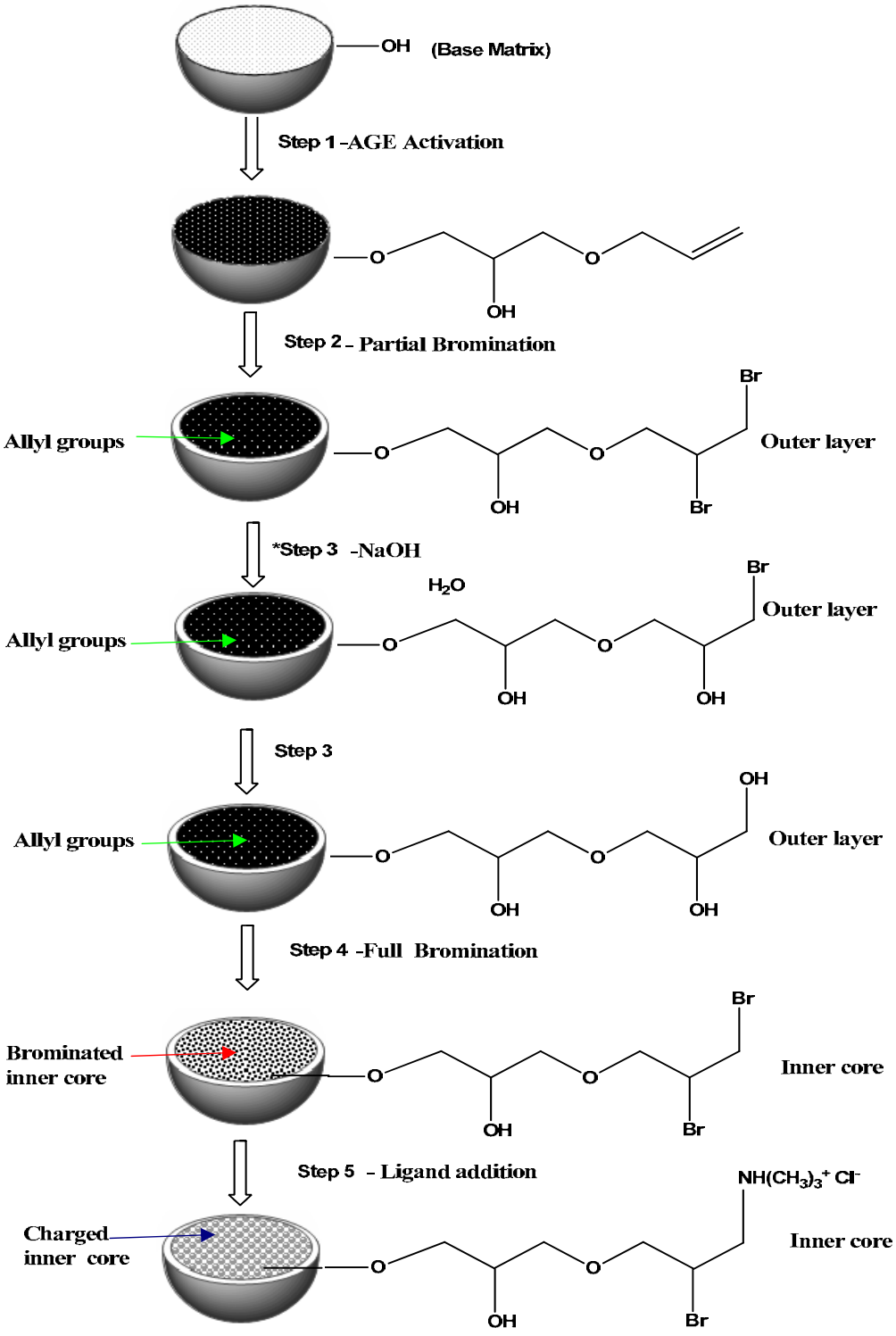

Figure 6.1: Synthetic scheme 1c for the preparation of SEC-AEC Sepharose CL-6B chromatography supports (Gustavsson *et al.*, 2004): (step 1) NaOH, $NaBH_4$, Na_2SO_4, AGE, 50°C, 24 h.(step 2) Sodium Acetate, Br_2, DMSO, 60 s.(Step 3) NaOH, $NaBH_4$, 40°C. (step 4) H_20, Br_2, Sodium Acetate. (step 5) $N(CH_3)_3$.HCl, NaOH, $NaBH_4$, 24 h. * during step 3, an three membered epoxide ring will form, but the base will continue to react to produce the final product.

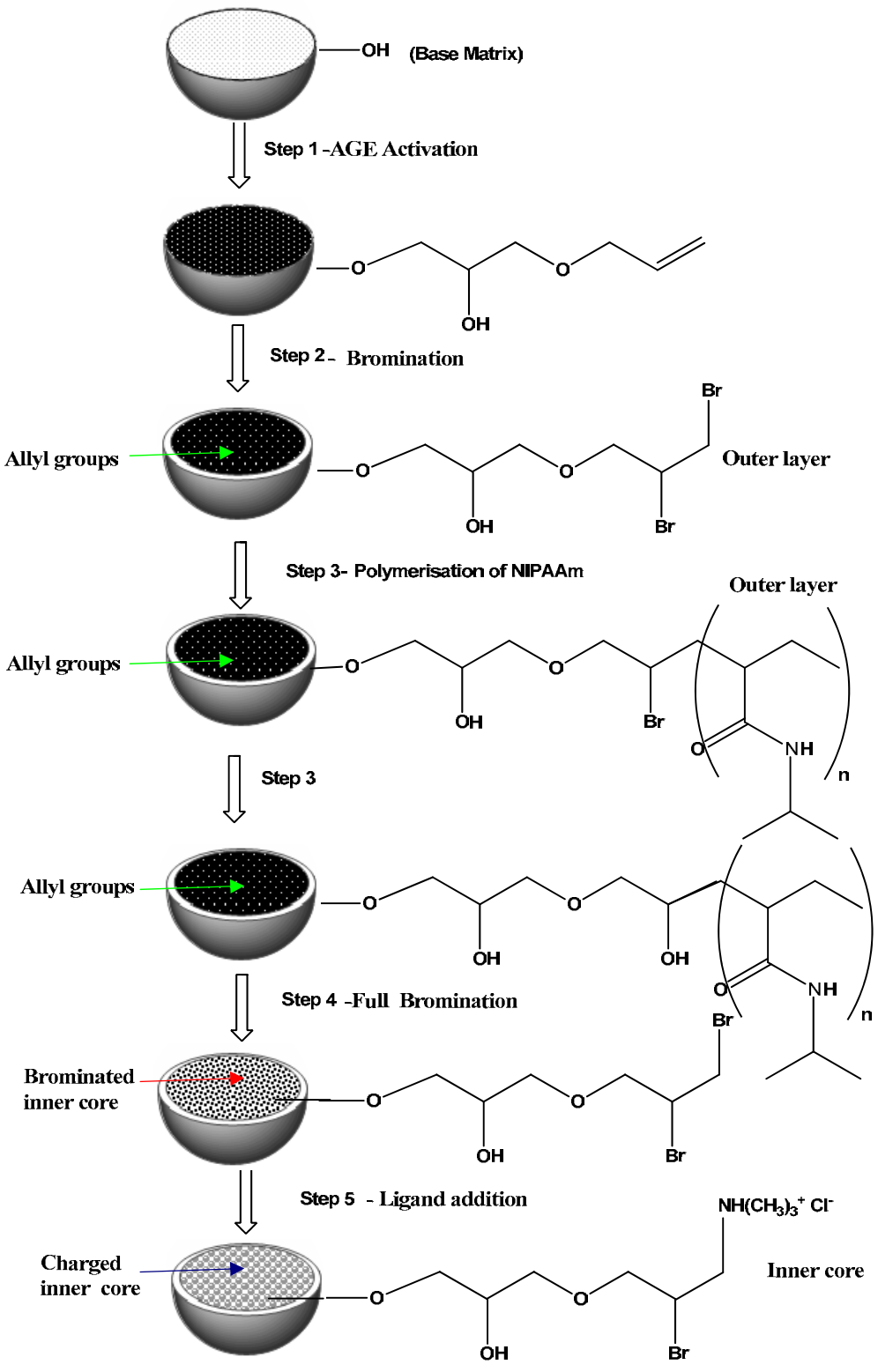

Figure 6.2: Synthetic scheme 1.0d, for the preparation of 'restricted access' anion exchange chromatography supports: (step 1) NaOH, $NaBH_4$, Na_2SO_4, AGE, 50°C, 24h. (step 2) DMSO, Br at 63°C. (Step 4) NIPAAm, CuBr ,2, 2'-Dipyridyl, MeOH (step 5) NaOH, $NaBH_4$, 50°C, 24 h. (step 6) Br_2, $N(CH_3)_3.HCl$, NaOH, $NaBH_4$, 24h.

6.4.2 Characterization and testing of bi-layered supports

This bi-layered support must possess an outer SEC layer that is as thin as possible so that a high binding capacity is maintained, and as inert as possible so that it will not bind nucleic acids and other contaminants (bi-layered supports are discussed in more detail in Chapter 2; Section 2.2). In this work plasmid binding is used as a model to test for layer inertness, due to it's large size it will not penetrate the pores of the support and only bind to the outer surface, if there is charge present. BSA is the protein used to test the binding capacity of supports. All the chemistry performed on the supports is monitored by assays for specific functional groups. Allyl group and ionic capacity density measurements provide a way to estimate the thickness of the layer. The results obtained from all the assays for each synthetic chemistry route are tabulated (Table 6.0)

Polymerization of NIPAAm onto the outer surface of the partially brominated allylated streamline supports was done by ATRP mechanism. The bromide groups present on the support introduced during the partial bromination step (Section 6.3.2.5; step 2) are used for surface polymerization by ATRP to attach NIPAAm on to the surface of the bead. The number of Bromide groups present was calculated using the bromine assay and the same number of moles Copper Bromide initiator was added for ATRP. The initiator used in this study was Copper Bromide which generates a radical on the support and allowed for the attachment of NIPAAm via ATRP. After the ATRP experiments FTIR analysis confirmed the presence of NIPAAm on the support, the FTIR spectrum (Figure 6.2) shows the peaks characteristic of PNIPAAm at 1640 cm^{-1} (C=O stretching and 1550 cm^{-1} (N-H bending) (Kim *et al.,* 2003). The amount of NIPAAm that reacted was calculated

by testing the solution before and after the reaction. It was then estimated that each chain attached to the support was 35 monomers in length. This estimation is based on the assumption that all bromide groups present on the bead were initiated and this resulted in the attachment of NIPAAm.

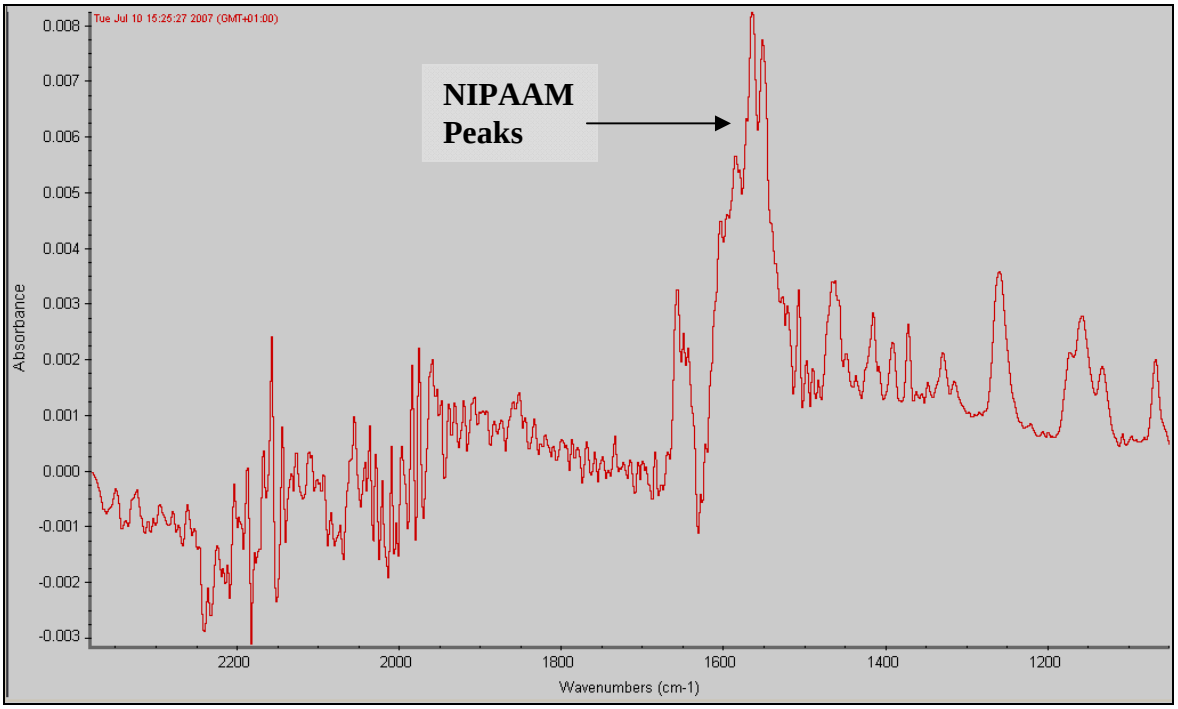

Figure 6.2: FTIR spectrum of NIPAAm attached onto the brominated Streamline support.

Further verification of NIPAAm attachment was obtained by examining the surface morphology of the beads before and after the attachment of the polymer. This was achieved by SEM. It is apparent from the images shown in Figures 6.3 & 6.4 that the bead with NIPAAm attached appears rougher and more crinkled.

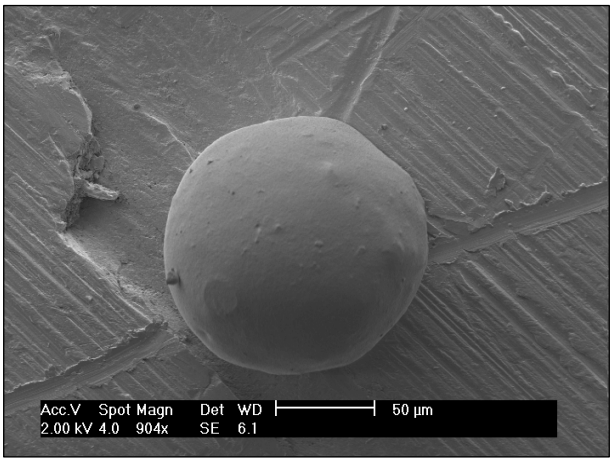

Figure 6.3. Scanning electron microscopy images of Streamline base matrix .

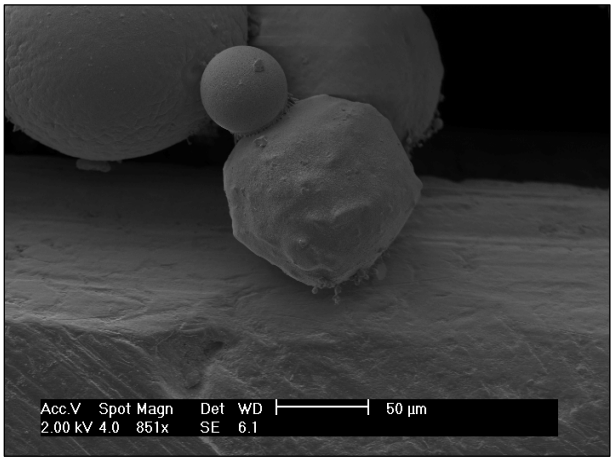

Figure 6.4. Scanning electron microscopy images NIPAAM –Streamline base matrix.

Table 6.0: Allyl group density, ionic capacity, static protein and DNA binding capacities for supports prepared via Synthetic routes 1a & 1b (Figures 6.0 & 6.1)

Support No.	**Reaction conditions**	**Allyl groups [a](%)**	**Ionic Capacity [b](%)**	**Protein binding capacity [c] (%)**	**DNA binding capacity [d](%)**
4.0	Control	100	100	100	100
4.1	DMSO, 63^0 C 10% Br_2, NIPAAM	87	79	84	66
4.2	DMSO, 63^0 C 10% Br_2 ,	87	90	86	50
4.3	DMSO, RT, 10 % Br_2 .	86	92	86	45

a:100% allyl group content = 670 μmol/mL; b:100% ionic capacity =476 μmol/mL; c:100% protein binding= 64 mg/mL; d: 100% pDNA = 69 μg/mL

The results displayed in Table 6.0 show that the AGE/Partial bromination chemistry performed at room temperature was the most the effective in eliminating plasmid DNA binding; with a 55% reduction on pDNA binding and a 14% reduction in protein binding. The support that bound the highest amount of pDNA was the NIPAAM-support, this was probably due to the plasmid interacting with the polymer present on the surface of the bead. The binding experiments were performed below LSCT of NIPAAm in which it would be in its hydrophilic state. No experiments were performed to test the transition of NIPAAM from its hydrophilic to hydrophobic states. Perhaps even below 32°C it still possessed some hydrophobic properties which resulted in plasmid interaction. None of the beads created proved to be that effective in eliminating outer surface binding.

The reasons into why this chemistry did not create two distinct layers, is discussed in detail in Chapter 3; Section 3.3.1. However, it was thought that under dynamic binding conditions a further reduction in outer surface binding would be observed. The fabricated EBA supports were then placed in an EBA column, however it became apparent during the experiment that the fluidisation properties of the streamline beads had changed

significantly. The beads appeared to be unable to settle and form a stable fluidised bed (Figure 6.5).

Figure 6.5: Photograph of the expanded bed containing NIPAAM activated streamline supports.

Further analysis, compared the settling velocity of both modified and unmodified streamline base matrix. These experiments were performed by placing on 1 mL of suction drained bed in 10 mL of water into a small measuring cylinder. The settling velocity of streamline base matrix was found to be 0.1875 cm/sec, whereas the settling velocity of the modified matrix was found to 0.05 cm/sec. Also observed during these experiments was that the chemistry modified matrix contained many fine particles which floated on the top of the liquid phase, this was a clear indication that the fluidisation property of the modified beads has been altered.

The size of these beads was then analysed (mastersizer, model hydro 2000, Malvern instruments, Worcestershire, UK). The size distribution data showed that the modified supports were approximately 37 μm bigger than the streamline base matrix (Table 6.1)

Table 6.1. Mastersizer results for supports

Support No.	**Support**	**Average bead size (μm)**
4.0	Base matrix	201
4.1	AGE Activated, DMSO, 63°C 10% Br_2, PNIPAAm	234
4.2	AGE activated, DMSO, 63°C 10% Br_2 ,	236
4.3	AGE activated, DMSO, RT, 10 % Br_2 .	243

Next the mechanical properties of these beads were tested using micromanipulation (the theory behind this technique is described in detail Chapter 4; Section 4.2.2. From the results displayed in Figure 6.6, it is obvious that the AGE/bromination chemistry had significantly weakened the mechanical strength of the base matrix. This AGE activation chemistry is used extensively for chromatography chemistry activations. Berg *et al.,* (2005) activated streamline base matrix with AGE and reported no changes to the beads properties after activation, however in Berg's study the EBA supports were not tested in a column after activation. During the partial bromination step, bromine can complex with DMSO and generate hydrogen bromide (Aida *et al*., 1976), which would significantly lower the pH of the reaction mixture. The recommended pH range for streamline based supports is 2-14 (Sandberg *et al.,* 1999); the measured pH of DMSO-Bromine solution is 2.48, which would be within the allowed pH range for streamline. Therefore it is highly unlikely it was the partial bromination step which damaged the streamline supports.

The stress (MPa) required to compress the NIPAAm activated beads (below the LSCT) is the same as the AGE activated support, indicating that it was that it was the first step in the synthesis (AGE activation) that changed the mechanical properties of these beads, and that it was this change that resulted in the beads no longer possessing the fluidisation properties required for EBA applications. The NIPAAM support compressed above its LSCT (42°C) showed to be mechanically stronger than the NIPAAM support compressed below its LSCT (32°C). This is probably due to the polymer chains collapsing into the pores of the support.

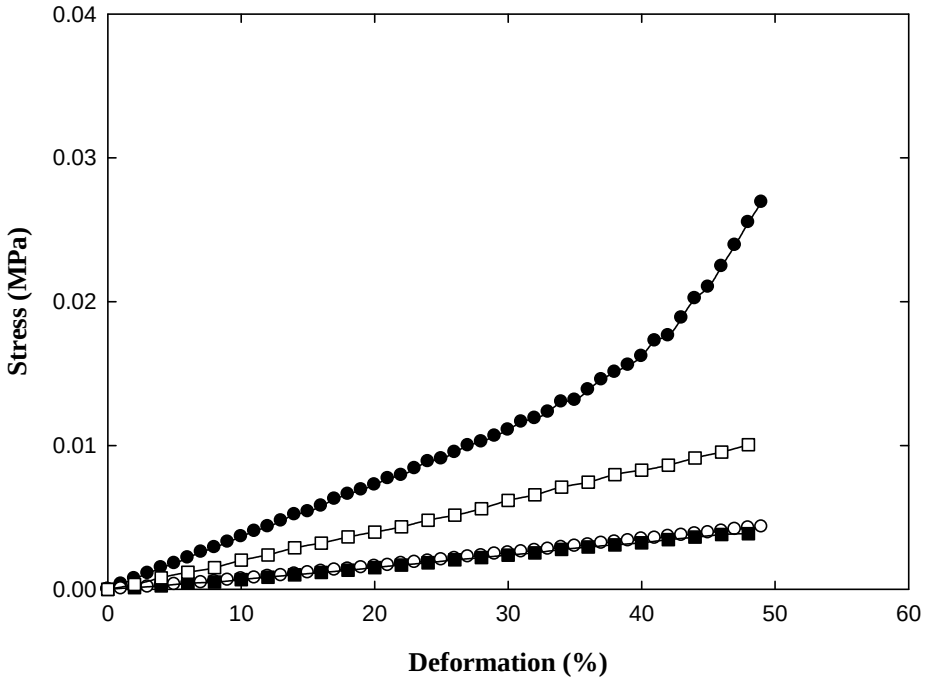

Figure 6.6: Stress versus deformation curves for supports. Symbols: (●) Base matrix ;(○) AGE partially brominated supports; (■) NIPAAm-activated support tested below LSCT ;(□) NIPAAm-activated supports tested above LSCT.

6.5 Conclusion

In this work a novel approach for creating bi-layered EBA adsorbents was attempted, these bi-layered supports could solve many of the problems which currently hamper EBA applications. However, the column performance of these fabricated beads was not satisfactory due to change in their fluidization properties. The chemical synthesis employed seemed to have changed the properties of these adsorbents. The settling velocity analysis revealed that the modification had lowered the density of modified adsorbents. Further micromanipulation analysis showed the mechanical properties of the beads changed significantly after the AGE partial bromination steps. Indicating that it was one or both of these chemical steps that induced the damage.

6.6 References

Aida T., Akasaka T., Furukawa N., Oae S. (1976) Catalytic Reduction of Sulfoxide by bromine-hydrogen bromide system.. *Chem. Soc. Japan* **49**: 1117-112

Anspach D., Cubelo D., Hartmann R., Garke G., Deckwer W. (1999) Expanded bed Adsorption Chromatography in primary protein purification. *J. Chromatogr. A* **865**: 129-144.

Berg H., Busson P., Carlsson M. (2005) Chromatographic two-layer particles. International patent number 2005/024037.

Bergström J., Berglund R., Soderberg L. (2002) Process for introducing functionality. International patent number WO98/39364.

Fernadez-Lahore H., Bolt K., Thömmes J. (2000) The influence of cell adsorbent interactions on protein adsorption in an expanded bed. *J. Chromatogr. A*. **873**: 195-208.

Ghose S.,Chase H. (2000) Expanded bed chromatography of proteins in small diameter columns. I. Scale down and validation. *Bioseparations* **9**: 21–28.

Gustavsson.P.E., Lemmens R., Nyhammar T., Busson P., Larson P.O. (2004) Purification of plasmid DNA with a new type of anion-exchange beads having a non-charged surface. *J. Chromatogr. A* **1038**: 131-140.

Karau A., Benken C., Thommes J., Kula M.R. (1997) The influence of particle size distribution and operating conditions on the adsorption performance in Fluidized bed. *Biotechnol. Bioeng.* **55**: 54-64 .

Kim D.J., Heo J.Y., Kim K.S., Choi S.I. (2003) Formation of Thermoresponsive Poly(N-iso-propylacrylamide)/Dextran Particles by Atom Transfer Radical Polymerization. *Macromol. Rapid Commun.* **24**: 517–521.

Langer E., Ranck J. (2006) Capacity bottleneck squeezed by downstream processes. *BioProcess Int.* **4**: 14–18.

Low D., O' Leary R., Pujar N.S. (2007) Future of antibody purification. *J. Chromatogr. A* **848**: 48-63.

Okano T., Yamato M., Kikuchi A. (2000) Rapid cell sheet detachment from Poly(N-isopropylacrylamide)-grafted porous cell culture membranes. *J. Biomed. Mater. Res.* **50:** 82-89.

Ping L., Xiu G., Mata V.G., Grande C.A., Rodrigues A.E. (2006) Expanded Bed Adsorption/Desorption of Proteins with Streamline Direct CST I Adsorbent. *Biotechnol. Bioeng*. **94**: 1155 -1163.

Pitfield I.D. (1992) Perfluorocarbon chromatographic supports. PhD Thesis University of Cambridge UK.

Sandberg L., Farenmark J., Gustavsson J., Largerlund I. (1999) Characterisation of Streamline Phenyl. *Bioseparation* **8**: 139-144.

Thommes J., Halfer M., Luthemeyer D., Amerskamp N., Kula M.R. (1999) Interaction of mammalian cell broth with adsorbents in expanded bed adsorption of monoclonal antibodies. *Process Biochem.* **34**: 59-165.

6.7:Technical information on Sepharose CL-6B (GE Healthcare)

% agarose	6
optimal mw for the separation of globular proteins	10 $x10^2$ - 4 x 10^5
Bead size range (µm)	45 -165
pH stability long term	3-13
pH stability short term	2-14

6.8 :Calibration curve for ionic capacity assay analysis in chapter 3

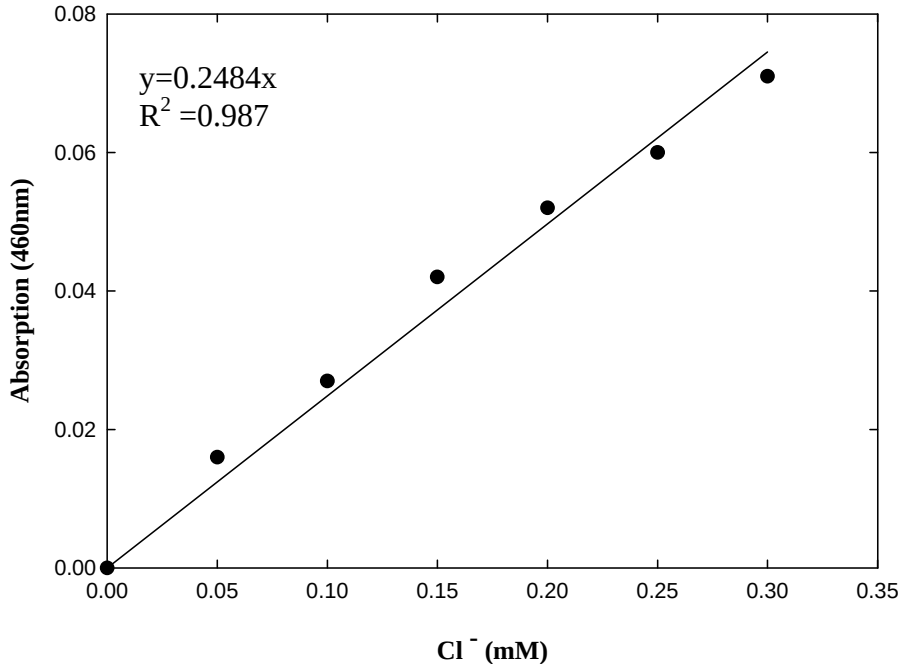

6.9: Protein calibration curve for protein binding analysis in chapter 3

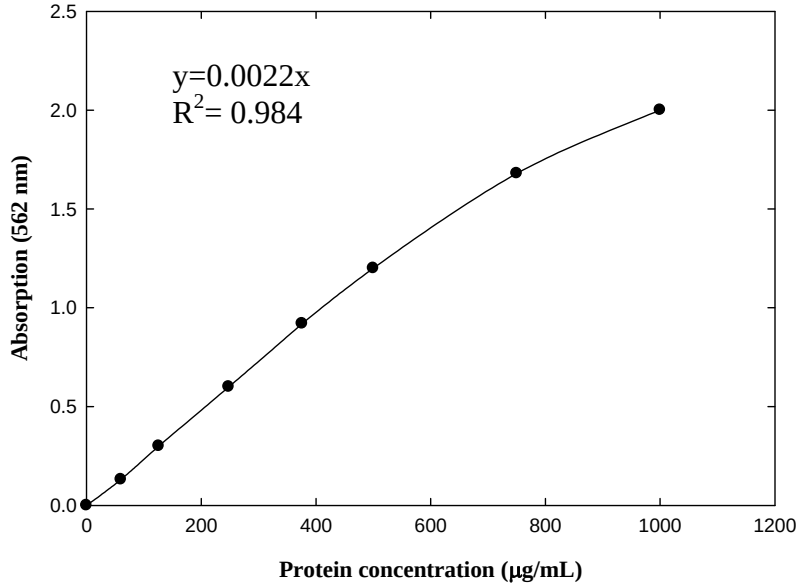

6.10:Calibration curve for bromine assay analysis in chapter 3

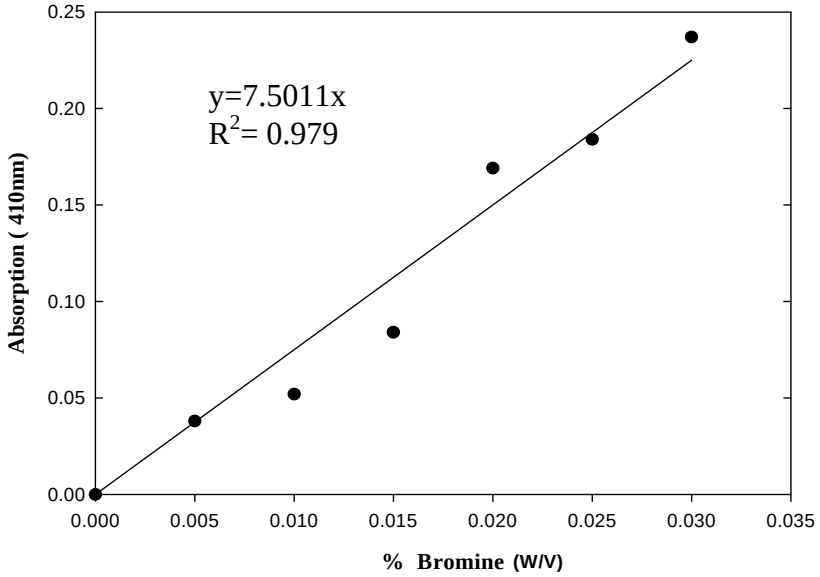

6.11: Allyl groups versus bromination for synthetic route 1 in chapter 3

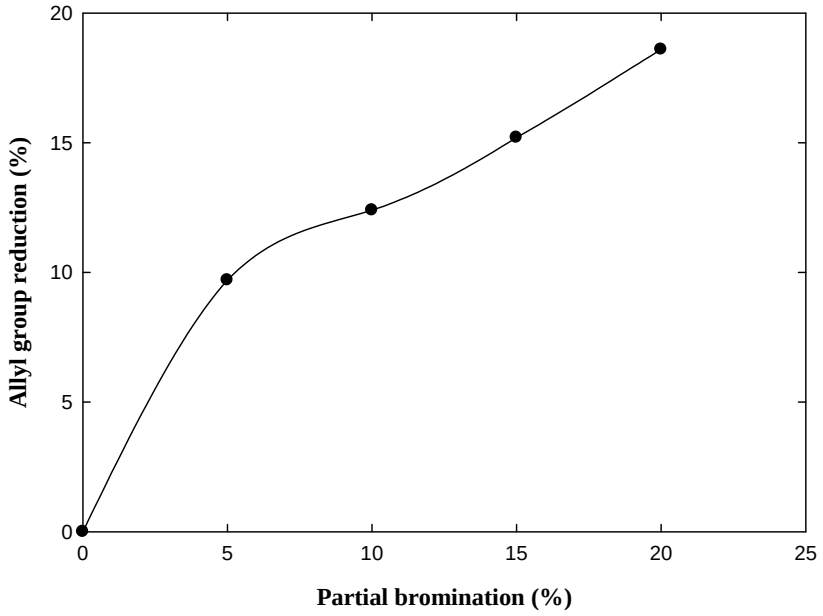

6.12: Allyl groups versus oxidation for synthetic route 2 in chapter 3

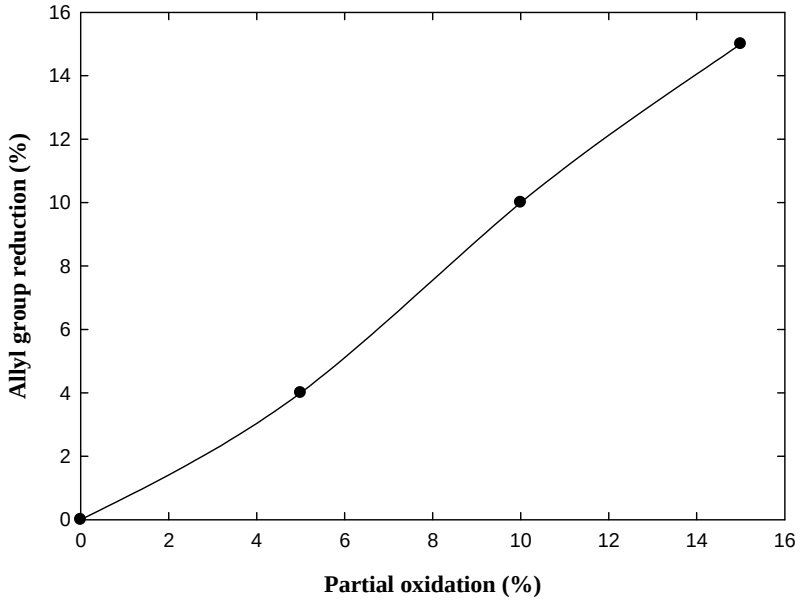

6.13: Epoxide groups versus hydrolysis for synthetic route 3 in chapter 3

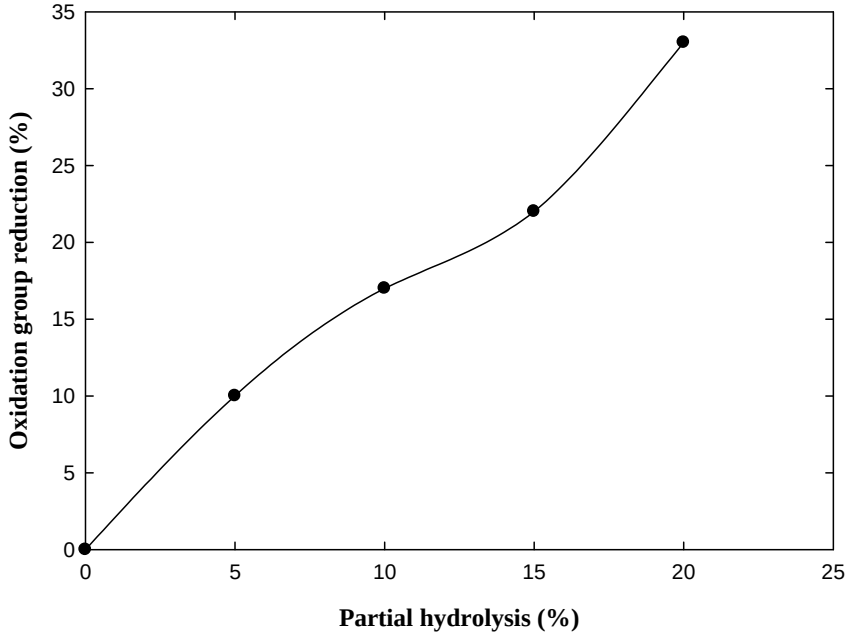

6.14: Plasmid used for binding studies in chapter 3

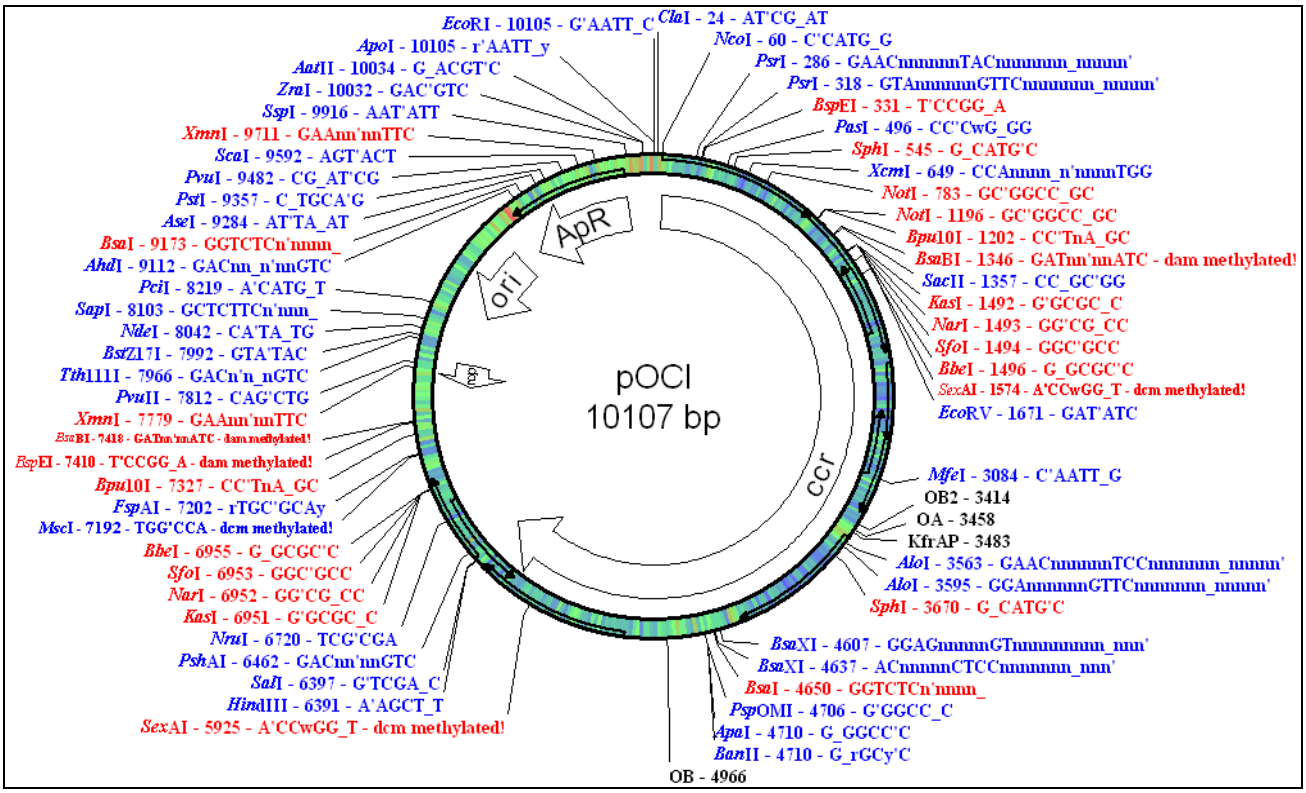

6.15: Light Micrographs discussed in Chapter 4

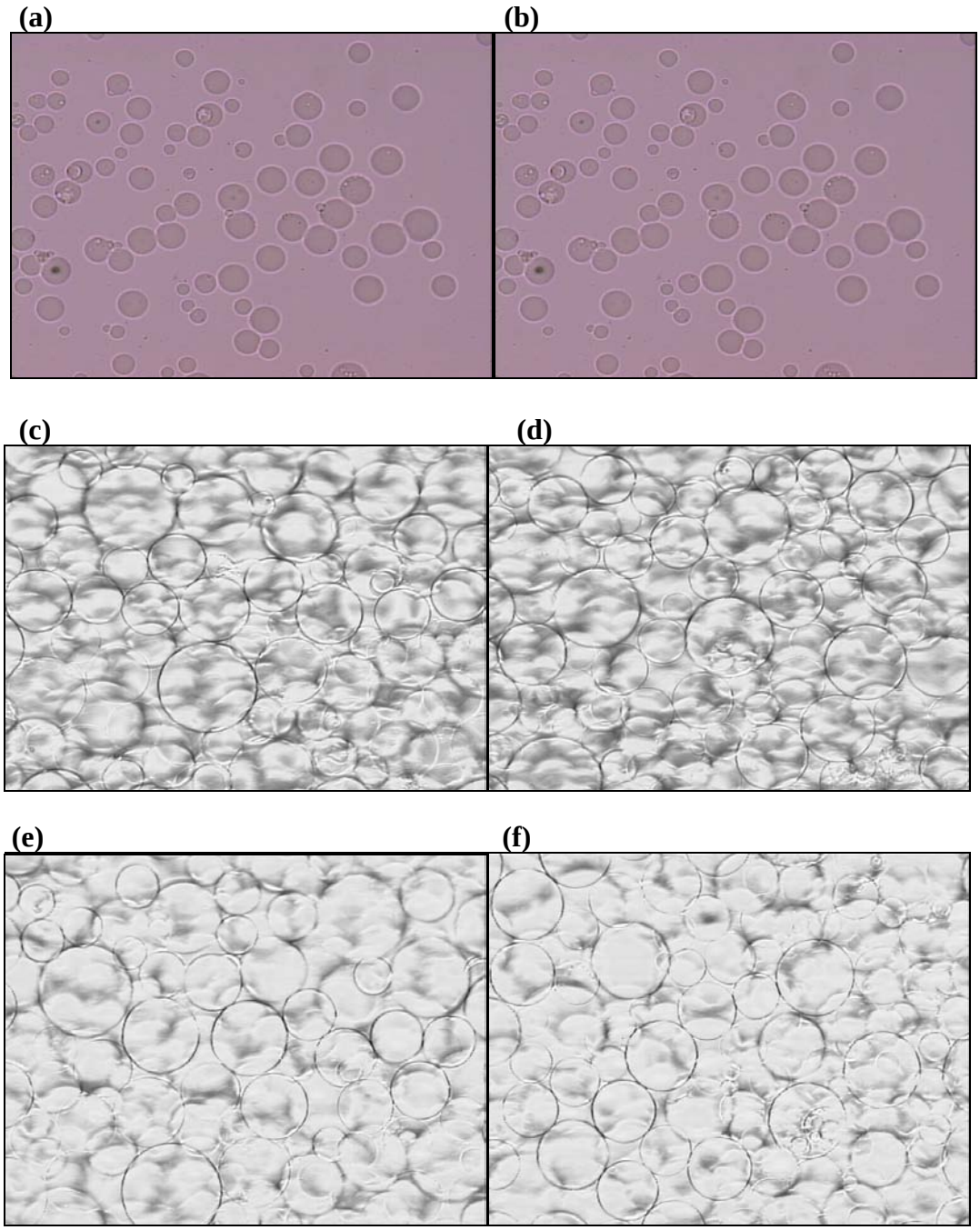

Figure 6.7: Light Micrographs of (a) Sepharose CL-6B ;(b) microwaved Sepharose CL-6B; (c) AGE activated Sepharose CL-6B; (d) microwaved AGE activated Sepharose CL-6B ; (e) Sepharose 6B ; (f) microwaved Sepharose 6B

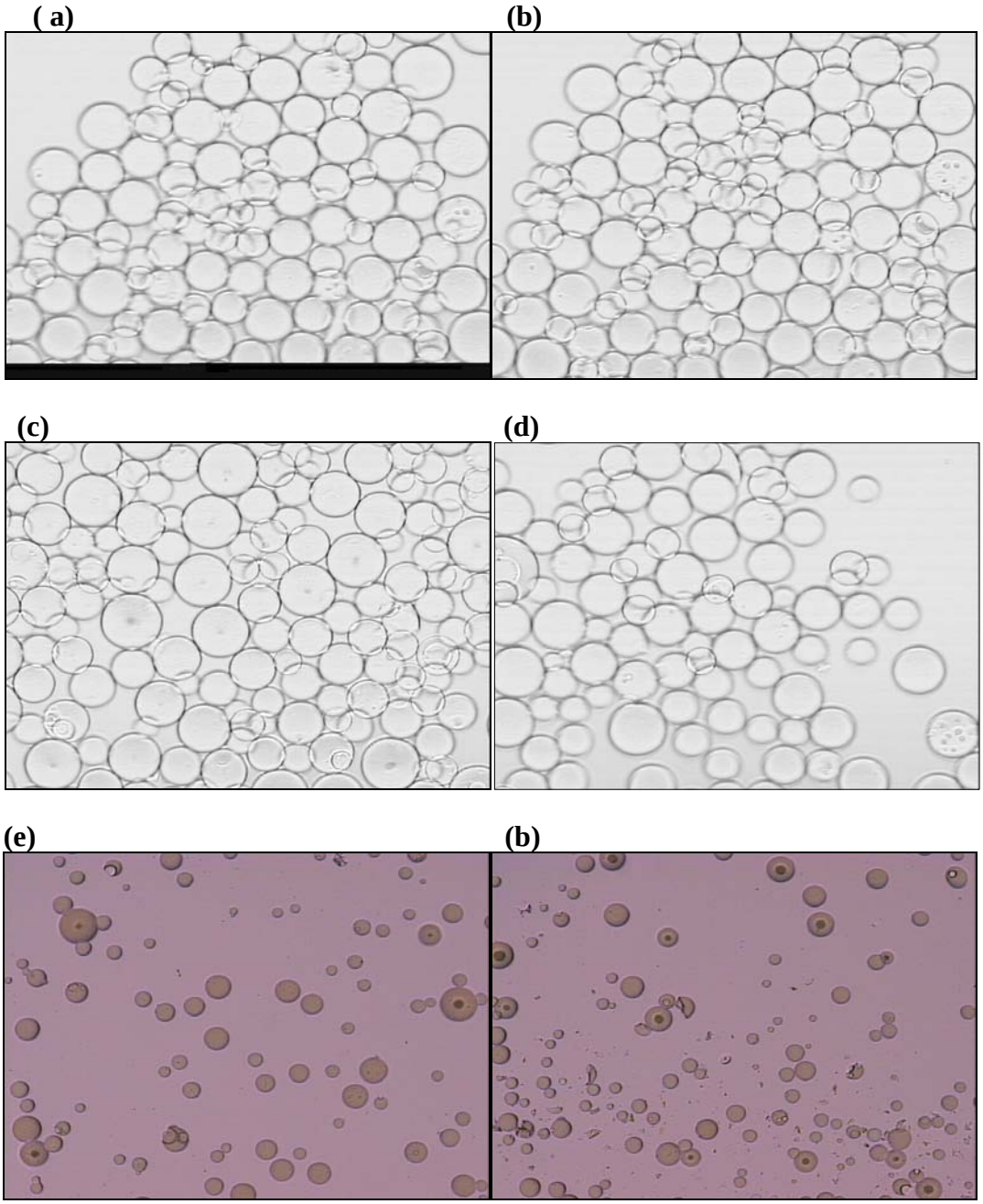

Figure 6.8: Light Micrographs of (a) Sepharose CM; (b) microwaved Sepharose CM ;(c) Phenyl Sepharose CM; (d) microwaved Phenyl Sepharose; (e) Sepharose DEAE FF; (f) microwaved Sepharose DEAE FF

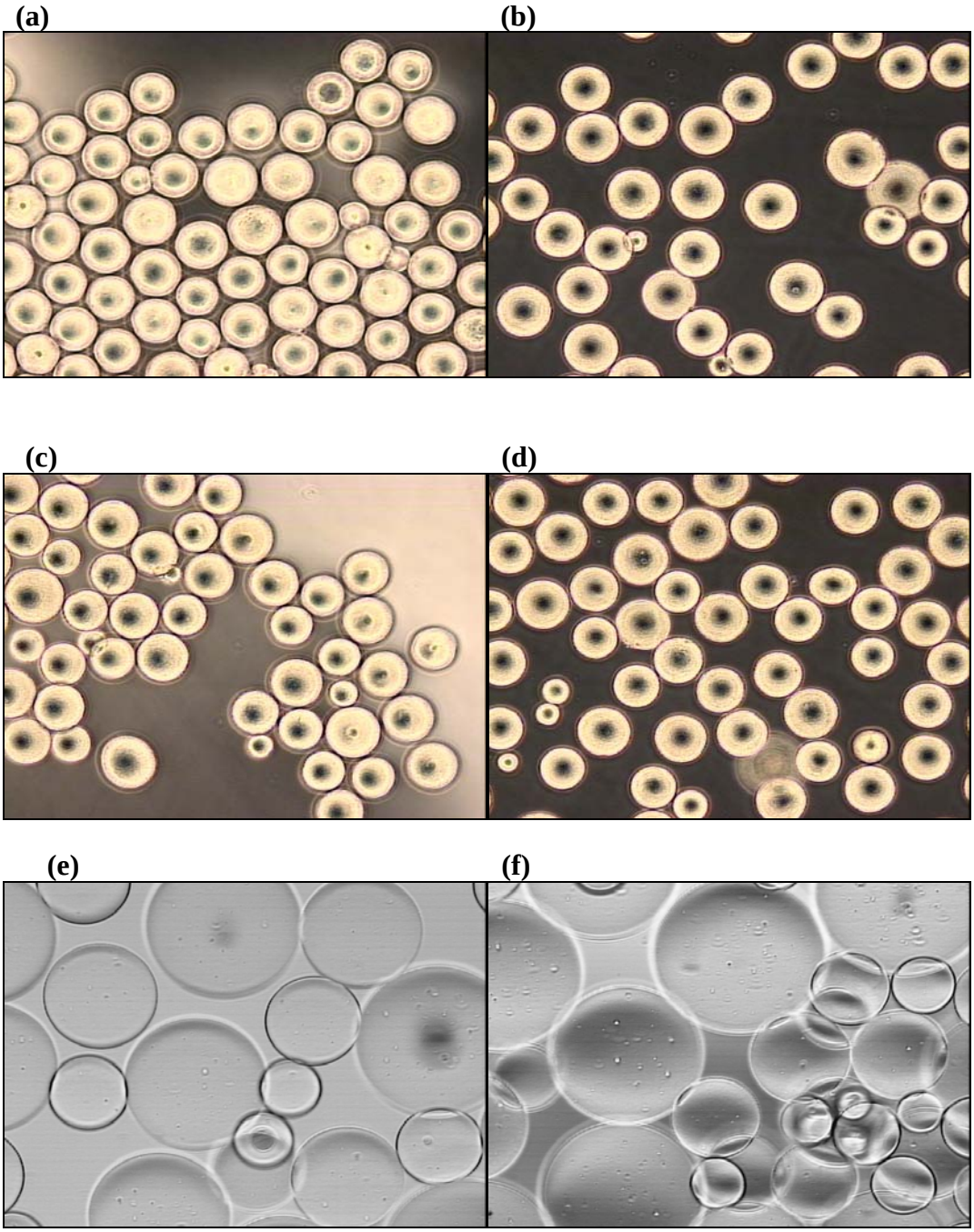

Figure 6.9: Light micrographs of: (a) HEA; (b) microwaved HEA; (c) PPA; (d) microwaved PPA; (e) Sephadex G50 ;(f) microwaved Sephadex G 50.

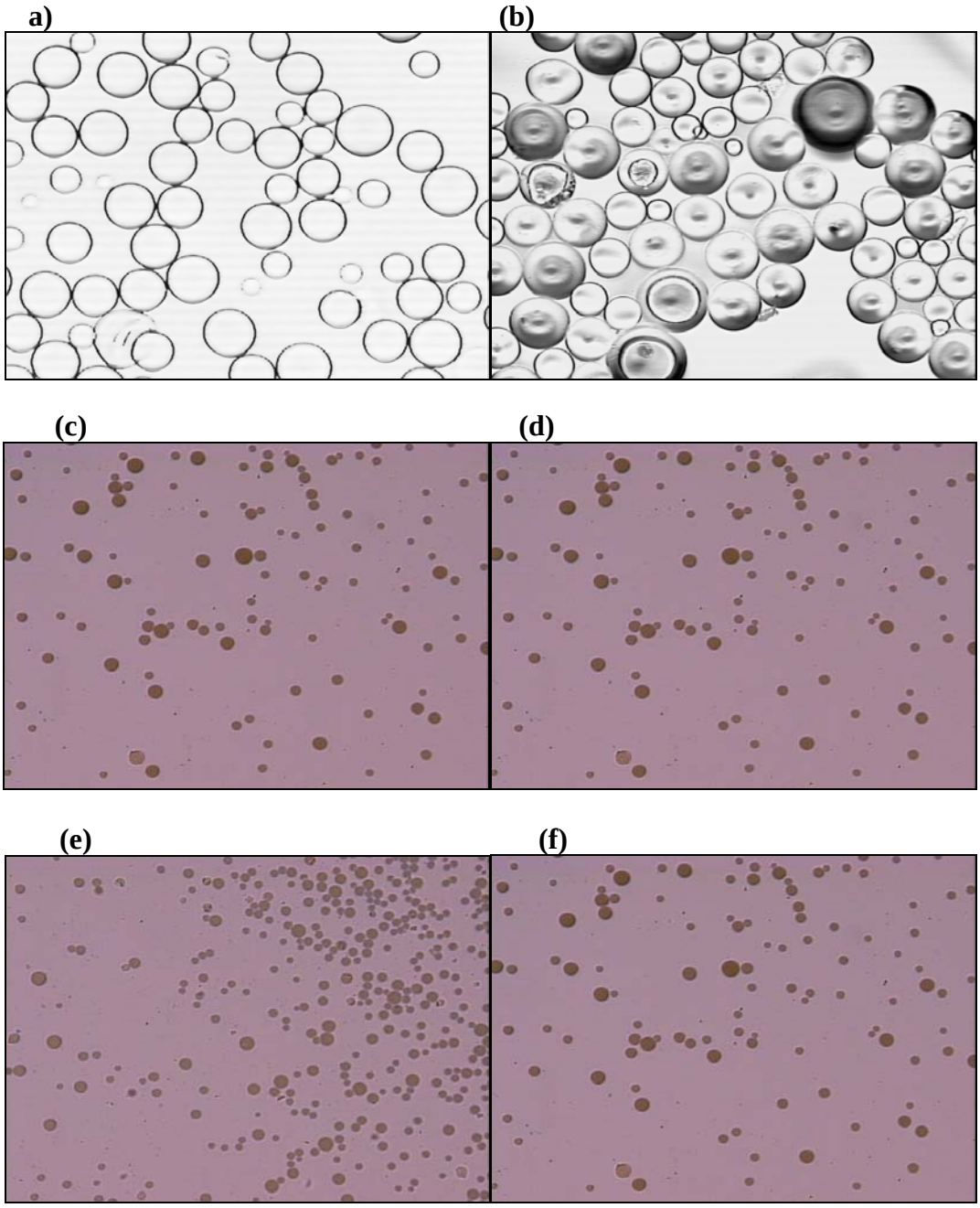

Figure 6.10: Light micrographs (a) Sephadex G 25; (b) microwaved Sephadex G 25; (c) Sephacryl S-HR 500; (d) microwaved Sephacryl S-HR 500; (e) Sephacryl S-HR 400; (f) microwaved Sephacryl S-HR 400.

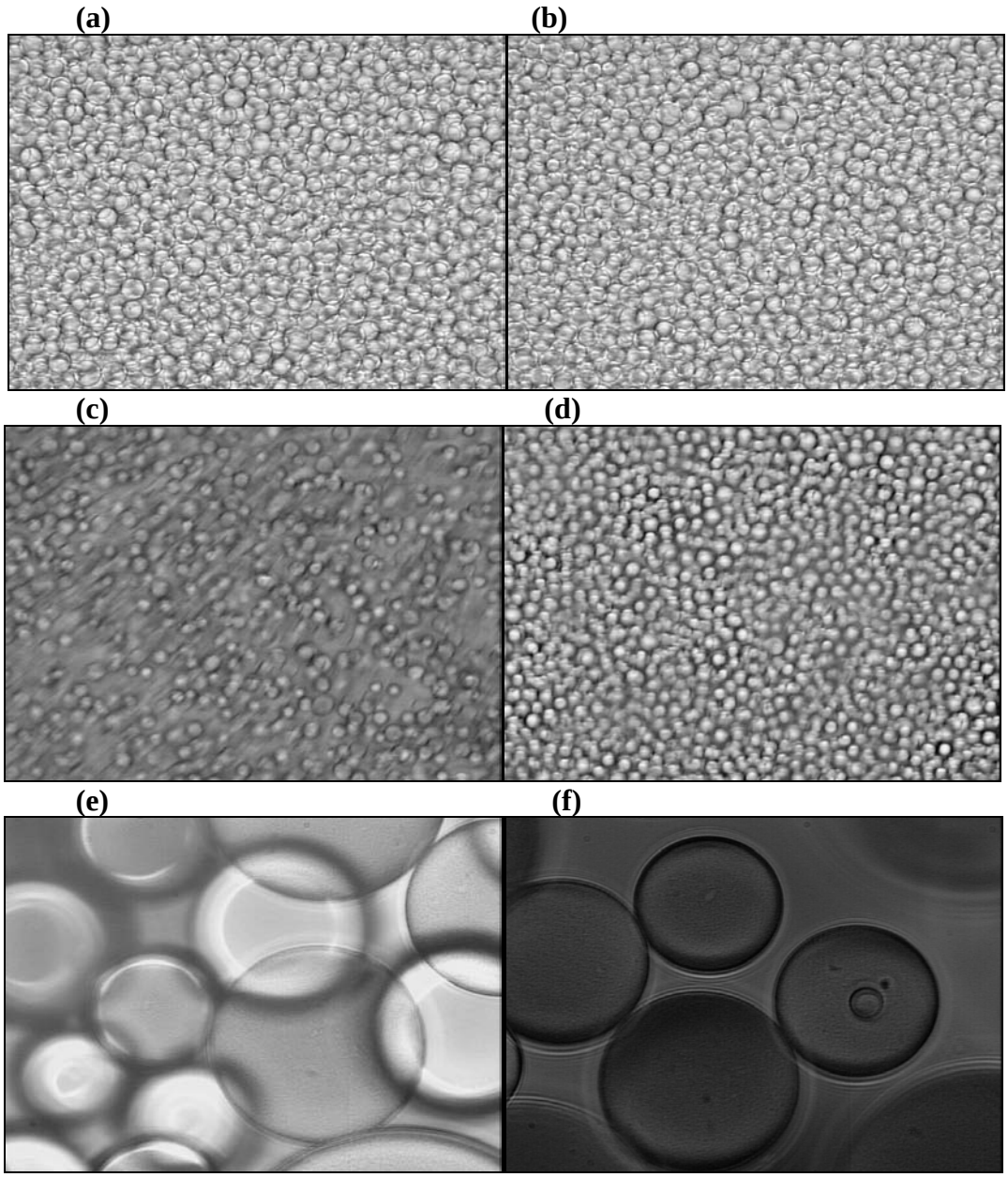

Figure 6.11: Light micrographs (a) Superdex 200; (b) microwaved Superdex 200; (c)Superdex 75; (d) microwaved Superdex 75; (e) Capto Q; (f) microwaved Capto Q

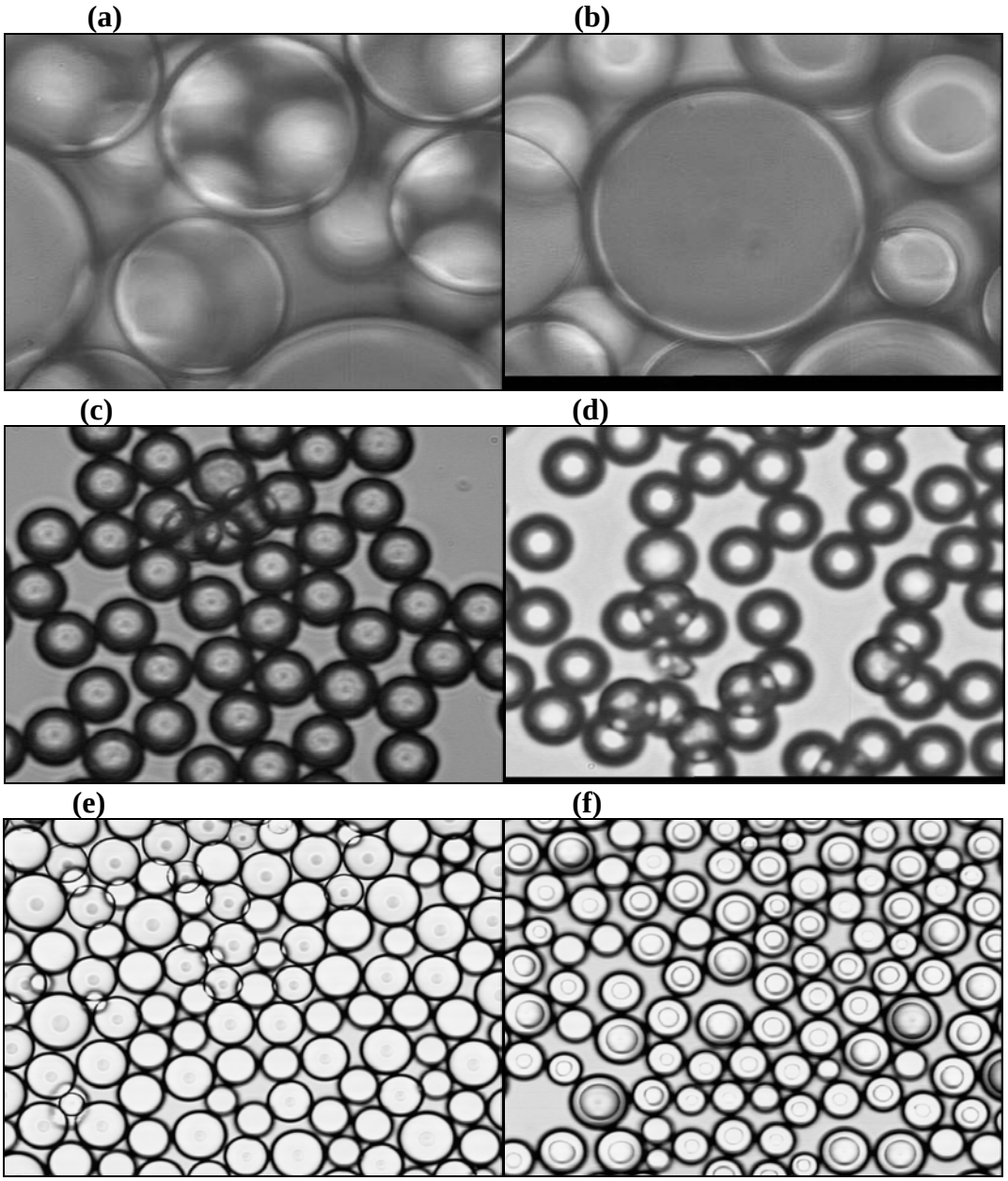

Figure 6.12: Light micrographs of (a) Capto S; (b) microwaved Capto S; (c) Source 15 Q ;(d) microwaved Source 15Q; (e) Toyopearl 40 C ; (f) microwaved Toyopearl 40C.

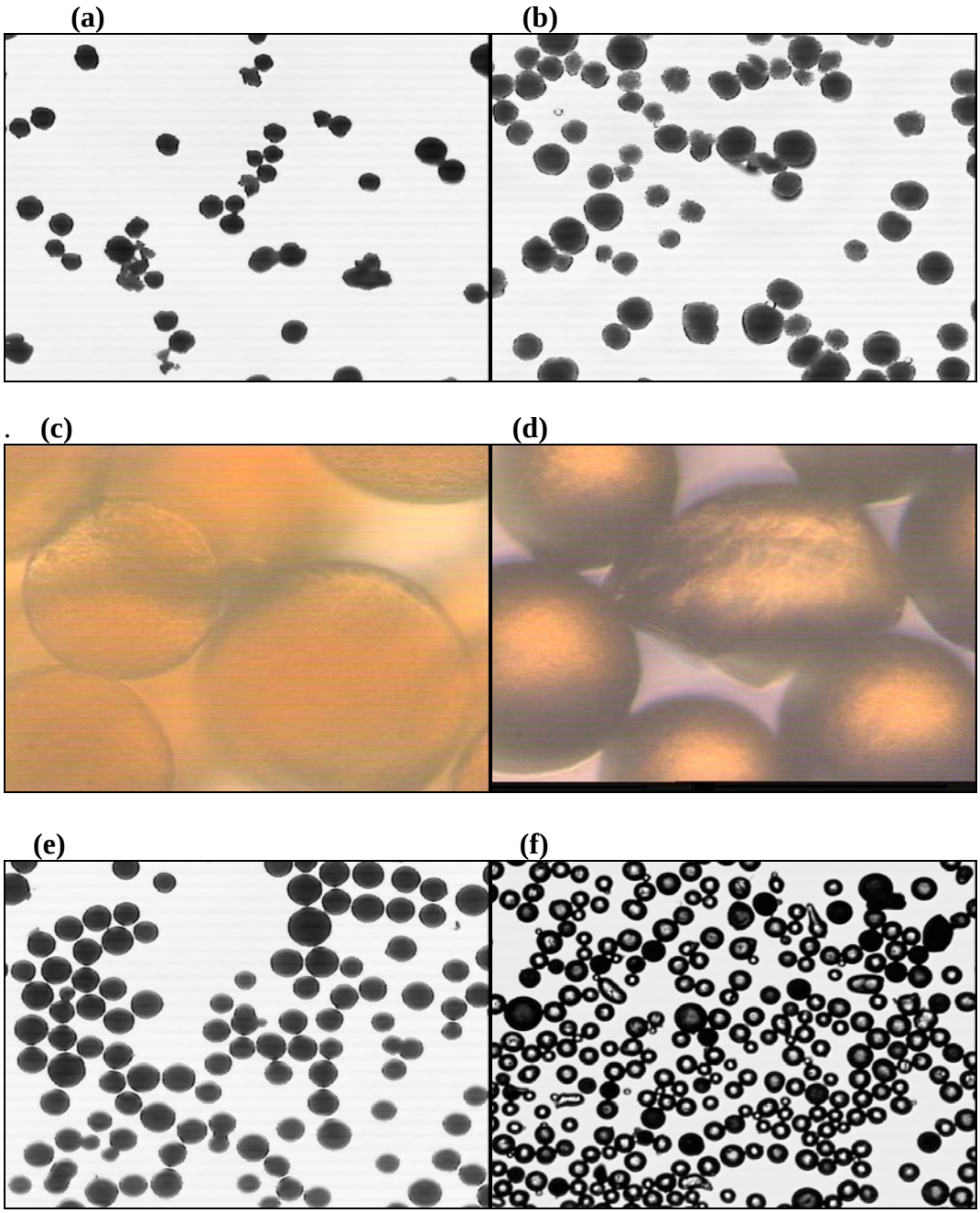

Figure 6.13 Light micrographs of (a) Toyopearl 75F; (b) microwaved Toyopearl 75F; (c) Fractogel EMD Control; (d) microwaved Fractogel EMD; (e) Zirconia Beads; (f) microwaved Zirconia Beads.

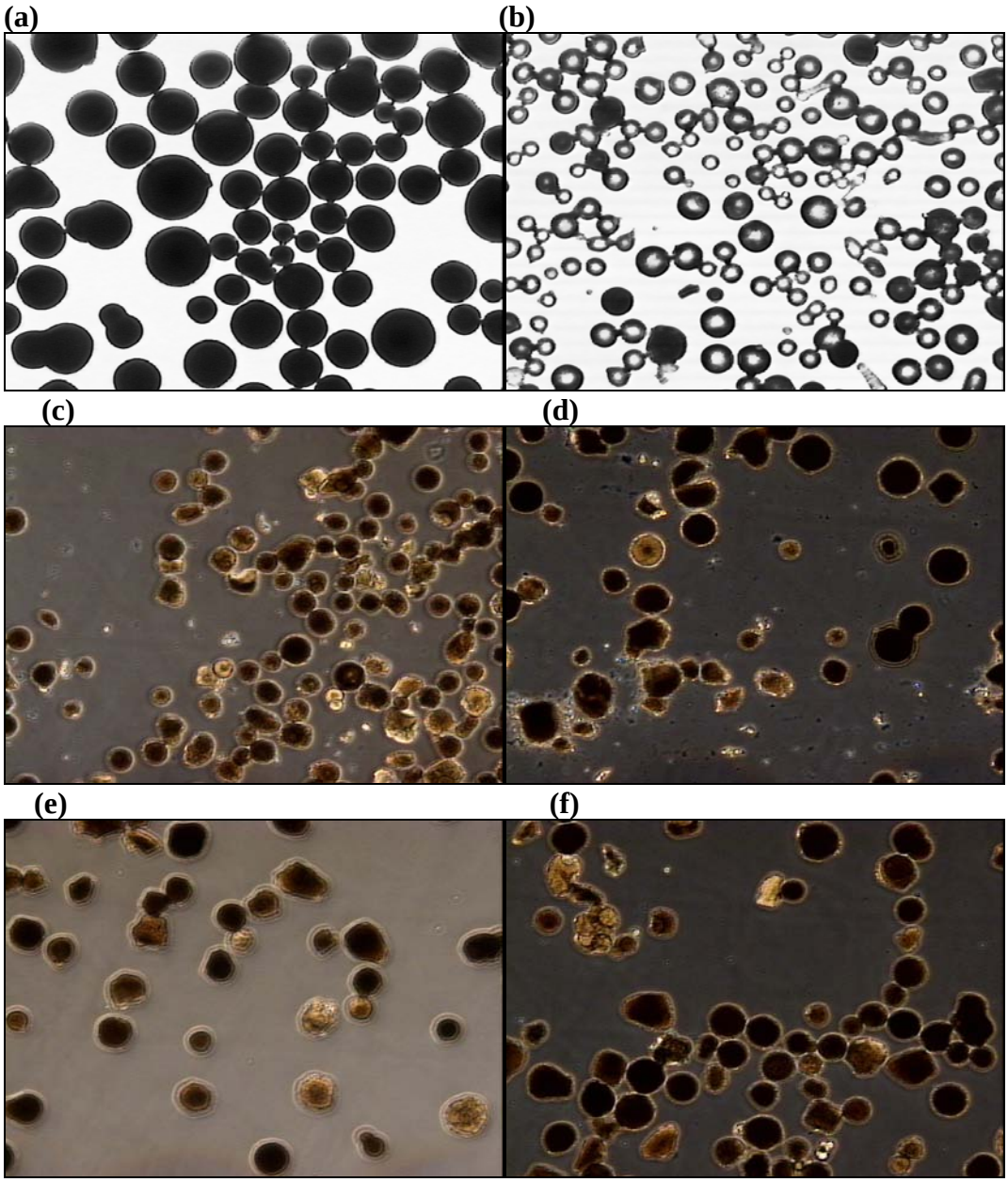

Figure 6.14 : Light micrographs of (a) CM Hyper Z; (b) microwaved CM Hyper Z; (c) S Hyper DF ;(d) microwaved S Hyper DF ; (e) Q Hyper DF (f) Q Hyper DF .

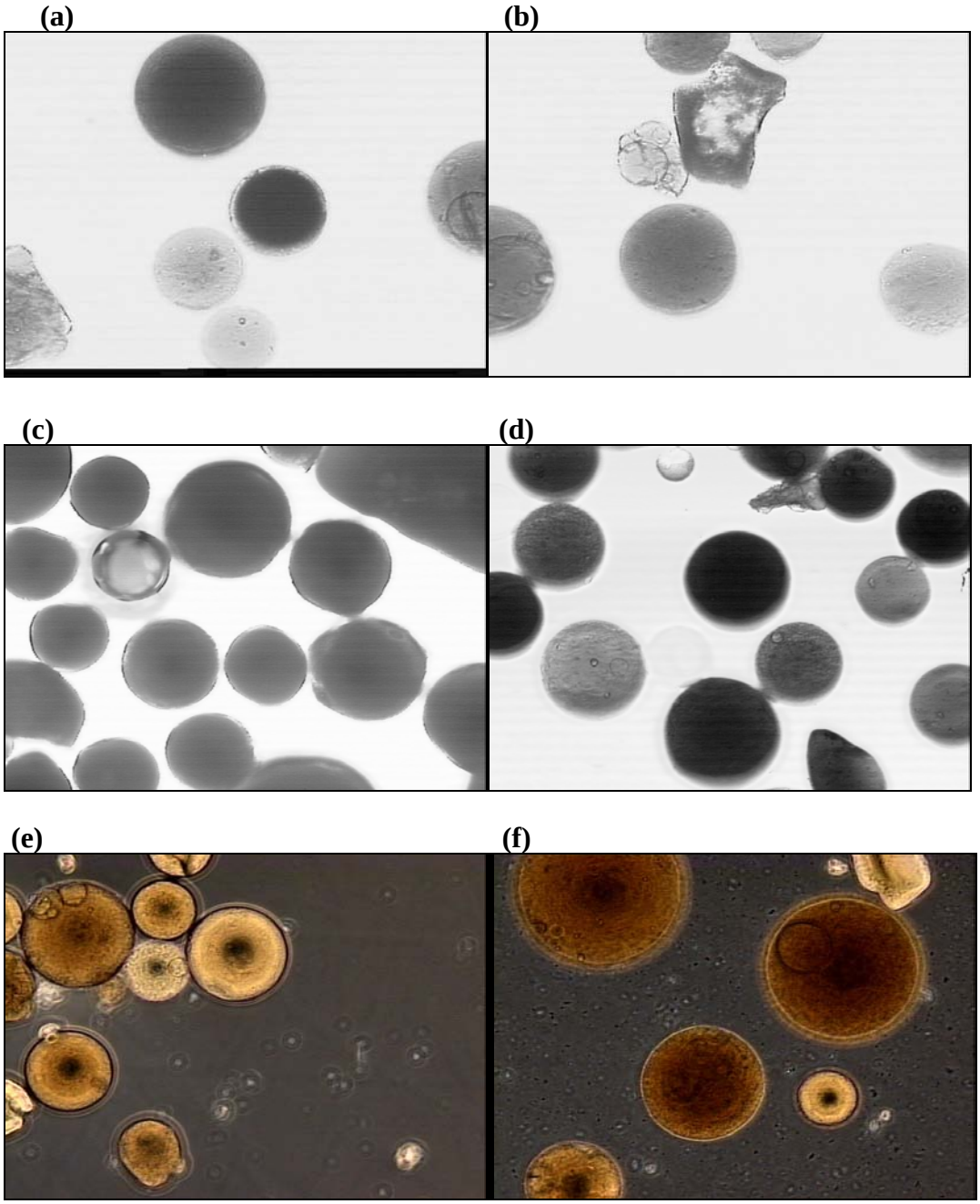

Figure 6.15: Light micrographs of: (a) SP SPHERSPOIL L; (b) microwaved SPHERSOIL ;(c) QMA SPHEROSIL LS, (d) microwaved QMA SPHEROSIL LS, (e) DEAE SPHERODEX LS ;(f) microwaved DEAE SPHERODEX LS

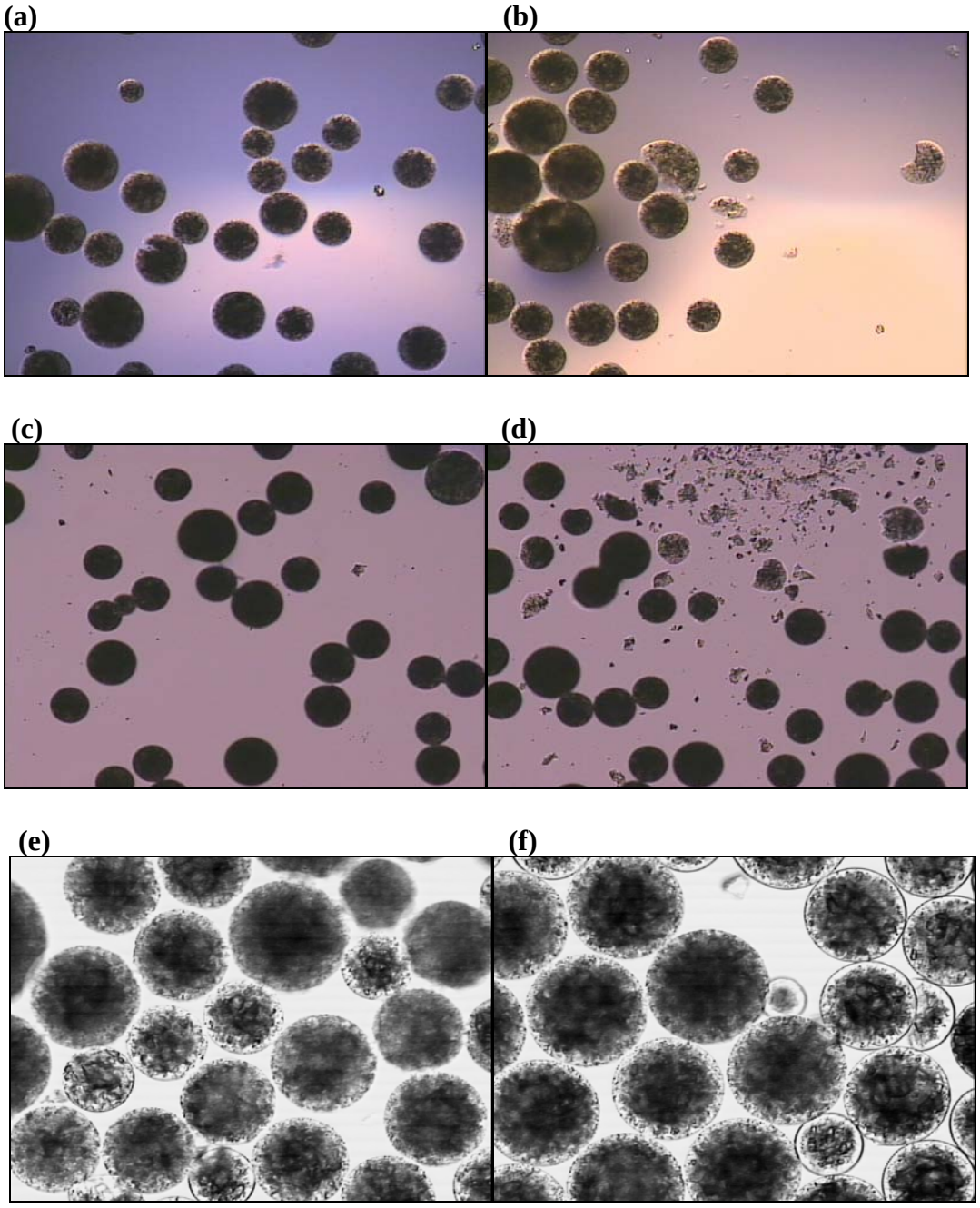

Figure 6.16: Light micrographs of: (a) Streamline base matrix; (b) microwaved Streamline base matrix ;(c) Streamline QXL, (d) microwaved Streamline OXL, (e) Streamline SP ;(f) microwaved Streamline SP

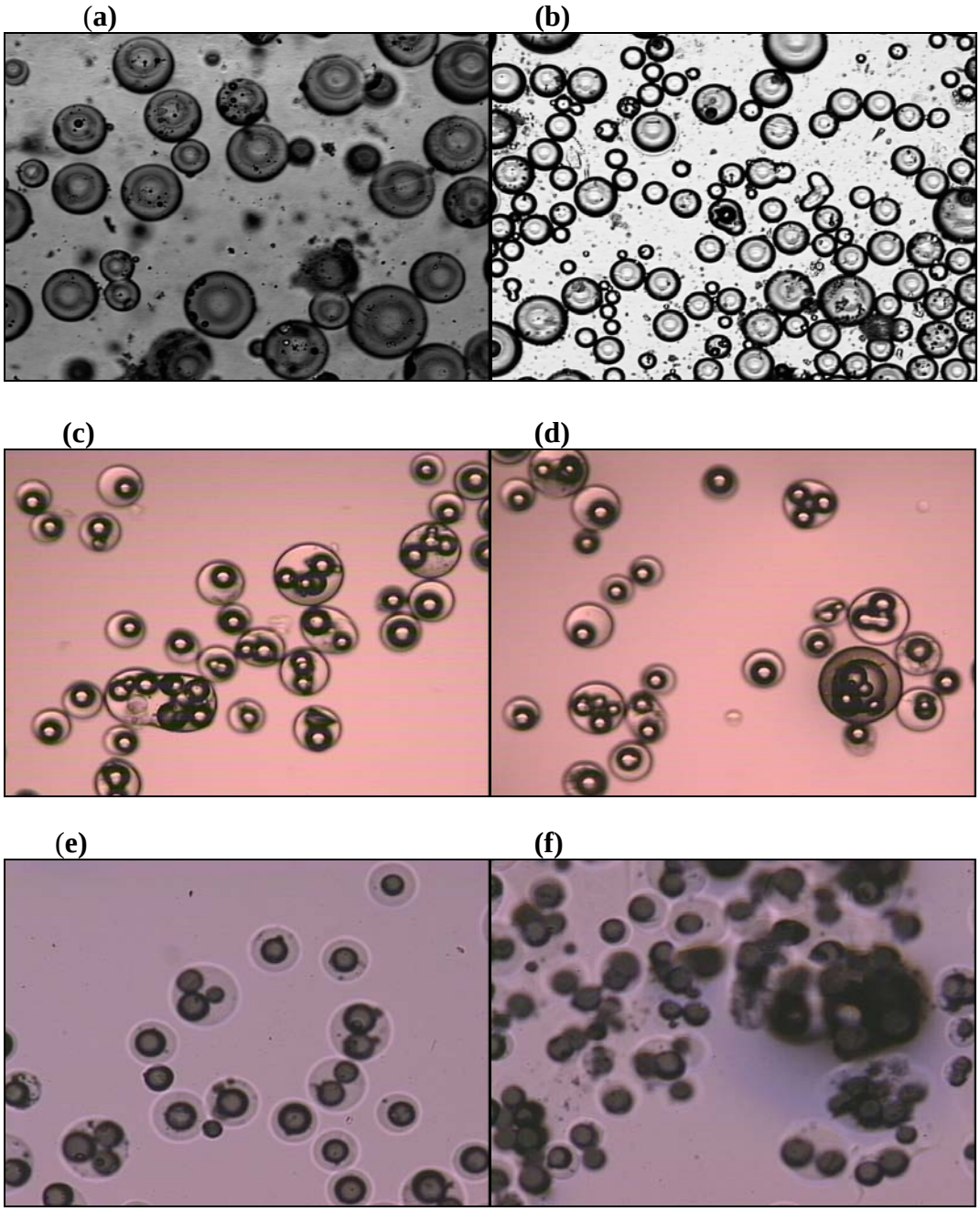

Figure 6.17: Light micrographs of: (a) UFC glass; (b) microwaved UFC glass;(c) UFC Steel PEI (d) microwaved UFC Steel PEI (e) UFC Steel ;(f) microwaved UFC steel

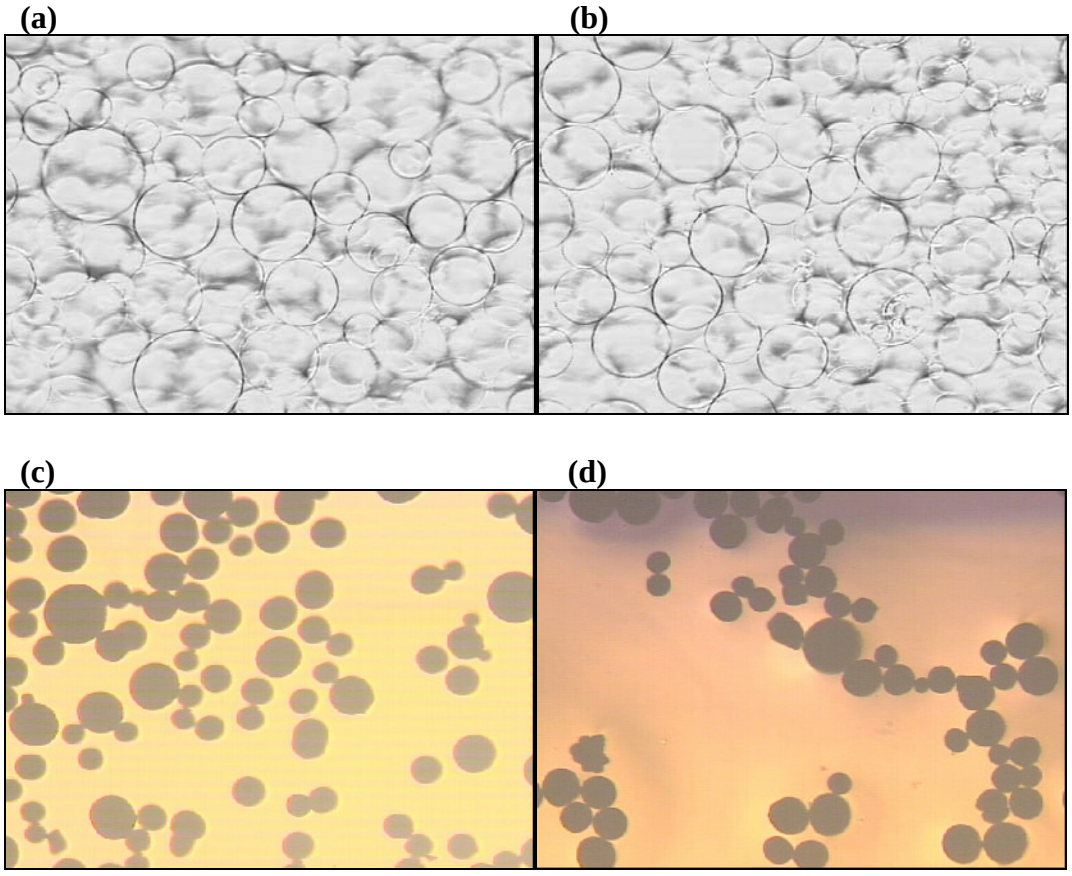

Figure 6.18: Light micrographs of: (a) Sepharose 6B; (b)microwaved Sepharose 6B; (c) Q Hyper z (d) microwaved Q Hyper Z